TECHNISCHE UNIVERSITÄT MÜNCHEN
Integrative Research Center Campus Straubing für Biotechnologie und Nachhaltigkeit

Thermosensitive bilayer actuators based on comb-type graft carboxymethylcellulose-g-poly-N-isopropylacrylamide hydrogels

Carla Meylín Chung Pinzás

Vollständiger Abdruck der von der promotionsführenden Einrichtung Campus Straubing für Biotechnologie und Nachhaltigkeit der Technischen Universität München zur Erlangung des akademischen Grades eines

Doktors der Naturwissenschaften (Dr. rer. nat.)

genehmigten Dissertation.

Vorsitzender:	Prof. Dr. Bastian Blombach
Prüfer der Dissertation:	1. Prof. Dr. Cordt Zollfrank
	2. Prof. Dr. Herbert Riepl

Die Dissertation wurde am 21.10.2019 bei der Technischen Universität München eingereicht und von der promotionsführenden Einrichtung Campus Straubing für Biotechnologie und Nachhaltigkeit am 03.03.2020 angenommen.

A mi padre Alfonso, mi madre Beatriz y mis hermanos Ramón y Gerardo…

An meinen Freund Alexander, seinen Vater Wolfram, seine Mutter Stilla und seine Brüder Christoph und Johannes…

Para mis amigos / To my friends / An meine Freunde…

A Dios…

Acknowledgements

First, I would like to thank my supervisor Prof. Dr. Cordt Zollfrank for his guidance throughout the research work from title's selection to finding the results. His immense experience, motivation and patience have given me more strength and courage to excel in the research writing. Conducting the academic study related to such a difficult topic couldn't be as simple as he made this for me. He is my mentor and a better advisor for my doctorate study beyond the imagination.

Besides my Supervisor, I won't forget to thank the rest of the team: Dr. Maria Naumann and Dr. Shahram Shafaei for giving the encouragement and sharing insightful suggestions. They all have participated in great measure in polishing my research writing skills. Their valuable guidance is hard to forget throughout my life.

I am also pleased to say thank you to Dr. Daniel Van Opdenbosch, Dr. Jörg Dörrstein, Dr. Matthias Petzold, M. Sc. Sabine Kugler, Dipl.-Ing. Steffi Deuerling, Sabine Witzel and Petra Peklo who facilitated my access to the research facilities and laboratory. It wouldn't have been possible to perform this research without their precious support. They all really mean a lot to me.

I would never forget my fellow labmates for the funny moments we experienced together, sleepless nights that gave us the spirit to complete tasks before deadlines and for stimulating the discussions. I would also like to thank my friends from Technical University München, Fraunhofer Institute, Technical University Dresden and Max Planck Institute for the Physics of Complex Systems. People who also helped me well throughout all this process are Prof. Dr. Brigitte Voit, Dr. Xavier Prudent, Dr. Rafael Guerra, Dr. Dimitar Denev and Dr. Francois Cardinali. Their immense support actually guided me to correct many mistakes that could create major challenges in the acceptance of my thesis.

In the end, I am grateful to my parents, siblings, my boyfriend (and his family), my friends and acquaintances who never forget me in their prayers for the ultimate success. I consider myself nothing without them. They provided me with enough moral support, encouragement and motivation to accomplish my personal goals. My parents have always supported me financially so that I only concentrate myself to the studies and achieving my objective without any difficulty on the way.

Summary

The main goal of this research was achieved through the development of a novel biomimetic bilayer actuator which fulfills the natural actuation mechanism “cell wall swelling (or shrinking)” (Burgert et al. (2009)) and has new thermosensitive actuation. Therefore, a novel material based on a polyamide 6 (PA6) passive layer and an active layer made of a CMC-g-PNIPAAm comb-type graft hydrogel was presented.

The developed synthetic path for developing comb-type graft hydrogels (main component of the active layer) involved three parts: First, the development of aminoterminated PNIPAAm oligomers by using the telomerization reaction proposed by Bokias et al. (2001) between the monomer N-isopropylacrylamide, the telomer 2-aminoethanothiol and the initiator ammonium persulphate. The functionalization of the PNIPAAm oligomers with amino end groups was verified with FTIR and NMR analysis. DSC analysis was used to confirm the existence of the PNIPAAm oligomers and also their phase transition behavior in water (Otake et al. (1990), Kano et al. (2009)) around 34-36 °C during the heating cycles. The increase of the LCST values (respect to non functionalized PNIPAAm oligomers) could be explained as a consequence of the amino end group attached to the PNIPAAm oligomers, due to restrictions of the amide-water interactions (Kokufuta et al. (2012)).

Second, the synthesis of novel copolymers by grafting the aminoterminated PNIPAAm oligomers on carboxymethyl cellulose polymers, by using a reaction with the coupling agent EDC (Bokias et al. (2001)). The grafting reaction was confirmed by FTIR with the characteristic PNIPAAm signals and CMC signals (Haleem et al. (2014)). Also DSC analysis confirmed the grafting reaction (Bokias et al. (2001)) by showing two phase transitions (Tg) at 53.9 and 146.6 °C for CMC backbones and PNIPAAm grafts, respectively, which corresponded to the Tg values for PNIPAAm (140.1 °C) and CMC (52.5 °C) obtained in previous measurements. The phase transition behavior in aqueous solutions of the graft copolymers was demonstrated, as in the case of the aminoterminated PNIPAAm oligomers, by the presence of a broad peak signal (Li et al. (2008)), Jin et al. (2013), Guo et al. (2015)) which was not visible at non-grafted CMC aqueous solution measurements. The reversibility of the phase transition was confirmed during the cooling cycles (Li et al (2008)).

Third and finally, new comb-type graft hydrogels were synthesized from the CMC-g-PNIPAAm graft copolymers by a crosslinking reaction either with $AlCl_3$ ions or with citric acid in a similar procedure like the one used by Demitri et al. (2008), where hydroxypropyl cellulose was used for promoting the intermolecular crosslinking rather than the intramolecular crosslinking between CMC chains (Demitri et al. (2008)) due to the HEC highly substituted C6 with OH groups (Sannino et al. (2005)). The crosslinking reaction with citric acid (and therefore the

formation of hydrogels) was validated with FTIR analysis. New signal occurred, which were not visible in the non-crosslinked graft copolymers (Demitri et al. (2008)). Also the crosslinking with citric acid and $AlCl_3$ ions was validated with DSC measurements performed to dried hydrogel samples that showed a shifting of the melting point peak from 174 °C (non-crosslinked graft copolymers) to 196.5 °C for hydrogels crosslinked with citric acid and 306 °C for hydrogels crosslinked with $AlCl_3$ ions.

The CMC-g-PNIPAAm comb-type graft hydrogels synthesized had faster equilibrium swelling times than the PNIPAAm comb-type graft hydrogels from Kaneko et al. (1995): Approximately 100 minutes (for crosslinking with citric acid) and 70 minutes (for crosslinking with Al^{3+} ions) versus more than 800 minutes for the PNIPAAm comb-type graft hydrogels. This could be explained because of the hydrophilic carboxylic groups from the CMC backbone matrix, since the constituents of the backbone matrix have an influence on the rapid equilibrium swelling times of hydrogels (Ju et al. (2001)). Also it was found that in the case of comb-type graft hydrogels crosslinked with Al^{3+} ions that the PNIPAAm grafts generated an heterogeneous volume structure with many pores that accelerated the hydrogel swelling kinetics (Kaneko et al. (1995), Hirasa et al. (1991), Kabra et al. (1991), Wu et al. (1992)), increasing their swelling degree (527%) in comparison to samples only composed of CMC (365%).

Studies of phase transition performed with digital photographs on hydrogel samples in aqueous media at 80 °C revealed that the comb-type graft hydrogels crosslinked with Al^{3+} ions contracted faster (first shrinking after 5 minutes) than samples crosslinked with citric acid (first shrinking after 15 minutes) and this could be explained because of the restriction of movement produced due to the covalent crosslinking with citric acid.

In acidic media (pH=2 and 3) at 80 °C the hydrogel samples crosslinked with citric acid contracted faster (46 minutes) than in aqueous media (120 minutes). This could be explained because at very low pH values the dissociation of carboxylic groups is inhibited, then a macroscopic phase separation might occur (Bokias et al. (2001)) and as consequence larger voids (Ju et al. (2001)) (or water release conducts (Kaneko et al. (1999)) are formed within the hydrogel matrix, releasing higher amounts of water. This allowed a faster contraction of the hydrogels. At higher or neutral pH values, the carboxylic groups are dissociated and the phase separation was partially inhibited, resulting in a slower contraction of the hydrogels than in acidic media (Bokias et al. (2001)).

The reversibility of the swelling and contraction with temperature of the comb-type graft hydrogels was validated by pulsatile temperature dependent analysis performed in water and buffer solution pH=3 between 80 and 4 °C. Here the influence of the pH in the intensity of the contraction and expansion was also demonstrated, since the hydrogels synthesized presented

a double sensitivity to temperature and pH, due to the carboxylic groups of the crosslinked CMC backbone (Ju et al. (2001)).

The preparation of the passive layer involved the surface functionalization of the PA6 substrate with two step-step glutaraldehyde reaction that was accomplished after an amino group activation (Isgrove et al. (2001)) was executed by using either an acidic (Pessoa de Amorim et al. (2014)) or aqueous hydrolysis. The glutaraldehyde provides the passive layer with the needed aldehyde groups that allows a covalent adhesion between the passive and active layer. The glutaraldehyde activation was validated with FTIR analysis by the presence and further intensity increase of the aldehyde peak (-COH) at 1720 cm^{-1}.

The covalent adhesion between the active and passive layer was confirmed by FTIR with the presence of an overlapped carboxylic group peak at 1718 cm^{-1} (-COOH), that would be a part of the citric acid structure that reacted with the OH-group of the CMC chains, as it was previously demonstrated by the FTIR studies of Demitri et al. (2008) in the crosslinking reaction progress between CMC and citric acid. It was inferred that in the same molecule its other carboxylic group reacts with the aldehyde group of the PA6 passive layer (Buhus et al. (2009)) (Figure 35), otherwise the adherence between both layers would not be possible. SEM micrographs also confirmed the adherence between active and passive layers.

The thermosensitive actuation in aqueous solutions of the bilayer actuators based on CMC-g-PNIPAAm comb-type graft hydrogel films with a bending angle of 10° after 45 minutes of residence time at 60 °C was confirmed with digital photographs. The bending was attributed to a thermosensitive contraction of the CMC-g-PNIPAAm comb-type graft hydrogel active layer and the non-contraction of the PA6 passive layer, this different behavior between both layers generated an interfacial stress (Ma et al. (2011)), which finally resulted in the bending action.

Gyration angle versus time measurements confirmed that the bending started 15 minutes after heating the sample between 40 to 60 °C and it was inferred that the contraction of the PNIPAAm grafts (dehydration of PNIPAAm) was high enough for producing release conducts (Kaneko et al. (1999)) or voids (Ju et al. (2001)), from where the water inside of the hydrogel was expulsed, producing the contraction of the hydrogel.

The present work opens the possibility of manufacturing other stimuli-sensitive bilayer actuators by using different comb-type graft CMC hydrogels that respond to light, magnetic or ionic strength external stimuli. The biodegradable CMC based hydrogel active layers make these bilayer actuators attractive candidates for biological and medical fields in the area of drug delivery and in the fabrication of miniaturized devices (Lab-on-a-Chip) with a fast reaction to a wide variety of external stimuli.

Zusammenfassung

Das Hauptziel dieser Forschung wurde durch die Entwicklung eines neuartigen biomimetischen Doppelschicht-Aktuators erreicht, der den natürlichen Aktuationsmechanismus „cell wall swelling (or shrinking)“ (Burgert et al. (2009)) erfüllt und eine neue thermosensitive Aktuation hat. Aus diesem Grund wurde ein neuartiges Material, basierend auf einer passiven Schicht aus Polyamid 6 (PA6) und einer aktiven Schicht bestehend aus einem CMC-g-PNIPAAm Kamm-Typ-Pfropfhydrogel, vorgestellt.

Der entwickelte Synthesepfad, um Kamm-Typ-Pfropfhydrogele (Hauptkomponente der aktiven Schicht) zu entwickeln, besteht auf drei Teilen: Als erstes wurden aminoterminierte PNIPAAm Oligomere durch die Telomerisationsreaktion entwickelt. Diese Reaktion ist von Bokias et al. (2001) zwischen dem N-Isopropylacrylamid Monomer, dem 2-Aminoethanothiol Telomer und dem Ammoniumpersulfat Initiator vorgeschlagen worden. Die Funktionalisierung der PNIPAAm Oligomere mit Aminoendgruppen wurde durch FTIR- und NMR-Analysen verifiziert. Die DSC-Analyse wurde verwendet, um die Existenz von PNIPAAm Oligomeren und ihr Phasenübergangsverhalten in Wasser (Otake et al. (1990), Kano et al. (2009)) bei etwa 34-36 °C (während der Wärmezyklen) zu bestätigen. Die Erhöhung der LCST-Werte (in Bezug auf nicht-funktionalisierte PNIPAAm Oligomere) könnte als Konsequenz der Einschränkungen der Amid-Wasser-Interaktionen der aminoterminierten Endgruppen, die mit den PNIPAAm Oligomeren verbunden wurden (Kokufuta et al. (2012)), gesehen werden.

Im zweiten Schritt wurden neuartige Copolymere durch Pfropfung von aminoterminierten PNIPAAm Oligomeren auf Carboxymethylcellulose-Polymere unter Verwendung einer Reaktion mit dem EDC Haftvermittler (Bokias et al. (2001)) synthetisiert. Die Pfropfreaktion wurde durch FTIR mit den charakteristischen Signalen von PNIPAAm und CMC (Haleem et al. (2014)) bestätigt. Auch die DSC-Analyse bestätigte die Pfropfreaktion (Bokias et al. (2001)) und wies zwei Phasenübergangstemperaturen (Tg) bei 53.9 und 146.6 °C für CMC Polymerrückgrate bzw. PNIPAAm Pfropfe auf, die den Tg Werten für PNIPAAm (140.1 °C) und CMC (52.5 °C) von früheren Messungen entsprachen. Das Phasenübergangsverhalten von den Pfropfcopolymeren in wässrigen Lösungen wurde, wie dies auch bei den aminoterminierten PNIPAAm Oligomeren der Fall war, durch die Präsenz eines breiten Peak-Signals (Li et al. (2008), Jin et al. (2013), Guo et al. (2015)) demonstriert. Dieses breite Peak-Signal war nicht sichtbar bei wässrigen Lösungsmessungen von nicht-gepfropften CMC Polymeren. Die Reversibilität des Phasenübergangs wurde während der Kühlzyklen bestätigt (Li et al (2008)).

Im dritten und letzten Schritt wurden neuartige Kamm-Typ-Pfropfhydrogele von den CMC-g-PNIPAAm Pfropfcopolymeren durch eine Vernetzungsreaktion entweder mit $AlCl_3$ Ionen oder

mit Zitronensäure, ähnlich wie bei der Vorgehensweise von Demitri et al. (2008), bei der vorzugsweise Hydroxypropylcellulose benutzt wurde, um die intermolekulare Vernetzung, anstatt der intramolekularen Vernetzung zwischen CMC Ketten (Demitri et al. (2008)) zu fördern, synthetisiert. Die intramolekulare Vernetzung ist aufgrund von HEC hochsubstituierten C6 mit OH Gruppen (Sannino et al. (2005)) entstanden. Die Vernetzungsreaktion mit Zitronensäure (und daher die Bildung von Hydrogelen) wurde mit FTIR-Analysen validiert. Neue Signale fanden statt, die nicht sichtbar in den nicht vernetzten Pfropfcopolymeren (Demitri et al. (2008)) waren. Auch die Vernetzungen mit Zitronensäure und $AlCl_3$ Ionen wurden mit DSC-Messungen validiert, die an getrockneten Hydrogelproben durchgeführt wurden, welche eine Verschiebung des Schmelzpunkts von 174 °C (für nicht vernetzte Pfropfcopolymere) auf 196.5 °C (für Hydrogele vernetzt mit Zitronensäure) und 306 °C (für Hydrogele vernetzt mit $AlCl_3$ Ionen) zeigten.

Die synthetisierten CMC-g-PNIPAAm Kamm-Typ-Pfropfhydrogele hatten schnellere Gleichgewichtsschwellungszeiten als die PNIPAAm Kamm-Typ-Pfropfhydrogele von Kaneko et al. (1995): Ungefähr 100 Minuten (für die Vernetzung mit Zitronensäure) und 70 Minuten (für die Vernetzung mit Al^{3+} Ionen) im Gegesatz zu mehr als 800 Minuten bei den PNIPAAm Kamm-Typ-Pfropfhydrogelen. Eine mögliche Erklärung hierfür kann in den hydrophilen Carboxylgruppen der CMC-Rückgratematrix gesehen werden, da die Komponenten der Rückgratematrix Einfluss auf die Gleichgewichtsschwellungszeiten der Hydrogele haben (Ju et al. (2001)). Auch wurde im Fall der mit Al^{3+} vernetzten Ionen Kamm-Typ-Pfropfhydrogele herausgefunden, dass die PNIPAAm Pfropfen eine heterogene Volumenstruktur mit vielen Poren generierten, die die Hydrogel-Schwellungskinetik beschleunigten (Kaneko et al. (1995), Hirasa et al. (1991), Kabra et al. (1991), Wu et al. (1992)), indem sie ihren Schwellungsgrad im Vergleich zu Proben, die nur aus CMC (365%) bestanden, steigerten (527%).

Studien zum Phasenübergang, die mittels digitaler Fotografien von Hydrogelproben in wässrigen Medien bei 80 °C durchgeführt wurden, zeigten, dass die mit Al^{3+} Ionen vernetzten Kamm-Typ-Pfropfhydrogele schneller schrumpften (erstes Schrumpfen nach 5 Minuten), als bei den Proben, die mit Zitronensäure vernetzt waren (erstes Schrumpfen nach 15 Minuten) und das eine mögliche Erklärung hierfür die aufgrund der kovalenten Vernetzung mit Zitronensäure entstandene Bewegungseinschränkung sein könnte.

In sauren Medien (pH=2 und 3) schrumpften bei 80 °C die mit Zitronensäure vernetzten Hydrogelproben schneller (46 Minuten) als in wässrigen Medien (120 Minuten). Eine mögliche Erklärung hierfür könnte sein, dass die Dissoziation der Carboxylgruppen bei sehr niedrigen pH-Werten gehemmt wird, woraufhin eine makroskopische Phasentrennung auftreten könnte (Bokias et al. (2001)). Als Konsequenz werden größere Poren (Ju et al. (2001)) (oder Wasserfreisetzungsleitungen (Kaneko et al. (1999)) innerhalb der Hydrogelmatrix gebildet,

wodurch größere Wassermengen freigesetzt werden. Dies erlaubte eine schnellere Schrumpfung der Hydrogele. Bei höheren oder neutralen pH-Werten wurden die Carboxylgruppen dissoziiert und die Phasentrennung teilweise gehemmt, sodass es eine langsamere Schrumpfung der Hydrogele als in sauren Medien gab (Bokias et al. (2001)).

Die Reversibilität von Schwellung und Schrumpfung mit der Temperatur der Kamm-Typ-Pfropfhydrogele wurde durch pulsatile temperaturabhängige Analyse zwischen 80 und 4 °C in Wasser und Pufferlösung (pH=3) bestätigt. Hier wurde auch der Einfluss des pH auf die Intensität von Schrumpfung und Schwellung demonstriert, weil die synthetisierten Hydrogele aufgrund der Carboxylgruppen des vernetzten CMC-Rückgrats (Ju et al. (2001)) eine zweifache Empfindlichkeit gegenüber Temperatur und pH zeigten.

Die Herstellung der passiven Schicht involvierte die Funktionalisierung der Oberfläche des PA6 Substrats durch eine zwei Schritt-Schritt Reaktion mit Glutaraldehyd. Diese Reaktion wurde erfüllt, nachdem eine Aktivierung der Aminogruppe entweder mit einer sauren (Pessoa de Amorim et al. (2014)) oder mit einer wässrigen Hydrolyse durchgeführt worden war (Isgrove et al. (2001)). Das Gluteraldehyd versorgt die passive Schicht mit den erforderlichen Aldehydgruppen, die eine kovalente Bindung zwischen passiver und aktiver Schicht erlauben. Die Aktivierung mit Glutaraldehyd wurde durch die Anwesenheit (und weitere Intensitätssteigerung) des Aldehyd-Peak (-COH) bei 1720 cm^{-1} mittels FTIR-Analyse validiert.

Die kovalente Bindung zwischen aktiver und passiver Schicht wurde durch die Anwesenheit eines überlappenden Carboxylgruppen-Peak bei 1718 cm^{-1} (-COOH) mit FTIR bestätigt. Die Carboxylgruppen waren ein Teil der Zitronensäurestruktur und reagierten mit den OH-Gruppen der CMC-Ketten, wie dies bereits zuvor durch die FTIR-Studien von Demitri et al. (2008) im Vernetzungsreaktionsverlauf zwischen CMC und Zitronensäure demonstriert worden war. Daraus ließ sich schließen, dass im gleichen Molekül die moleküleigene andere Carboxylgruppe mit der Aldehyd-Gruppe der PA6 passiven Schicht (Buhus et al. (2009)) (Abbildung 35) reagiert. Andernfalls wäre die Adhärenz zwischen beide Schichten nicht möglich. SEM-Micrographen bestätigten auch die Adhärenz zwischen, den aktiven und passiven Schichten.

Die thermosensitive Aktuation in wässrigen Lösungen der Doppelschicht-Aktuatoren, basierend auf CMC-g-PNIPAAm Kamm-Typ-Pfropfhydrogelen Filmen, wurde mit digitalen Fotografien bestätigt. Die Fotografien zeigten einen 10° Biegewinkel nach 45 Minuten Aufenthaltszeit bei 60 °C. Diese Biegung wurde einer thermosensitiven Schrumpfung der CMC-g-PNIPAAm Kamm-Typ-Pfropfhydrogel aktiven Schicht und einer nicht-Schrumpfung der PA6 passiven Schicht zugeschrieben. Das unterschiedliche Verhalten zwischen beiden

Schichten generierte eine Grenzflächenspannung (Ma et al. (2011)), die schließlich in der vorgenannten Biegung resultierte.

Drehwinkel verglichen mit Zeitmessungen bestätigten, dass die Biegung begann, nachdem die Probe 15 Minuten zwischen 40 und 60 °C erwärmt worden war. Daraus ließ sich schließen, dass die Schrumpfung der PNIPAAm Pfropfen (Dehydrierung von PNIPAAm) stark genug war, um Freisetzungsleitungen (Kaneko et al. (1999)) oder Poren (Ju et al. (2001)) zu erzeugen, von denen aus das Wasser aus dem Inneren des Hydrogels herausgestoßen wurde, um die Schrumpfung des Hydrogels auszulösen.

Die vorliegende Arbeit eröffnet die Möglichkeit der Herstellung anderer stimulisensitiver Doppelschicht-Aktuatoren, indem unterschiedliche Kamm-Typ-Pfropfhydrogele, die auf lichtsensitive, magnetische oder starke ionische äußere Stimuli reagieren, Verwendung finden. Die biodegradierbaren CMC-basierten hydrogelaktiven Schichten machen diese Doppelschicht-Aktuatoren zu attraktiven Kandidaten für biologische und medizinische Anwendungsfelder auf dem Gebiet des Drug Delivery sowie bei der Herstellung von miniaturisierten Vorrichtungen (Lab-on-a-Chip), die eine schnelle Reaktion gegenüber einer Vielzahl von äußeren Stimuli haben.

Table of Contents

Acknowledgements ..... **I**
Summary ..... **II**
Table of Contents ..... **IX**
Abbreviations ..... **XIII**

Theoretical and Experimental Parts

1. Motivation and Goals **1**

2. Theoretical Background **3**

2.1. Biomimetic Actuators 3
2.1.1. “Smart” Biomimetic Actuation 3
2.1.2. “Smart” Bilayer Actuators 6
2.1.3. Thermosensitive bilayer and multilayer actuators 9

2.2. Synthesis of Bilayer Actuators based on CMC-g-PNIPAAm comb-type graft hydrogel films 14
2.2.1. Synthesis of Aminoterminated PNIPAAm oligomers 14
2.2.1.1. Poly(N-isopropylacrylamide) – PNIPAAm 14
2.2.1.2. Functionalization of Polymers (amino end groups) 21
2.2.1.3. Telomerization 25
2.2.2. Synthesis of CMC-g-PNIPAAm graft copolymers 28
2.2.2.1. Carboxymethyl cellulose (CMC) 28
2.2.2.2. Grafting “onto” polymerization and couple reaction 33
2.2.3. Synthesis of comb-type graft hydrogels 36
2.2.3.1. Chemically crosslinked hydrogels 36
2.2.3.2. Ionically crosslinked hydrogels 37
2.2.3.3. Thermosensitive hydrogels 39
2.2.4. Synthesis of Bilayer Actuators based on CMC-g-PNIPAAm comb-type graft hydrogel films 43
2.2.4.1. Bilayer Actuators with hydrogel substrates 43
2.2.4.2. Bilayer Actuators with PA6 unidirectional substrates 43

2.3. Bilayer Actuators based on CMC-g-PNIPAAm comb-type graft hydrogel films 43
2.3.1. Chemical Bonding between Active and Passive Layers in Bilayer Actuators based on CMC-g-PNIPAAm comb-type graft hydrogel films 44
2.4. Thermal and Actuation Properties from Bilayer Actuators 44
2.4.1. DSC measurements of LCST in PNIPAAm oligomers 44
2.4.2. DSC measurements of LCST in thermosensitive graft copolymers 47
2.4.3. Thermosensitive swelling degree in comb-type graft hydrogels vs homopolymer gels 49
2.4.4. Stimulus-sensitive actuation in bilayers measured by digital photographs 57
2.4.5. Quantitative measurement of stimulus-sensitive actuation in bilayers from digital photographs 60

3. Experimental Part 67

3.1. Analytical Methods 67
3.1.1. FTIR spectroscopy (ATR and KBr pallets) 67
3.1.2. Nuclear Magnetic Resonance (NMR) 67
3.1.3. Elemental Analysis 67
3.1.4. Gel Permeation Cromatography (GPC) 67
3.1.5. Differential Scanning Calorimetry (DSC) 68
3.1.6. Equilibrium Swelling Ratio 69
3.1.7. Equilibrium Temperature-Responsive Swelling Behavior 69
3.1.8. Pulsatile Temperature-Responsive Swelling Behavior 69
3.1.9. Digital photographs and videos 70

3.2. Synthesis of aminoterminated PNIPAAm oligomers 70

3.3. Synthesis of CMC-g-PNIPAAm graft copolymers 72

3.4. Synthesis of CMC-g-PNIPAAm comb-type graft hydrogels 72
3.4.1. CMC-g-PNIPAAm comb-type graft hydrogel crosslinked with Al^{3+} ions 72
3.4.2. CMC-g-PNIPAAm comb-type graft hydrogel crosslinked with citric acid 74
3.4.3. CMC-g-PNIPAAm comb-type graft hydrogels: Crosslinking with Al^{3+} ions vs crosslinking with citric acid 76

3.5. Synthesis of bilayer actuators based on CMC-g-PNIPAAm comb-type graft hydrogel films 76
3.5.1. Preparation of CMC-g-PNIPAAm comb-type graft pre-gel solutions 76
3.5.2. Synthesis of bilayer actuators with PA6 substrates 78
3.5.2.1. Functionalization of PA6 substrates 78
3.5.2.2. Synthesis of bilayer actuators with PA6 substrates 80
3.5.3. Synthesis of bilayer actuators with hydrogel substrates 83

4. Results 84

4.1. Synthesis and structural characterization of aminoterminated PNIPAAm oligomers 84
4.1.1. Amount and %yield 84
4.1.2. Gel Permeation cromatography 84
4.1.3. Elemental analysis 84
4.1.4. FTIR 84
4.1.5. NMR 87
4.1.6. DSC (Dry) 87

4.2. Characterization of phase transition activity in aminoterminated PNIPAAm oligomers 87
4.2.1. Reversibility of Phase Transition in Water 87

4.3. Synthesis and structural characterization of CMC-g-PNIPAAm graft copolymers 90
4.3.1. Amount and %yield 90

4.3.2. Elemental analysis 91
4.3.3. FTIR 92
4.3.4. DSC (Dry) 93

4.4. Characterization of Phase Transition Activity in CMC-g-PNIPAAm graft copolymers 104
4.4.1. Reversibility of Phase Transition in Water and in Buffer Solutions 104

4.5. Synthesis and Structural Characterization of comb-type graft hydrogels 104
4.5.1. FTIR 104
4.5.2. DSC (Dry) 104
4.5.3. Swelling Kinetics and Equilibrium Ratio 107

4.6. Characterization of phase transition activity in comb-type graft hydrogels 108
4.6.1. Characterization of phase transition activity by digital photographs 108
4.6.2. Deswelling kinetics in water and in buffer solution pH=3 at 80 °C 109
4.6.3. Pulsatile temperature dependent kinetics in water and buffer solution pH=3 at 80 °C and 4 °C 109

4.7. Synthesis and structural characterization of functionalized PA6 substrates 109
4.7.1. EA until initial activation with glutaraldehyde 109
4.7.2. FTIR until final activation with glutaraldehyde 111

4.8. Synthesis and structural characterization of bilayer actuators based on CMC-g-PNIPAAm comb-type graft hydrogel films 114
4.8.1. FTIR 114
4.8.2. SEM 116

4.9. Characterization of temperature dependent actuation property in bilayer actuators based on CMC-g-PNIPAAm comb-type graft hydrogel films 116
4.9.1. Photographs of actuation 116
4.9.2. Gyration Angle 125

5. Discussion of Results 128

5.1. Introduction 128

5.2. Synthesis of Bilayer actuators based on CMC-g-PNIPAAm comb-type graft hydrogels 129
5.2.1. Aminoterminated poly(N-Isopropylacrylamide) semitelechelic oligomers as thermosensitive polymers 129
5.2.1.1. Antecedents and secondary hypothesis proposed 129
5.2.1.2. Amount and %yield 129
5.2.1.3. Gel permeation cromatography and elemental analysis 130
5.2.1.4. FTIR and NMR 130
5.2.1.5. DSC (Dry) 130
5.2.1.6. DSC (In solution) 131
5.2.2. Thermal modification of carboxymethyl cellulose polymers with

Aminoterminated PNIPAAm oligomers by coupling reaction with EDC 132
5.2.2.1. Antecedents and secondary hypothesis proposed.....132
5.2.2.2. Amount and %yield.....132
5.2.2.3. Elemental analysis and FTIR 133
5.2.2.4. DSC (Dry).....133
5.2.2.5. DSC (In solution) 133
5.2.3. CMC-g-PNIPAAm comb-type graft hydrogels 135
5.2.3.1. Antecedents and secondary hypothesis proposed.....135
5.2.3.2. Amount and %yield.....135
5.2.3.3. FTIR 135
5.2.3.4. DSC (Dry).....137
5.2.3.5. Swelling kinetics and equilibrium ratio 137
5.2.3.6. Phase transition activity by digital photographs 138
5.2.3.7. Deswelling Kinetics in Water and in Buffer Solution pH=3 at 80 °C 139
5.2.3.8. Pulsatile temperature dependent kinetics in water and buffer solution pH=3 at 80 °C and 4 °C 140
5.2.4. Aldehyde functionalization of PA6 unidirectional substrates by acidic hydrolysis 140
5.2.4.1. Antecedents and secondary hypothesis proposed.....140
5.2.4.2. Elemental Analysis 141
5.2.5. Chemical bonding between active and passive layers in bilayer actuators 141
5.2.5.1. Antecedents and secondary hypothesis proposed.....141
5.2.5.2. FTIR 142
5.2.5.3. SEM 142

5.3. Thermal and actuation properties from bilayer actuators based on CMC-g-PNIPAAm comb-type graft hydrogel films 143
5.3.1. Antecedents and secondary hypothesis proposed.....143
5.3.2. Photographs of actuation 143
5.3.3. Gyration angle 144

6. Bibliography 146

Suplementary Information

7. Index of Figures 155

8. Index of Tables 163

9. Appendix I: Protocols 172

9.1. Elemental analysis protocol.....172

10. Appendix II: Tables 187

Abbreviations

AA	Acrylic acid
AAc	Acetic Acid
AB	Telogen
ACVA	4, 4-azobis(4-cyanovaleric acid)
AESH	2-aminoethanethiol
AET	2-aminoethanethiol
AET.HCl	Aminoethanethiol hydrochloride
AFM	Atomic force microscope
AGU	Anhydro Glucose Unit
AIBN	Azobisisobutyronitrile
APS	Ammonium persulfate
A(m)nB	Telomer
AMPS	2-Acrylamido-2-methyl propane sulfonic acid
ATR	Attenuated Total Reflectance
ATRP	Atom-transfer radical-polymerization
Au	Gold
BA	Benzophenone acrylate
Bpy	Bipyridine
C6M	1, 4-di-(4-(6-acryloyloxyhexyloxy)benzoyloxy)-2-methylbenzene
$CDCl_3$	Deuterated chloroform
CHO	Aldehyde
CM	Carboxymethyl
CMC	Carboxymethyl cellulose
CMC-g-PNIPAAm	Carboxymethylcellulose grafted with poly(N-Isopropylacrylamide) oligomers
CNTs	Carbon nanotubes
CP	Cross Polarization
CRP	Controlled radical polymerization
DCC	1,3-dicyclohexylcarbodiimide
DCCI	Dicyclohe-xylcarbodiimide
DHEBAAm	Dihydroxyethylene-bis-acrylamide
% Dif.	Percentage of Difference
DMAAM	N,N-dimethylacrylamide
DMAP	4-(dimethylamino) pyridine

DMF	Dimethylformamide
DMSO	Dimethyl sulfoxide
DP	Degree of polymerization,
DP(Graft)	Degree of Polymerization per Graft
DS	Degree of substitution
DSC	Differential Scanning Calorimetry
DVS	Divinyl sulfone
ECP	2-chloropropionate
EDC	1-(3-dimethylamino-propyl)-3-ethyl-carbodiimide hydrochloride
FTIR	Fourier-transform infrared
ΔG	Free energy variation
GAN	Comb-type graft hydrogels of alginate grafted with PNIPAAM oligomers
GG	Comb-type graft hydrogels
GG2900	Comb-type graft with 2900 g/mol graft chain length hydrogels
GG4000	Comb-type graft with 4000 g/mol graft chain length hydrogels
GG9000	Comb-type graft with 9000 g/mol graft chain length hydrogels
GOD	Glucose oxidase
GPC	Gel Permeation Cromatography
%Graft(THEO)	Theoretical Graft Weight Percentage
%Graft(EXP)	Experimental Graft Weight Percentage
HEC	Hydroxyethyl cellulose
HPC	Hydroxypropyl cellulose
ΔHm	Enthalpy associated with the melting of the samples
HPAEC	High-Performance Anion Exchange Cromatography
HPLC	High-performance liquid chromatography
HPMC	Hydroxyl propyl methyl cellulose
ID-GG	Comb-type graft PNIPAAm grafted with poly(NIPAAM-co-DMAAM) hydrogels
ID-NG	Non grafted poly(NIPAAM-co-DMAAM) hydrogels
IPAAm	N-isopropylacrylamide
IPN	Interpenetrated network

IP-GG	Comb-type graft poly(NIPAAM-co-DMAAM) grafted with PNIPAAm hydrogels
IP-NG	Poly(N-isopropylacrylamide) homopolymer hydrogels
KPS	Potassium persulfate
LC	Liquid crystal
LCST	Lower Critical Solution Temperature
LDPE	Low density polyethylene
MAS	Magic Angle Spinning
Me_6TREN	CuCl/tris[2-(dimethylamino)ethyl]-amine
MMA	Methyl-methacrylate
Mn	Molecular Weight - Number
Mw	Molecular Weight – Weight
MTF	Muscular thin films
Mw	Molecular Weight
Mw(Graft)(EXP)	Experimental Molecular Weight per Graft
Mw(Graft)(THEO)	Theoretical Molecular Weight per Graft
Mw(EXP)	Experimental Molecular Weight
Mw(THEO)	Theoretical Molecular Weight
Mw(Total)	Molecular Weight Backbone + Grafts
NG	PNIPAAm hydrogels
NG	PNIPAAm homopolymer hydrogels
NH2-PNIPAAm	Aminoterminated poly(N-isopropylacrylamide)
NHS	N-hydroxysuccinimide
NiPA	N-isopropylacrylamide
NIPA	N-isopropylacrylamide
NIPAAm	N-isopropylacrylamide
NIPAAM	N-isopropylacrylamide
NIPAm	N-isopropylacrylamide
NIPAM	N-isopropylacrylamide
NiPMA	N-isopropylmethacrylamide
nM	Taxogen
NMP	N-methylpyrrolidone
NMR	Nuclear magnetic resonance
NnPA	N-n-propylacrylamide
NnPMA	N-n-propylmethacrylamide
NOA	Mercapto ester prepolymer
nOBA	n-oxy benzoic acid

PA6	Polyamide 6
PAA	Poly(acrylic acid)
PAAm	Poly(acrylamide)
PAAM	Poly(Acrylamide)
PAD	Pulsed Amperometric Detection
PAH	Poly(allylamine hydrochloride)
PCL	Polycaprolactone
PDMA	Poly(dimethylacrylamide)
PDMAAM	Poly(N,N-dimethylacrylamide)
PDMS	Polydimethylsiloxane
PEG	Polyethylenglycol
PEGDMA	Poly(ethylene glycol dimethacrylate)
PEGMA	Poly(ethylene glycol methacrylate)
PEI	Polyethyleneimine
PEO5	Aminoterminated O-(2-Aminoethyl)-O'-methyl polyethylene oxide
PEODA	Poly-ethylene oxide diacrylate
PET	Polyethylene terephthalate
PEPO	Poly(ethylene oxide-co-propylene oxide)
pH	Hydrogen Potential
PIPAAm	Poly(N-isopropylacrylamide)
pKa	Potential of the acid dissociation constant
PMMA	Poly(methyl-methacrylate)
PNiPA	Poly(N-isopropylacrylamide)
PNIPAA	Poly(N-isopropylacrylamide)
PNIPAAm	Poly(N-Isopropylacrylamide)
PNIPAAM	Poly(N-isopropylacrylamide)
pNIPAM	Poly(N-isopropylacrylamide)
P(NIPAM-AA)	Poly(N-isopropylacrylamide-co-acrylic acid)
P(NIPAM-AA-BA)	Poly(N-isopropylacrylamide-co-acrylic acid-co-benzophenone acrylate)
P(NIPAM-BA)	Poly(N-isopropylacrylamide-co-benzophenone acrylate)
polyNIPAAm	Poly(N-isopropylacrylamide) or polyNIPAAm (pNIPAM)
poly(PEGMA-co-PEGDMA)	Copolymer poly(poly(ethylene glycol methacrylate)-co-poly(ethylene glycol dimethacrylate))
PS	Polystyrene
PSS	Polymer Standards Service

PVDC	Polyvinylidene chloride
PyCP	1-pyrenyl 2-chloropropionate
RH	Relative humidity
ΔS	Entropy
SAC-MALLS	Symmetry adapted cluster-multiangle laser light scattering
SEM	Scanning Electro Microscopy
SWNT	Single-walled carbon nanotube
Tc	Lower Critical Solution Temperature estimated from the onset of T% vs Temperature graphs in transmittance measurements
Tc1	Average Lower Critical Solution Temperature value obtained from the onset of the endotherm in in Differential Scanning Calorimetry measurements
Tc2	Average Lower Critical Solution Temperature value obtained from the peak temperature of the endotherm in Differential Scanning Calorimetry measurements
T_{CP}	Cloud Point Temperature
TEA	Triethylamine
TEMED	Tetramethylethylenediamine
Tg	Glass transition temperatures
THF	Tetrahydrofuran
Tm	Melting point
Tmax	Maximal Temperature
UV	Ultraviolet
% (v/v)	Volume Percentage
WSC	Water soluble carbodiimide
Wt%	Weight Percentage

1. Motivation and Goals

Actuation in natural systems is produced by different kinds of plants as a reaction to external stimuli. For example, pine cones are natural actuators that react towards changes in environmental humidity by opening when they are dry and closing when they are wet (Dai et al. (2013), Dawson et al. (1997)). The movement capability of this stimulus sensitive actuators can be replicated by developing synthetic actuation structures based on “smart polymers”, which are able to provide a reaction when an external trigger is applied (Dai et al. (2013)). One nature replicating biomimetic approach of natural actuators is the manufacture of bilayer actuators with an active hydrogel layer made from smart polymers and a passive layer that acts as a substrate.

Hydrogels are polymeric networks where polymer chains are distributed in a three dimensional arrangement and interconnected by chemical or physical crosslinking (Haldorai et al. (2014)). They are capable of absorbing and retaining water and the intensity of these properties is related with the amount of hydrophilic units present in the polymer chains. Cellulosic polymers are cellulose derivatives in which cellulose is modified with hydrophilic groups in its backbone, to improve interaction with water. Carboxymethyl cellulose (CMC) is a cellulosic polymer with a cellulose backbone modified with carboxylic groups, making it an economically attractive water absorbing base material. CMC hydrogels have been developed in the past and have been modified with other polymers, however, there are not so frequently used in the development of actuators.

The main goal of this research is the replication of the natural actuation mechanism “cell wall swelling (or shrinking)” (Burgert et al. (2009)) by the manufacture of a novel biomimetic bilayer actuator, based on novel thermosensitive CMC-g-PNIPAAm (carboxymethyl cellulose grafted with poly(N-Isopro-pylacrylamide) oligomers) Comb-type graft hydrogels, with potential medical applications. In order to achieve this goal, the developed procedure is as follows: Aminoterminated PNIPAAm oligomers are synthetized and grafted to CMC, obtaining CMC-g-PNIPAAm graft copolymers, which later are ionically and covalently crosslinked and as result, new CMC-g-PNIPAAm comb-type graft hydrogels are synthetized. In order to obtain passive layers, a first group is prepared from PA6 (polyamide 6) substrates that are functionalized by different chemical treatments. The second group was prepared from highly concentrated CMC-g-PNIPAAm covalently crosslinked comb-type graft hydrogel films. For the generation of active layers, comb-type graft pre-gel solutions are prepared from CMC-g-PNIPAAm graft copolymers. Finally, these pre-gel solutions are casted over the functionalized PA6 substrates, and the highly concentrated CMC-g-PNIPAAm covalently crosslinked comb-type graft

hydrogel films, and new bilayer actuators, based on new CMC-g-PNIPAAm comb-type graft hydrogels are obtained.

2. Theoretical Background

2.1. Biomimetic Actuators

2.1.1. "Smart" Biomimetic Actuation

In nature, one finds different kinds of plants capable of producing movement (actuation). Biomimetics is the copy of natural models, systems and elements with the task of giving a solution to complex engineering problems (Vincent et al. (2006)). Many of these actuation systems could be seen as prototypes from which biomimetic principles are derived (Burgert et al. (2009), Shahinpoor et al. (1995), Taya et al. (2003), Skotheim et al. (2005), Matthews (2006), Fratzl et al. (2008)). Burgert et al. (2009) explained actuation with the following mechanisms: Cell growth, turgor pressure, cohesion forces and cell wall swelling (or shrinking). We will center our attention on the last three mechanisms, since they are triggered by external stimuli producing "smart" actuation.

Turgor pressure. The turgor pressure is defined as "the pressure exerted on a plant cell wall by water passing into the cell by osmosis. It is also called: hydrostatic pressure" (Collins Dictionaries (2014)). An example of actuation explained by the mechanism of turgor pressure can be found in the Venus flytrap (Figure 1).

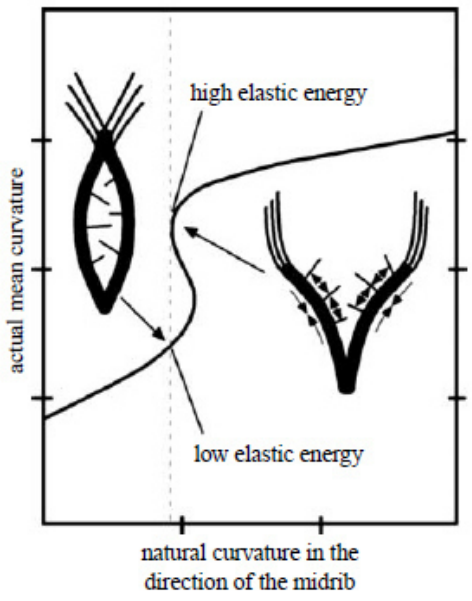

Figure 1. Venus flytrap showing its closed and opened stages (Burgert et al. (2009)). The curve drawn was based from values obtained by Forterre et al. (2005). It shows a metastable path is produced going from a state with high elastic energy (opened stage) to a one with low elastic energy (closed stage) when external stimulation is applied to the plant (Burgert et al. (2009)).

Volkov et al. (2008) applied external stimulation (of mechanical and electrical type) to a Venus flytrap during the opened stage and studied the mechanism followed until the closed stage of the trap was achieved. In order to arrive to this stage, the closure of the trap goes through three specific steps: A step without any visible motion, followed by a fast motion of the lobes and finally the closed stage with a reduction of tension of the lobes.

Cohesion forces. A cohesion force is defined as "the force that holds together the atoms or molecules in a solid or liquid, as distinguished from adhesion" (Collins Dictionaries (2014)). An example of actuation by cohesion forces is represented by how fern spores are distributed with a launch mechanism (Burgert et al. (2009)). According to Burgert et al., spore containers are surrounded (by forming a ring) by specially design cells, known as annular cells. In a cross-section profile of these cells (Figure 2), it is observed that they are u-shaped because of the presence of densely cell walls in three sides of the cell.

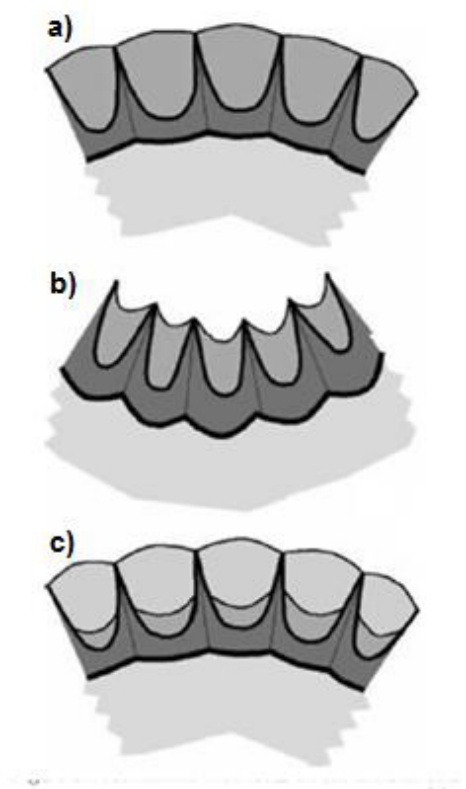

Figure 2. Cross-section at different stages of annular cells which forms a ring around a fern container: a) Anullar cells completely full of water, b) decrease of ring perimeter due to dehydration, and c) return to initial state of the system after the surpassing of water cohesion forces (Burgert et al. (2009), Lüttge et al. (2005)).

During the elimination of water from the cell cavities, the cohesion forces of water attract together the two ends of the cells that have a shape of an "U" (Burgert et al. (2009)). The

consequence is a decreasing of the annulus ring perimeter that surrounds the fern container, producing transversal tensile stresses, which breaks, at a specific position, and the seeds are released. Water cohesion forces are exceeded by the increasing stress of the ring-like cell walls. Finally, this results into returning to the initial position of the annular cells and as a consequence a breaking of the fern container with a subsequent release of the ferns (Haupt et al. (1977)).

Cell wall swelling (or shrinking). Finally, an example of cell wall swelling or shrinking is represented by the release of ripe seeds from pine cones (Figure 3).

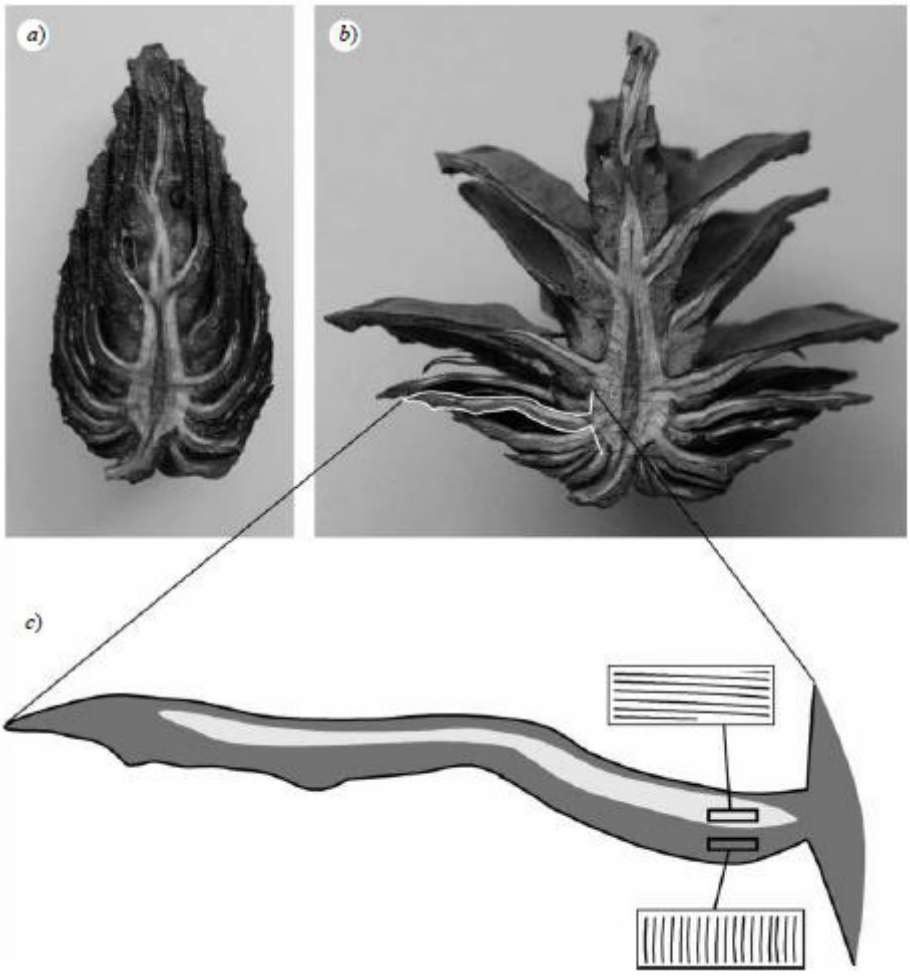

Figure 3. Longitudinal section of a pine cone: a) Wet (closed state) and b) dry (opened state) (Burgert et al. (2009)). c) Sketch of one pine cone scale during the opened state, showing the cellulose fibril orientation inside the cell walls, at the top side of the scale (----------) and at the bottom side of the scale (Burgert et al. (2009), Dawson et al. (1997)).

Fluctuations in the relative humidity of the environment induced movement on the scales of pine cones, these scales are the support of pine cone seeds (Burgert et al. (2009)). When the

pine cone is dry, the scales move to the open stage liberating the seeds (Burgert et al. (2009), Dawson et al. (1997)). When the pine cone is wet, the scales move to the closed stage (Burgert et al. (2009)).

The cellulose fibrils are responsible the flexing mechanism of the scale, which is dependent on the orientation of the fibrils that direct the cells hygroscopic dilatation at the bilayer system of the scale (Figure 3) (Burgert et al. (2009)).

2.1.2. "Smart" Bilayer Actuators

Actuation in plants shows many specifications that can be used in the manufacture of biomimetic actuators (Burgert et al. (2009)). The scale movements in pine cones, based on the actuation mechanism cell wall swelling (or shrinking), are a intrinsic material function and they do not require a vivid metabolism. These "smart" actuating systems are adequate for bioinspiring technical actuating artifacts made of gels, under the format of "smart" bilayer actuators.

Hu et al. (1995) developed a bilayer actuator, consisting of a poly(acrylamide) (PAAM) layer interpenetrated from one side by N-isopropylacrylamide-NIPAAm (NIPA) gel. This smart bilayer actuator is sensitive to temperature fluctuations and to the concentration of e.g. acetone in the environment (Figure 4).

The bilayer actuator (or bigel strip) actuates itself towards an increase of temperature or acetone concentration by folding until almost a circumference (Hu et al. (1995)).

Guan et al. (2005) fabricated a bilayer actuator consisting of one chitosan layer and the other made of the copolymer poly(poly(ethylene glycol methacrylate)-co-poly(ethylene glycol dimethacrylate)) or poly(PEGMA-co-PEGDMA) with different PEGMA:PEGDMA weight proportions. These bilayers were made by using soft-lithographic methods and the obtained structures that are able to fold in water resulting in different 3D shapes (Figure 5).

The bilayer actuator developed by Feinberg et al. (2007), consisted of a layer of polydimethylsiloxane (PDMS) elastomer thin film and a layer of myocardium tissue (cardiac muscle) named muscular thin films (MTF) that was sensitive to electric pulses. The myocardium layer was built from the culturing of neonatal rat cardiac cells (ventricular cardiomyocites) over the film of PDMS previously micropatterned with proteins. The researchers concluded that the performance of the bilayer actuator was dependent to the configuration of the myocardium tissue, the shape of the thin film of PDMS, and the frequency of the electrical pulse applied to the actuator.

Polyethylene oxide diacrylate / N-isopropylacrylamide(NIPAAm)-acetic acid or PEODA / NIPAm-AAc hydrogel bilayers were made by Bassik et al. (2010) by spin coating on a silicon

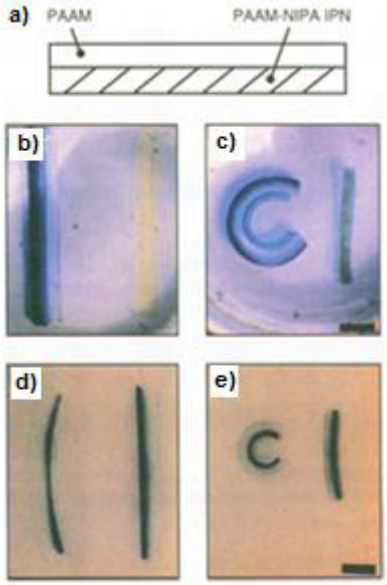

Figure 4. Thermo- and solvent-sensitive folding in a bilayer actuator: a) Drawing of the actuator displaying a PAAM gel (blank area) interpenetrated by one side with a NIPA gel, forming an interpenetrated PAAM-NIPA gel net (hatched area). Images showing the thermosensitive folding of the bilayer actuator at b) 30.0 °C and c) 37.8°C. For an optimum viewing sample was dyed with blue color. Reference sample located at the right side is a pure NIPA gel stripe. Images showing the acetone solvent concentration-sensitive folding of the bilayer actuator in an aqueous environment at d) 20% and e) 45% per weight of total solution mixture. Reference sample located at the right side is a pure PAAM gel stripe. Scale: 5 mm (Hu et al. (1995)).

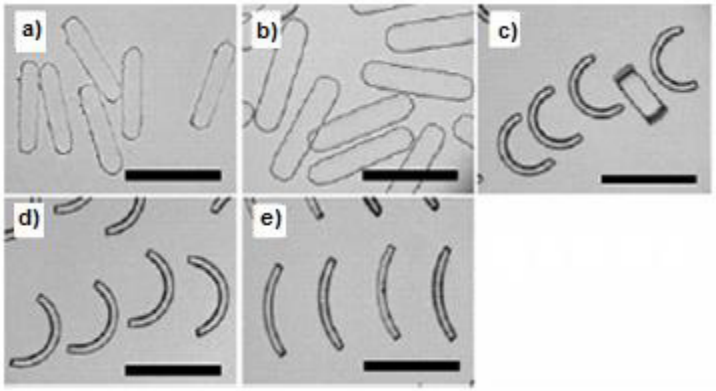

Figure 5. Micro photographs of hydrogel bilayers in water: a) Monolayer made of chitosan; b) monolayer made from the copolymer poly(PEGMA-co-PEGDMA) with 5:1 PEGMA:PEGDMA weight proportion; c), d), e) Bended bilayers of chitosan and copolymer poly(PEGMA-co-PEGDMA) with 5:1, 3:1 and 1:1 PEGMA:PEGDMA weight proportions. Scale: 100 µm. (Guan at al. (2005))

wafer, a PEODA pregel solution for non contact photopatterning, with a later spin coating over this layer of NIPAm-AAc pregel solution again for non-contact photopatterning. These bilayers folded in aqueous solutions at different pH and ionic strength values (Figure 6).

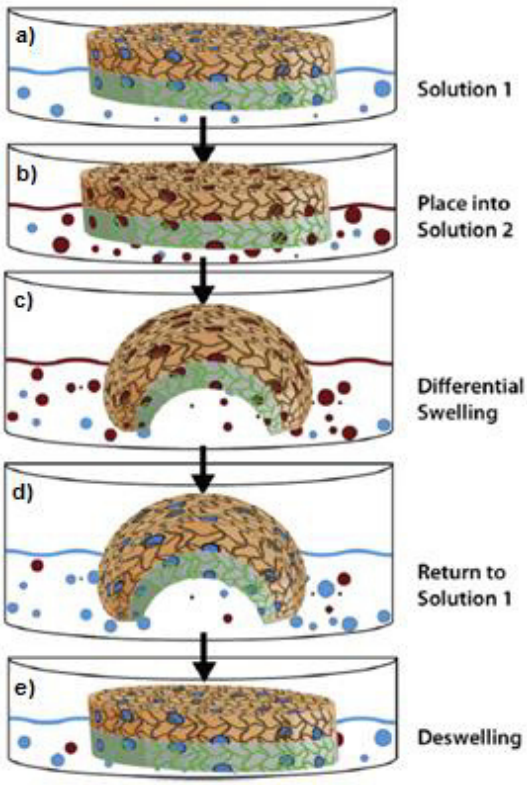

Figure 6. Representation of the actuation process for a PEODA/NIPAm-AAc hydrogel bilayer. a) Bilayer actuator is submerged in an aqueous solution (solution 1) with determined pH and ionic strength values. b) The bilayer actuator is translated to solution 2, which has different pH and ionic strength values. c) A differential swelling occurs as a consequence from changing the solution. d) Bilayer actuator is returned again to solution 1. e) Bilayer actuators deswells as a consequence of changing the pH and ionic strength (Bassik et al. (2010)).

Simpson et al. (2010) developed a thermosensitive bilayer actuator, with one layer made of a polydimethylsiloxane (PDMS) film with a micrometer thickness, and a second layer made of a gold (Au) film with a thickness in the order of nanometers. They demonstrate that it remained unfolded showing a flat configuration (2D geometry) when the bilayer was heated. However once the bilayer was cooled down, it started to fold (Figure 7). They also showed that this behavior was reversible. This folding was explained because during the cooling the PDMS layer tends to reduce their dimension faster than the Au layer and a compression stress is developed on the PDMS layer.

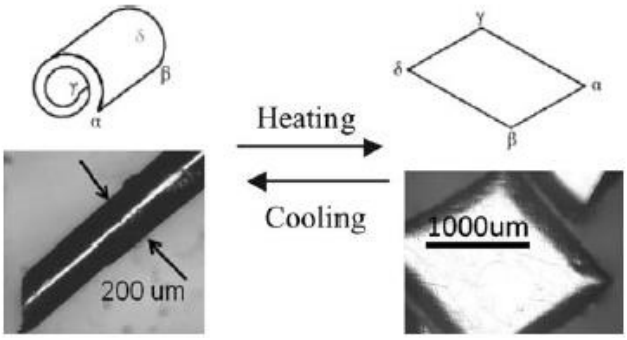

Figure 7. Thermosensitive and reversible folding of a PDMS/Au bilayer (Simpson et al. (2010)).

A humidity sensitive bilayer actuator based on poly(acrylic acid) (PAA) and poly(allylamine hydrochloride) (PAH) was developed by Ma et al. (2011). It comprised a layer of 30 PAA/PAH bilayers ((PAA/PAH)*30) fabricated by the layer-by-layer technique and crosslinked with temperature, while the other layer was mercapto ester prepolymer crosslinked by UV.

Dai et al. (2013) generated a humidity sensitive bilayer actuator provided with a layer of oriented polyamide 6 (PA6) substrate layer which was a liquid crystalline (LC) polymer, composed of the monomer n-oxy benzoic acid (nOBA) covalently crosslinked by the mesogen 1, 4-di-(4-(6-acryloyloxyhexyloxy)benzoyloxy)-2-methylbenzene (C6M), and photocrosslinked by the pho-toinitiator Irgacure 819. LC phase forms a net because of the presence of hydrogen bridges. In order to activate the bilayer actuator this must be submerged in a solution with basic pH, in order to break the hydrogen bonds of the net, then the bilayer at high humidity values maintained straight, while at low values tended to bend.

The pH and ionic strength sensitive bilayer actuator developed by Haldorai et al. (2014), was composed of a layer made of a PA6 film substrate and another one of hydrogel made from the copolymer PAA-co-PAAm (poly(acrylic acid)-co-poly(acrylamide)) grafted onto carboxymethyl cellulose (CMC). The reversible actuation was evaluated by submerging the bilayer in water (for expansion of the hydrogel layer) and in ethanol (for subsequent contraction).

2.1.3. Thermosensitive bilayer and multilayer actuators

LeMieux et al. (2006) developed a two-material cantilever based on a thermosensitive multilayer actuator (Figure 8) that consisted of a passive layer of rigid polysilicone (normally used as probes in AFM microscopy) and multiple active layers of polystyrene (PS), with a thickness between 20 to 200 nm that were deposited on the passive layer by using the method plasma-enhanced chemical vapor deposition.

The thermal behavior of the PS nanolayers provide a fast reaction towards external temperature variations.

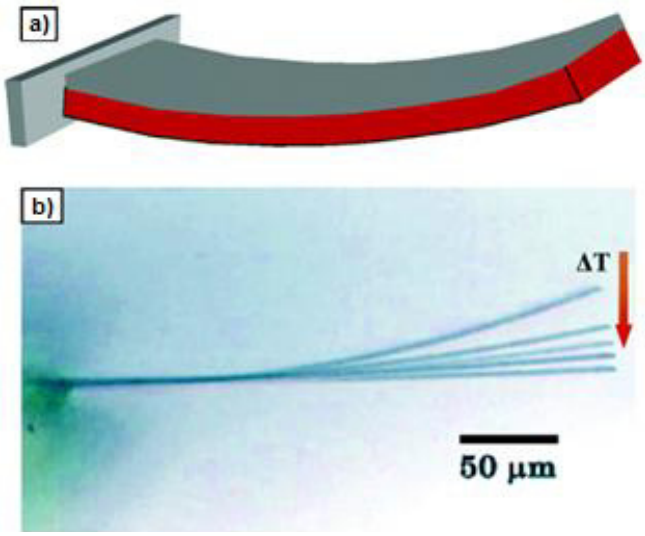

Figure 8. a) Graphical representation of the two-material cantilever during its flexing due to increment of temperature. b) Optical picture of the multilayer actuator flexing when temperature rises from 20 to 40 °C (LeMieux et al. (2006)).

The combination of these two materials in a multilayer actuator, resulted in the generation of stresses originated from temperature variations, producing a bending effect with thermal sensitivities higher than the ones produced by conventional metal-ceramic designs (Figure 9) (LeMieux et al. (2006)).

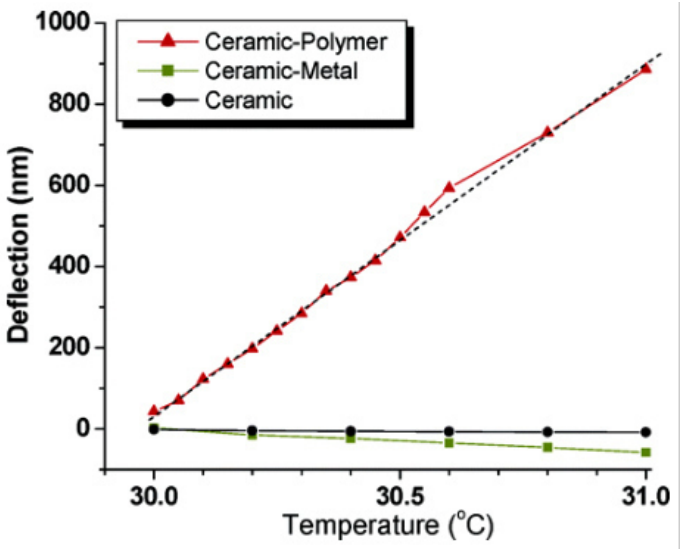

Figure 9. Comparison between the thermosensitive deflections of cantilevers made of silicon/PS, silicon/metal and only silicon during the heating interval (LeMieux et al. (2006)).

Zhang et al. (2011) manufactured a thermosensitive actuator by developing a bilayer with a passive layer of low density polyethylene (LDPE) and an active layer, which was a composite material composed of a poly(N-isopropylacrylamide) or polyNIPAAm (pNIPAM) hydrogel matrix, reinforced with single-walled carbon nanotube (SWNT) fillers (Figure 10). They managed to increase five times the thermic reaction of these bilayer actuators, when the single-walled carbon nanotube concentration was of 0.75 mg/mL. This means that the time required for a thermosensitive reaction could be tuned by the amount of filler loaded. The developed actuators also showed an optically sensitive responsiveness.

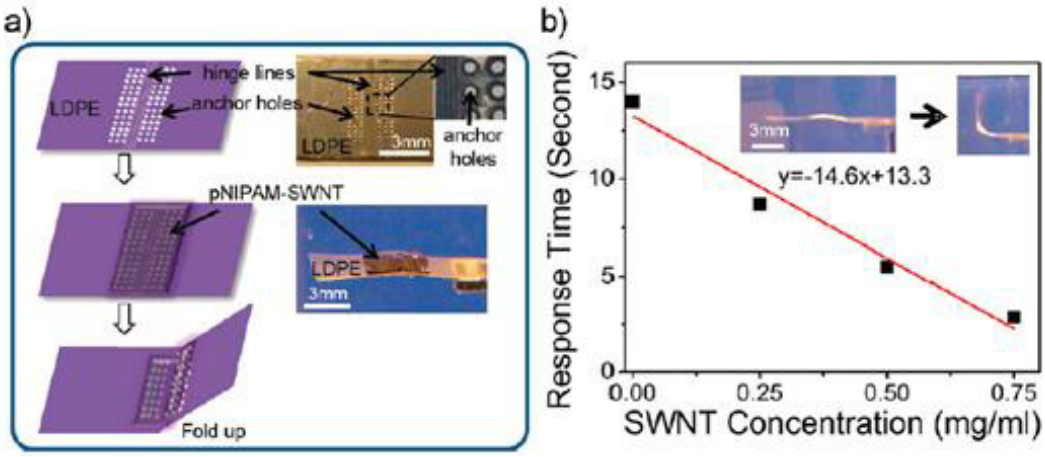

Figure 10. a) Manufacture process for elaboration of SWNT-pNIPAM/LDPE bilayer actuators, including amplification of certain portion with optical photos. b) Response time for reaching a 90° bending versus SWNT concentration with photo images of the bilayer actuator at the left before and at the right after flexing (Zhang et al. (2011))

Stoychev et al. (2012) performed a study on the influence of the aspect ratio and relative thickness of active layers on the folding of thermosensitive hydrogel bilayers. For that purpose with a photolithographic technique, they developed bilayers with a passive hydrophobic layer made of either polycaprolactone (PCL), or a random-type copolymer poly(methyl-methacrylate-co-benzophenone acrylate) (P(MMABA)); and an active thermosensitive layer made of either poly(N-isopropylacrylamide-co-acrylic acid-co-benzophenone acrylate) (P(NIPAM-AA-BA)), or poly(N-isopropylacrylamide-co-benzophenone acrylate) (P(NIPAM-BA)), both photocrosslin-ked. They established that the hydrophobic passive layer limited the shrinking and swelling of the active layer, and therefore as a consequence folding and unfolding occurred with different configurations (Figure 11).

Stoychev et al. (2013) also developed thermoresponsive bilayer actuators of photocrosslinked layers, with a passive of hydrophobic poly(methylmethycrylate) (PMMA) and active layer of a thermosensitive random-type copolymer of poly(N-isopropylacrylamide-co-acrylic acid)

(P(NIPAM-AA)). It was found that the bilayer actuator unfolded at 70 °C, but at a temperature T>70°, the folding of the bilayer occurred (Figure 12). They managed to determine empirical rules that would allow to control the type of folding of a bilayer. Their hypothesis were demonstrated in the design of a 3D pyramid (Figure 12).

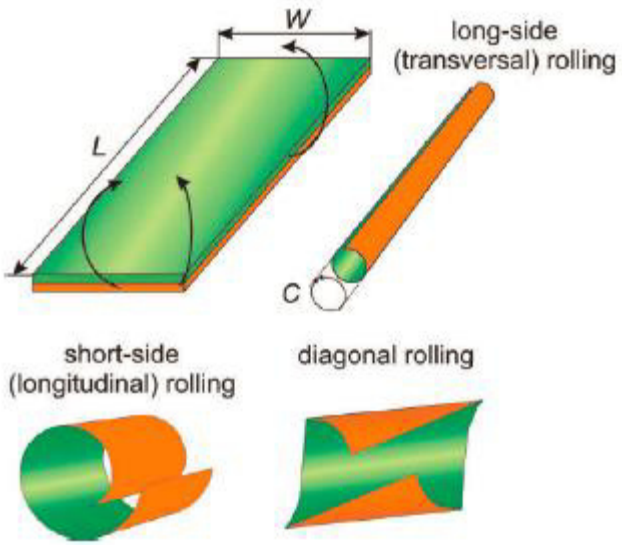

Figure 11. Different possibilities of folding for a bilayer actuator: short-side, long-side and diagonal (Stoychev et al. (2012)).

Yamamoto et al. (2015) studied the thermal response actuation in air by developing a bilayer actuator consisting of a passive layer made of polyethylene terephthalate (PET), patterned as line trenches of 80 μmx13 mm dimensions and with holes of circa 150 μm diameter. The holes were made on the passive layer with a laser tool and in order to assure the adhesion of the active layer made of a polyNIPAAm (pNIPAM) in water. The active layers were divided in two groups: One loaded with carbon nanotubes (CNTs) and the other one without CNTs. The bilayer actuator was tested with a packaging technique, where the bilayer actuator was packed in a polyvinylidene chloride (PVDC) film. The packaging technique allowed the study of thermal responsive actuation in air (Figure 13).

Stroganov et al. (2015) investigated the reversible thermosensitive actuation and its potential use in cell encapsulation of bilayers, with a passive layer made of gelatine films and an active layer made of polycaprolactone (PCL). The passive layer of gelatine caused the bending of the bilayer because of its swelling in water. The thermosensitive actuation occurred above the melting point of PCL (55-60 °C) with a folding of the bilayer actuator and an unfolding during the cooling cycle until room temperature. The authors stated that the reversible actuation was related with the alignment of the PCL chains during the melting and crystallization stages.

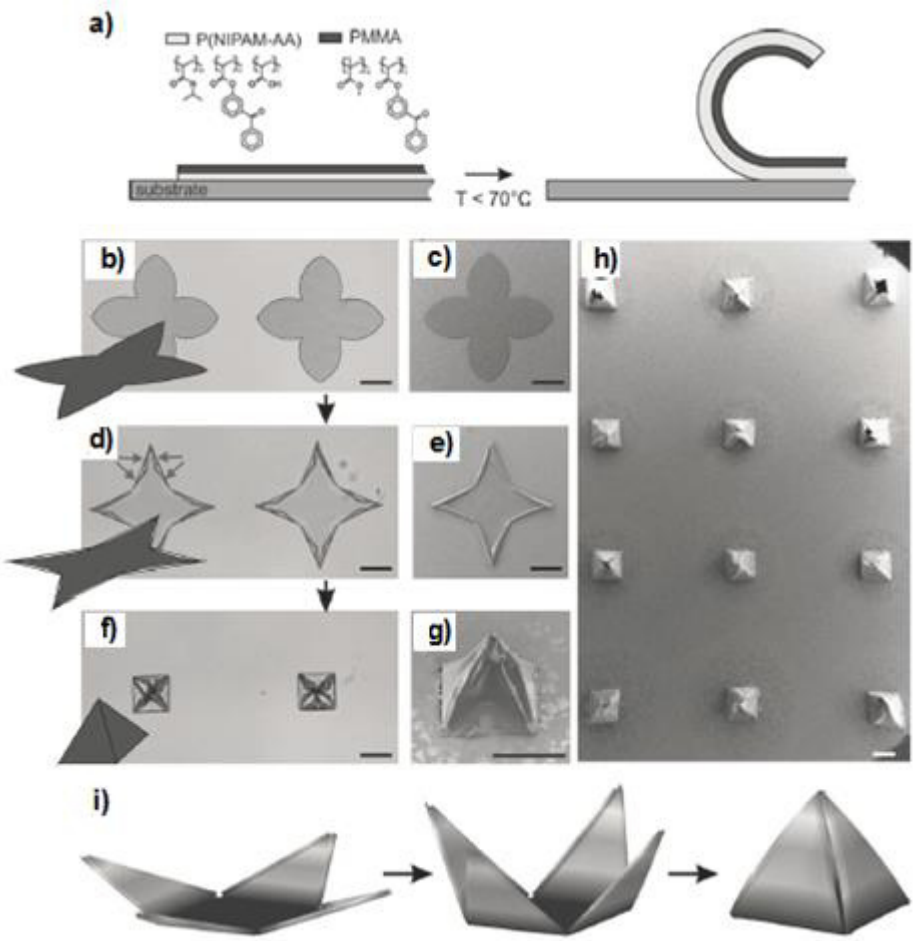

Figure 12. Folding of a bilayer actuator: a) Graphic representation of the thermosensitive bending of a PMMA/P(NIPAM-AA) bilayer actuator (Stoychev et al. (2013)). Step by step actuation until pyramids of four shaft star bilayer actuators: b), c) Unactivated bilayer actuator. d), e) Shriveling of peripherical shaft region into pipes, during first part of bending (indicated by arrows). f) – h) Bending of shafts directing to pyramids formation. Scale bar = 200 µm each. i) Simulation of the bending of a four shaft star (Stoychev et al. (2013)).

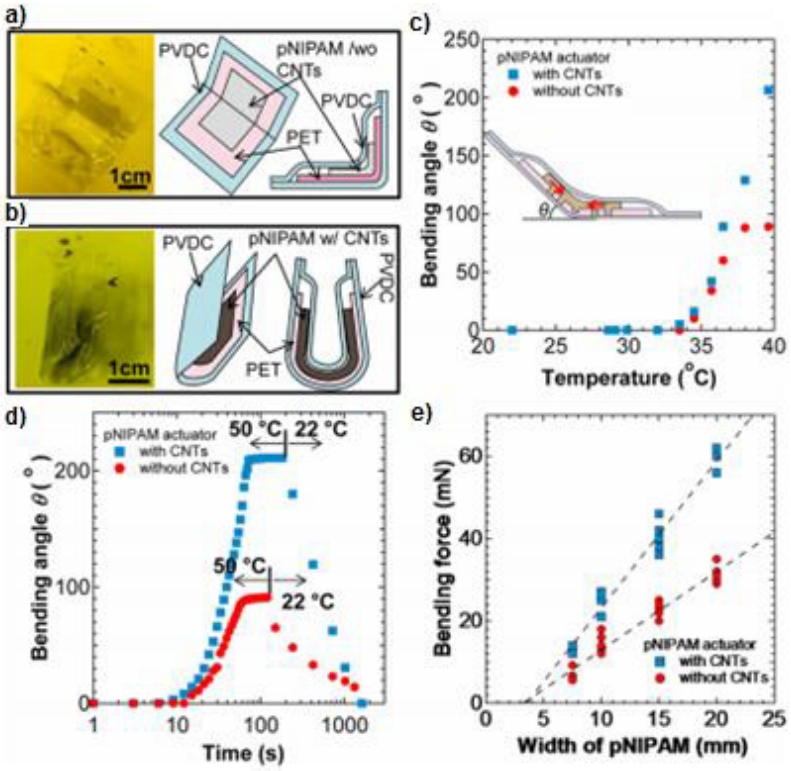

Figure 13. PolyNIPAAM/PET thermosensitive bilayer actuator. a) Figures and photographs of the bilayer actuator (with CNTs) over a heating plate at 50°C. b) Bilayer actuator at 50°C without CNTs. c) Bilayer actuator bending angle versus heating plate temperature. d) Reaction times of bilayer actuator at 50 and 22 °C. e) Bending force versus Width of pNIPAAM layer in bilayer actuators with and without CNTs (Yamamoto et al. (2015)).

2.2. Synthesis of Bilayer Actuators based on CMC-g-PNIPAAm comb-type graft hydrogel films

2.2.1. Synthesis of Aminoterminated PNIPAAm oligomers

2.2.1.1. Poly(N-isopropylacrylamide) – PNIPAAm

a) N-isopropylacrylamide monomer

The monomer N-isopropylacrylamide (NIPAAm) belongs to the group of acrylamides and can be synthesized by the Ritter reaction between acrylnitrile and isopropyl alcohol (Figure 14-a)) (Kirk-Othmer (1991)). Acrylamides are interesting bifunctional monomers, that contain a double bond (electron deficient) and an amide group (Kirk-Othmer (1991)). Because of its double bonds, these monomers can be polymerized in simple polymeric chains or gels of poly(N-isopropylacrylamide) (Figure 14-b)) (PNIPAAm).

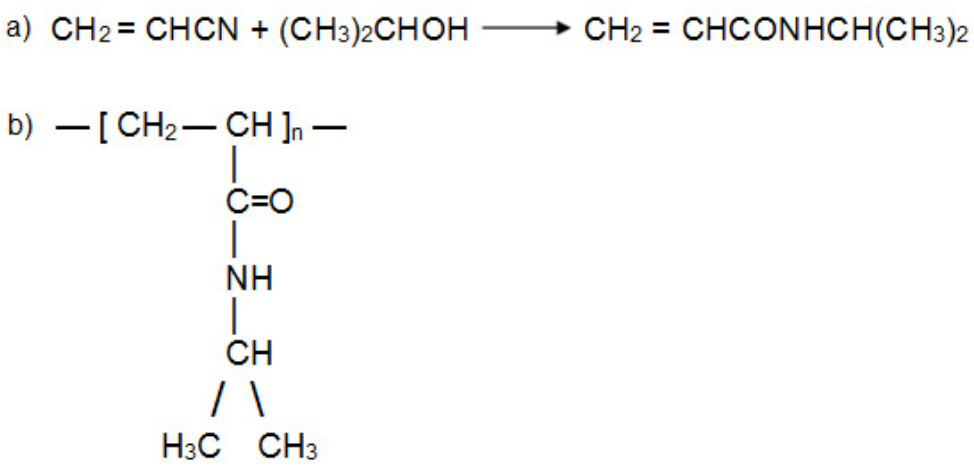

Figure 14. a) Synthesis of N-isopropylacrylamide (Kirk-Othmer (1991)) b) Molecular structure of PNIPAAm (Schild et al. (1992)).

The main reason for using PNIPAAm in different applications has been its thermal behaviour in aqueous media (Schild et al. (1992)). It is maybe because of this reason, that PNIPAAm became very popular between a group of polymers that show an inverse solubility during heating. This uncommon property consists in the dissolution of the polymer in water when the solution is cooled down and the phase separation of the polymer from the solution, when this is heated over a characteristic temperature known as lower critical solution temperature (LCST). It was experimentally found, that for PNIPAAm this temperature ranges between 30 to 35 °C and is a function of the macromolecule microstructure. PNIPAAm can be found with different molecular structures, as linear chains, macroscopic gels, microgels, latex, thin films, membranes, coatings and fibres (Schild et al. (1992)).

b) Synthesis methods for PNIPAAm polymers

PNIPAAm can be synthesized by using a variety of methods, the most frequently used are: Free radical initiation in organic solutions (Table 1) and redox initiation in aqueous media (Table 2) (Schild et al. (1992)). There has been also reports on using ionic initiators and radiation in some way in the construction of PNIPAAm systems (Schild et al. (1992)). Some markers and functional groups have been introduced by comonomer substitution. When the comonomer is bifunctional, a gel can be obtained by subsequent crosslinking. These gels can be of macroscopic type or microgels (latex).

c) Thermo- and pH-sensitive properties of PNIPAAm solutions

PNIPAAm goes through an abrupt spiral-globule transition at a temperature of 32 °C (LCST), changing from a hydrophilic state below this temperature to an hydrophobic state above this temperature (Dimitrov et al. (2007)).

The ordering of solutes like PNIPAAm in aqueous solutions results from specific orientations with hydrogen bond bridges with the previously ordered water molecules (Dimitrov et al. (2007)). Water molecules reorient through the non-polar regions of the PNIPAAm solutes, diminishing the probability of hydrogen bonding with them. This results in the so called clathrate structures. The phenomenum known as hydrophobic effect, gives as a consequence a decreased entropy during the mixing (entropy difference ΔS negative).

Table 1
Free radical initiators and organic solvents for PNIPAAm synthesis (Schild et al. (1992))

Organic Solvent	Initiator
Methanol	AIBN
Benzene	AIBN
Benzene/Acetone	AIBN
THF	AIBN
Benzene/THF	AIBN
t-Butanol	AIBN
Dioxane	AIBN
Benzene	Benzoyl peroxide
Chloroform	Lauryl peroxide

Table 2
Redox initiators (and their accelerators) used in aqueous media for PNIPAAm synthesis (Schild et al. (1992))

Initiator	Acelerator
APS	Sodium metabisulfite
APS	Tetramethylethylenediamine
KPS	Sodium metabisulfite
KPS	Tetramethylethylenediamine

At higher temperatures the entropic term dominates over the exothermic enthalpy of the already formed hydrogen bridge bonds between the water molecules and the polymer polar groups, which are the driving forces of the dissolution (Dimitrov et al. (2007)). Once the free energy variation (ΔG) adopts a positive value during the mixing, the consequence is a phase separation at the LCST of PNIPAAm. If the polymer concentration is high enough then the replacement of contact points polymer-water by polymer-polymer and water-water is visible by

the presence of precipitation. The temperature – induced phase transition of PNIPAAm is shown in Figure 15 (Dimitrov et al. (2007)).

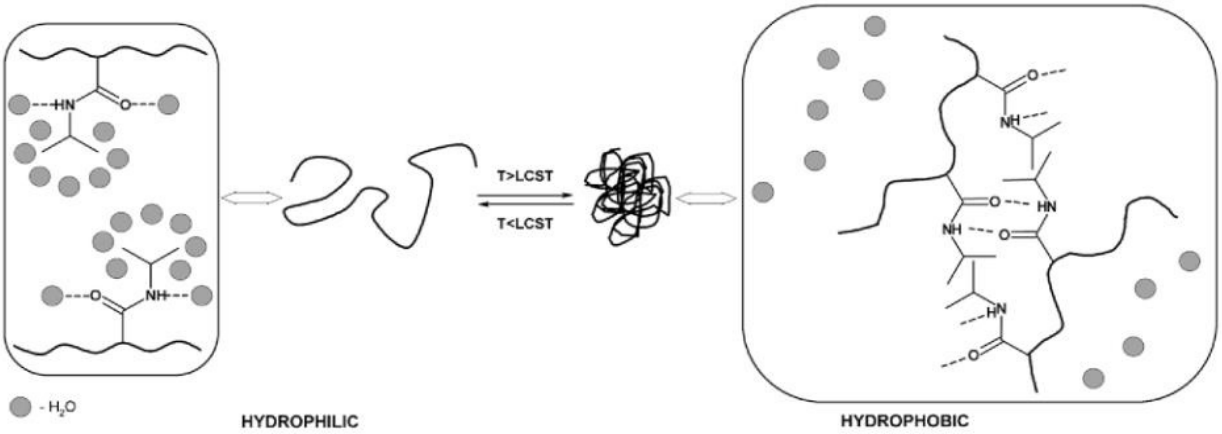

Figure 15. Temperature – induced phase transition of poly(N-isopropylacrylamide) (Dimitrov et al. (2007)).

Under this critical temperature, a spiral structure is favored allowing a maximal interaction between the polymer and water molecules (Dimitrov et al. (2007)). In systems where it is possible to form hydrogen bridge bonds, this interactions decrease the Free Gibbs dissolution energy considerably.

At the LCST, it seems that the individual polymer chains collapse before aggregation and this can be more probable in more diluted solutions (Dimitrov et al. (2007)). At higher temperature the hydrogen bridge bonds turn weak, the system tends to minimize the contact between water molecules and hydrophobic surfaces, then the transition from a spiral to a globular structure occurs.

The T_{CP} (cloud point temperature) or LCST from PNIPAAm aqueous solutions can be modified by adding to the polymer chain, small amounts of hydrophilic and hydrophobic comonomers (Dimitrov et al. (2007)). Additionally, the presence of ionizable units is the base of pH sensitivity in polymers, because these induce the neutralization of opposite charges.

NIPAAm monomer has been copolymerized with different other monomers, in order to change and tune the phase transition temperatura of copolymer aqueous solutions (Dimitrov et al. (2007)). The use of comonomers with ionizable groups such as carboxylic acids and tertiary amines, shows an advantage over other comonomers, since their hydrophilicity/hydrophobicity can be modified from changes on the solution pH resulting in tunable LCST values.

When hydrophilic monomers are copolymerized with NIPAAm, the LCST of the resulting polymer is shifted to higher temperatures, while the copolymerization with hydrophobic

monomers, will result in more hydrophobic polymers and the LCST will occur at lower temperatures (Dimitrov et al. (2007)).

Moreover, NIPAAm copolymerization with monomers that contain ionizable groups is an interesting approach, since they give the opportunity to adjust the thermosensitivity to values near the corporal temperature (Dimitrov et al. (2007)). Acrylic acid is the more commonly monomer used for this purpose, but it limits the thermosensitivity to specific pH values, because at high pH values, the carboxylic groups are ionized (until carboxylate groups) and the polymer becomes more hydrophilic, then its thermosensitivity decreases.

This can be attributed to the combined characteristic of the ionic monomer residues of breaking the PNIPAAm chain sequences in smaller and non-cooperative segments (Dimitrov et al. (2007)). The excess of hydration and electrostatic repulsion set by ionized monomers like for example acrylic acid, will debilitate the thermically driven hydrophobic assembly of the collapsed PNIPAAm chains. Then, the amount of comonomer cannot be so much incremented, since the LCST value could disappear because the copolymer becomes soluble in water at every temperature.

Variations in the LCST temperature produced by the random inclusion of comonomers, are due to changes in the total hydrophilicity of the polymer (Dimitrov et al. (2007)). The hydrophilicity and the charged comonomers, increase the LCST because the hydrophilicity of the polymer is increased, since they do not affect directly the interaction of water molecules with the hydrophobic groups.

Another issue that needs to be comprehensively understood is the effect of the hydrogen bridge bonds with respect to PNIPAAm copolymers behavior. It is obvious that these bonds perform an important part in the case of acid comonomers (Dimitrov et al. (2007)).

In the case of NIPAAm – acrylic acid copolymer, the carboxylic acid pendant groups can form hydrogen bridge bonds with the amide pendant groups of the PNIPAAm portion (Figure 16) (Dimitrov et al. (2007)).

This will yield to additional polymer-polymer interactions, producing a phase separation during a heating cycle that is less endothermic in comparison with pure PNIPAAm, since less sites will be available for the bonding between water molecules and NIPAAm units (Dimitrov et al. (2007)). The hydrogen bridge bonds are related to the pH tuning of LCST temperature. In general, if a strong base is added to a PNIPAAm/acrylic acid solution, the protons of the carboxylic acid groups will be bonded with the protons of the strong base, then the formed carboxylate groups will not be able to form hydrogen bridge bonds with the pendant amide groups of the NIPAAm units. Also the polymer-polymer interactions will be weak because of

electrostatic charge repulsion, and as a result the LCST temperature will be shifted to higher temperatures.

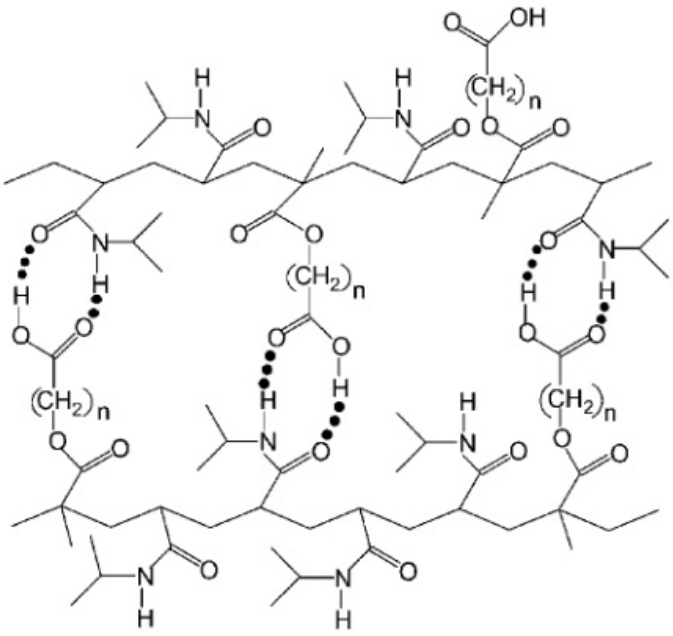

Figure 16. Hydrogen bridge bond interactions proposed for aleatory NIPAAm – carboxylic acid copolymers (Dimitrov et al. (2007)).

However, this occur only if all of the carboxylic groups are simultaneously ionized, and this will might proceed according the acidity constant (Dimitrov et al. (2007)). With only a partial ionization, the electrostatic charge repulsion between ionizable units will be diminished by the attractive forces exerted from the hydrogen bridge bonds that belong to the not ionized units. At the first pH stage (at low pH) when the majority of carboxylic groups are not ionized, the LCST temperature will experience a decrease with an increment in the number of acid units. In a second stage (at high pH) when the majority of carboxylic units are ionized, the LCST temperature will be increased, also with an increment in the number of acid units.

d) Methods for estimating the LCST

- Cloud point or turbidimetric method

Heskins and Guillet managed to estimate the LCST temperature, by the visual observation of a macroscopic phase separation during a heating cycle (Schild et al. (1992)). This method is known as cloud point method. Other researchers have quantified this method by using UV-visible standard spectrophotometers.

- Differential scanning calorimetry (DSC).

Henskins and Guillet were the first on reporting the presence of an endotherm at the LCST temperature during the heating cycle of PNIPAAm aqueous solutions (Schild et al. (1992)). Other researchers have reported that height, width and position of the LCST endotherm peak were found to be independent of the PNIPAAm concentration, at least for the range between 0.4-4.0 mg/L. It is interesting to point out, that polymers with different molecular weight distribution presented endotherms with different shape and height, even when the same enthalpy (6.3 KJ/mol) was observed, which is typical for hydrogen bridge bonds.

- Light scattering.

Information about the size, shape and macromolecule interactions can be obtain by using a light scattering (Schild et al. (1992)). This methods offers more structural information than the turbidimetric method. Recent measurements were performed by using either static as dynamic light scattering in diluted solutions in an attempt to detect the coil-globule transition.

In this case, intermolecular polymer-polymer bonds who replace the polymer-water, interactions are replaced by intramolecular polymer-polymer bonds. This is because neighbouring polymer chains are so distant, one from the other (Schild et al. (1992)). In theory, it would be possible to obtain a rigid sphere ($R \sim N^{1/3}$).

- Viscosimetry

The first studies about viscosimetry in PNIPAAm aqueous solutions were performed in 1968 by Heskins and Guillet (Schild et al. (1992)). They observed that the intrinsic viscosity was decreasing while the temperature was increasing, even when the volumetric molecular weight was high. The estimations were made with precipitation experiments, and the aim was to conclude that under the LCST temperature, the polymer was more like a flexible coil than a rod.

This work has been criticized, because their samples had a wide molecular weight distribution with a polydispersity of 3.4 (Schild et al. (1992)). A higher understanding of the polymer structure could be obtained from the Mark-Houwink-Sakurada equation:

$$[\eta] = KM_v^a$$

This equation is a useful tool for the determination of the molecules shape in solution (Schild et al. (1992)). For higher values of “a” (> 1.0) the polymer have the shape of a rod.

2.2.1.2. Functionalization of Polymers (amino end groups)

a) Telechelic Polymers

The word 'telechelic' is derived from the greek words: *Tele,* which means 'remote' (Arens (1968)) and *chele* means 'claw', 'nipper' (Lo Verso et al. (2008)). Telechelic polymers are macromolecules that were modified at their ends by functionalization with terminal end groups, which are reactive and capable of binding with other molecules, through forming inter- or intra molecular bonds. In the majority of cases, these macromolecules are functionalized at both of their ends, however the term telechelic is also applied to polymers which have have a part of the chain with terminal end groups (Figure 17).

Telechelic polymers can be synthetized by a variety of polymerization techniques, for example: ionic polymerization, conventional radical polymerization, polycondensation and controlled radical polymerization (CRP) (or telomerization) (Lo Verso et al. (2008)).

But why is it necessary to functionalize polymers or synthesize telechelic polymers? The end functionalization of macromolecules is necessary in order to allow them to be bound to other polymers, giving as a result the building of macromolecules with more complex structures, such as block and graft copolymers, star and dendrimer polymers, etc. (Figure 17) (Lo Verso et al. (2008)). The attachment of different polymers to a telechelic macromolecule results in a polymer with new physical properties that can be stimuli-sensitive and this sensitivity can be regulated by external trigger parameters, like for example temperature, pH or solution salinity. Besides that, the rheological properties of the final polymer can be modified, in comparison to the original telechelic macromolecule.

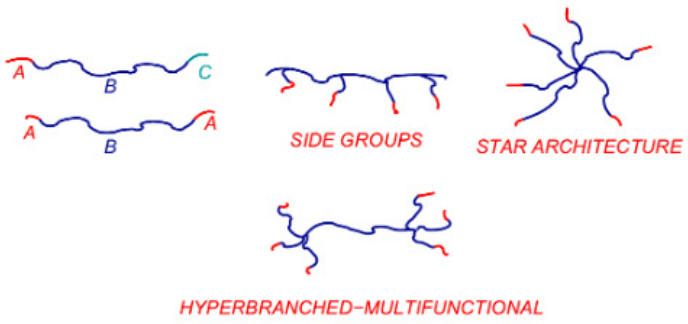

Figure 17. Types of telechelic polymers: Top-left, diblock and triblock copolymers; top-center, graft copolymer with telechelic graft groups; top-right, a telechelic star polymer and down-center, a telechelic dendritic polymer (Lo Verso et al. (2008)).

b) PNIPAAm telechelic and semitelechelic polymers

Yoshida et al. (1995) prepared semitelechelic PNIPAAm (PIPAAm) polymers by functionalizing one end of the macromolecules with amino end groups. The reaction used was the

telomerisation (controlled radical polymerization) of the NIPAAm (IPAAm) monomers in DMF by using the telogen 2-aminoethanethiol (AET or AESH) and the initiator azobisisobutyronitrile (AIBN). The resulting semitelechelic polymers were then grafted to a covalently crosslinked PNIPAAm network, giving as a result a comb type graft hydrogel with improved deswelling properties in comparison with the conventional PNIPAAm covalently crosslinked hydrogels.

PNIPAAm semitelechelic polymers functionalized with amino end groups were also prepared by Durand et al. (1999) by the telomerization in water of NIPAAm monomers at 29 °C and under inert atmosphere. Aminoethanethiol hydrochloride (AET,HCl) was used as telogen and potassium persulfate (KPS) was used as an initiator.

Bokias et al. (2001) obtained also PNIPAAm semitelechelic polymers functionalized with amino end groups, by performing the same reaction used by Durand et al. (1999), but they used ammonium persulfate (APS) as an initiator instead of KPS.

Smithenry et al. (2001) prepared PNIPAAm (PNIPAAM) telechelic polymers by functionalizing both of their ends with carboxylic end groups. They accomplished this synthesis by conventional radical polymerization of the NIPAAm monomer in acetonitrile at 82 °C, under inert atmosphere and with reaction times between one and four hours. The carboxylic functional group was provided by the initiator 4,4′-Azobis(4-cyanovaleric acid) (ACVA) and the reaction was performed in DMF (Figure 18). They managed to regulate the size of the telechelic polymers by varying the ratio monomer:initiator. However, samples with M_n (Number average molecular weight) values between 8.3-12.2 KDa presented polymer aggregates that were impossible to deaggregate.

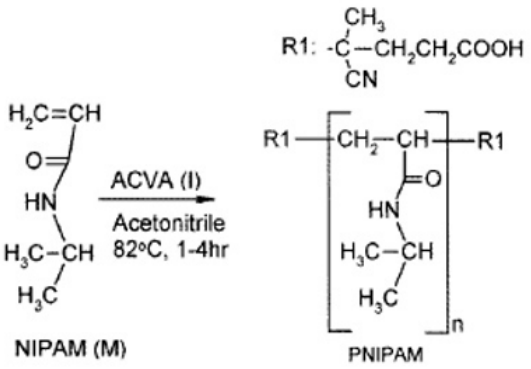

Figure 18. Synthesis reaction used for telechelic PNIPAM (Smithenry et al. (2001))

Masci et al. (2004) functionalized PNIPAAm polymers with bipyridine (bpy) end groups. The chosen reaction method was ATRP in water-based mixtures, because of the already proven good ligand performance of bpy in this type of reaction solvent systems. The solvent system

used was DMF:water with a ratio of 50:50 (volume based) at 20 °C for three hours, with the initiator ethyl 2-chloropropionate (ECP) and the catalytic system CuCl/bpy. The resulting conversion was low (13%) and it was not possible to control either the molecular weight or the polydispersity of the obtained PNIPAAm polymers.

ATRP was also used by Bontempo et al. (2005) in the polymerization of the NIPAAm monomer, giving as a result low polydispersity PNIPAAm telechelic polymers with a biotin end group. The polymerization was performed in deuterated DMSO at 20 °C with a biotinylated initiator, and CuCl:$CuCl_2$:tris(2-dimethylaminoethyl) amine (Me_6TREN) was used as a catalytic system. The biotinylated initiator was obtained from a 8 hour reaction in DMF between biotin with N,N'-disuccinimidyl carbonate (DSC) in triethylamine (TEA). After the completion of this reaction, the product was reacted with 2-(2-aminoethoxy)ethanol obtaining biotinylated alcohol, which after a recrystallization undergo a esterification reaction with 2-chloropropionic acid in a reaction mixture of 1,3-dicyclohexylcarbodiimide (DCC) and 4-(dimethylamino) pyridine (DMAP). The PNIPAAm telechelic polymers developed in this research were bound with the protein streptavidin.

PNIPAAm telechelic polymers functionalized with pyrenyl end groups were synthesized by Duan et al. (2006) with ATRP in DMF/water at 20°C. 1-pyrenyl 2-chloropropionate (PyCP) was used as initiator and the catalytic system was CuCl/tris[2-(dimethylamino)ethyl]-amine (Me_6TREN) (Figure 19). The telechelic PNIPAAm polymer presented a low LCST of 21.7 °C in aqueous solution, in comparison with the LCST of 32 °C attributed to the non-functionalized PNIPAAm polymer. The author explained that this lowering of the LCST was due to the formation of aggregates, and this aggregation was diminished by adding β-cyclodextrin to the aqueous solution, increasing the LSCT value of the PNIPAAm telechelic polymer to about 26 °C. It was also concluded the role of PyCP in the synthesis of PNIPAAm telechelic polymers with tunable LCST.

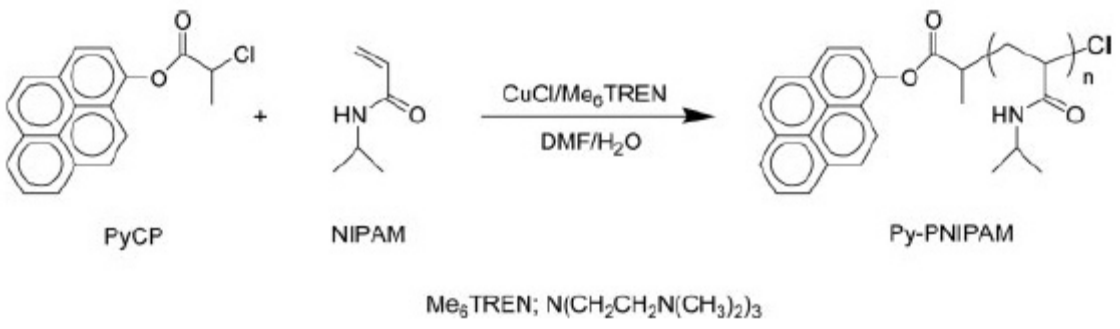

Figure 19. Synthesis of telechelic PNIPAAm polymers functionalized with pyrenyl end groups (Duan et al. (2006)).

Fischer et al. (2006) prepared a PNIPAAm telechelic polymer with carboxylic end groups in a microwave oven, by telomerization of NIPAAm monomers with the telogen 3-mercaptopropionic acid ($HOOC(CH_2)_2SH$) and the initiator AIBN. The reaction mixture received a radiation of 350 W and the reaction time was of 150 seconds (Figure 20). Once the reaction is completed, the polymer is dissolved in acetone and then precipitated with hexane. The polymer obtained had a low polydispersity and therefore a narrow distribution of the molar mass.

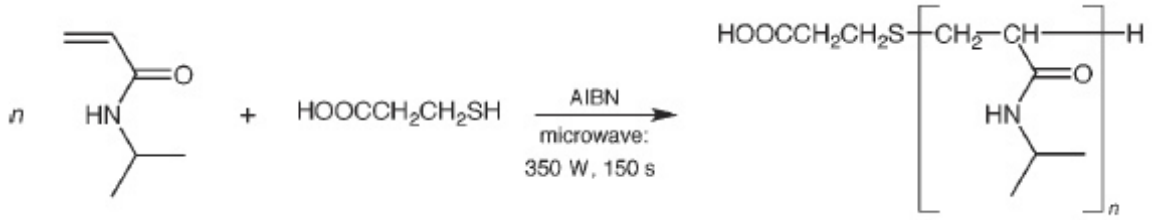

Figure 20. Telomerization of PNIPAAm at a microwave oven and by using AIBN initiator and 3-mercaptopropionic acid chain-transfer agent (Fischer et al. (2006)).

Kujawa et al. (2006) polymerized NIPAAm monomers with RAFT polymerization, and obtained as a result hydrophobically modified PNIPAAm telechelic polymers with n-octadecyl end groups. The reaction was performed in dioxane, and the chain transfer agent used was *S*-1-*n*-octadecyl-*S*‘-(α,α‘-dimethyl-α‘‘-*N*-*n*-octadecylacetamide) trithiocarbonate. The polydispersity obtained was low (circa 1.20). It was also observed that due the hydrophobic end groups bound to the telechelic polymers, the cloud point was diminished significantly while the concentration of these polymers was increased. The author stated that this happened, because of the aggregation of n-octadecal end groups and the hydrated PNIPAAm polymer chains.

Hydrophobically modified PNIPAAm telechelic polymers were also prepared by Liu et al. (2006), by polymerizing NIPAAm monomers with RAFT polymerization in dioxane, at 65 °C and under inert atmosphere. The initiator used was AIBN and the chain transfer agent used was a trithiocarbonate. They obtained the semitelechelic C_{18}-$PNIPAMC_3$ and the telechelic C_{18}-PNIPAM-C_{18} polymers by using the chain transfer agents N-isopropyl-2-n-octadecylsulfanyl-thiocarbonylsulfanyl-2-methylpropionamide for first one, and N-n-octadecyl-2-n-octadecylsulfanyl-thiocarbonylsulfanyl-2-methylpropionamide for the se-cond one.

Ritter et al. (2012) obtained pNIPAAm with amino end groups by telomerization of NIPAAm monomers with the telogen 2-aminoethanethiol hydrochloride. When the reaction was performed in water (at 25 °C and for 4 hours) ammonium persulfate was used as initiator, and AIBN was used as an initiator when the reaction was performed in ethanol (at 65 °C and for

12 hours). In both cases after the respective reaction time was achieved, triethylamine was added to the reaction mixtures.

2.2.1.3. Telomerization

a) Concept

Telomerization or radical chain transfer polymerization is a type of controlled radical polymerization (CRP), which has been used in order to adjust the length of polymers (Fischer et al. (2006)). In this polymerization technique participates a highly reactive chain transfer agent, some examples of very effective ones are the mercaptans like mercaptopropionic acid.

A general telomerization reaction and its constituent components is shown in Figure 21: *Taxogen* (nM) is the monomer to be polymerized, *telogen* (AB) is the chain transfer agent employed and the product of this reaction is known as *telomer* (A(m)nB) or semitelechelic polymer, which is a polymer with one reactive end group (Fischer et al. (2006)). This reaction was designed so oligomers (polymers with low molecular weight) with one end group can be synthetized. The end group (A) can be distinguished in the telogen and is known as *taxonom*.

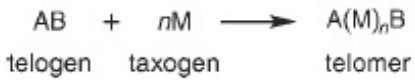

Figure 21. Telomerization reaction and its components (Fischer et al. (2006)).

b) Types of telomerization

In literature, different types of telomerization reactions are mentioned, each one varies according to the end group or taxonom present in the telomer. The following types are observed (Behr et al. (2009)):

- Telomerization with OH nucleophiles such as water (Monflier et al. (1995)), alcohols (mono-alcohols) (Clement et al. (2008)), polyols (Behr et al. (2009)) and acids (Rose et al. (1973));
- Telomerization with amines; e.g. telomerization of butadiene (Kaneda et al. (1981)) and isoprene (Leca et al. (2006)) with amines;
- Telomerization with carbon oxides, having as examples telomerization of butadiene (Musco et al. (1978)) and isoprene (Dinjus et al. (1995)) with CO_2, besides the carboxytelo-merization (Billups et al. (1971)) and finally
- Telomerization by heterogeneous catalysts (Lazutkin et al. (1978)).

- **Telomerization with OH Nucleophiles**

Telomerization with water. Montflier et al. (1995) telomerized butadiene with water in a

cojointed colloidal system, obtaining the telomer 2,7-octadien-1-ol. The telomerization was performed in absence of a solvent and with carbon dioxide and a non-ionic surfactant. This neutral surfactant had an encouraging effect when it was used over the critical micelle concentration and the configuration of hydrophilic part determined the grade of conversion and selectivity of the reaction.

Telomerization with alcohols (monoalcohols). 1,3-butadiene was telomerized by Clement et al. (2008) by using methanol as chain transfer agent and palladium-carbene complexes as catalysts (Figure 22), the telomer obtained was 1-methoxyoct-2,7-diene (1), a major product from this reaction, which has a high commercial interest for the industry as an intermediate component for the synthesis of plasticizer alcohols. In addition, it was reported that other three secondary products (2, 3 and 4) were obtained and some of them are also of commercial interest.

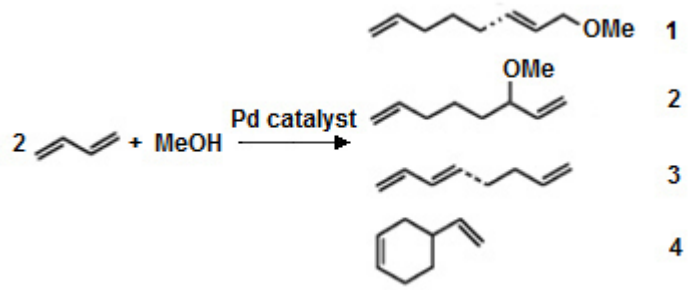

Figure 22. Telomerization reaction for 1,3-butadiene with methanol (Clement et al. (2008)).

Telomerization with alcohols (polyols). Behr et al. telomerized butadiene with the chaim transfer agent ethylene glycol obtaining isomeric monotelomers 2-**(1a)** (2,7-octadienyloxy) ethanol and **(1b)** 2-(1-ethenyl-5-hexenyloxy) ethanol, **(2)** ditelomers and **(3)** butadiene dimers 1,3,7-octatriene and 4-vinyl-1-cyclohexene (Figure 23) (Behr et al (2003)).

Telomerization with acids. Butadiene was telomerized by Rose et al. by using acetic acid as chain transfer agent, catalized with palladium in the presence of orto-aryl substituted phosphite, that act as ligands, the telomers obtained were acetoxyoctadienes (Rose et al. (1973)).

- **Telomerization with amines**

Telomerization of butadiene with amines. Kaneda et al. (1981) telomerized butadiene with the amine telogen morpholine, with a palladium and a tetrakis(triphenylphosphine)palladium$_{(0)}$ heterogeneous and homogeneous catalyst systems, respectively. They evaluated the

influence of solvents in the reaction and arrived to the conclusion that the highest yield reactions were achieved when acetone, benzene or THF were used as solvents in both types of catalytic reactions. At the end they chose acetone for reaction with non-aromatic amines and dioxane for aromatic amines like aniline.

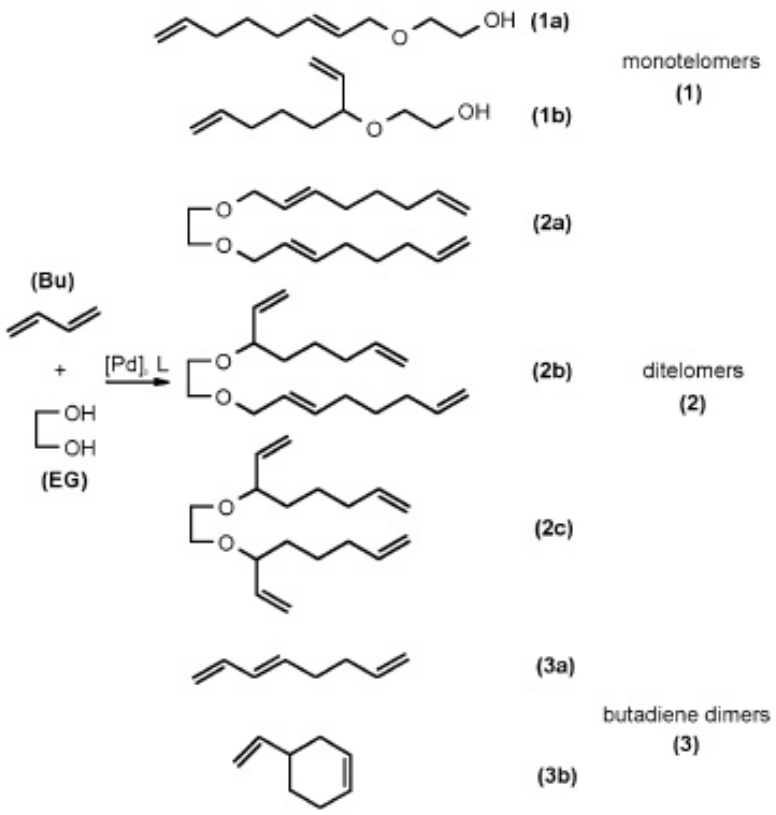

Figure 23. Products obtained by the telomerization of butadiene with ethylene glycol (L: ligand of carbene of phosphine ligand) (Behr et al (2003)).

Telomerization of isoprene with amines. Leca et al. (2006) telomerized isoprene with the telogen diethylamine, 2-pyridyl-2-phospholenes ligands and catalyzed with palladium. They showed that a high activity can be achieved by using acetic acid as an acidic complementary catalyst. They also managed to activate this system with UV radiation for the first time.

- **Telomerization with carbon oxides**

Telomerization of butadiene with CO_2. Musco et al. (1978) used carbon dioxide (CO_2) as a telogen agent for telomerizing butadiene in the presence of the palladium catalyst $(C_4H_7PdOAc)_2$ and the phosphorous ligand $P(C_6H_{11})_3$ in presence (or absence) of benzene and water at 70 °C for 48 hours. They obtained as products from these reactions, esters such as the octadienyl esters of 2-ethylidenehepta-4,6-dienoic acid, and lactones such as the lactone (E)-2-ethylidenehept-6-en-5-olide.

Telomerization of isoprene with CO_2. Dinjus et al. (1995) used a palladium based catalyst and the ligand 1 ,3- bis(dicyclohexylphosphino)propane in the telomerization of isoprene with carbon dioxide (CO_2) in acetonitrile solvent. The reaction was performed at 90 °C for 20 hour with an initial pressure between 25-30 bar and a final pressure of 15 bar. The products obtained were different kinds of lactones.

Carboxy-telomerization. Billups et al. (1971) telomerized in ethanol, butadiene with the telogen carbon monoxide (CO), the catalyst palladium acetylacetonate $Pd(acac)_2$ and the ligand triphenylphosphine. The reaction temperature was between 70 and 80 °C and the reaction time was of 4 hours. Ethyl-nona-3,8-dienoate was the product obtained from this reaction.

- **Telomerization by heterogeneous catalysts**

Lazutkin et al. (1978) used heterogeneous catalyst like palladium-tin complexes supported over a SiO_2 surface, in the telomerization of butadiene with diethylamines. The suitability of these catalysts is due its high activity and low miscibility in diethylamine-butadiene media.

2.2.2. Synthesis of CMC-g-PNIPAAm graft copolymers

2.2.2.1. Carboxymethyl cellulose (CMC)

In order to transform polysaccharides into sustainable and high-value raw materials, it is necessary to chemically functionalize of these biopolymers (Heinze (2005), Heinze et al. (2001)). These modifications can be accomplished by using the same chemical reactions that work for low molecular weight organic molecules. But the development of new products have been limited. New research works aim at upgrading the synthesis methods and the products available, along with the development of novel synthetic routes.

New products with a spectra of interesting properties can be obtained by chemically modifying polysaccharides by using the synthetic path known as carboxymethylation (Heinze et al. (2005), Balser et al. (1986)). With the Williamson ethers synthesis a carboxymethyl (CM) polysaccharide derivative is obtained from a polysaccharide that was previously activated with aqueous alkali hydroxide (e.g. sodium hydroxide). Besides starch and cellulose, carboxymethylation can be applied to other polysaccharides. Some of the polysaccharides to whom carboxymethylation were applied are presented in Table 3. In 1918, carboxymethyl cellulose was synthetized for first time and in 1920, IG Farbenindustrie AG in Germany produced on a commercial scale (Balser et al. (1986)).

From the polysaccharide cellulose many cellulose derivatives are produced. Cellulose is a biopolymer that can be found in nature and is part of 1/3 of every plant material. It also forms

part of cells walls of many high vegetable organisms (Cash et al. (2009)). Between 40-50% of

Table 3

Various polysaccharides used for carboxymethylation (Heinze et al. (2005), Balser et al. (1986))

Polysaccharide Type	Source	Structure
Cellulose	Plants	β-(1→4)-D-glucose
Chitin	Animals	β-(1→4)-D-(*N*-acetyl)glucosamine
Chitosan		β-(1→4)-D-glucosamine
Curdlan	Bacteria	β-(1→3)-D-glucose
Dextran	Bacteria	α-(1→6)-D-glucose main chain
Pullulan	Fungi	α-(1→6)linked maltotriosyl units
Scleroglucan	Fungi	β-(1→3)-D-glucose main chain, β-(1→6)-D-glucose branches
Schizophyllan	Fungi	β-(1→3)-D-glucose main chain, D-glucose branches
Starch	Plants	
Amylose		α-(1→4)-D-glucose
Amylopectin		α-(1→4)- and α-(1→6)-D-glucose

cellulose is found in wood and 85-97% in cotton. Some examples of cellulose derivatives are listed:

- Carboxymethyl cellulose or sodium carboxymethyl cellulose or cellulose gum (CMC).
- Ethyl cellulose.
- Hydroxypropyl cellulose.
- Methyl cellulose and hydroxypropylmethyl cellulose, known as modified cellulose gums.

Carboxymethyl cellulose is a cellulose derivative of anionic type and also soluble in water (Cash et al. (2009)). It has no odor, taste, its color ranges from white to light tan, and is a hygroscopic free-flowing powder. Cellulose gums are the name given to carboxymethyl cellulose grades that have a purity of at least 99.5%. The degree of polymerization (DP), of carboxymethyl cellulose substitution (DS) and how uniform this substitution is will determine its mixing properties. In Figure 24 is shown that per each Anhydro Glucose Unit (AGU) of CMC, there are three available substitution sites, then the maximum DS of CMC is 3, but high DS levels have no commercial use. It is more commonly used to find DS levels of 1.5 and DS values less than 0.4 corresponding to insoluble CMC (Zecher et al. (1997)).

Large growths in viscosity are obtained by small rises of molecular weight of cellulose derivatives. In Table 4 the most common and commercial average DP and molecular weights of CMC found in the market are shown.

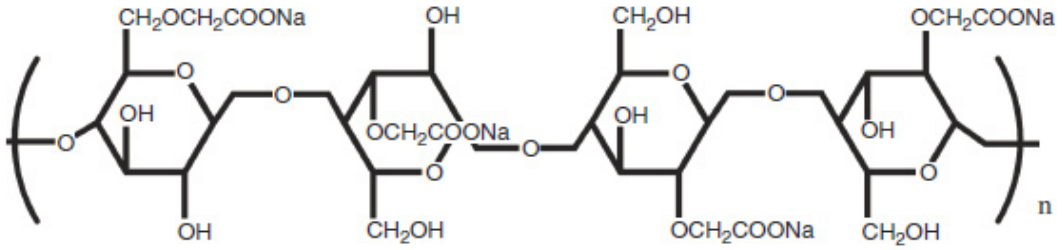

Figure 24. Theoretical chemical structure of CMC (Reproduced with permission of Hercules incorporated, a subsidiary of Ashland Inc.) (Cash et al. (2009)).

Table 4

Molecular weight and degree of polymerization (DP) of more commercial CMC with a DS=0.7 (Cash et al. (2009))

DP	Molecular Weight
3,200	700,000
1,100	250,000
400	90,000

Many progress have been made in engineering science, in quality control effectiveness in production (Heinze et al. (2005), Stigsson et al. (2001)). A review about the production of CMC and the potential future developments was published (Stigsson et al. (2001)). Different types and grades of CMC are applied in different industrial sectors and also in human life (Table 5).

a) Properties

The carboxymethylation of cellulose for producing CMC is performed in order to obtain a cellulose derivative that can be dissolved in water, and that can find many applications like the take over of the flow behavior from aqueous solutions and preparations (Heinze et al. (2005), Heinze et al. (1997)). CMC is a polyelectrolyte. Clay and latex systems are stabilized with CMC. The effect exerted on the draining, the rheology and layering operation of the system by the molecular weight of CMC was measured. No strong effect was discovered.

CMC is mainly used as a sodium salt form which is soluble in water. With acids of mineral origin a CMC in acid form is obtained with a pKa of 3.2 (water solubility is decreased) (Heinze et al. (2005), Sandas et al. (1993)).

However, the pKa value estimated is an average one since it is affected by the functionalization pattern of the carboxymethyl groups. For example a CMC with a pKa of 3.0 are functionalized at O-2, while a pKa of 3.3 can be attributed to a CMC with a functionalization oriented to O-6 (Heinze et al. (2005), Kötz et al. (1990)).

Table 5

Types and grades of CMC and its applications (Heinze et al. (2005), Stigsson et al. (2001))

Quality of CMC	Examples of application areas	Content of CMC (%)	Salt content (%)
Technical	Detergents, mining flotation	< 75	> 25
Semi-purified	Oil and gas drilling muds	75 - 85	15-25
Purified	Paper coating, textile sizing and printing, ceramic glazing, oil drilling muds	> 98	< 2
Extra purified (Cellulose gum)	Food, toothpaste, pharmaceuticals	> 99.5	< 0.5

The H-form of CMC are applied for metal ion adsorption, such as in the treatment of waste water (Heinze et al. (2005), Hoogendam et al. (1998)).

CMC solutions behave like non-Newtonian fluids, which means that at low shear rates they will possess a Newtonian viscosity, but at a critical shear rate the viscosity will decrease (Heinze et al. (2005)). A tendency to a pseudoplasticity is commonly observed due an orientation of the polymer chains to the direction of the flow, when a stress is applied. CMC was used as an additive in blends with aqueous solutions of other polysaccharides like konjac or glucomannan (Heinze et al. (2005), Sungur et al. (1996)). The presence or absence of hydrogen bridge bonds will influence on the mechanical properties of the blend, and therefore these can be controlled by the ratio of components in the blend.

- Solubility

The solubility of CMC can be affected by the length of the polymer chain. Solubility in water will increase while DP decreased (Cash et al. (2009)). Carboxymethyl cellulose types with a same DS but with different DP will possess different water solubility. The solubility of CMC in water will be increased when the DS is increased. A decrease in the DS will mean that non substituted areas of the molecule are associated one with the other, and the dissolution in water will be decreased. A uniform carboxymethyl substitution at the main chain, avoids this kind of behavior because solubility in water will be increased.

- Viscosity

By the regulation of the polymer chain and the degree of polymerization (DP) of CMC, it is possible to adapt the viscosity of the polymer (Cash et al. (2009)). High viscosity values are observed in long polymer chains of CMC. Besides that, the degree of substitution (DS) of CMC has an effect in its viscosity. As it was stated before, a few or not uniform substitution, leads to association of no substituted domains, then the solubility in water is decreased and the polymer exhibit a high viscosity. The viscosity of CMC aqueous solutions is affected by their DP and DS.

The existence of non-solvents has an impact on the viscosity of CMC (Cash et al. (2009)). Solvents soluble in water, like alcohol and glycerol, increase the viscosity of CMC because they restrict the amount of aqueous solvent available, and a result the CMC solution turns into a more concentrated one. In these systems, the increase of non-solvent quantity contributes to an augmentation of viscosity, because associative bonds between CMC regions are encouraged.

CMC tolerates the presence of ethanol in its solution (Cash et al. (2009)). In solvent systems of water and 50% or more of ethanol, CMC solutions are clear. The tolerance of alcohol from CMC increments when its degree of substitution (DS) is higher, more amounts of CMC can be dissolved in water ethanol mixtures. CMC with low viscosities accepts organic solvents, in comparison with middle and high viscosity CMCs.

- Dispersion and dissolution techniques

Hot or cold water can dissolve CMC. In water, carboxymethyl particles exhibit an agglomeration tendency by generating particles. This is explained by the fast hydration of this polysaccharide (Cash et al. (2009)). The formation of bulks is almost avoid by the use of efficient dispersion techniques and by addition of special additives. Mixers capable of creating vortexes by strong agitation, will decrease the generation of bulks, because they are going to help to keep particles separated and therefore they could be hydrated independently. It is also advisable the a previous mixing with other dry components like for example sugar, in order to avoid the bulk formation by keeping particles non-agglomerated. Methanol, ethanol and glycerol acts as dispersive agents with CMC, since it is not soluble in these polar solvents. In food industry corn, fructose or invert syrup are used in CMC recipes as dispersive agents.

Different particle size distributions CMC are found in commercial grade products (Cash et al. (2009)). CMC with gross particles will absorb water slowly then the formation of bulks will be diminished. CMC grades that are used in dry mixers have refined particles, because these can be separated and the bulking when water is added will be avoided. When there is rivalry

between ingredients for water availability, then the size of CMC particles plays an important role, since fine particles are faster hydrated.

b) Analytical tools for the structure characterization carboxymethylated cellulose and starch

The properties of CMC are determined by its degree of substitution (DS), which is defined as the number of carboxymethylated groups introduced to the polymer chain (Heinze et al. (2005)). The properties are also influenced by the pattern of the functionalization. Therefore, in order to improve the reaction conditions and to understand the relation between property and structure, it is necessary to know the DS and the pattern of functionalization. The carboxymethylated groups at the AGU can be located at different positions (2, 3 and 6) and therefore the different possibilities of AGUs that will set up the polymer chain and that will happen between polymer chains. Between different CMC chain distribution patterns might be observed.

- Determination of the degree of substitution of carboxymethyl groups

In order to determine the degree of substitution of CMC, the carboxylic groups acidity is used. The carboxymethyl cellulose functional group of CMC in its sodium salt form is treated by reaction with hydrogen chloride in ethanol resulting the acid form of the carboxylate group, which later can be titrated with sodium hydroxide (Heinze et al. (2005), Eyler et al. (1947)).

The back titration method is a commonly used as reference method for CMC (Heinze et al. (2005), ASTM (1995)).

- Characterization of the functionalization pattern

In order to define the functionalization pattern of the CMC polymers, the techniques used are Cross Polarization Magic Angle Spinning (CP/MAS) and solution ^{13}C-NMR spectroscopy, ^{1}H-NMR spectroscopy and High-Performance Anion Exchange Cromatography with Pulsed Amperometric Detection (HPAEC-PAD) and HPLC chromatographic techniques, and liquid gas chromatography (Heinze et al. (2005), Sjostrom et al. (1989)) executed after complete depolymerization of the samples (Heinze et al. (2005), Käuper et al. (1998)). The degree of substitution (DS) can be calculated from the CP/MAS ^{13}C-NMR spectra **(Heinze et al. (2005)).**

2.2.2.2. Grafting "onto" polymerization and coupling reaction

2-Acrylamido-2-methyl propane sulfonic acid (AMPS) was linearly copolymerized with acrylic acid (AA), in aqueous media and at 20°C, using the redox initiator ammonium persulphate / N,N,N',N'-tetramethyl-ethylenediamine ($(NH_4)_2S_2O_8$/ TEMED) (Figure 25) (L'Alloret et al. (1995)). Subsequent grafting of this backbone with the semitelechelic aminoterminated O-(2-aminoethyl)-O'-methyl polyethylene oxide (PEO5), by using as a coupling agent 1-(3-

dimethylamino-propyl)-3-ethyl-carbodiimide hydrochloride (EDC) at 60 °C, at pH=8 and in aqueous media (Figure 26).

The graft copolymers obtained presented thermosensitive behavior during heating, due to the formation of microdomains from the PEO5 grafts when they reached their LCST temperature, these microdomains acted as croslinker agents between the other copolymer chains, increasing the viscosity of the aqueous solutions (L'Alloret et al. (1995)).

Hourdet et al. (1997) performed with the coupling agent EDC couple reactions at pH=8, between the semitelechelic polyether, polyethylene oxide (PEO5: Molecular weight 5000 g/mol) and carboxymethyl cellulose (CMC), a water soluble backbone bearing carboxylic pendant groups.

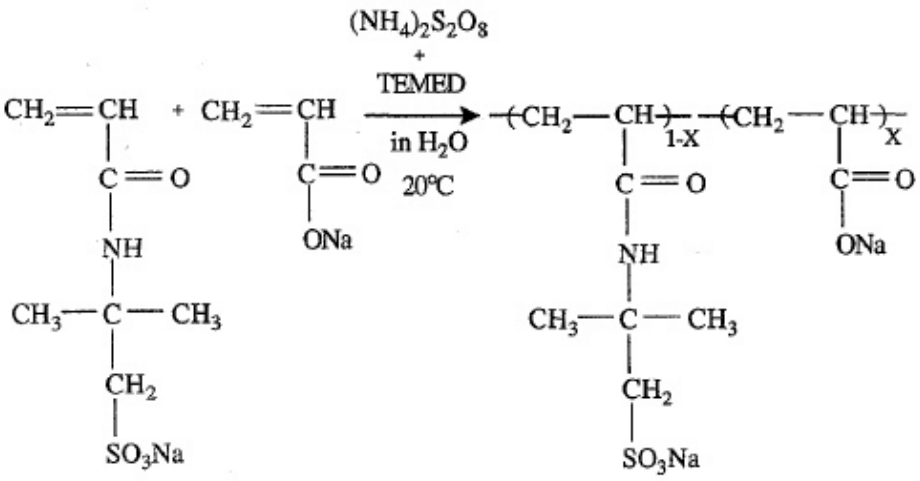

Figure 25. Synthesis reaction of 2-acrylamido-2-methyl propane sulfonic acid (AMPS) / acrylic acid (AA) linear copolymers (L'Alloret et al. (1995)).

Since the polyether grafts (PEO) presented a phase transition upon heating (and therefore LCST), the resulting graft copolymer displayed thermosensitive properties in solution upon heating, with a phase segregation of the polyether grafts and an increment in the solution viscosity (Hourdet et al. (1997)).

Hourdet et al. (1998), also studied the phase transition behavior by light scattering analysis in semidilute solutions of graft copolymers with different polyacrylic acid backbones (homo and copolymers) grafted with polyetheroxide (PEO) oligomers, similar to the ones used in a previous publication (Hourdet et al. (1997), Hourdet et al. (1998)). They determined in their light scattering analysis that a phase transition of the polyetheroxide grafts is triggered by temperature or salt concentration critical values (Hourdet et al. (1998)). This was established by a correlation found between the presence of scattering peaks and the formation of polyether

oxide (PEO) microdomains. Durand et al. (1999) developed PAA-g-PNIPAAm graft copolymers by grafting semitelechelic aminotermi-nated PNIPAAm oligomers to polyacrylic acid backbones with the coupling agent dicyclohe-xylcarbodiimide (DCCI). The reaction was performed for 20 hours at 60 °C and N-methylpyrrolidone (NMP) was used as a solvent. The thermosensitive behavior of the obtained copolymers was evaluated with rheological measurements on the viscosity of semidilute aqueous solutions (Durand et al. (1999)). Upon heating it was observed an increment in the viscosity of the solutions (thermothickening behaviour), when the temperature reached was over the LCST temperature of PNIPAAM. Bokias et al. (2001) modified carboxymethyl cellulose polymers making them thermosensitive by grafting them with aminoterminated PNIPAAm, performing a coupling reaction using the coupling agent 1-(3-dimethylamino-propyl)-3-ethyl-carbodiimide hydrochloride (EDC). The reaction was performed for 8 hours at room temperature, at pH=8 and in aqueous media (Figure 27).

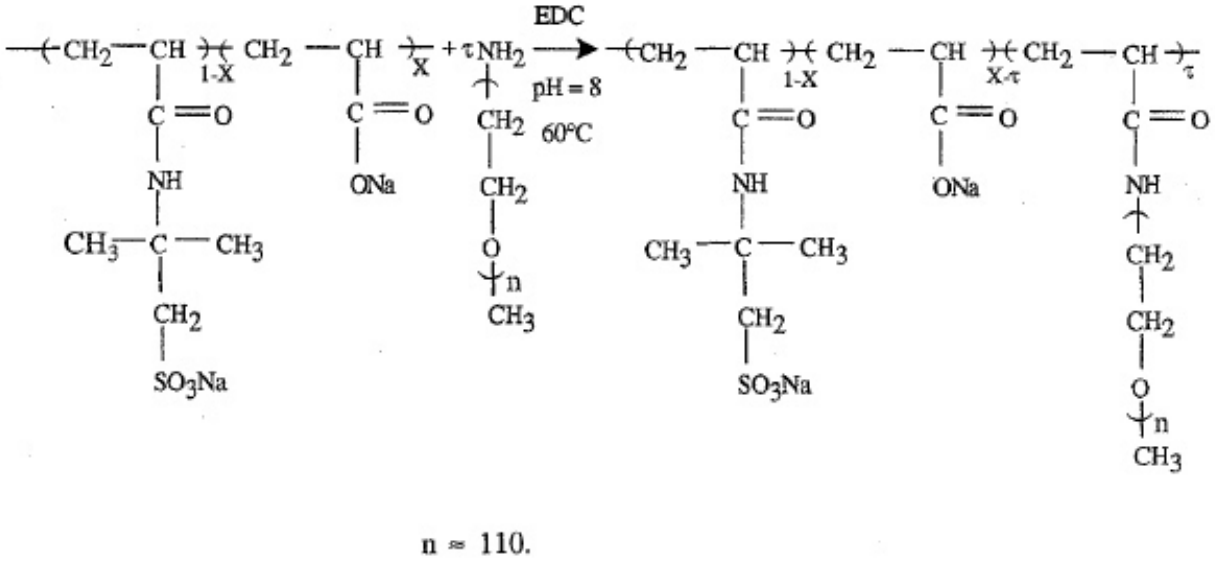

Figure 26. Grafting reaction of aminoterminated O-(2-aminoethyl)-O'-methyl polyethylene oxide (PEO5) to 2-acrylamido-2-methyl propane sulfonic acid (AMPS) / acrylic acid (AA) linear copolymers (L'Alloret et al. (1995)).

The thermosensitive nature of the obtained copolymers was demonstrated and compared with carboxymethyl cellulose and aminoterminated PNIPAAm samples by turbidimetry, viscosimetry, fluorescence and rheology tests (Bokias et al. (2001)). Rheological measurements (and also viscosimetric tests) confirmed the thermothickening behavior of the grafted copolymers (Durand et al (1999)).

Karakasyan et al. (2008) coupled aminoterminated poly(ethylene oxide-co-propylene oxide) (PEPO) (with a 84% mol content of propylene oxide) to a carboxymethyl cellulose polymer backbone, by using EDC and NHS (N-hydroxysuccinimide) as coupling agents. The reaction was performed at 10°C, in water, at pH=5 and for 16 hours. The efficiency of grafting was low (between 30-40%) due to the thermothickening behavior of the CMC solutions with high viscosities even at low polymer concentrations.

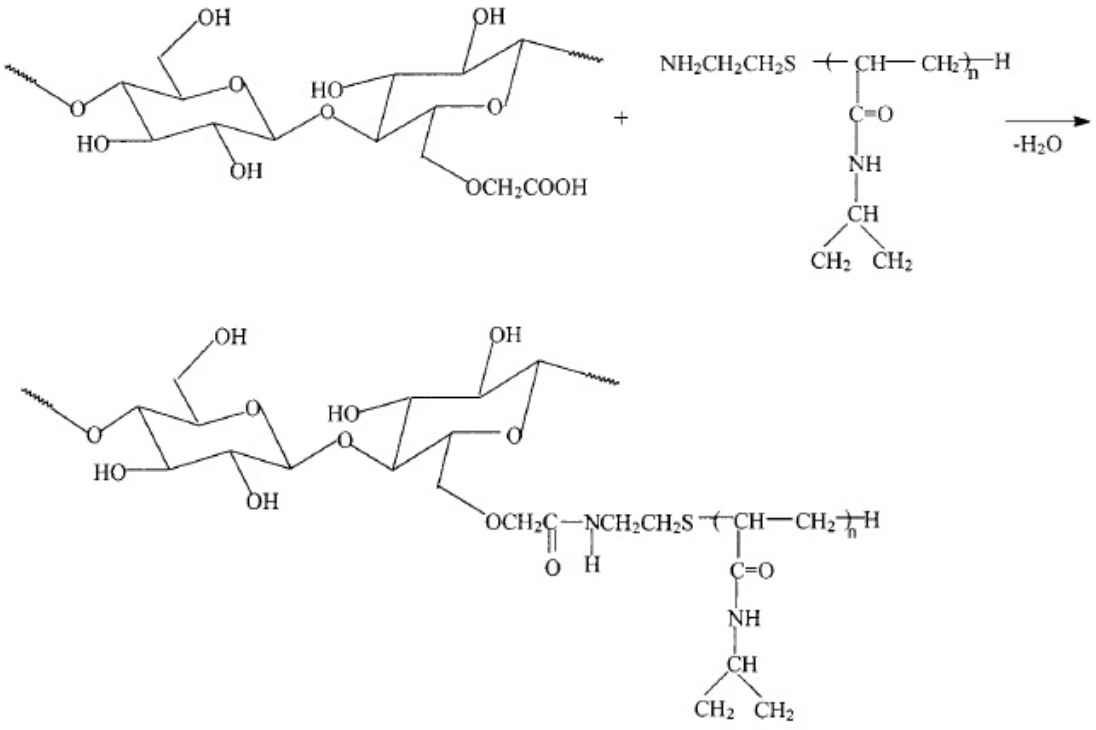

Figure 27. Synthesis reaction for CMC grafted with PNIPAAM (Bokias et al. (2001)).

2.2.3. Synthesis of comb-type graft hydrogels

2.2.3.1. Chemically crosslinked hydrogels

In order to improve packaging materials by making them more hydrophobic, Coma et al. (2003) developed a hydrogel from hydroxyl propyl methyl cellulose (HPMC) by crosslinking with citric acid at 190 °C for 15 minutes. The solvent used was a mixture of distilled water and absolute ethanol (2:1 parts) with 1 part of polyethylenglycol (PEG-400), which was used as a plasticizer. Then the crosslinker citric acid was added and also NaH_2PO_4 in order to make the reaction mixture reaching a pH of 2.65. After a 15 minutes of mixing and a degassing stage, the reaction mixture was poured over a polypropylene support forming films, which were dried at 60 °C for 60 minutes. The films were then pealed off and used in the subsequent crosslinking reaction. A new polyelectrolyte hydrogel was developed by Sannino et al. (2005) by crosslinking a

mixture of carboxymethyl cellulose (CMC)/hydroxyethyl cellulose (HEC) with the crosslinking agent divinyl sulfone (DVS) at a pH of 12.5 under air and at room temperature. The reaction was performed at different CMC/HEC ratios and with different DVS concentrations, in order to study the influence of the polyelectrolyte nature of the backbone and the crosslinking degree in the swelling performance of the obtained hydrogel.

A bulking agent for hypocaloric diets was also developed by Sannino et al. (2006). A blend of carboxymethyl cellulose (CMC)/hydroxyethyl cellulose (HEC) (ratio 3:1) was crosslinked and a hydrogel was made by using the water soluble carbodiimide (WSC) 1-ethyl-3-(3-dimethylaminopropyl)carbo-diimide hydrochloride. Citric acid was used as a catalyst for the reaction. The reaction was performed for a few hours at room temperature in air. The solvent used was water and the CMC/HEC concentration was 3 wt%, the crosslinking agent was at a concentration of 5 or 2.5% and the catalyst was a 1 wt% aqueous solution. The crosslinking bond in the cellulosic hydrogel is an ester bond formed as a result of the reaction between the carboxylic acid groups from the carboxymethyl cellulose (CMC) and the water soluble carbodiimide (WSC) (Sannino et al. (2006)).
CMC/HEC (ratio 3:1) was also crosslinked for making hydrogels by Demitri et al. (2008) but instead of a WSC, citric acid was used as a crosslinker. They explained that in the polymer blend, HEC is an additive for improving the crosslinking efficiency between different CMC polymer chains and not through the same chain. The polymer blend was dissolved in water, with a concentration of 2 %wt, different concentrations of citric acid (with respect of the weight of the polymer blend) were added (1.75%, 2.75%, 3.75%, 10% and 20% w/w polymer) in order to obtain different grades of crosslinking. The reaction was performed at 80 °C for 24h after a predrying at 24h at 30 °C. They studied the crosslinking reaction between citric acid and the carboxylic groups of the CMC by using Fourier transform infrared spectroscopy (FTIR). A possible crosslinking mechanism (Figure 28) based on comparisons with a previous study made by Zhou et al. (1995) was proposed, where it was stated that the citric acid and the multifunctional carboxylic acid groups reacted with the cellulosic hydroxyl groups of different polymer chains via esterification reactions via the formation of intermediate anhydride groups (Demitri et al. (2008)).

2.2.3.2. Ionically crosslinked hydrogels

Ionically crosslinked hydrogels or ionotropic gels of carboxymethyl cellulose are polymer aggregates stabilized by the electrostatic interplay between the carboxylic pending groups of CMC and multicharged metal cations (Heinze et al. (2005)). These gels are also insoluble in water because of the electrostatic interactions between OH groups of CMC and the multicharged ions. Ionically crosslinked hydrogels are possible to be manufactured as spheres. A review about the synthesis, the structure of these gels, made from natural or modified

biogenic polymers, provided with carboxylic pending groups and multicharged metal cations is available (Heinze et al. (1993), Heinze et al. (2005)).

The specification of the interplay between the CMC carboxylic pending groups and the multicharged metal ions, have caught the attention of many researchers (Heinze et al. (2005)). Ionically crosslinked hydrogels find application in controlled liberation of active biological substances and immobilization of cells. CMC ionotropic gels have been applied in controlled liberation of drugs, where the polysaccharide has been used as a container and the drug liberated was erythomycia (Heinze et al. (1990), Heinze et al. (2005)).

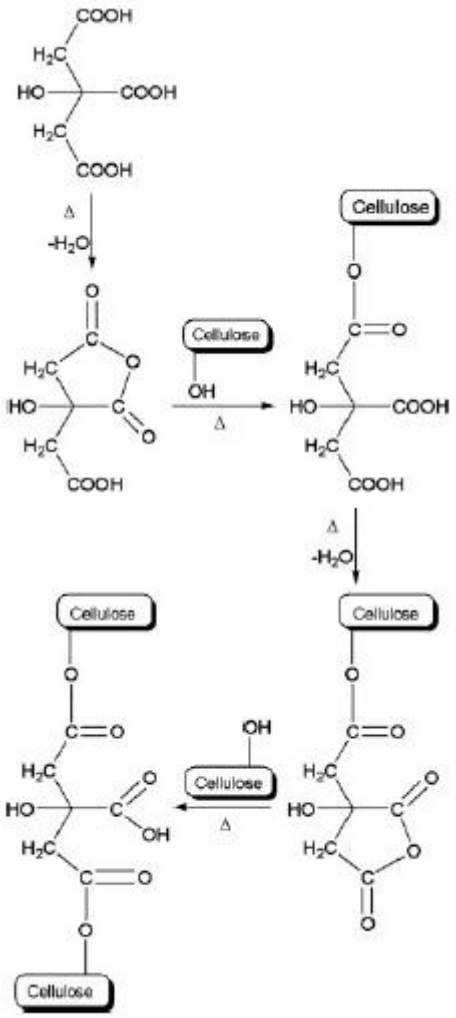

Figure 28. Possible mechanism proposed for the crosslinking reaction between CMC and citric acid (Demitri et al. (2008))

Biodegradable beads were obtain by the ionic crosslinking of CMC with Fe^{3+} ions. These beads were coated with a blend of gelatin and CMC and crosslinked, with this the controlled liberation of substances was improved (Heinze et al. (2005)). Important for the synthesis of ionically crosslinked gels is the macroscopic properties characterization of pregel polymer solutions

bythe evaluation of their molecular parameters. Molecular parameters such as the radius of gyration, molecular weight of polymers, branching degree and flexibility influence the viscosity of CMC

pregel solutions. The persistence length is related to the rigidity of the polymer backbone, which is the molecular parameter that characterizes the thickening properties of the pregel solutions. Sandas et al. (1993) determined with SAC-MALLS and potentiometric titrations that for DS between 0.75 and 1.25 (commercial grades) the intrinsic persistence length for CMC was of 16 nm by applying the worm-like theory (Sandas et al. (1993), Heinze et al (2005)). Saeedi et al. (2009) studied different tablets formulations for extended-liberation of the drug theophylline by the crosslinking carboxymethyl cellulose with different amounts of cation Ca^{2+} (from $CaCl_2.2H_2O$) and Al^{3+} (from $AlCl_3x6H_2O$). Magnesium stearate was also added to the formulations. They performed dissolution studies and determined that the drug liberation speed diminished by an increment of the metal cation concentration. They also concluded that the type of metal cations (and their concentrations and charges) affected the extended-liberation of the drug and its kinetics.

In order to avoid large gastric adverse effects produced by non-steroidal anti-inflamatory drugs, Kaushik et al. (2012) developed tablets from carboxymethyl cellulose crosslinked with Al^{3+} (from $Al(OH)_3$) by using wet granulation, in order to diminish the liberation of the drug aceclofenac to the gastric mucosal surface. Magnesium stearate was also included in the formulations. During this research, it was studied how the liberation of aceclofenac in acid (pH=1.2) and phosphate buffer dissolution (pH=6.8), can be affected by the proportion polymer:$Al(OH)_3$, the amount of drug contained in the tablet and the amount of compression used for the manufacture of the tablet. Their study managed to demonstrate that it was possible to regulate the drug liberation in the stomach and to extend it at the small intestine, only with an adequate formulation and compression force.

Braihi et al. (2014) developed a blend of carboxymethyl cellulose and starch which was crosslinked with Al^{3+} ions (from aluminium sulfate octadecahydrate, $Al_2(SO_4)_3.18H_2O$). By using ignition tests in crosslinked CMC samples, they observed the presence of a precipitate of white color, which was aluminium oxide, confirming the presence of aluminium ions in the crosslinked structures. Flame tests performed to CMC samples confirmed the replacement of Na ions by Al^{3+} ions. Also FTIR spectra from the carboxymethyl cellulose and starch blend samples confirmed the existence of crosslinking reaction between the molecules of starch and CMC.

2.2.3.3. Thermosensitive hydrogels

Wu et al. (1992) synthesized a thermosensitive macroporous hydrogel (Figure 29) by crosslinking PNIPAAm with dihydroxyethylene-bis-acrylamide (DHEBAAm) and by using

hydroxypropyl cellulose (HPC) as a porogen agent. The hydrogel was prepared by polymerization of recrystallized NIPAAm dissolved in water at a concentration of 18 wt%. After degassing with N_2, the reaction was initiated with the redox initiator pair ammonium persulfate (APS)/*N,N,N',N'*-tetramethylethylenediamine (TEMED) at 50 °C in order to precipitate the porogen agent HPC (LCST=42°C). The hydrogels were characterized by thermosensitive swelling and deswelling tests.

A PNIPAAm comb-type graft hydrogel (Figure 30) was developed by Yoshida et al. (1995) by a three step synthesis: First, a semitelechelic aminoterminated PNIPAAm oligomer was made by telomerization reaction; second, an acrylate group was inserted to the oligomers, by reacting at 15 °C for 1 day their amino functionality with *N*-acryloxysuccinimide obtaining as a result a PNIPAAm macromonomer; and finally, comb-type graft hydrogels are synthesized by reacting the acrylate groups (of the resulting macromonomers) with NIPAAm monomers, in a polymerization reaction in water. The PNIPAAm comb-type graft hydrogels were characterized by their shrinking kinetics versus PNIPAAm homopolymers between 10 and 40 °C. Using the three step comb-type graft hydrogel synthesis reaction performed by Yoshida et al. (1995), Kaneko et al. (1995) studied the influence of the graft length (molecular weight) on the swelling and deswelling behavior of the PNIPAAm hydrogels, by developing three groups of PNIPAAm macromonomers with molecular weight values of 2900, 4000 and 9000 g/mol. The swelling (and deswelling) performance of these samples was contrasted with conventional PNIPAAm hydrogel without macromonomer grafts (Figure 31). Comb-type graft PNIPAAm hydrogels presented a more pronounced shrinking at lower temperatures in comparison with conventional (non grafted) PNIPAAm hydrogels, and the longer the graft chain, the more pronounced the thermosensitive shrinking resulted (Figure 32). Differential Scanning Calorimetry (DSC) analysis certified the fast dehydration of the grafts during the thermosensitive shrinking.

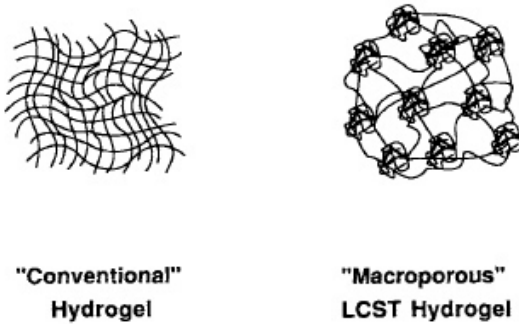

Figure 29. Possible representation of structures of conventional and macroporous hydrogel (Wu et al. (1992)).

Ju et al. (2001) studied the swelling properties of a comb-type graft alginate with PNIPAAm grafts hydrogel and contrasted them with alginate – PNIPAAm semi-interpenetrated network hydrogels also prepared during their research (Figure 33). The alginate grafted with PNIPAAm comb-type graft hydrogels were prepared by simultaneously reacting previously synthetized semitelechelic aminoterminated PNIPAAm oligomers with N-hydroxysuccinimide (NHS), 1-Ethyl-(3-3-dimethylaminopropyl) carbodiimide hydrochloride (EDC) and the carboxyl groups of the alginate polymers and crosslinked with Ca^{2+} (from $CaCl_2$). For the comb-type graft hydrogels, in order to create amide bonds between the amine end group of the PNIPAAm semitelechelic oligomers and the carboxylic groups of the alginate polymers, different molar amounts of the oligomers were dissolved in solutions with a molar proportions of alginate carboxylic groups:EDC:NHS of 2:2:1 and mixed at room temperature overnight (Ju et al. (2001)).

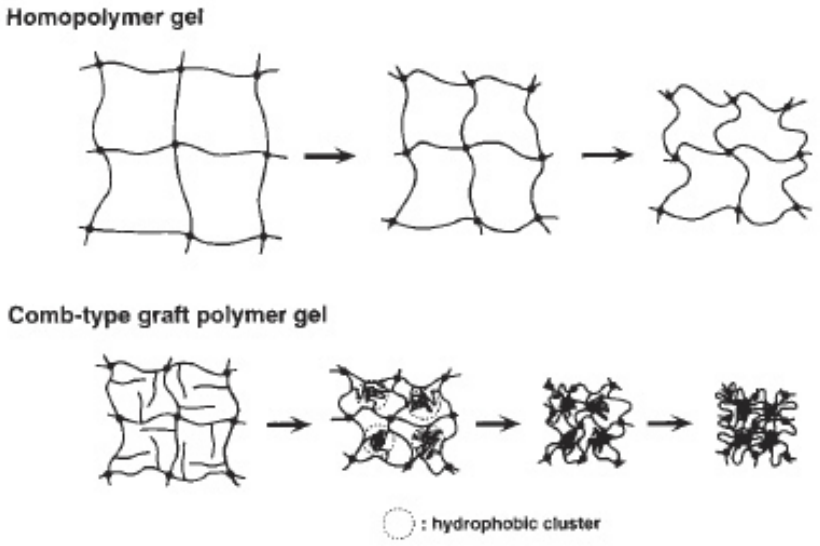

Figure 30. Configuration and thermosensitive deswelling of homopolymer and comb-type graft PNIPAAm hydrogel (Yoshida et al. (2001)).

The PNIPAAm-alginate semi-interpenetrated network hydrogels were prepared by mixing aqueous solutions of alginate (5 wt%) and of the semitelechelic aminoterminated PNIPAAm oligomer (20 wt%) at different proportions by weight (Ju et al. (2001)).
From the swelling and deswelling tests it was concluded that the comb-type graft alginate with PNIPAAm grafts hydrogels showed a faster shrinking in comparison with the PNIPAAm-alginate semi-interpenetrated network hydrogels (Ju et al. (2001)). All the hydrogels developed were sensible to changes in pH and temperature and also to the ionic strength of the media.

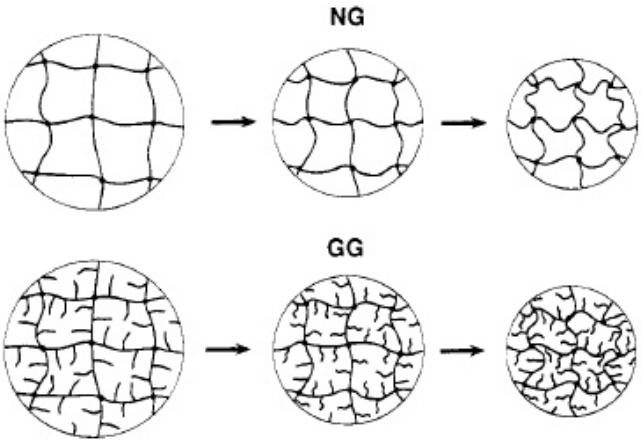

Figure 31. Deswelling at LCST temperatures of conventional PNIPAAm hydrogels (NG) vs comb-type graft hydrogels (GG) (Kaneko et al. (1995)).

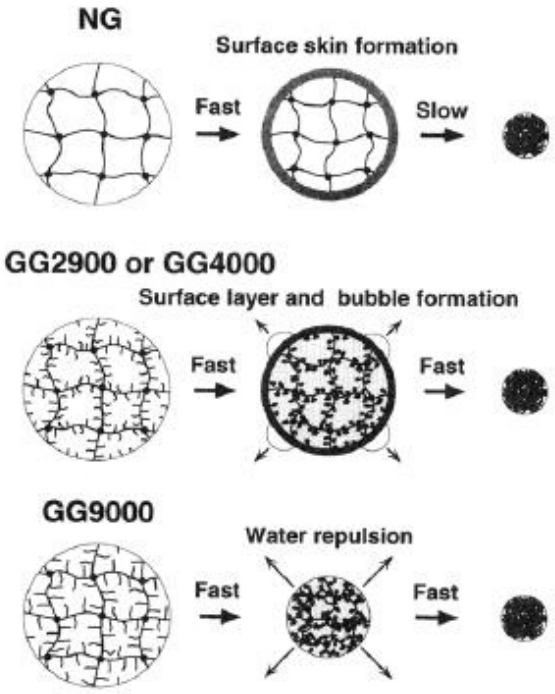

Figure 32. Influence of graft length in the deswelling at LCST temperatures of comb-type graft hydrogels (GG) vs conventional PNIPAAm hydrogels (NG) (Kaneko et al. (1995)).

2.2.4. Synthesis of Bilayer Actuators based on CMC-g-PNIPAAm comb-type graft hydrogel films

2.2.4.1. Bilayer Actuators with hydrogel substrates

Non thermosensitive bilayer actuators were fabricated by Hu et al. (1995), Guan at al. (2005) and Bassik et al. (2010) (See section 2.1.2. “Smart” Bilayer Actuators) and also bilayer actuators with thermosensitive properties were made by Stoychev et al. (2012), Stoychev et al. (2013) and Stroganov et al. (2015) (See section 2.1.3. Thermosensitive bilayer and multilayer actuators).

2.2.4.2. Bilayer Actuators with PA6 unidirectional substrates

A humidity- and a solvent-sensitive bilayer actuators were developed by Dai et al (2013) and Haldorai et al. (2014), respectively (See section 2.1.2. “Smart” Bilayer Actuators).

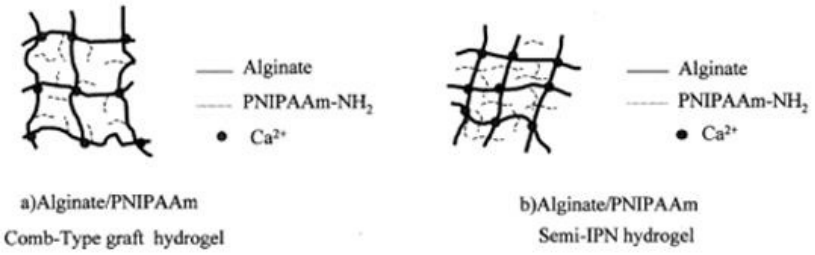

Figure 33. Representation of the structures for: (a) comb-type graft alginate with PNIPAAm grafts hydrogel and (b) PNIPAAm-alginate semi-interpenetrated network hydrogels (Ju et al. (2001)).

2.3. Bilayer Actuators based on CMC-g-PNIPAAm comb-type graft hydrogel films

Aminoterminated Poly(N-Isopropylacrylamide) oligomers were presented by Yoshida et al. (1995), Durand et al. (1999), Bokias et al. (2001) and Ritter et al. (2012), respectively (See section 2.2.1.2.b PNIPAAm telechelic and semitelechelic polymers). Grafting of carboxymethyl cellulose polymers with semitelechelic oligomers by coupling reaction with EDC were shown by Hourdet et al. (1997), Bokias et al. (2001) and Karakasyan et al. (2008) (See section 2.2.2.2. Grafting “onto” polymerization and couple reaction). Isgrove et al. (2001) generated on polyamide 6 (PA6) specific binding sites for immobilization of the enzyme β-glucosidase, by blocking non-specific binding sites and with this to avoid enzyme loss by leaking. In order to achieve this goal, they adhered aldehyde groups binding sites on the PA6 films. Vasileva et al. (2004) immobilized the enzyme glucose oxidase (GOD) on polyamide 6 (PA6) films by creating aldehyde functional groups over the film surface as binding sites. Pessoa de Amorim et al. (2014) modified polyamide 6 (PA6) films in order to generate aldehyde groups (Figure 34) for

covalent bonding of the commercial enzyme laccase, for a further application in dye decoloration for the textile industry.

2.3.1. Chemical Bonding between Active and Passive Layers in Bilayer Actuators based on CMC-g-PNIPAAm comb-type graft hydrogel films

Haldorai et al. (2014) produced a good adhesion between the passive and active layer of their PA6/poly(PNIPAAM-co-PAA)-g-CMC hydrogel bilayer actuators by generating with photocrosslinking, covalent bonds between the amide groups from the PA6 passive layer and the PNIPAAM segments of the grafts from the poly(PNIPAAM-co-PAA)-g-CMC hydrogel active layer. Demitri et al. (2008) presented a possible reaction mechanism of the crosslinking of carboxymethyl cellulose chains with citric acid for the synthesis of superabsorbent carboxymethyl hydrogels. The mechanism suggests the formation of covalent bonding (ester bonding) from the reaction of the carboxylic groups from citric acid and the hydroxyl groups from the carboxymethyl cellulose (Figure 28). Buhus et al. (2009) reported about synthesis of carboxymethyl cellulose (CMC) – gelatine hydrogels and claimed the existence of different crosslinking reactions between the CMC, the gelatin chains and the crosslinker glutaraldehyde (Figure 35). The glutaraldehyde crosslinker provides aldehyde groups that can react with the amino groups from gelatin to form imine type bonds, and with the hydroxyl groups from CMC to form acetal or semiacetal rings type bonds. Pessoa de Amorim et al. (2014) immobilized the enzyme lacasse by forming covalent bonds between the amino groups of the enzyme and the aldehyde groups of the polyamide 6 (PA6) film substrate (Figure 36), generated by acidic hydrolysis, polyethylene imine and glutaraldehyde treatment.

2.4. Thermal and Actuation Properties from Bilayer Actuators

2.4.1. DSC measurements of LCST in PNIPAAm oligomers

Schild et al. (1990) performed DSC measurements to PNIPAAm polymer samples with different molecular weights (Table 6) in aqueous solutions and studied the effect of salt concentration in the intensity of the phase transition (Figure 37). They demonstrated the phase transition of PNIPAAm in aqueous solutions by the presence of endotherms and determined the respective LCST temperatures, with the temperatures of the endotherm peaks. In order to validate these results, they compared them with LCST determinations via optical density measurements (Table 6).

Otake et al. (1990) studied the phase transition in PNIPAAm gels, and stated that their thermoshrinking was associated with the coil-globule phase transition behavior of the linear PNIPAAm polymers that conformed the gel structure. This was validated by DSC measurements performed to both, PNIPAAm gels and linear homopolymers that showed

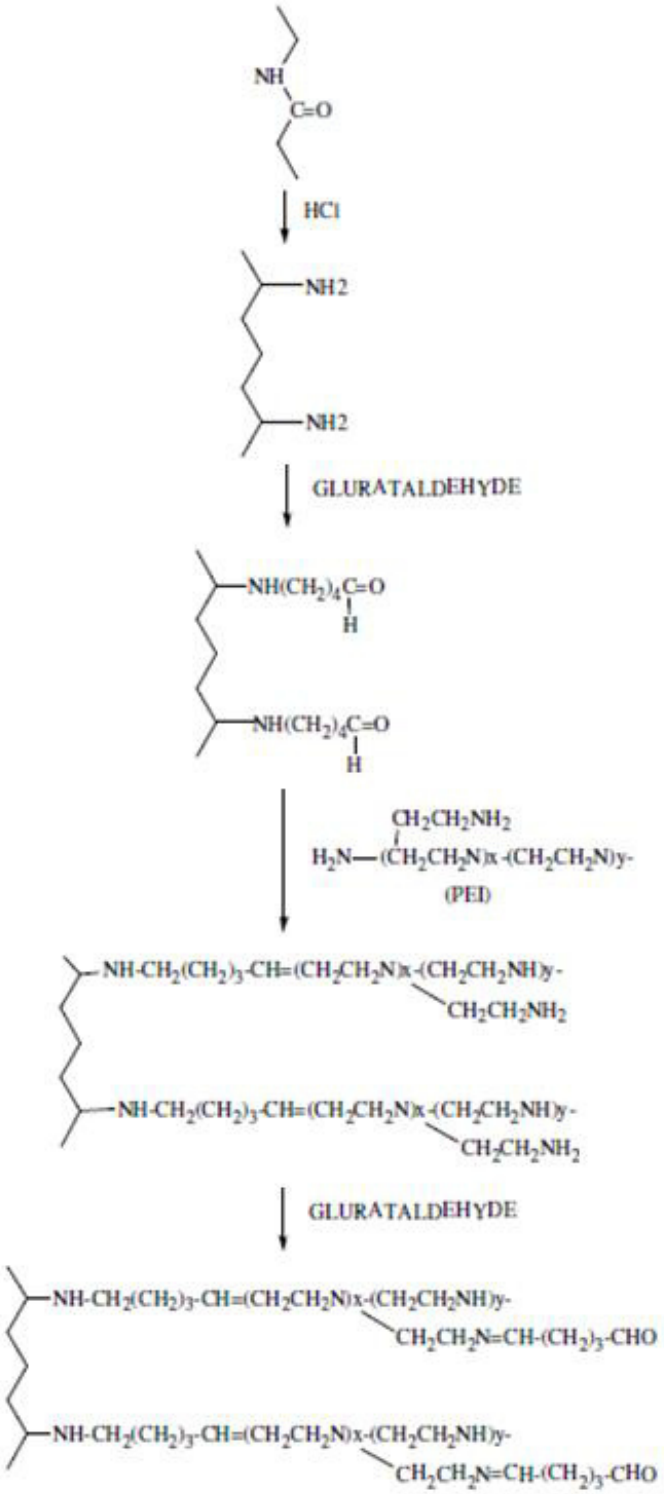

Figure 34. Reaction treatment of polyamide 6 PA6 films for generating aldehyde functional groups (Extracted from a Figure of Pessoa de Amorim (2014)).

similar LCST values. The LCST values obtained with DSC and light scattering measurements (Figure 38) for PNIPAAm linear homopolymers solutions, were similar to the ones obtained by cloud point measurements.

Kano et al. (2009) compared the phase transition behavior of PNIPAAm (PNiPA) gels and linear homopolymers with others based on other N-propylacrylamides (N-n-propylacrylamide – NnPA) and N-propylmethacrylamides (N-isopropylmethacrylamide – NiPMA and N-n-propylmethacrylamide - NnPMA) by performing DSC and transmittance measurements (Table 7 and Figure 39). They arrived to the conclusion that the LCST varies in the polymer aqueous solutions are in accordance to the type of acrylamide monomer used and with following this order NiPMA > NiPA > NnPMA > NnPA and the endotherm peak intensity varies with NnPMA > NnPA ≈ NiPMA > NiPA.

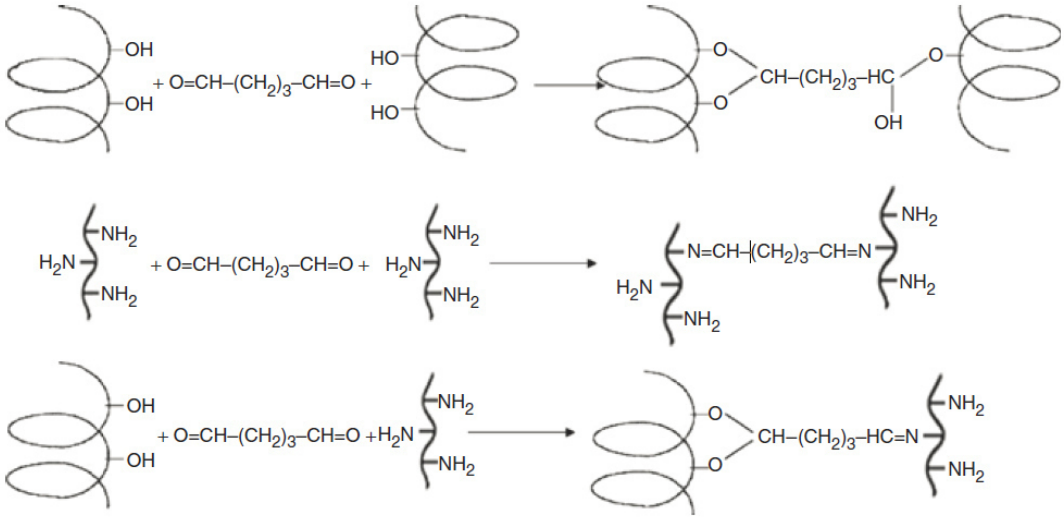

Figure 35. Possible crosslinking reactions between OH groups from CMC, NH2 groups from gelatin chains and the aldehyde groups from the crosslinker glutaraldehyde (Buhus et al. (2009)).

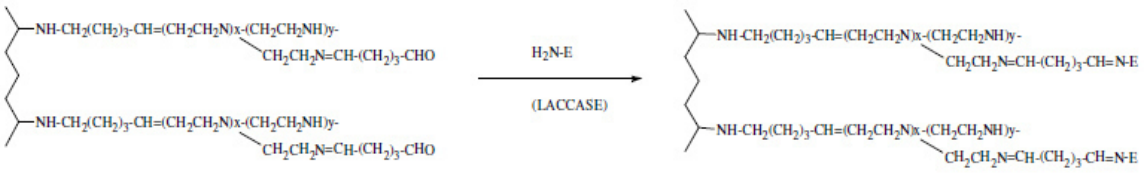

Figure 36. Reaction between aldehyde (CHO) groups of modified PA6 film and amino (H_2N) groups of lacasse enzyme (Extracted from a Figure of Pessoa de Amorim (2014)).

Kokufuta et al. (2012) extended the LCST studies previously made by Kano et al. (2009) to aqueous solutions of copolymers made from NIPAAm (NiPA) and N-isopropylmethacrylamide

(NiPMA). Like in the previous study, they performed DSC measurements and estimated the LCST data from the endotherms obtained. They found that the LCST of the copolymers increased with an increment of the NiPMA quantity present in the copolymer starting from 32 °C (pure NiPA homopolymer) to 42 °C (pure NiPMA homopolymer), however it was mentioned that the isopropyl groups of NiPMA restricted the existence of hydrophilic interactions between the amide groups and water, then the elevation of LCST with the increment of NiPMA monomers in the copolymers is not necessarily translated in an increment of enthalpy at the phase transition temperature LCST.

2.4.2. DSC measurements of LCST in thermosensitive graft copolymers

Li et al. (2008) synthetized graft copolymers cellulose-g-poly(ethylene glycol) with different molecular weights and graft percentages of poly(ethylene glycol) (PEG). They managed to provide a thermosensitive property to the cellulose polymers, in addition to tuning the LCST temperature by varying the amount and molecular weight (or length) of the PEG grafts ($PEG_{1.1K}$ – 1100 g/mol and PEG_{2K} – 2000 g/mol) (Figure 40).

Table 6

PNIPAAm polymer samples and data obtained from measurements to their aqueous solutions (Schild et al. (1990))

Sample	M_w[a] (g/mol)	M_n[a] (g/mol)	M_w/M_n	Cloud Point[b] (°C)	T_{max}[c] (°C)
N1	530,000	146,000	3.7	35.7	35.5
A1	440,000	160,000	2.8	32.2	32.4
R1	400,000	73,000	5.5	33.2	33.5
R2A	160,000	49,000	3.2	33.9	34.0
R2B	76,000	11,000	6.9	34.2	34.1, 35.1
N12	14,000	5,400	2.3	34.3	ca. 35

[a]Estimated with Gel Permeation Cromatography (GPC) in THF and with polystyrene standards. [b]LCST values obtained from optical density measurements. [c]LCST estimated from temperature peak values of endotherms in DSC measurements.

Jin et al. (2013) made thermal sensitive hydroxypropyl cellulose (HPC) by a grafting reaction of the cellulosic backbone with NIPAAm monomers. They used single-electron transfer living radical polymerization (SET-LRP) and they regulate the NIPAAm conversion by using solvents with different water/THF proportions. The solvent with lower water amount, provided a lower NIPAAm conversion. The graft copolymers synthesized, therefore presented different grafts lengths, and because of this feature they managed to regulate the LCST temperature (Figure 41). They demonstrate this last achievement by performing DSC measurements of the different graft copolymer aqueous solutions (Figure 42).

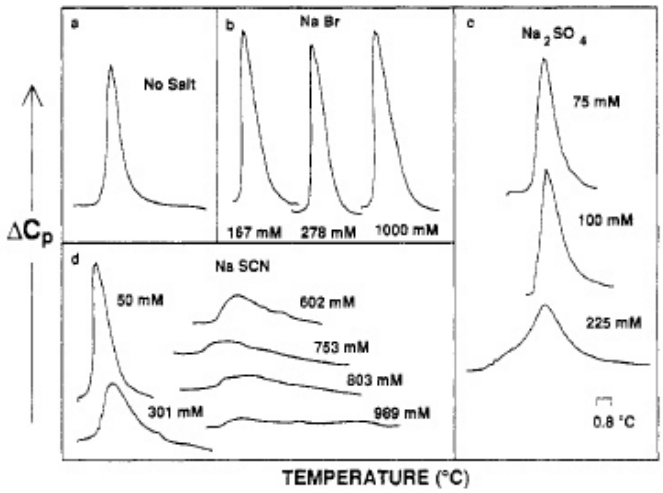

Figure 37. Effect of type of salt and salt concentration shown from microcalorimetric endotherms from DSC measurements performed on aqueous solutions (0.40 mg/mL) of PNIPAAm polymer sample A1: (a) Without salt, (b) with NaBr, (c) with Na_2SO_4 and (d) with NaSCN (Schild et al. (1990)).

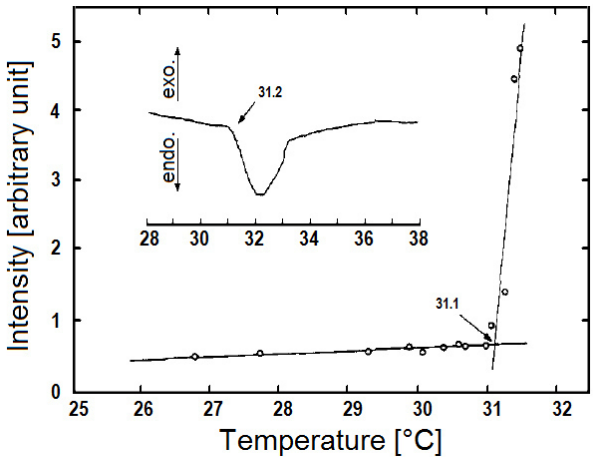

Figure 38. LCST determination in a DSC thermogram embedded in a 90° light scattering analysis for LCST measurement of PNIPAAm linear homopolymer sample aqueous solution (7.8 x 10^{-5} mol PNIPAAm/g sol). The LCST values obtained for this sample (31.2 °C for DSC vs 31.1 °C for light scattering) are similar (Otake et al. (1990)).

Table 7

LCST data obtained from DSC and transmittance measurements on aqueous solutions of PNIPAAm (PNiPA), other N-propylacrylamides and N-propylmethacrylamides (Kano et al. (2009))

Sample	T_c[a] (°C)	T_{c1}[b] (°C)	T_{c2}[b] (°C)
PNiPA	31.2	30.9	32.1
PNiPMA	41.2	41.8	42.0
PNnPA	23.2	23.0	24.5
PNnPMA	27.2	26.9	28.0

[a]LCST estimated from the onset of T% vs temperature graphs in transmittance measurements. [b]Average LCST values obtained from the onset (T_{C1}) and the peak temperature of the endotherm (T_{C2}) in DSC measurements.

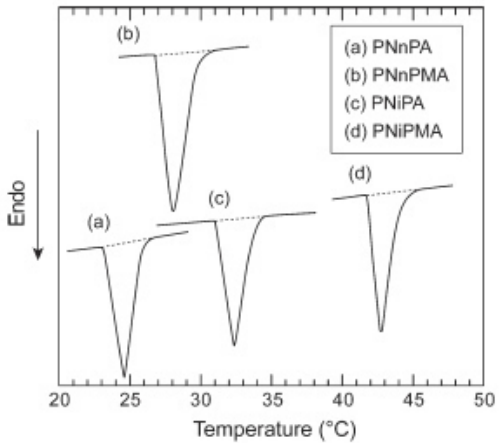

Figure 39**. LCST endotherms determined by DSC measurements of linear homopolymer aqueous solutions (Kano et al. (2009)).**

Guo et al. (2015) synthesized two groups graft copolymers of poly(dimethylacrylamide) (PDMA) and PNIPAAm, the first group had grafts of PDMA (PNIPAAm-g-PDMA) and the second group, grafts of PNIPAAm (PDMA-g-PNIPAAm). From the DSC measurements performed in aqueous solutions of both graft copolymer, it can be observed the different phase transition behaviors present in the graft copolymers (Figure 43).

2.4.3. Thermosensitive swelling degree in comb-type graft hydrogels vs homopolymer gels

Yoshida et al. (1995) evaluated the thermosensitive swelling of their comb-type graft PNIPAAm hydrogels, by measuring the equilibrium swelling (or swelling ratio) in water and at different temperatures, ranging from 10 to 40 °C and compare these results with measurements performed to the PNIPAAm homopolymer gel (Figure 44), showing that under the LCST

temperature, the comb-type graft hydrogel had a higher equilibrium swelling degree and the authors assumed that this was due to the presence of the PNIPAAm grafts that have free polymer chains in contact with water.

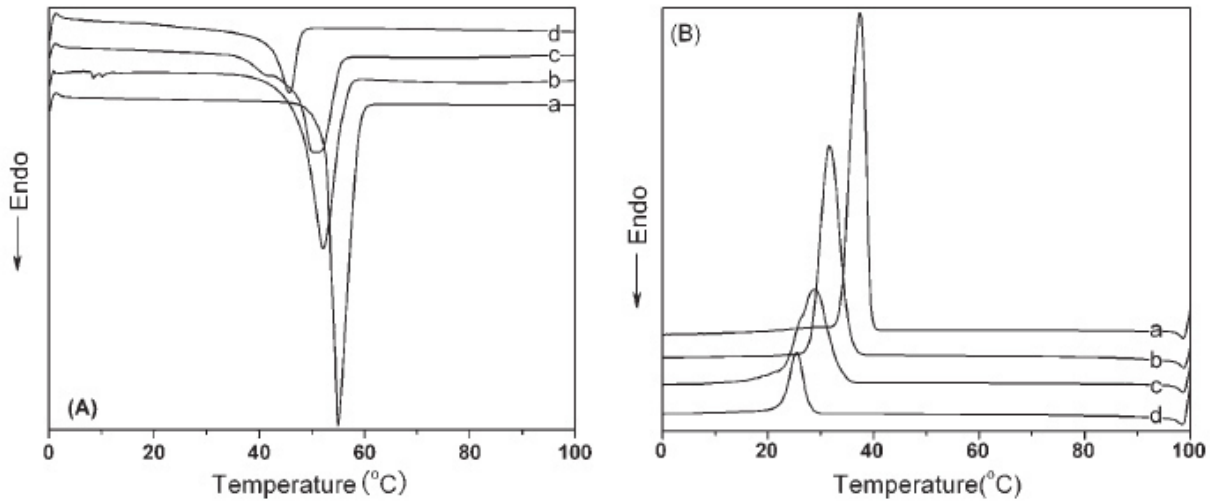

Figure 40. Heating (A) and cooling (B) cycles from DSC measurements showing the variation of LCST temperatures by changing the PEG content in cellulose-g-PEG2k graft copolymers: (a) 100% PEG_{2k}, (b) 94% PEG_{2k}, (c) 85% PEG_{2k} and (d) 50% PEG_{2k} (Li et al. (2008)).

They also evaluated the deswelling kinetics of their PNIPAAm comb-type graft hydrogels and compare their results with measurements, also performed to PNIPAAm homopolymer gels, in water (Figure 44) (Yoshida et al. (1995)). They observed that the deswelling of the PNIPAAm homopolymer gel was slow in comparison with the comb-type graft hydrogel sample. They stated that the deswelling happens first with a shrinking in the surface and then this shrinking is propagated inside de gel, and the water is released due to this collapse (Yoshida et al. (1995)). In the case of the PNIPAAm homopolymer gel, the water release is slow due to the collapse of the external layer of polymer producing water permeation, then the deswelling is slowly. However, the water release in the comb-type graft hydrogel is faster, and therefore the deswelling, due to a strong sagging derived from bigger collapsing gel due to the presence of the grafts, then the water is fast expulsed from the gel.

Kaneko et al. (1995) developed PNIPAAm comb-type graft hydrogels with different molecular weights (or polymer lengths) by using the synthesis method proposed by Yoshida et al. (1995) and measured the thermosensitive swelling. Their results were contrasted with the ones obtained from a PNIPAAm homopolymer hydrogel. They measured the equilibrium swelling at different temperatures (from 10 to 40 °C), and concluded that the movement of the graft chains

influence the swelling degree. Like Yoshida et al. (1995) they concluded that below the LCST temperature the PNIPAAm comb-type graft hydrogels presented a higher deswelling in comparison with the homopolymer hydrogel. With increasing length of the graft, the swelling at low temperatures becomes larger. The equilibrium swelling of the gels can be tuned by controlling the length of the grafts (Figure 45).

From the measured swelling degree of the samples at 10 °C in water (Figure 45), they presented almost equal swelling kinetics. This was due at 10 °C the grafts are “frozen” and therefore cannot contribute to the swelling and the hydration of the comb-type graft hydrogels. Therefore the swelling process was governed by the backbone network, and since all of the sample have the same PNIPAAm backbone network, similar swelling kinetics were expected (Figure 46) (Kaneko et al. (1995)).

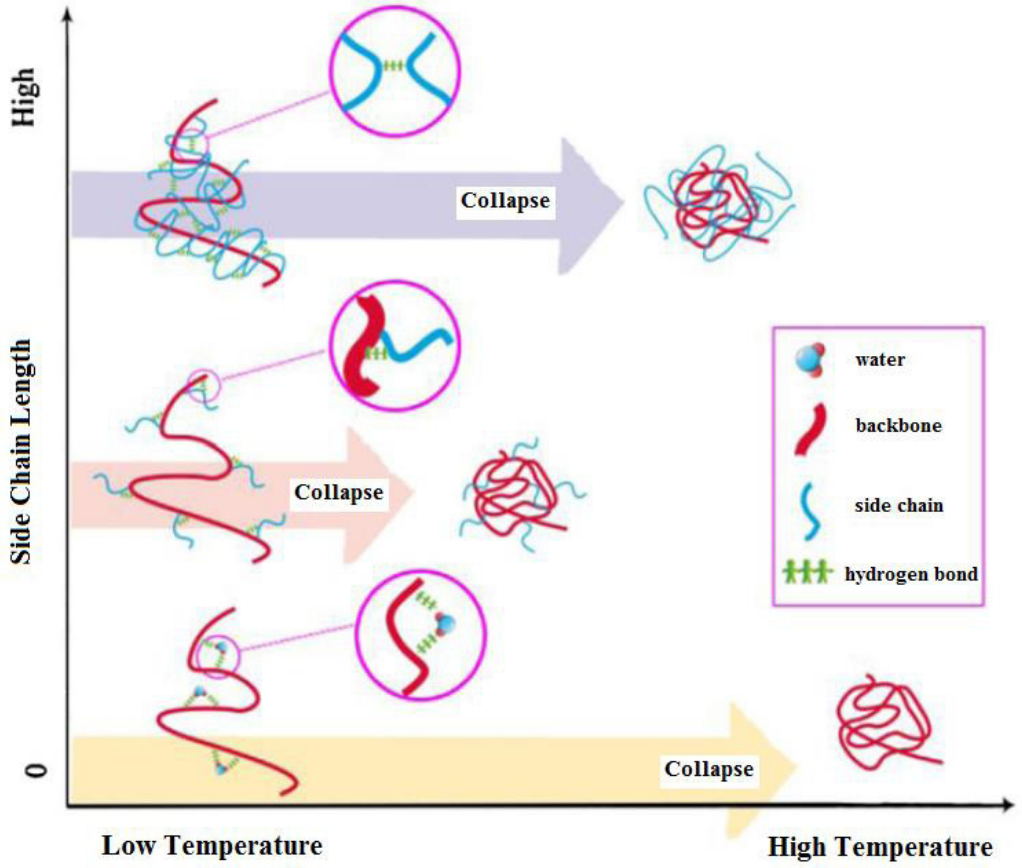

Figure 41. LCST tunning of HPC-g-PNIPAAm by changing the length of the PNIPAAm grafts (Jin et al. (2013)).

Kaneko et al. (1999) also developed PNIPAAM homopolymer hydrogels (IP-NG) and hydrogels based on PNIPAAM and poly(N,N-dimethylacrylamide) (PDMAAM) copolymers: A non grafted poly(NIPAAM-co-DMAAM) (ID-NG), a comb-type graft poly(NIPAAM-co-DMAAM)

grafted with PNIPAAm (IP-GG) and a comb-type graft PNIPAAm grafted with poly(NIPAAM-co-DMAAM) (ID-GG) hydrogels. They measured the equilibrium swelling between 10 and 50 °C (Figure 46). The results showed that the gels deswelled at temperatures over the LCST, also the gels presented transparency at the swelling and deswelling state, which indicate that no large polymer aggregation were formed.

The inclusion of the DMAAM comonomer contributed to increase the LCST for the deswelling and the decreasing of the LCST for the swelling equilibria (Kaneko et al. (1999)). They explained that this comonomer interfered with the collapse of the PNIPAAm segments in the backbone and therefore higher LCST were observed in the ID-NG sample in comparison with IP-NG, and the comb-type graft variation ID-GG showed a more marked phase transition in comparison with homopolymer type ID-NG and in the case of the sample with PNIPAAm grafts IP-GG, the displacement of the LCST is even higher in comparison with the ID-NG sample.

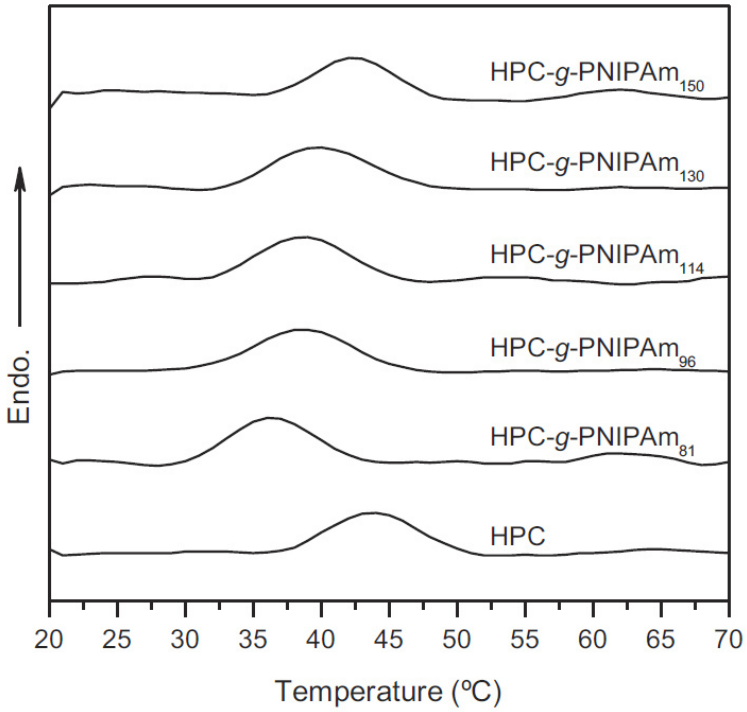

Figure 42. LCST tunning demonstrated by DSC thermograms of HPC and HPC-g-PNIPAAm with different PNIPAAm graft lengths (150, 130, 114, 96 and 81). The graft length is represented by the numerical subindex written at the end of the polymer name (Jin et al. (2013)).

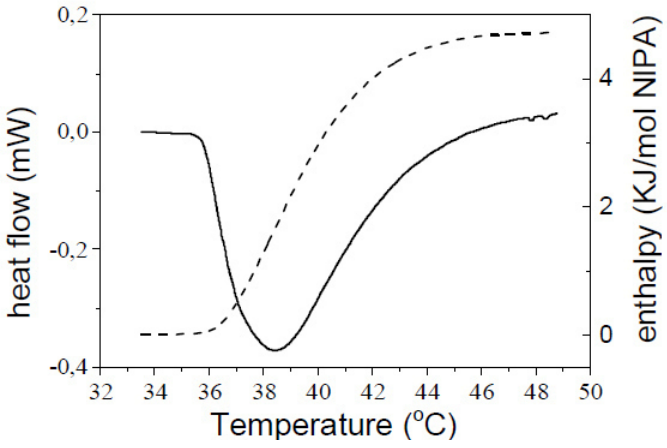

Figure 43. DSC measurements of PNIPAAm-g-PDMA (dash line) and PDMA-g-PNIPAAm (solid line) aqueous solutions. PNIPAAm-g-PDMA sample showed the lowest LCST (36°C) while PDMA-g-PNIPAAm, an LCST of 38 °C (Guo et al. (2015)).

The deswelling kinetics between two different temperature values (10-50 °C) were measured (Figure 47 and 48) (Kaneko et al. (1999)). The non-grafted sample ID-NG presented faster deswelling kinetics in comparison with the grafted samples for measurements until a maximal value of 36 °C, but it turned slower for temperatures higher than 38 °C. This could be explained because of the external layer collapse and a permeation blocking effect to the water released. In the case of the grafted samples the deswelling was accelerated with increasing temperature. Ju et al. (2001) elaborated comb-type graft hydrogels (GAN) of alginate grafted with PNIPAAM oligomers and semi-interpenetrated network or semi-IPN (IPN) hydrogels composed of alginate polymers and aminoterminated PNIPAAM oligomers and compared the performance of both structures. A higher swelling equilibrium can be achieved with a higher amount of PNIPAAm graft chains and a lower amount of crosslinkable alginate (Figure 49). They also measured the deswelling kinetics (Figure 50) of the comb-type graft hydrogels and compared these results with the measurements performed to a semi-IPN hydrogel with 50% alginate content (IPN55) (Ju et al. (2001)). The author claimed that the fast deswelling equilibrium achieved by the comb-type graft hydrogels was due the free movement of the PNIPAAM graft chains, that over the LCST contribute to a marked hydrophobic aggregation of the chains, increasing the pore volume of the hydrogel and with this contributing to a fast release of water. Thermosensitive pulsatile measurements between 25 and 40 °C were also performed (Figure 51) (Ju et al. (2001)). The authors confirmed with these measurements that the swelling and deswelling was repetitive and reversible.

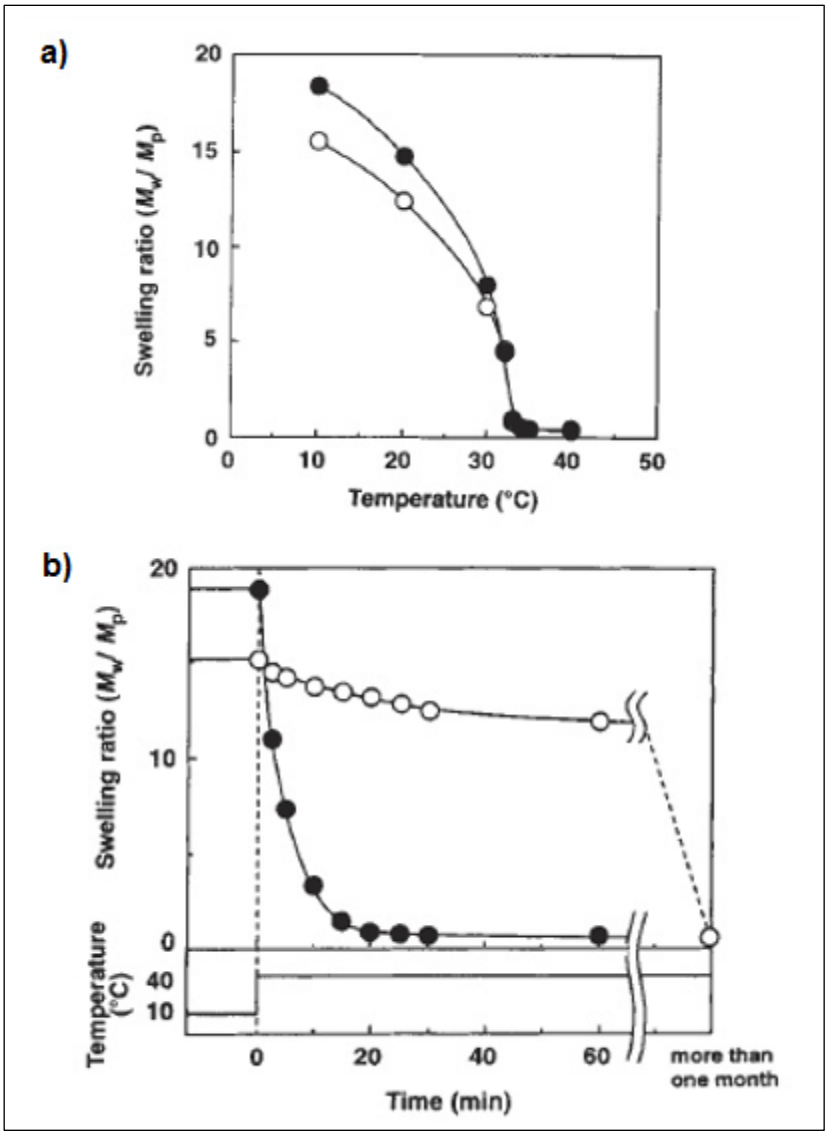

Figure 44. a) Equilibrium swelling (swelling ratio) at different temperatures for the PNIPAAm homopolymer (○) and comb-type graft (●) gels. Swelling ratio is described as weight of absorbed water per weight of dried gel sample (M_w/M_p) (Yoshida et al. (1995)). b) Deswelling kinetics (measured as swelling ratio) at 40 °C (starting from an equilibrium swelling at 10 °C) of PNIPAAm homopolymer (○) and comb-type graft (●) gels (Yoshida et al. (1995)).

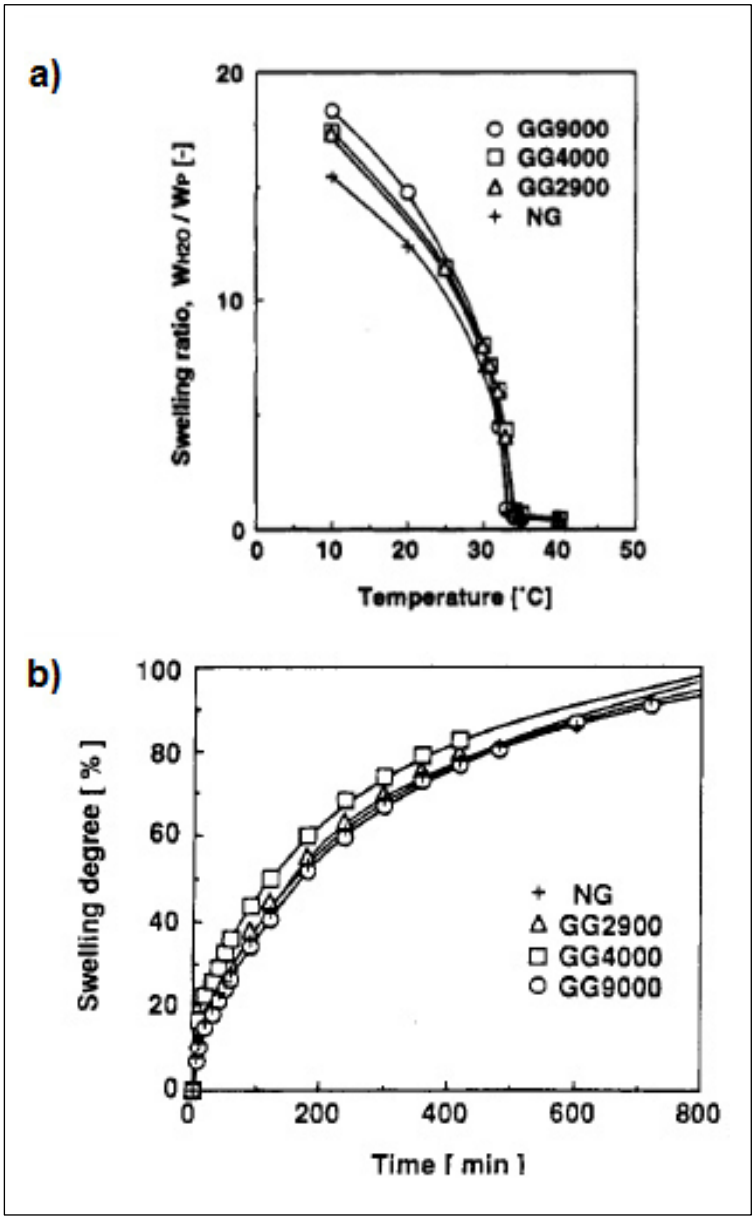

Figure 45. a) Deswelling kinetics (measured as swelling ratio) at different temperatures (starting from an equilibrium swelling at 10 °C) of PNIPAAm homopolymer (NG) and comb-type graft with 2900 g/mol graft chain length (GG2900), 4000 g/mol graft chain length (GG4000) and 9000 g/mol graft chain length (GG9000) hydrogels (Kaneko et al. (1995)). b) Swelling degree at 10 °C (starting from an equilibrium swelling at 10 °C) of PNIPAAm homopolymer (NG) and comb-type graft with 2900 g/mol graft chain length (GG2900), 4000 g/mol graft chain length (GG4000) and 9000 g/mol graft chain length (GG9000) hydrogels (Kaneko et al. (1995)).

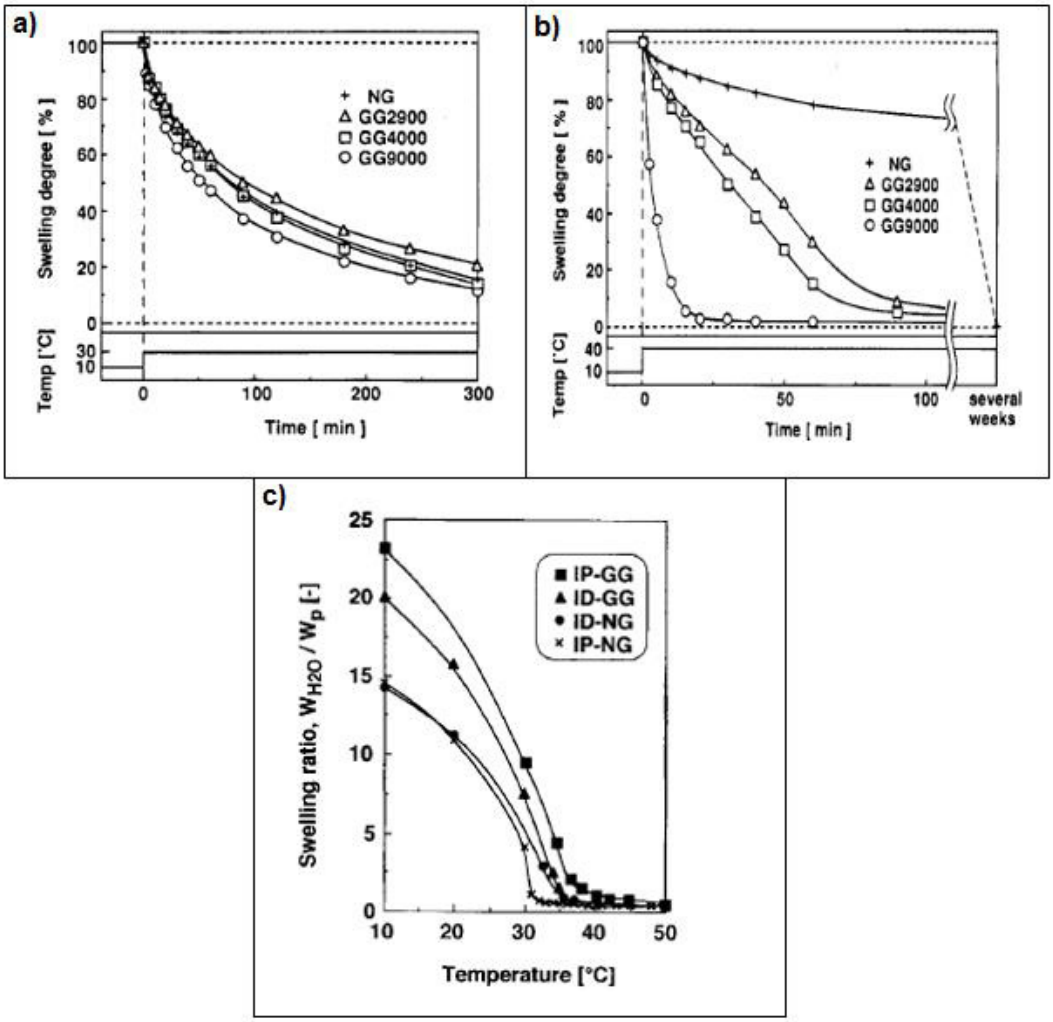

Figure 46. Deswelling kinetics (measured as swelling degree) at: a) 30 and b) 40 °C (starting from an equilibrium swelling at 10 °C) of PNIPAAm homopolymer (NG) and comb-type graft with 2900 g/mol graft chain length (GG2900), 4000 g/mol graft chain length (GG4000) and 9000 g/mol graft chain length (GG9000) hydrogels (Kaneko et al. (1995)). c) Deswelling kinetics (measured as swelling ratio) at different temperatures (starting from an equilibrium swelling at 10 °C) of non-grafted (IP-NG and ID-NG) and comb-type graft (ID-GG and IP-GG) hydrogels (Kaneko et al. (1995)).

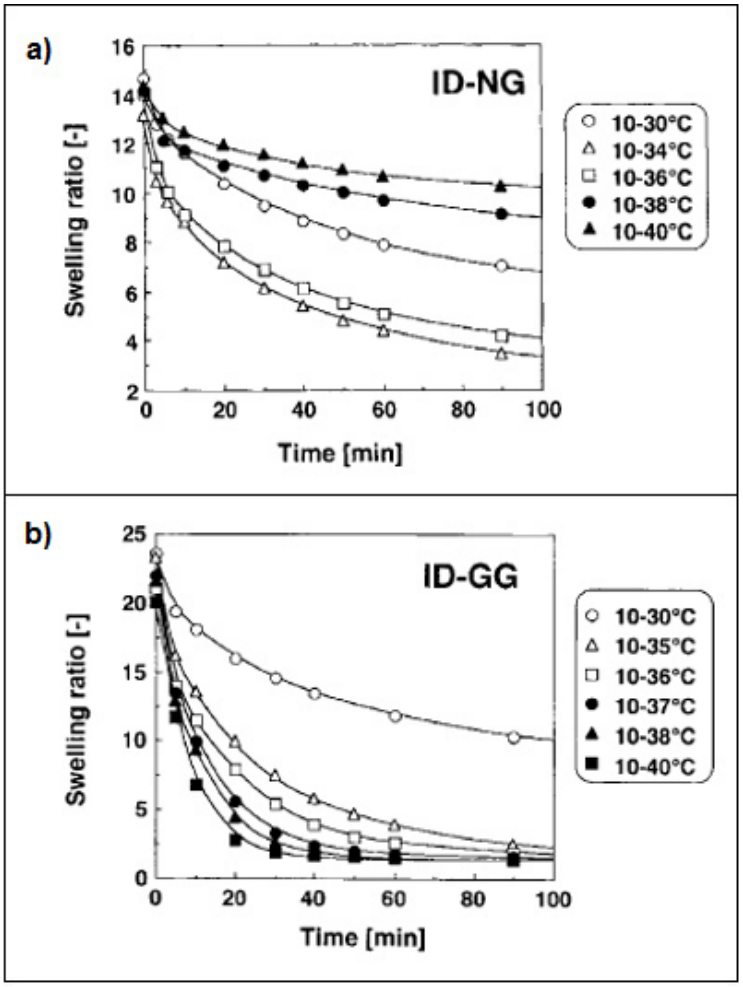

Figure 47. a) Deswelling kinetics (measured as swelling ratio) between 30 and 40 °C (starting from an equilibrium swelling at 10 °C) for non grafted ID-NG hydrogels (Kaneko et al. (1999)). b) Deswelling kinetics (measured as swelling ratio) between 30 and 40 °C (starting from an equilibrium swelling at 10 °C) for comb-type graft ID-GG hydrogels (Kaneko et al. (1999)).

2.4.4. Stimulus-sensitive actuation in bilayers measured by digital photographs

As a first example of measurement from stimulus-sensitive actuation in bilayer actuators, Feinberg et al. (2007) measured with digital photographs (Figure 52) the electrical-sensitive actuation of their robotic grippers (bilayer actuators), which were composed of polydimethylsiloxane (PDMS) elastomer thin film and a layer of myocardium tissue (cardiac muscle). When the contraction is produced due to an electric pulse, both extremes (yellow circles) of the robotic gripper touch each other after 0.60 seconds.

The humidity sensitive-actuator bilayers of 30 PAA/PAH bilayers ((PAA/PAH)*30) and mercapto ester prepolymer crosslinked with UV (NOA 63) made by Ma et al. (2011) were tested against decrements and increments of relative humidity (Figure 53). For all tests one end of the bilayer was fixed (Ma et al. (2011)). In the first test, relative humidity was decremented from 12 to 5%, and exhibited as a consequence a shrinking of the (PAA/PAH)*30 active layer, while the NOA 63 passive layer remained unaltered (Ma et al. (2011)). This shrinking difference produced an interfacial stress between the two layers and as a result after 9 seconds a bending of the bilayer from left to right was produced (Figure 53-left column). The second test (made on the same sample) was started immediately after the first one, by incrementing the relative humidity from 5 to the original level of 12% (Ma et al. (2011)). This increment in the relative humidity allowed a swelling of the (PAA/PAH)*30 active layer due to water absorption, a bending from right to left was produced and the initial position of the actuator was achieved after 27 seconds (Figure 53-right column).

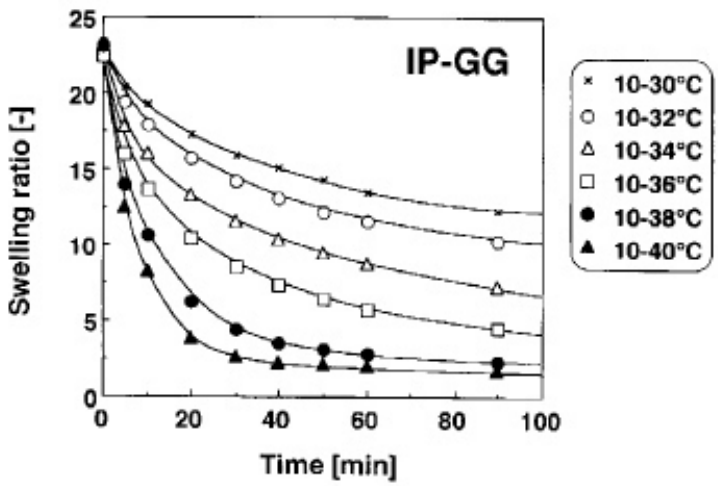

Figure 48. Deswelling kinetics (measured as swelling ratio) between 30 and 40 °C (starting from an equilibrium swelling at 10 °C) for comb-type graft IP-GG hydrogels. (Kaneko et al. (1999)).

Dai et al. (2013) synthesized a humidity-sensitive actuator composed of polyamide 6 (PA6) and a liquid crystal (LC) bilayer. The bilayer was placed in a humidity chamber, and a relative humidity gradient was produced. Figure 54 shows that the actuator had a major bending on the side of the LC, therefore humidity does not influence the PA6 layer. The bending is produced after 15 seconds. The bending is heterogenous, probably because of surface flaws at the edge of the bilayer.

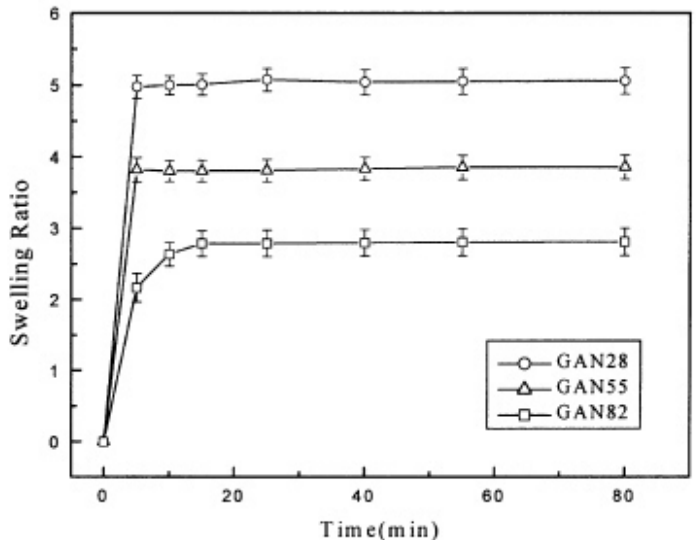

Figure 49. Swelling kinetics (measured as swelling ratio) at 25 °C in pH=5.4 aqueous solutions of comb-type graft hydrogels (samples GAN28, GAN55 and GAN82) (Ju et al (2001)).

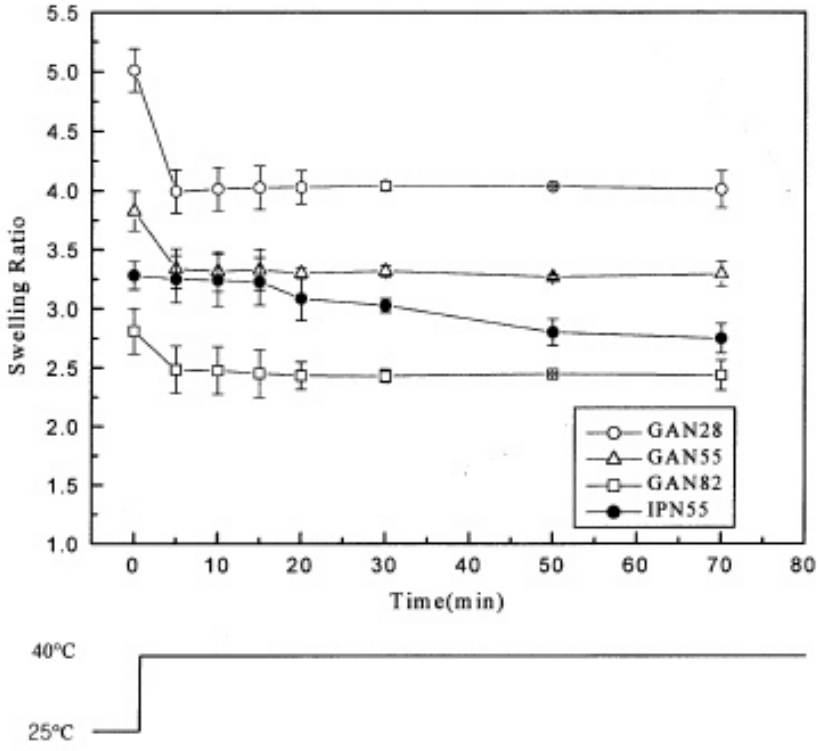

Figure 50. Deswelling kinetics (measured as swelling ratio) in water at 40 °C (starting from an equilibrium swelling at 25 °C) of comb-type graft (samples GAN28, GAN55 and GAN82) and semi-IPN (sample IPN55) hydrogels (Ju et al (2001)).

The pH and ionic strength sensitive reversible actuation of the PA6/poly(PNIPAAM-co-PAA)-g-CMC hydrogel bilayer actuator developed by Haldorai et al. (2014), was tested (and registered with photos) in water (Figure 55 – row (b)) and immediately after in ethanol (Figure 55 – row (c)). While curving of the bilayer in water happened due to swelling of the PNIPAM-co-PAA hydrogel by water absorption, the counter-curving in ethanol happened due of dissolving of water by ethanol, producing the release of water from the hydrogel layer and therefore deswelling. [19]

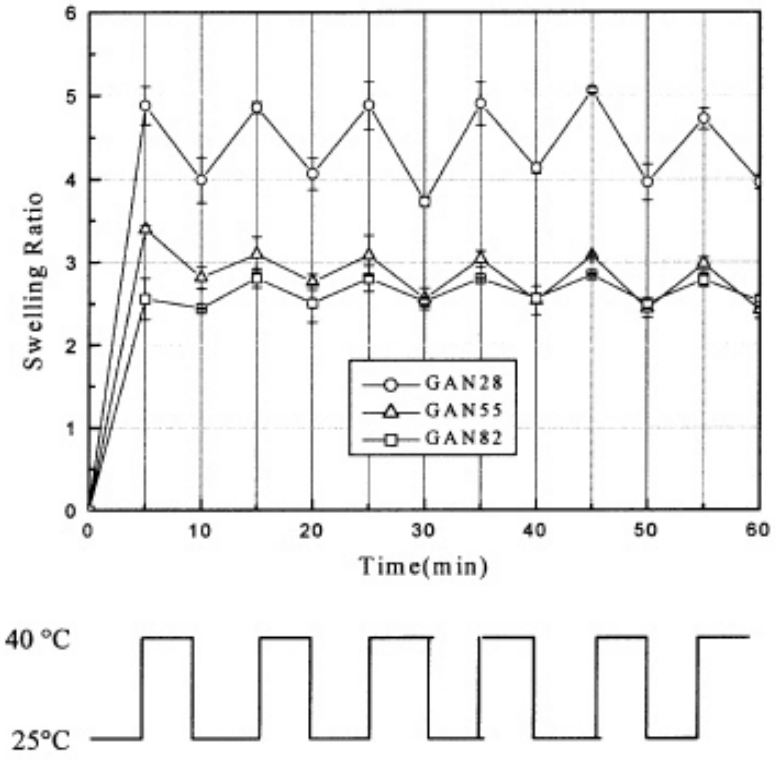

Figure 51. Thermosensitive pulsatile measurements in water and between 25 and 40 °C of comb-type graft (samples GAN28, GAN55 and GAN82) hydrogels (Ju et al (2001)).

2.4.5. Quantitative measurement of stimulus-sensitive actuation in bilayers from digital photographs

Feinberg et al. (2007) applied to their electrical-sensitive bilayer actuators (robotic grippers) a controlled pacing frequency from 0.25 to 5.0 Hz in order to regulate the systolic curving of the bilayer and keep a maximum tip separation (yellow circumferences in Figure 52). Instead of an instantaneous open- close movement, the bilayer went from an diastolic open state to a systolic closed state by incrementing the pacing rate until the total contact of the tips was achieved at 5.0 Hz (Figure 56).

The deflection angles versus time of the humidity sensitive actuator bilayers developed by Ma et al. (2011) were measured for decrements and increments of relative humidity (Figure 57). They observed that in every measurement the bilayer first curved 57° in 4 seconds (Figure 57 - top) and then needed 8 seconds to uncurve until its initial position (Figure 57 - bottom). These measurements demonstrated the reversible character of the actuation in these bilayers.

Dai et al. (2013) quantified the humidity-sensitive actuation of their polyamide 6 (PA6)/liquid crystal (LC) bilayers. In a humidity chamber for different relative humidity (RH) values,

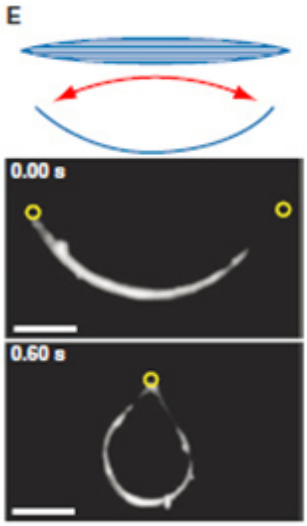

Figure 52. Bilayer actuators (robotic grippers) sensitive to electric pulses applied to the structure at different frequencies. (E) The robotic "gripper" was a rectangular PDMS thin film, provided on the concave side of it with longitudinally aligned myocardium tissue, the tips (yellow circunferences) of the gripper joined together during contraction of the muscle due to electric pulse. Scale: 1 mm (Extracted from a figure shown in Feinberg et al. (2007))

they measured the correspondent curvature (1/inverse radius r) of the bilayer, they estimated a high curvature for low RH values and the bilayer was curved with the PA6 layer located outside of the curve Figure 58. The bilayer turned flat as the RH was increased, implying less bending. The test was repeated two times in order to establish the reproducibility and reversibility of the actuation.

Haldorai et al. (2014) measured the pH and ionic strength sensitive reversible actuation of their PA6/poly(PNIPAAM-co-PAA)-g-CMC hydrogel bilayer actuators, by estimating from the actuation photos, the K (curvature=1/radius) value (Figure 59). From these results, they deduced that the curving in water needed more time than the uncurving in ethanol.

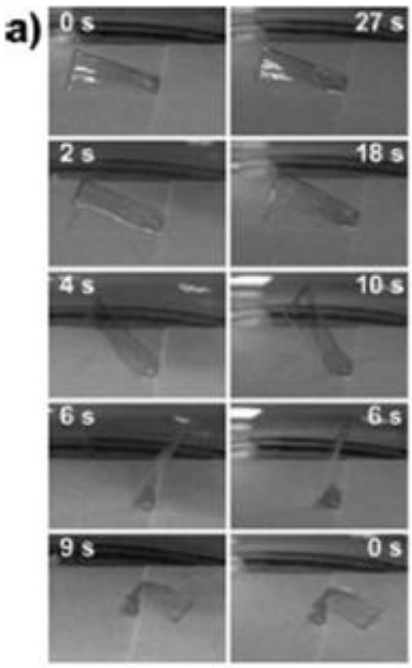

Figure 53. a) Folding and unfolding of (PAA/PAH)*30/NOA 63 bilayer actuator (0.5 X 0.8 cm) measured time outlines versus different relative humidity (RH) values. Left column: Relative humidity decreased from 12 to 5% RH. Right column: Relative humidity increased from 5 to 12% RH. (Extracted from a figure shown in Ma et al. (2011))

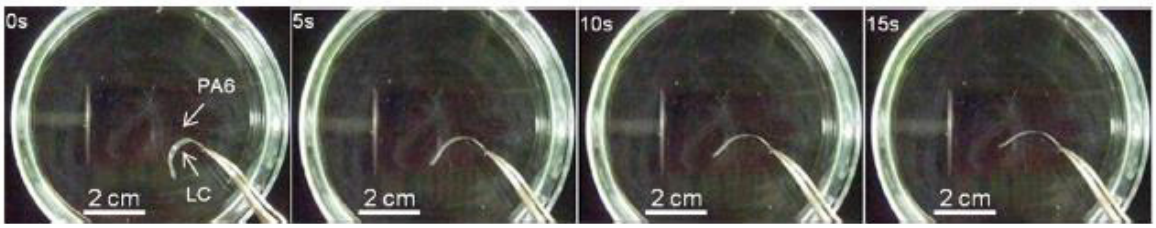

Figure 54. Humidity sensitive actuation of the PA6/LC bilayer after activation in basic solution and exposition to water vapor (Dai et al. (2013)).

Figure 55. (Rows b and c) photos during the folding in water of the bilayer actuator (Photos (i) to (vi) taken each 102 s) and in ethanol for the unfolding ((i) to (vi) taken each 66 s) (Extracted from a figure shown in Haldorai et al. (2014)).

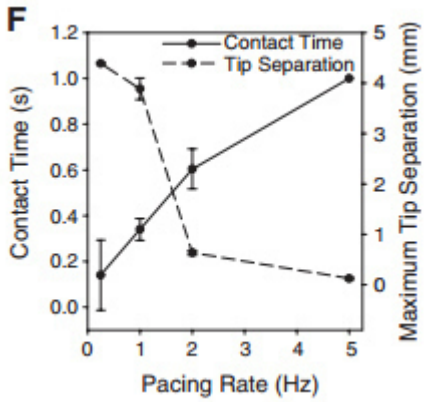

Figure 56. Bilayer actuators (robotic grippers) sensitive to electric pulses applied to the structure at different frequencies. (F) Measurement of actuation expressed in terms of maximum tip separation and its correspondent contact time, for different frequencies (pacing rate) of applied electric pulses (pacing rate). The tips are the extremes of the bilayer presented as yellow circunferences in Figure 52 (Extracted from a figure shown in Feinberg et al. (2007))

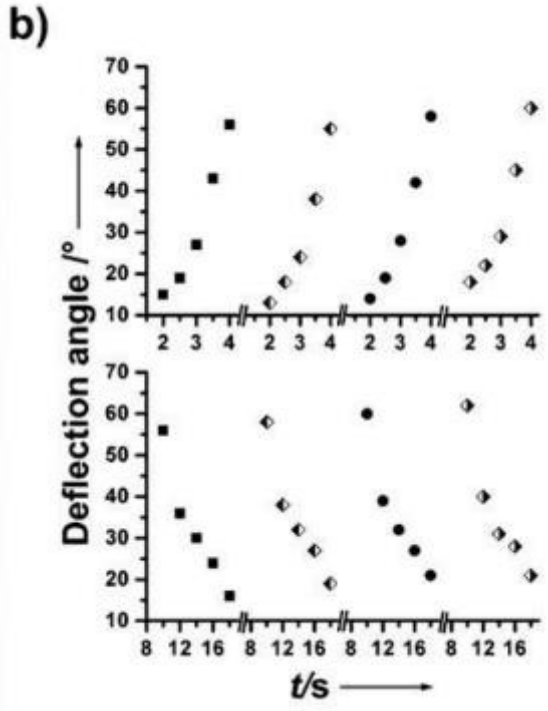

Figure 57. b) Bending angles (deflection angles) vs time of (PAA/PAH)*30/NOA 63 bilayer actuator (0.5 X 0.8 cm) measured when relative humidity decreased from 12 to 5% RH (top) and relative humidity increased from 5 to 12% RH (bottom). Measurements made from actuation photos of Figure 53. (Extracted from a figure shown in Ma et al. (2011))

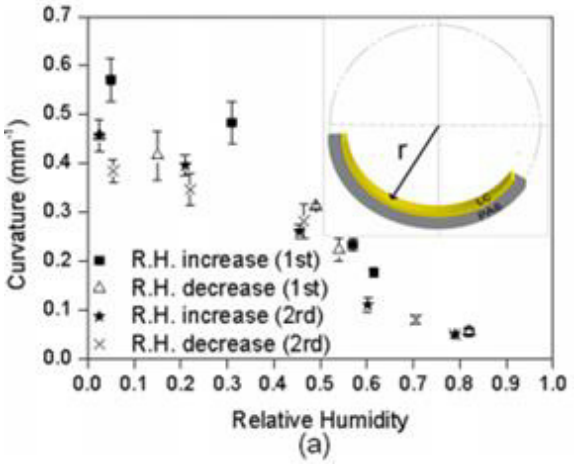

Figure 58. Curvature of a PA6/LC bilayer versus relative humidity. Testing was done two times. First the relative humidity was incremented and then decremented in order to see the respective reactive actuation. The embedded figure shows the deflection radius r defined for the bilayer actuator (Extracted from a figure shown in Dai et al. (2013)).

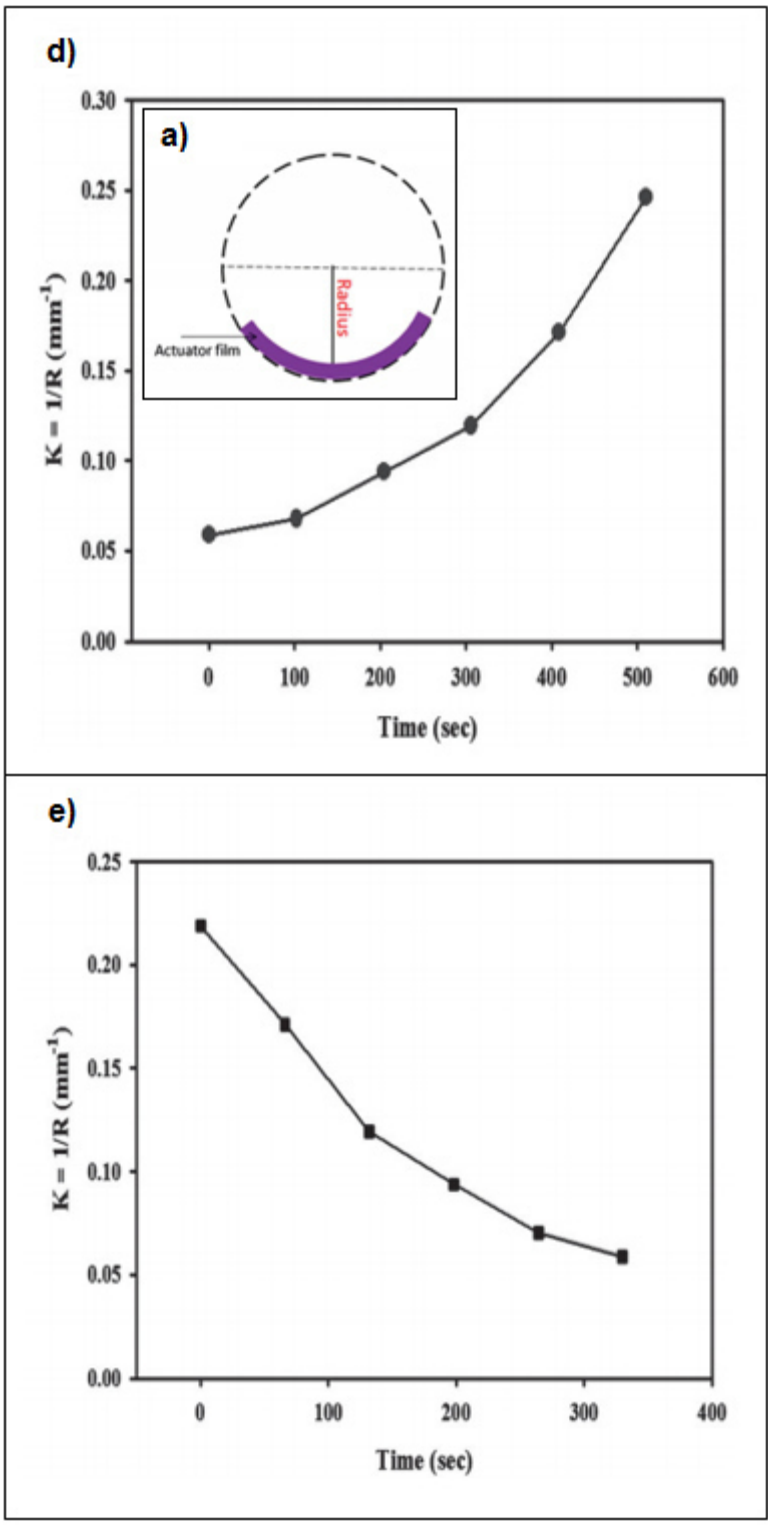

Figure 59. (a) Determination of the R of curvature. Curvature (K=1/R) versus time measured during (d) the folding in water of the bilayer actuator (photos (i) to (vi) from Figure 55 taken each 102 s) and (e) in ethanol for the unfolding (photos (i) to (vi) from Figure 55 taken each 66 s) (Extracted from a figure shown in Haldorai et al. (2014)).

They assumed that this occurred because water needed more time to be absorbed by diffusion to the hydrogel layer, than the time it needed for its release due to a good miscibility between water and ethanol.

In the present work, for the first time, a thermosensitive bilayer actuator is successfully fabricated by crosslinking CMC-g-PNIPAAm graft copolymers with aldehyde-activated PA6 and using citric acid as a crosslinking agent. Also a new comb-type graft hydrogel material with temperature sensitivity is manufactured by grafting aminoterminated PNIPAAm oligomers onto CMC, then mixing the resulting graft copolymers with HEC and finally crosslinking the mixture system with citric acid. The actuation properties of the manufactured bilayers and the swelling behavior of the comb-type graft hydrogels are evaluated at different temperatures and pH values.

Neither thermosensitive bilayer actuators based on CMC polymers nor interfacial chemical bonding with citric acid between a CMC based hydrogel active layer and a PA6 passive layer were never been reported before. Only chemoresponsive CMC based bilayer actuators have been fabricated (Haldorai et al. (2014)) and interfacial photocrosslinking with UV-radiation between CMC based hydrogel active layers and PA6 substrates have been performed (Haldorai et al. (2014)).

3. Experimental Part

3.1. Analytical Methods

3.1.1. FTIR spectroscopy (ATR and KBr pellets)

0.5 mg of the respective compound (aminoterminated PNIPAAm oligomers or CMC-g-PNIPAAm graft copolymers) were mixed and milled in a mortar with 300 mg of dry potassium bromide (KBr), and pressed into pellets. CMC-g-PNIPAAm comb-type graft hydrogels, functionalized (or not) PA6 substrates and samples of bilayer actuators were prepared as films for Attenuated Total Reflectance (ATR) measurements.

Both, pellets and films, were analyzed in a FT-IR spectrometer Nicolet 380 with resolution of 4 cm^{-1}, with 32 scans and a wavenumber range from 4000 cm^{-1} to 450 cm^{-1}.

3.1.2. Nuclear Magnetic Resonance (NMR)

NMR samples were prepared by dissolving 4 mg of the respective compound (aminoterminated PNIPAAm oligomer) in 0.6 mL of deuterated chloroform ($CDCl_3$). 400 MHz ^1H NMR spectra of each sample were measured in a NMR spectrometer (Jeol JNM-ECS400, Jeol Ltd.) at room temperature.

3.1.3. Elemental Analysis

For determination of molecular weight (for oligomers and graft copolymers), degree of polymerization (for oligomers), graft percentage and number of grafts per CMC chain, samples between 1-3 mg (for CHNS element analysis) and 1-2 mg (for O element analysis) of aminoterminated PNIPAAm oligomers (or CMC-g-PNIPAAm graft copolymers (after soxhlet extraction)) were weighed. For inspection of the carbon weight percentages (%C) to validate functionalization, samples between 1-3 mg (for CHNS element analysis) of functionalized PA-6 substrates were also weighed. The weighed samples were wrapped in zinc cartridges (for CHNS element analysis) and in silver cartridges (for O element analysis).

The wrapped samples were measured in an elemental analyser (Euro EA 3000, HEKAtech GmbH) for determining the weight percentage of CHNS and O atoms.

Data analysis of the results corresponding to CMC-g-PNIPAAm graft copolymer samples, was performed by using a correlation formulated by Touzinsky et al. (1979) (Detailed data analysis procedures from these and other samples (and their replicas) are listed in in Appendix I (See section 9. Appendix I: Protocols).

3.1.4. Gel Permeation Cromatography (GPC)

5 mg of aminoterminated PNIPAAm oligomers (or pullulan standards) were dissolved in DMSO for preparing 5 mL of 1 mg/mL sample solutions (or standard solutions). Lithium nitrate was

dissolved in DMSO for preparing 5L of 0.075 M eluent solution. The molecular weight and polydispersity of aminoterminated PNIPAAm oligomers were measured by injecting the standards, samples and eluent solutions at 50 °C and with a flow rate of 0.4 mL/min, in a GPC equipment (EcoSEC GPC Instrument, Tosoh Bioscience GmbH) equipped with three columns from PSS Polymer Standards Service GmbH (PSS GRAM Vorsäule, PSS GRAM 30 A and PSS GRAM 1000 A) and one column from AppliChrom® (AppliChrom ABOA DMSO-Phil-P-300). The detection outside the column was performed by using a refractive index detector (PSS SECcurity RI, PSS Polymer Standards Service GmbH).

3.1.5. Differential Scanning Calorimetry (DSC)

Thermal analysis was performed on NIPAAm monomer, aminoterminated PNIPAAM oligomers, CMC polymer, CMC-g-PNIPAAm graft copolymers and CMC-g-PNIPAAm comb-type graft hydrogels, by using two differential scanning calorimeters (DSC): A Mettler Toledo TA Instrument DSC12E and a Mettler Toledo DSC 3+, both operated with a heating rate of 10 °C min^{-1} and under N_2 atmosphere. The analysis was operated with dried samples (with weigths between 3-4 mg) and with 7 %w/w aqueous (and buffer) sample solutions (with weights between 16-17 mg). Each of the dried samples and aqueous sample solutions were placed in preweighted-empty aluminium pans (Mettler Toledo) and then sealed with covering pans. The data analysis for the DSC scans was performed by using two softwares: Mettler Toledo System Software TA89A (for the DSC12E) and STARe Evaluation software (for the DSC 3+).

Dried samples. The thermal properties of each of the dried samples were measured by using three scans: The first scan started with a 5 min isotherm at -5 °C and a preheating until 40 °C, the second scan was a cooling until -5 °C and the third scan, which was the measuring scan, started with a 5 min isotherm at -5 °C and ended with a heating until 380 °C. The three scans were performed at a heating rate of 10 °C min^{-1}. The glass transition temperatures (T_g), the melting point (T_m) and the enthalpy associated with the melting of the samples were calculated. For the calculation of T_g, and T_m, were used the values that appeared from the third scan and the onset temperature and the peak of the melting signal were used.

Aqueous (and buffer) sample solutions. Thermal properties of each of the aqueous (and buffer) sample solutions were measured by using three scans: The first scan started with a 5 min isotherm at -5 °C, a preheating until 90 °C, the second scan was a 5 min isotherm at 90 °C and a cooling until -5 °C and the third scan, started again with a 5 min isotherm at -5 °C and ended with a heating until 90 °C. The three scans were also performed at a heating rate of 10 °C min^{-1}. The lower critical solution temperature (LCST) was calculated. For the calculation of the LCST were used the values that appeared from the second and third scans. Buffer solutions were prepared from mixtures of 0.05 M $NaHCO_3$ and 0.2 M KCl with: 0.2 M NaOH

(for buffer pH=12) and 0.1 M NaOH (for buffer pH=10). Also were mixed 0.1 M KH_2PO_4 with 0.1 M NaOH (for buffer pH=7) and 0.1 M potassium hydrogen phthalate with 0.1 M HCl (for buffers pH=3.5, 3, 2.5 and 2). For the exact quantities used for each buffer solution, please refer to Table 36 in Appendix II (See section 10. Appendix II: Tables).

3.1.6. Equilibrium Swelling Ratio

A circa 2mm x 3mm x 0.5mm dried CMC-g-PNIPAAm comb-type graft hydrogel film (sample CCH-C3(8)MONO-1(Al).1) was weighed (0.164 g) and immersed in a water bath, at room temperature and at different time intervals (10, 30, 30, 30, 30, 60 and 180 minutes). The sample was then removed from the bath, excess water on the surface of the swollen gel was removed with a paper towel, and finally the sample was weighed. This procedure was repeated until no change in the weight of the swollen gels was registered. The Swelling Degree (%) was calculated by using the following equation:

$$\text{Swelling Degree (\%)} = \frac{(\text{Weight}_{\text{swelled}} - \text{Weight}_{\text{dried}})}{\text{Weight}_{\text{dried}}} \times 100 \quad \text{.....(1)}$$

Where:
Swelling Degree: Swelling Degree of a hydrogel sample at a specific period of time
$\text{Weight}_{\text{swelled}}$: Weight of swelled hydrogel sample at a specific period of time
$\text{Weight}_{\text{dried}}$: Weight of dried hydrogel sample

3.1.7. Equilibrium Temperature-Responsive Swelling Behavior

Two circa 2mm x 3mm x 0.5mm dried CMC-g-PNIPAAm comb-type graft hydrogel films (samples CCH-C3(8)MONO-1(Al).1 and CCH-C3(8)MONO-1(CA).2), were weighed (0.096 and 1.277 g) and immersed in a water bath at room temperature overnight. At the next day, the samples were taken out from the bad and weighed (0.557 and 6.260 g). After that, they were immersed at different time intervals, in a water (sample CCH-C3(8)MONO-1(Al).1) and in a buffer solution pH=3 (sample CCH-C3(8)MONO-1(CA).2) baths and both of them were at 80 °C. The samples were then taken out from their respective baths, water and buffer solution excess on the surface of the swollen gels were removed with a paper towel, and finally samples were weighed. This procedure was repeated until no change in the weight of the swollen gels was registered. The Swelling Degree (%) was calculated by using equation (1).

3.1.8. Pulsatile Temperature-Responsive Swelling Behavior

Two circa 2 mm x 3 mm x 0.5 mm dried CMC-g-PNIPAAm comb-type graft hydrogel films (cut from sample CCH-C3(8)MONO-1(CA).1), were weighed (1.890 and 2.453 g) and immersed in a water bath at room temperature overnight. At the next day, the samples were removed from the bath. After that, they were immersed for 30 minutes, one sample in a water and the other

one in a buffer solution pH=3 baths and both of them were at 80 °C. The samples were then removed from their respective baths, water and buffer solution excess on the surface of the swollen gels were removed with a paper towel, and finally the samples were weighed (7.279 and 5.680 g). Subsequently, they were immersed for another 30 minutes, one sample in a water and the other one in a buffer solution pH=3 baths and both of them were at 4 °C. The samples were then removed again from their respective baths, water and buffer solution excess on the surface of the swollen gels was removed with a paper towel, and finally samples were weighed. The whole procedure was repeated 4 more times. The Swelling Degree (%) was calculated by using equation (1).

3.1.9. Digital photographs and videos

Digital photographs. Circa 0.5 mm width CMC-g-PNIPAAm comb-type graft hydrogel dried films (samples CCH-C3(8)MONO-1(CA) and CCH-C3(8)MONO-1(Al)) with different sizes, were immersed overnight in a water (or pH=2 or 3 buffer solution) bath at room temperature. At the next day, the samples were removed from the bath, put on a flat surface with a 2 mm x 2 mm square pattern and digital photographs (from a horizontal perspective) of the samples, were taken with a digital camera Canon EOS 550 D. Then, the samples were returned to their respective baths (previously heated until 80 °C) and removed out at different time intervals, in order to make (from a horizontal perspective) digital photographs over the square pattern surface. The same procedure (with a water bath) was applied to circa 0.5 mm width CMC hydrogel dried films (samples CCH-C3(8)MONO-2(CA) and CCH-C3(8)MONO-2(Al)).

Actuation tests. Bilayer actuators composed of a CMC-g-PNIPAAm comb-type graft hydrogel film on a PA6 substrate (samples CCH-C3(8)BI-56 and CCH-C3(8)BI-40), were vertically fixed from one of their extremes with laboratory tweezers and submerged in a water bath, which was heated first, until 40 °C and then until 60 °C in order to visualize the thermosensitive actuation behavior of the bilayer samples. In other tests, the samples were left cooling down until room temperature (and later around 5 °C), in order to verify the reversibility or the thermosensitive actuation. During these tests, digital photos were taken automatically each 30 seconds, with the digital camera fixed in a graduated support. Digital photos were later processed with the program ImageJ version1.45s, and videos of the thermosensitive actuation tests were obtained. Data analysis of the photos was made with the program Tracker version 4.92, and gyration angles were measured and plotted against time, for the whole duration of all tests. These tests were also performed to an untreated PA6 (sample CCH-C3(8)BI-Blanc(8)) and a functionalized PA6 (sample CCH-C3(8)BI-Blanc(4)) film substrates.

3.2. Synthesis of aminoterminated PNIPAAm oligomers

Based on the synthesis performed by Bokias et al. (2001), aminoterminated PNIPAAm oligomers with theoretical molecular weights of 5,000, 7,000 and 9,000 g/mol were synthetized

from NIPAAm monomers, by using a telomerization technique in aqueous media. Table 8 shows the experimental design that was used (matrix 1x3) and the samples that were synthetized.

Table 8

Experimental Design for synthesis of aminoterminated PNIPAAm oligomers

Mw(THEO)* (g/mol) / Monomer	5,000	7,000	9,000
NIPAAm	Sample CCH-A15-1** Sample CCH-A15-2** Sample CCH-A15-3** Sample CCH-C1-1** Sample CCH-C1(2)-1**	Sample CCH-B4-1*** Sample CCH-C1-2*** Sample CCH-C1(2)-2***	Sample CCH-B4-2**** Sample CCH-C1-3**** Sample CCH-C1(2)-3**** Sample CCH-C1(2)-3.2**** Sample CCH-C1(2)-3.3****

*$Mw_{(THEO)}$: Theoretical Molecular Weight of aminoterminated PNIPAAm oligomers

**This sample belongs to Group of Samples A ($Mw_{(THEO)}$ = 5,000 g/mol)

***This sample belongs to Group of Samples B ($Mw_{(THEO)}$ = 7,000 g/mol)

****This sample belongs to Group of Samples C ($Mw_{(THEO)}$ = 9,000 g/mol)

Procedure

(Sample CCH-A15-1) 11.3163 g (0.1 moles) of NIPAAm monomer (Purity ≥ 99%, Sigma-Aldrich) was dissolved in 80 mL (4.44 moles) of millipore water, then the aqueous solution was purged with argon. By using a water bath, the temperature of the solution was set to 29 °C. 0.2282 g ($1.1x10^{-3}$ moles) of the activator APS (Purity ≥ 98% (ACS), VWR Chemicals) and 0.2502 g ($2.2x10^{-3}$ moles) of the initiator AET•HCl (Purity ≥ 97%, Sigma-Aldrich) were dissolved separately in two aqueous solutions with 10mL (0.55 moles) of millipore water. After about 1 h, to the monomer solution was added first, the AET•HCl aqueous solution, followed then by the APS solution. After a reaction time of 3 hours, the product was dialyzed in a water bath, by using a dialysis membrane (12,000 Da cutoff, Sigma) and finally was freeze-dried. For a detailed amount of reagents used per each sample, please refer to Tables 37, 38 and 39 at Appendix II (See section 10. Appendix II: Tables).

3.3. Synthesis of CMC-g-PNIPAAm graft copolymers

Based on the synthesis performed by Bokias et al. (2001), CMC-g-PNIPAAm graft copolymers with theoretical molecular weights per graft of 5,000, 7,000 and 9,000 g/mol and theoretical graft weight percentages of 40, 50 and 80%, were synthetized by coupling grafts of aminoterminated PNIPAAM oligomers to a CMC backbone. Here 1-(3-dimethylamino-propyl)-3-ethyl-carbodiimide hydrochloride (EDC) was used as a coupling reagent. Table 9 shows the experimental design that was used (matrix 3x3) and the samples that were synthetized.

Procedure

Exemplarily, the synthesis conditions of sample CCH-A27-1, with a %Graft$_{(THEO)}$ = 40% and a Mw(Graft)$_{(THEO)}$ = 5,000 g/mol of aminoterminated PNIPAM oligomer are as follows: 2.7049 g ($3.86x10^{-6}$ mol) of CMC (Mw ≈ 700,000 g/mol, Sigma-Aldrich) and 1.3515 g ($2.70x10^{-4}$ mol) of aminoterminated PNIPAM oligomer (sample CCH-A15-1) were added to 160 and 35 mL of millipore water, respectively. The solutions were stirred overnight. Another aqueous solution was made by adding 0.2013 g ($1.05x10^{-3}$ mol) of the coupling reagent EDC (Purity ≥ 99%, Sigma-Aldrich) to 5 mL of millipore water. The three aqueous solutions were purged with argon for 1 hour. The CMC aqueous solution was mixed with the aminoterminated PNIPAM solution. Then, a small amount of a 2 M NaOH aqueous solution was added, in order to adjust the pH of the mixture to 8. The next step was to add the EDC aqueous solution (0.04 g/mL) to the mixture at room temperature. The reaction mixture was stirred for 12 h. The product was dialyzed in a water bath, by using a dialysis membrane (12,000 Da cutoff, Sigma) and finally was freeze-dried. Detailed amount of reagents used per each sample are listed in Tables 40, 41, 42, 43, 44, 45, 46, 47 and 48 at Appendix II (See section 10. Appendix II: Tables).

3.4. Synthesis of CMC-g-PNIPAAm comb-type graft hydrogels

3.4.1. CMC-g-PNIPAAm comb-type graft hydrogel crosslinked with Al^{3+} ions

Based on the synthesis performed by Demitri et al. (2008) and Ju et al. (2001), a new procedure was proposed for the synthesis of CMC-g-PNIPAAm comb-type graft hydrogels. First, a pre-gel stock solution of 30% polymer concentration by weight of water (solution CCH-C3(4)-2(30%)), was made by mixing in distilled water, CMC-g-PNIPAAm graft copolymer and hydroxyethyl cellulose (HEC) with a weight ratio of 3/1 (for a detailed amount of reagents used in this pre-gel stock solution, please refer to Table 49 at Apendix II (See section 10. Appendix II: Tables)). Films made from this pre-gel stock solution were crosslinked with Al^{3+} ions present in 1, 1.5, 2, 2.5, 3, 3.5, 3.75 and 15 % weight percentage $AlCl_3$ aqueous solutions (for a detailed amount of $AlCl_3$ used per aqueous solution, please refer to Table 50 at Apendix II (See section 10. Appendix II: Tables)). Table 10 shows the experimental design that was used (matrix 1x8) and the samples that were synthetized.

Table 9

Experimental Design for synthesis of CMC-g-PNIPAAm graft copolymers

%Graft$_{(THEO)}$[b] (%) / Mw(Graft)$_{(THEO)}$[a] (g/mol)	40	50	80
5,000	Sample CCH-A27-1[c,**] Sample CCH-C2-1.40[c,*] Sample CCH-C2(2)-1.40[c,*]	Sample CCH-B5-1.50[f,**] Sample CCH-C2(2)-1.50[f,*]	Sample CCH-C2(2)-1.80[i,*]
7,000	Sample CCH-B5-2.40[d,**] Sample CCH-C2(2)-2<1>.40[d,*] Sample CCH-C2(2)-2.40[d,*]	Sample CCH-B5-2.50[g,**]	Sample CCH-C2(2)-2<1>.80[j,*] Sample CCH-C2(2)-2.80[j,*]
9,000	Sample CCH-B5-3.40[e,**] Sample CCH-C2(2)-3.40[e,*]	Sample CCH-B5-3.50[h,**] Sample CCH-C2(2)-3.50[h,*]	Sample CCH-C2(2)-3.80[k,*]

[a] Mw(Graft) (**THEO**): Theoretical Molecular Weight per Graft.

[b] %Graft(**THEO**): Theoretical Graft Weight Percentage.

[c] This sample belongs to Group of Samples A (Mw(**THEO**) = 5,000 g/mol) - Sub-Group A.1 %Graft(**THEO**)=40%).

[d] This sample belongs to Group of Samples A (Mw(**THEO**) = 5,000 g/mol) - Sub-Group A.2 (%Graft(**THEO**)=50%).

[e] This sample belongs to Group of Samples A (Mw(**THEO**) = 5,000 g/mol) - Sub-Group A.3 (%Graft(**THEO**)=80%).

[f] This sample belongs to Group of Samples B (Mw(**THEO**) = 7,000 g/mol) - Sub-Group B.1 (%Graft(**THEO**)=40%).

[g] This sample belongs to Group of Samples B (Mw(**THEO**) = 7,000 g/mol) - Sub-Group B.2 (%Graft(**THEO**)=50%).

[h] This sample belongs to Group of Samples B (Mw(**THEO**) = 7,000 g/mol) - Sub-Group B.3 (%Graft(**THEO**)=80%).

[i] This sample belongs to Group of Samples C (Mw(**THEO**) = 9,000 g/mol) - Sub-Group C.1 (%Graft(**THEO**)=40%).

[j] This sample belongs to Group of Samples C (Mw(**THEO**) = 9,000 g/mol) - Sub-Group C.2 (%Graft(**THEO**)=50%).

[k] This sample belongs to Group of Samples C (Mw(**THEO**) = 9,000 g/mol) - Sub-Group C.3 (%Graft(**THEO**)=80%).

*Sample synthetized by using CMC with 90,000 g/mol of molecular weight.

**Sample synthetized by using CMC with 700,000 g/mol of molecular weight.

Procedure

Pre-gel stock solution CCH-C3(4)-2(30%) was prepared as follows: 0.0750 g ($8.33x10^{-7}$ mol) HEC was first dissolved in 1 mL ($5.55x10^{-2}$ mol) water and mixed overnight, resulting into a slightly viscous clear dissolution; then, 0.2250 g ($2.74x10^{-5}$ mol) of CMC-g-PNIPAAm copolymer (for an exact sample composition of the copolymer see Table 49 at Apendix II (See section 10. Appendix II: Tables)) was mixed with the dissolution overnight, obtaining at the end a more viscous clear dissolution. The dissolution obtained was distributed in glass molds for making films. The molds were left drying at room temperature overnight. The next step was to demold the films from the molds in an atmosphere saturated of vapor. For example, for film sample CCH-C3(4)-2(30%) (Al Ions)-1%: First, 10 mL $AlCl_3$ aqueous solution of 1% weight percent concentration was prepared. Subsequently, dry film sample CCH-C3(4)-2(30%) (Al Ions)-1% was submerged in 10 mL of the previously prepared 1% $AlCl_3$ aqueous solution and this was shaken for 10 minutes. Finally, the film sample was washed with water and dried at room temperature in a desiccator overnight.

3.4.2. CMC-g-PNIPAAm comb-type graft hydrogel crosslinked with citric acid

To synthesize CMC-g-PNIPAAm comb-type graft hydrogels, the following procedure based on a previous synthesis (Demitri et al. (2008)) was proposed: Pre-gel stock solutions of 15, 20, 25, 30, 35 and 40 % polymer concentration by weight of water, were prepared by combining in distilled water, CMC-g-PNIPAAm graft copolymer (or CMC) and HEC with a weight ratio of 3/1 (for a detailed amount of reagents used in these pre-gel stock solutions, please refer to Table 51 at Apendix II (See section 10. Appendix II: Tables)). From this pre-gel stock solutions, the films prepared were crosslinked with citric acid, present in the reaction mixture at a weight percentage of 3.75 %, respect of the weight of the polymer. The experimental design that was used (matrix 2x6) and the synthesized samples are shown in Table 11.

Procedure

Preparation of pregel stock solution CCH-C3(5)-2(15%): In 1 g ($5.56x10^{-2}$ mol) water was dissolved 0.0377 g ($4.19x10^{-7}$ mol) HEC and left stirring overnight, as a result an slightly viscous clear dissolution was obtained; subsequently, the dissolution was overnight mixed with 0.1125 g ($3.89x10^{-7}$ mol) CMC-g-PNIPAAm graft copolymer (sample CCH-C2(2)-2.80(1)) and a more viscous clear dissolution was obtained. Finally, 0.0056 g ($2.91x10^{-5}$ mol) citric acid was added to the reaction dissolution and mixed until it was dissolved. Films were made by distributing the dissolution in glass molds and by leaving them at room temperature drying overnight. Then the dried samples were left in an oven at 80 °C for 24 hours. Later, with a vapor chamber the debonding of the films from the molds was performed. To conclude, after washing the film samples with water, they were left drying overnight at room temperature in a desiccator.

Table 10

Experimental Design for synthesis of CMC-g-PNIPAAm comb-type graft hydrogels crosslinked with Al ions.

Pre-Gel Stock Solution / $AlCl_3$* (%)	1	1,5	2	2,5	3	3,5	3,75	15
CCH-C3(4)-2(30%)	Sample CCH-C3(4)-2(30%) (Al Ions)-1%	Sample CCH-C3(4)-2(30%) (Al Ions)-1,5%	Sample CCH-C3(4)-2(30%) (Al Ions)-2%	Sample CCH-C3(4)-2(30%) (Al Ions)-2,5%	Sample CCH-C3(4)-2(30%) (Al Ions)-3%	Sample CCH-C3(4)-2(30%) (Al Ions)-3,5%	Sample CCH-C3(4)-2(30%) (Al Ions)-3,75%	Sample CCH-C3(4)-2(30%) (Al Ions)-15%

* $AlCl_3$: Weight percentage concentration of Al^{3+} in aqueous solutions.

3.4.3. CMC-g-PNIPAAm comb-type graft hydrogels: Crosslinking with Al^{3+} ions vs crosslinking with citric acid

CMC-g-PNIPAAm graft copolymer and CMC polymers were crosslinked with $AlCl_3$ and citric acid. CMC polymers were only crosslinked with $AlCl_3$. Table 12 shows the experimental design that was used (matrix 2x2) and the samples that were synthetized.

Procedure

Group of samples CCH-C3(8)MONO-1(Al) and CCH-C3(8)MONO-2(Al) were prepared, from pre-gel stock solutions of 35% polymer concentration by weight of water (samples CCH-C3(8)-2.1(35%) and CCH-C3(8)-1a(35%)) (for a detailed amount of reagents used in these pre-gel stock solutions, please refer to Table 52 and 53 at Apendix II (See section 10. Appendix II: Tables)). The correspondent sample films were crosslinked with Al^{3+} ions present in 2.5% weight percentage $AlCl_3$ aqueous solutions. These pre-gel stock solutions and films were prepared by following the procedure presented in 3.4.1.

Group of samples CCH-C3(8)MONO-1(CA) were prepared, from pre-gel stock solution CCH-C3(8)-2.1(35%) and by mixing with citric acid at a weight percentage of 3.75 %, respect of the weight of the polymer. The films were prepared by following the procedure presented in 3.4.2.

3.5. Synthesis of bilayer actuators based on CMC-g-PNIPAAm comb-type graft hydrogel films

3.5.1. Preparation of CMC-g-PNIPAAm comb-type graft pre-gel solutions

Based on the synthesis performed by Demitri et al. (2008), a procedure was proposed for the preparation of CMC-g-PNIPAAm comb-type graft pre-gel solutions from pre-gel stock solutions.

First, 2 pre-gel stock solutions (CCH-C3(8)-2.2(35%) and CCH-C3(8)-2.3(35%)) of 35 % polymer concentration by weight of water, were prepared by mixing in distilled water, CMC-g-PNIPAAm graft copolymer and HEC with a weight ratio of 3/1.

Procedure

For pre-gel stock solution CCH-C3(8)-2.2(35%): In 4 g (2.21×10^{-1} mol) distilled water were mixed 1.0281 g (4.98×10^{-6} mol) CMC-g-PNIPAAm graft copolymer and 0.3505 g (3.89×10^{-6} mol) HEC with a weight ratio of 3/1 (for a detailed amount of reagents used in this and the other pre-gel stock solutions, please refer to Tables 54 and 55 at Apendix II (See section 10. Appendix II: Tables)). Second, the pre-gel solutions were made from this 2 pre-gel stock solutions, by diluting them with water until obtaining 4, 6, 8, 10, 12 and 35 % pre-gel stock solution concentrations by weight of pre-gel solution. Finally different amounts of citric acid

Table 11

Experimental Design for synthesis of CMC-g-PNIPAAm comb-type graft hydrogels crosslinked with citric acid

Polymer \ Concentration of Polymer (%)	15	20	25	30	35	40
CMC (1)	Sample CCH-C3(5)-1(15%)	Sample CCH-C3(5)-1(20%)	Sample CCH-C3(5)-1(25%)	Sample CCH-C3(5)-1(30%)	Sample CCH-C3(5)-1(35%)	Sample CCH-C3(5)-1(40%)
CMC-g-PNIPAAm (2)	Sample CCH-C3(5)-2(15%)	Sample CCH-C3(5)-2(20%)	Sample CCH-C3(5)-2(25%)	Sample CCH-C3(5)-2(30%)	Sample CCH-C3(5)-2(35%)	Sample CCH-C3(5)-2(40%)

Table 12

Experimental Design for synthesis and comparison between CMC-g-PNIPAAm comb-type graft hydrogels crosslinked with citric acid versus crosslinking with Al^{3+}

Polymer \ Crosslinker	$AlCl_3$	Citric Acid
CMC-g-PNIPAAm (1)	Sample CCH-C3(8)MONO-1(Al)	Sample CCH-C3(8)MONO-1(CA)
CMC (2)	Sample CCH-C3(8)MONO-2(Al)	-

(3.75 or 20 % respect the weight of CMC-g-PNIPAAm graft copolymer and HEC) were added as a crosslinker.

Procedure

For preparation of 2 g pre-gel solution CCH-C3(8)BI-Sol(1): 0.0842 g of pre-gel stock solution CCH-C3(8)-2.2(35%) was mixed with 0.0011 g citric acid and diluted with 1.9147 g deionized water until 4 % of pre-gel stock solution concentration by weight of pre-gel solution was obtained (for a detailed amount of reagents used in this and the other pre-gel solutions, please refer to Table 56 at Apendix II (See section 10. Appendix II: Tables)).

Finally, Table 13 shows the experimental design that was used (matrix 1x6) and the pre-gel solutions that were synthetized.

3.5.2. Synthesis of bilayer actuators with PA6 substrates

3.5.2.1. Functionalization of PA6 substrates

Based on the procedures proposed by Isgrove et al. (2001) and Vasileva et al. (2004) PA6 substrates were functionalized with aldehyde groups, by performing either a concentrated acidic hydrolysis, an aqueous hydrolysis or a diluted acidic hydrolysis. The activation method used for the PA6 substrates involved, either a reaction with glutaraldehyde alone or a reaction with glutaraldehyde and polyethyleneimine (PEI). Table 14 shows the experimental design that was used (matrix 3x2) and the substrates that were prepared.

Procedure

7 PA6 film pieces measuring 30mmx30mm were cut from a roll and were divided in 3 sample groups: Concentrated acidic hydrolysis (2 PA6 film pieces), aqueous hydrolysis (2 PA6 film pieces) and diluted acidic hydrolysis (3 PA6 film pieces).

Concentrated Acidic Hydrolysis. The 2 PA6 film pieces were incubated for 2 h at 37 °C in a 2.9 M HCl aqueous solution and then were washed thoroughly in water. After that, the PA6 films were immersed in 25 Wt% aqueous solution of glutaraldehyde at 4 °C for 60 minutes. One of the PA6 films was left drying under the hood overnight, and the other one was immersed for 60 minutes at 37 °C, in 1 V/V% polyethyleneimine (PEI) in 0.1 M sodium phosphate pH=8 solution. After that, it was washed thoroughly in water and finally left drying overnight under the hood (for a detailed amount of reagents and solutions used per each sample, please refer to Table 57 at Apendix II (See section 10. Appendix II: Tables)).

Aqueous hydrolysis. The two PA6 film pieces were incubated for 24 h at 37 °C in water. After that the PA6 films were immersed in 25 Wt% aqueous solution of glutaraldehyde at 4 °C for 60 minutes. One of the PA6 films was left drying under the hood overnight, and the other one was immersed for 60 minutes at 37 °C, in 1 V/V% polyethyleneimine (PEI) in 0.1 M Sodium

Table 13

Experimental design for preparation of CMC-g-PNIPAAm comb-type graft pre-gel solutions used in bilayers with hydrogel or PA6 substrates

Pre-Gel Stock Solution / Concent. Pre-Gel Stock Solution (%)	4	6	8	10	12	35
Stock Solution CCH-C3(8)-2.2(35%)	Solution CCH-C3(8)BI-Sol(1)	Solution CCH-C3(8)BI-Sol(2)	Solution CCH-C3(8)BI-Sol(3)	Solution CCH-C3(8)BI-Sol(4)	Solution CCH-C3(8)BI-Sol(5)	Solution CCH-C3(8)BI-Sol(6)*
Stock Solution CCH-C3(8)-2.3(35%)	-	-	-	-	-	

* Prepared with a mixture of CCH-C3(8)-2.2(35%) and CCH-C3(8)-2.3(35%) pregel stock solutions

Table 14

Experimental Design for functionalization of PA6 substrates

PA6 Film Activation Method / NH_2 Production Method	**Glutaraldehyde (a)**	**Glutaraldehyde + PEI (b)**
Concentrated Acidic Hydrolysis (1)	Substrate CCH-C3(8)BI-PA6(1a)	Substrate CCH-C3(8)BI-PA6(1b)
Aqueous Hydrolysis (2)	Substrate CCH-C3(8)BI-PA6(2a)	Substrate CCH-C3(8)BI-PA6(2b)
Diluted Acidic Hydrolysis (3)	Substrate CCH-C3(8)BI-PA6(3a)	Substrate CCH-C3(8)BI-PA6(3b)
		Substrate CCH-C3(8)BI-PA6(3b.2)

Phosphate pH=8 solution. Subsequently, it was washed thoroughly in water and finally left drying overnight under the hood (for a detailed amount of reagents and solutions used per each sample, please refer to Table 57 at Apendix II (See section 10. Appendix II: Tables)).

Diluted acidic hydrolysis. The three PA6 film pieces were incubated for 30 min at 40 °C in 6 wt% HCl aqueous solution and then were washed thoroughly in water. After that, the PA6 films were immersed in 10 Wt% aqueous solution of diethylamine at 40 °C for 60 minutes. Then the films were immersed in 25 wt% aqueous solution of glutaraldehyde at 4 °C for 60 minutes. One of the PA6 films was left drying overnight, and the other two were immersed for 60 minutes at 37 °C, in 1 V/V% polyethyleneimine (PEI) in 0.1 M sodium phosphate pH=8 solution, after that they were washed thoroughly in water and later, they were incubated in 25 Wt% aqueous solution of glutaraldehyde at 4 °C for 60 minutes, to finally be left drying overnight (for a detailed amount of reagents and solutions used per each sample, please refer to Table 57 at Apendix II (See section 10. Appendix II: Tables)).

3.5.2.2. Synthesis of bilayer actuators with PA6 substrates

A new procedure was proposed for the synthesis of bilayers with functionalized PA6 substrates. Bilayer samples were synthetized, with active layers made of the previously prepared CMC-g-PNIPAAm comb-type graft pre-gel solutions, and passive layers made of the functionalized PA6 substrates obtained previously. Another group of bilayer samples were synthetized, with active layers also made of the previously prepared pre-gel solutions, but

Table 15

Experimental Design for synthesis of bilayer actuators with PA6 substrates

Active Layer / Passive Layer	Solution CCH-C3(8)BI-Sol(1)	Solution CCH-C3(8)BI-Sol(2)	Solution CCH-C3(8)BI-Sol(3)	Solution CCH-C3(8)BI-Sol(4)	Solution CCH-C3(8)BI-Sol(5)	Solution CCH-C3(8)BI-Sol(6)	NONE
Substrate CCH-C3(8)BI-PA6(1a)	Sample CCH-C3(8)BI-1	Sample CCH-C3(8)BI-14	Sample CCH-C3(8)BI-27	Sample CCH-C3(8)BI-40	Sample CCH-C3(8)BI-53	Sample CCH-C3(8)BI-66	Sample CCH-C3(8)BI-Blanc(1)
Substrate CCH-C3(8)BI-PA6(1b)	Sample CCH-C3(8)BI-2	Sample CCH-C3(8)BI-15	Sample CCH-C3(8)BI-28	Sample CCH-C3(8)BI-41	Sample CCH-C3(8)BI-54	Sample CCH-C3(8)BI-67	Sample CCH-C3(8)BI-Blanc(2)
Substrate CCH-C3(8)BI-PA6(2a)	Sample CCH-C3(8)BI-3	Sample CCH-C3(8)BI-16	Sample CCH-C3(8)BI-29	Sample CCH-C3(8)BI-42	Sample CCH-C3(8)BI-55	Sample CCH-C3(8)BI-68	Sample CCH-C3(8)BI-Blanc(3)
Substrate CCH-C3(8)BI-PA6(2b)	Sample CCH-C3(8)BI-4	Sample CCH-C3(8)BI-17	Sample CCH-C3(8)BI-30	Sample CCH-C3(8)BI-43	Sample CCH-C3(8)BI-56	Sample CCH-C3(8)BI-69	Sample CCH-C3(8)BI-Blanc(4)
Substrate CCH-C3(8)BI-PA6(3a)	Sample CCH-C3(8)BI-5	Sample CCH-C3(8)BI-18	Sample CCH-C3(8)BI-31	Sample CCH-C3(8)BI-44	Sample CCH-C3(8)BI-57	Sample CCH-C3(8)BI-70	Sample CCH-C3(8)BI-Blanc(5)
Substrate CCH-C3(8)BI-PA6(3b)	Sample CCH-C3(8)BI-7	Sample CCH-C3(8)BI-20	Sample CCH-C3(8)BI-33	Sample CCH-C3(8)BI-46	Sample CCH-C3(8)BI-59	Sample CCH-C3(8)BI-71	Sample CCH-C3(8)BI-Blanc(6)
Substrate CCH-C3(8)BI-PA6(3b.2)	Sample CCH-C3(8)BI-8	Sample CCH-C3(8)BI-21	Sample CCH-C3(8)BI-34	Sample CCH-C3(8)BI-47	Sample CCH-C3(8)BI-60	Sample CCH-C3(8)BI-72	Sample CCH-C3(8)BI-Blanc(7)
Substrate PA6	Sample CCH-C3(8)BI-84	Sample CCH-C3(8)BI-85	Sample CCH-C3(8)BI-86	Sample CCH-C3(8)BI-87	Sample CCH-C3(8)BI-88	Sample CCH-C3(8)BI-89	Sample CCH-C3(8)BI-Blanc(8)

Table 16

Experimental Design for synthesis of bilayer actuators with hydrogel substrates

Active Layer / Passive Layer	**Solution CCH-C3(8)BI-Sol(1)**	**Solution CCH-C3(8)BI-Sol(2)**	**Solution CCH-C3(8)BI-Sol(3)**	**Solution CCH-C3(8)BI-Sol(4)**	**Solution CCH-C3(8)BI-Sol(5)**	**Solution CCH-C3(8)BI-Sol(6)**
Solution CCH-C3(8)BI-Sol(6)	Sample CCH-C3(8)BI-9	Sample CCH-C3(8)BI-22	Sample CCH-C3(8)BI-35	Sample CCH-C3(8)BI-48	Sample CCH-C3(8)BI-61	Sample CCH-C3(8)BI-73
Solution CCH-C3(8)BI-Sol(6)	Sample CCH-C3(8)BI-10	Sample CCH-C3(8)BI-23	Sample CCH-C3(8)BI-36	Sample CCH-C3(8)BI-49	Sample CCH-C3(8)BI-62	Sample CCH-C3(8)BI-74
Solution CCH-C3(8)BI-Sol(6)	Sample CCH-C3(8)BI-11	Sample CCH-C3(8)BI-24	Sample CCH-C3(8)BI-37	Sample CCH-C3(8)BI-50	Sample CCH-C3(8)BI-63	Sample CCH-C3(8)BI-75
Solution CCH-C3(8)BI-Sol(6)	Sample CCH-C3(8)BI-12	Sample CCH-C3(8)BI-25	Sample CCH-C3(8)BI-38	Sample CCH-C3(8)BI-51	Sample CCH-C3(8)BI-64	Sample CCH-C3(8)BI-76
Solution CCH-C3(8)BI-Sol(6)	Sample CCH-C3(8)BI-13	Sample CCH-C3(8)BI-26	Sample CCH-C3(8)BI-39	Sample CCHC3(8)BI-52	Sample CCH-C3(8)BI-65	Sample CCH-C3(8)BI-65
Solution CCH-C3(8)BI-Sol(6)	Sample CCH-C3(8)BI-75	Sample CCH-C3(8)BI-76	Sample CCH-C3(8)BI-77	Sample CCH-C3(8)BI-78	Sample CCH-C3(8)BI-79	Sample CCH-C3(8)BI-80

passive layers made of not functionalized PA6 substrates. Blanc samples were prepared only with passive layers made of treated and untreated PA6 films, without active layers made of pre-gel solutions. Table 15 shows the experimental design that was used (matrix 8x7) and the samples that were synthetized.

Procedure

Thin films were obtained by casting (with a microliter syringe) CMC-g-PNIPAAm comb-type graft pre-gel solutions over the previously functionalized PA6 substrates. Then, the samples were left drying at room temperature overnight. At the next day, they were heated at 80 °C in a preheated oven for 24 hours. After that time, the samples were removed from the oven and kept in flask for subsequent actuation experiments.

3.5.3. Synthesis of bilayer actuators with hydrogel substrates

A new procedure was proposed for the synthesis of bilayer actuators with hydrogel substrates. Bilayer samples were manufactured with active layers, made of the previously prepared CMC-g-PNIPAAm comb-type graft pre-gel solutions, and passive layers made of the previously obtained pre-gel solution CCH-C3(8)BI-Sol(6). Table 16 shows the experimental design that was used (matrix 6x6) and the samples that were synthetized.

Procedure

0.4898 g pre-gel solution CCH-C3(8)BI-Sol(6) was mixed with 0.0064 g ($3x10^{-5}$ mol) citric acid, added to the reaction mixture at a weight percentage of 3.75 %, respect of the weight of the polymer. The dissolution obtained was distributed in glass molds for making films. The molds were left drying at room temperature overnight. Then, the dried films were left in an oven at 80 °C for 24 hours. The next step was to demold the films from the molds, by using a vapor chamber. The films were washed with water, and dried at room temperature in a desiccator overnight. At the next day, over these films, thin films were made by casting (with a microliter syringe) CMC-g-PNIPAAm comb-type graft pre-gel solutions. Then, the bilayer samples were left drying at room temperature overnight. After that time, they were heated in oven preheated at 80 °C for 24 hours. Finally, the bilayer samples were removed from the oven and kept in flasks for subsequent actuation tests.

4. Results

4.1. Synthesis and structural characterization of aminoterminated PNIPAAm oligomers

4.1.1. Amount and %yield

The synthesis of aminoterminated PNIPAAm oligomers could be successfully performed, however, with a low to medium yield (Table 17). Sample CCH-C1(2)-2 presented the highest value with 43% and sample CCH-C1(2)-3.2 the lowest value, with 7%. Due to the high amount of some reaction solutions to be purified, and the limited capacity of the dialysis membranes, some reaction solutions were purified in parts, therefore some samples were divided in sample fractions.

4.1.2. Gel Permeation cromatography

The results from gel permeation cromatography (Figure 60 and Table 18) showed that it was possible to synthesize aminoterminated PNIPAAm oligomers with three different groups of molecular weight values. From the three groups of samples presented (A, B and C), it was observed that group of samples A and C had molecular weight values, close to the theoretical ones chosen during the experimental design. However, that was not the case for group of samples B. This group of samples managed to partially differentiate its molecular weight values from groups A and C, because some values of some sample fractions were inside the range of values of group of samples A. High polydispersity values were also observed for the three group of samples: Between 1.5-2.1 for group of samples A, between 1.7-3.1 for group of samples B and between 1.5-2.3 for group of samples C. It should be noted that the results obtained by this analysis are not absolute values, but are only relative values that depend on the molecular standard that was used.

4.1.3. Elemental analysis

The results of the Elemental Analysis (Table 19) also revealed that it was possible to obtain aminoterminated PNIPAAm oligomers with three different groups of molecular weight values. The three groups of samples A, B and C had molecular weight values that were close to the theoretical values chosen during the experimental design. Also the analysis allowed the estimation of the respective degrees of polymerization: Between 43-44 for group of samples A, around 60 for group of samples B and between 76-78 for group of samples C. The results observed are average values calculated between the fractions of each group of samples. In this analysis was not possible to measure polydispersity values. The results obtained by this analysis are absolute values. Detailed measurement data from all samples, their sample fractions and their replicas are listed from Table 113 to Table 133 in Appendix II (See section 10. Appendix II: Tables).

4.1.4. FTIR

The FTIR spectra (Figure 61) confirmed the structure of the aminoterminated PNIPAAm

oligomers obtained. Characteristic amide and secondary amine peaks are found at 1,648 cm^{-1} (group -N-C=O) and 1,545 cm^{-1} (group –NH-), The functionalization of the aminoterminated PNIPAAm oligomers by amino end groups (primary amine), is confirmed by the peak found at 3,439 cm^{-1} (group $–NH_2$) and also by the peak found at 1,545 cm^{-1}. FTIR measurement data from other samples, their sample fractions and their replicas are listed in Tables 58, 59 and 60 at Appendix II (See section 10. Appendix II: Tables).

Table 17

Amount and %yield for

Groups of Samples A, B and C

Group of Samples A ($Mw_{(THEO)}$ = 5,000 g/mol)			
Sample	**N° of Sample Fractions**	**Amount (g)**	**%Yield (%)**
CCH-A15-1	1	3.462	29.4
CCH-A15-2	1	0.538	18.2
CCH-A15-3	1	0.956	32.4
CCH-C1-1	2	2.988	34.5
CCH-C1(2)-1	6	10.791	40.4
Group of Samples B ($Mw_{(THEO)}$ = 7,000 g/mol)			
Sample	**N° of Sample Fractions**	**Amount (g)**	**%Yield (%)**
CCH-B4-1	1	1.538	42.6
CCH-C1-2	2	1.371	16.0
CCH-C1(2)-2	6	11.340	43.2
Group of Samples C ($Mw_{(THEO)}$ = 9,000 g/mol)			
Sample	**N° of Sample Fractions**	**Amount (g)**	**%Yield (%)**
CCH-B4-2	1	0.965	20.9
CCH-C1-3	2	3.633	42.6
CCH-C1(2)-3	6	7.334	28.5
CCH-C1(2)-3.2	6	1.913	7.4
CCH-C1(2)-3.3	6	3.538	13.8

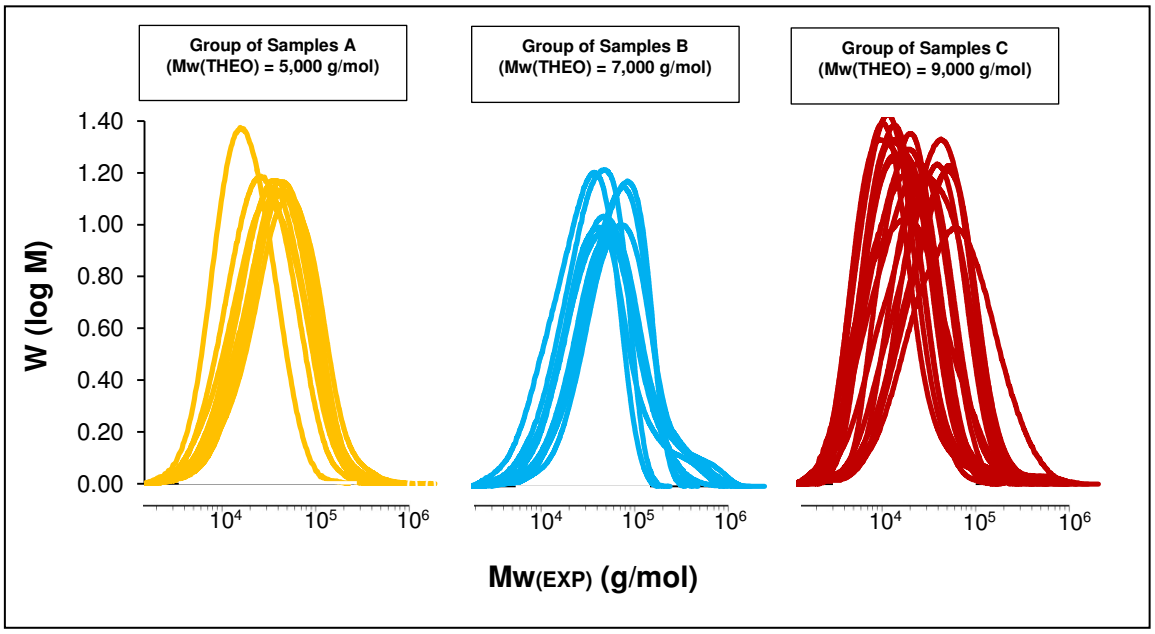

Figure 60. Gel Permeation Cromatography elugrams for group of samples A, B and C

Table 18

Molecular Weight and Polydispersity values for Groups of Samples A, B and C

Group of Samples A ($Mw_{(THEO)}$ = 5,000 g/mol)		
Sample	**$Mw_{(EXP)}$ (g/mol)**	**Polydispersity**
CCH-A15-1	4,113	1.95
CCH-A15-2	Not measured	Not measured
CCH-A15-3	3,700	1.87
CCH-C1-1	2,927-4,787	1.53-1.96
CCH-C1(2)-1	3,438-4,517	1.72-2.09
Group of Samples B ($Mw_{(THEO)}$= 7,000 g/mol)		
Sample	**$Mw_{(EXP)}$ (g/mol)**	**Polydispersity**
CCH-B4-1	5,083	1.98
CCH-C1-2	4,329-4,971	1.73-1.99
CCH-C1(2)-2	4,391-5,256	2.20-3.08

Table 18

(Cont.)

Group of Samples C ($M_{W(THEO)}$ = 9,000 g/mol)		
Sample	**$M_{W(EXP)}$ (g/mol)**	**Polydispersity**
CCH-B4-2	Not measured	Not measured
CCH-C1-3	5,993-7,701	1.95-2.34
CCH-C1(2)-3	7,391-9,357	1.65-1.99
CCH-C1(2)-3.2	8,589-9,950	1.46-1.66
CCH-C1(2)-3.3	9,939-11,250	1.58-1.75

4.1.5. NMR

The NMR spectra (Figure 62) also confirmed the structure of the aminoterminated PNIPAAm oligomers obtained. Characteristic peaks are found at 1.901 ppm (group CHCO) and 3.781 ppm (group CHNH), The functionalization of the aminoterminated PNIPAAm oligomers by amino end groups (primary amine), is confirmed by the peak found at 3.388 ppm (group CH_2NH_2) and also by the peaks found at 3.088 ppm (group CH_2CH_2S) and 2.110 ppm (group SCH_2CH). NMR measurement data from other samples (and their sample fractions) are listed in Tables 61, 62 and 63 at Appendix II (See section 10. Appendix II: Tables).

4.1.6. DSC (Dry)

The DSC measurements (Figure 63 and 64) performed on dried samples of NIPAAm monomer and aminoterminated PNIPAAm oligomers, confirmed that the polymerization of the NIPAAm monomer was successfully made, because the analysis (Figure 63) showed a displacement of the melting temperature (T_m) from 66.5 °C for NIPAAm monomers to 175.2 °C for aminoterminated PNIPAAm oligomers (sample CCH-C1(2)-1(3)). The melting enthalpy of both samples was also calculated: 129 J/g for NIPAAm monomer and 102 J/g for aminoterminated PNIPAAm oligomers (sample CCH-C1(2)-1(3)). Figure 64 shows, another evidence of a successful polymerization: The presence of a signal at 140.1 °C that correspond to the glas transition temperature (T_g) of the aminoterminated PNIPAAm oligomers (sample CCH-C1(2)-1(3)). DSC measurements from other samples (and their sample fractions) are listed in Tables 64, 65 and 66 at Appendix II (See section 10. Appendix II: Tables).

4.2. Characterization of phase transition activity in aminoterminated PNIPAAm oligomers

4.2.1. Reversibility of Phase Transition in Water

The DSC measurements performed with aqueous solutions of NIPAAm monomers and

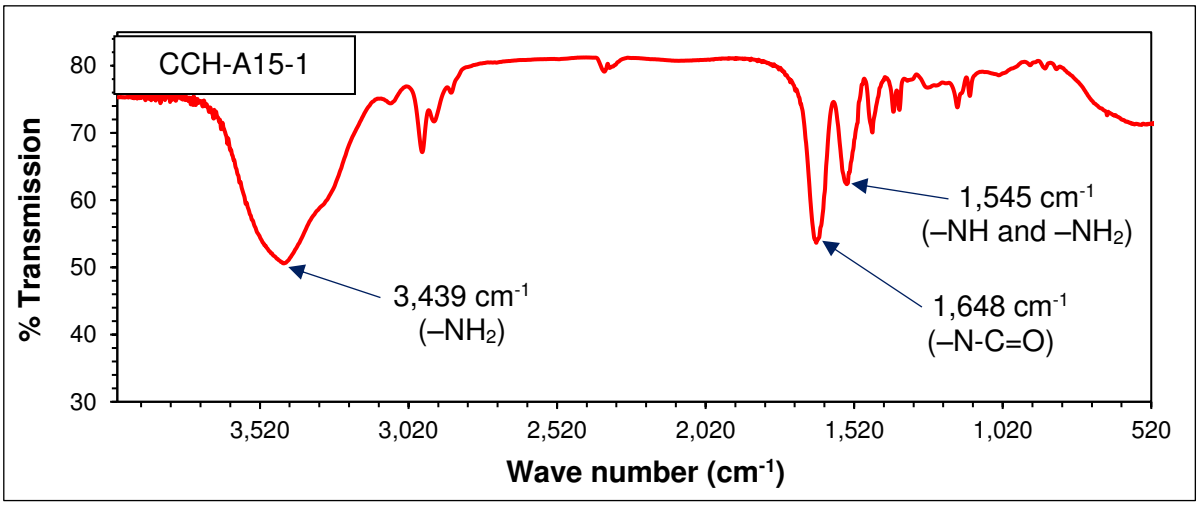

Figure 61. FTIR spectrum of aminoterminated PNIPAAm oligomer (Sample CCH-A15-1)

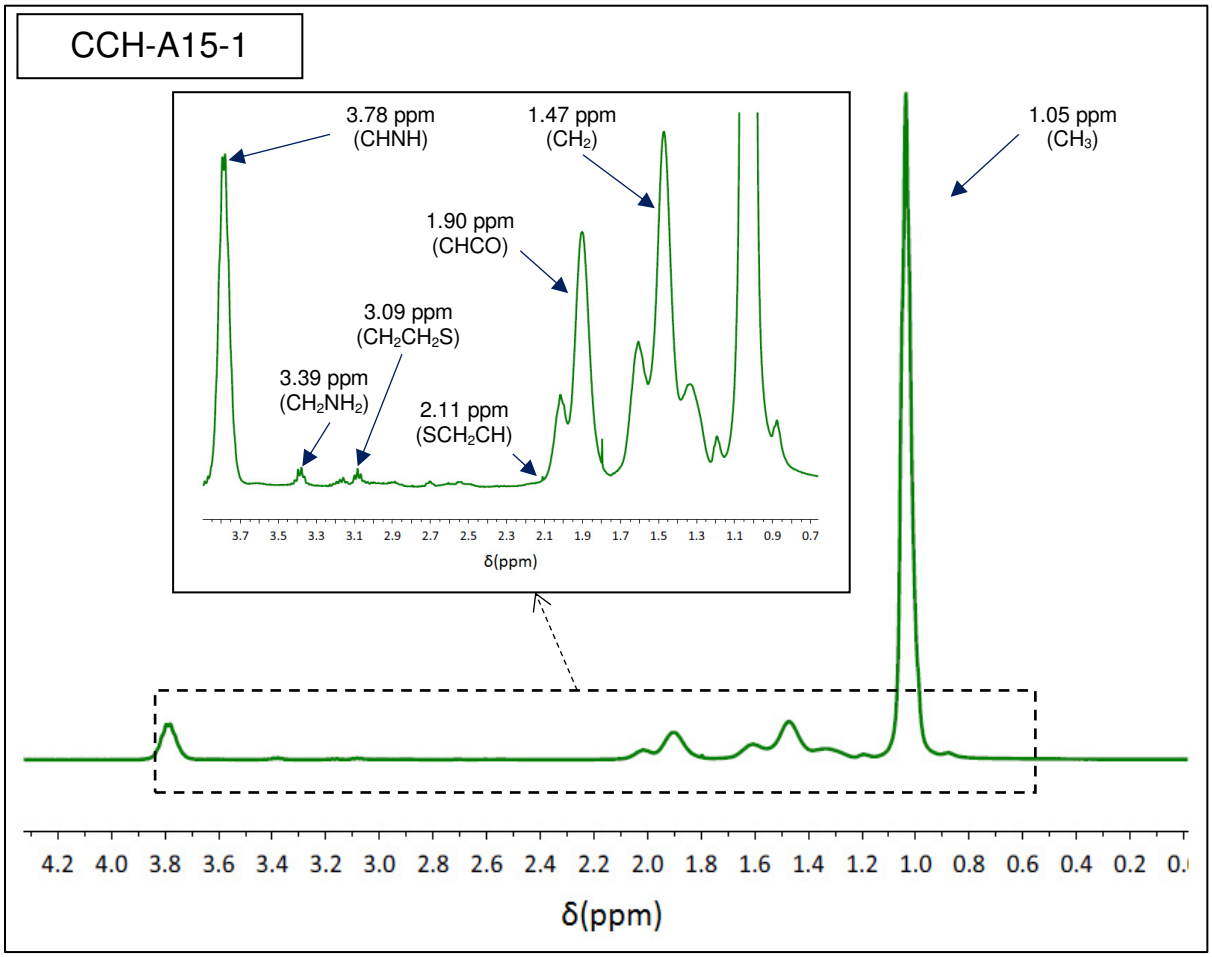

Figure 62. ^{1}H-NMR spectra of aminoterminated PNIPAAm oligomer (Sample CCH-A15-1)

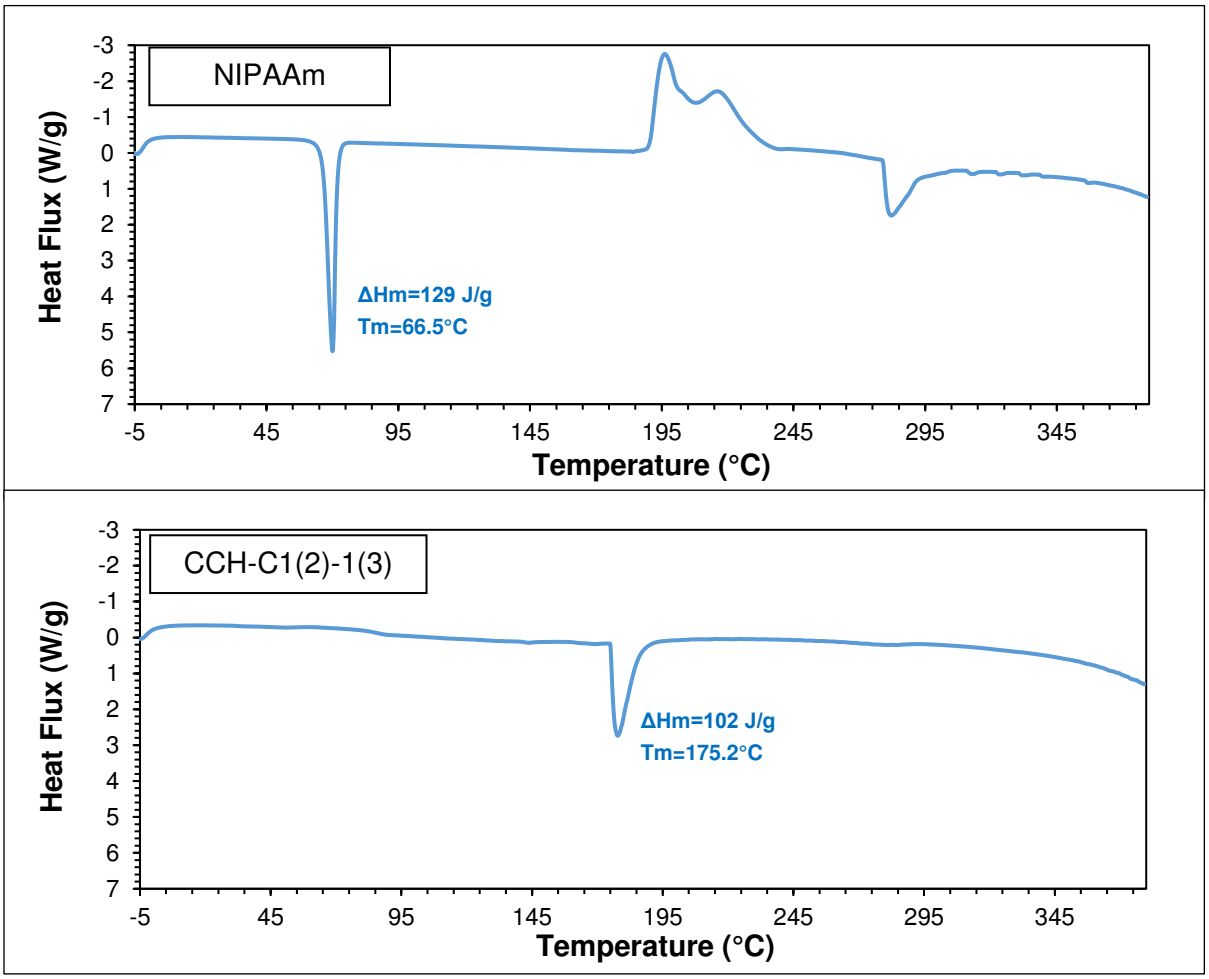

Figure 63. T_m and ΔH_m of NIPAAm monomer versus aminoterminated PNIPAAm oligomer (Sample fraction CCH-C1(2)-1(3))

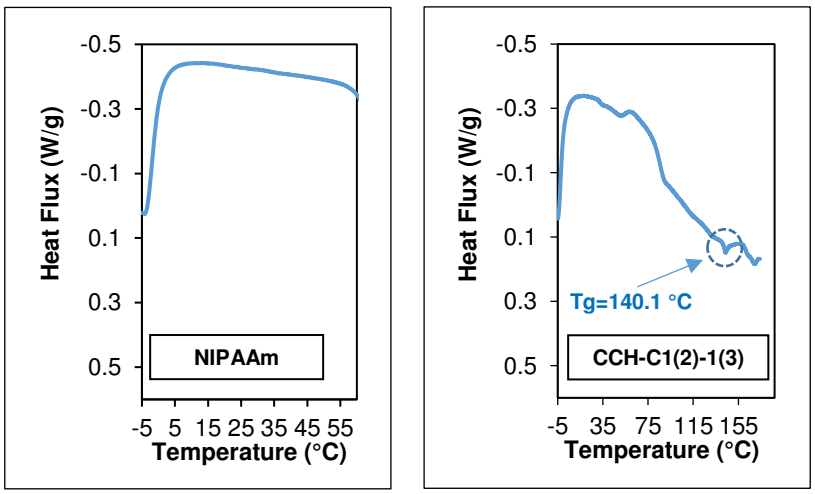

Figure 64. Tg of NIPAAm monomer versus amino-terminated PNIPAAm oligomer (Sample fraction CCH-C1(2)-1(3))

Table 19

Molecular Weight ($Mw_{(EXP)}$) and Experimental Degree of Polymerization (n_{exp})

Group of Samples A ($Mw_{(THEO)}$ = 5,000 g/mol)		
Sample	**$Mw_{(EXP)}$ (g/mol)**	**n_{exp}**
CCH-A15-1	5,101.34	44
CCH-A15-2	5,053.38	43
CCH-A15-3	5,033.28	43
CCH-C1-1	5,145.60	44
CCH-C1(2)-1	5,063.89	43
Group of Samples B ($Mw_{(THEO)}$ = 7,000 g/mol)		
Sample	**$Mw_{(EXP)}$ (g/mol)**	**n_{exp}**
CCH-B4-1	7,048.21	60
CCH-C1-2	7,102.51	60
CCH-C1(2)-2	7,054.55	60
Group of Samples A ($Mw_{(THEO)}$ = 9,000 g/mol)		
Sample	**$Mw_{(EXP)}$ (g/mol)**	**n_{exp}**
CCH-B4-2	9,169.14	79
CCH-C1-3	9,037.69	77
CCH-C1(2)-3	9,009.74	76
CCH-C1(2)-3.2	9,047.88	77
CCH-C1(2)-3.3	9,206.69	77

aminoterminated PNIPAAm oligomers (Figure 65) revealed the thermosensitive activity of the latter, showed by a peak signal, which was not visible in the measurements of the NIPAAm monomer aqueous solutions. The low critical solution temperatures (LCST) estimated for the aminoterminated PNIPAAm oligomers were between 34-36 °C (heating cycle) and 34-39 °C (cooling cycle). The analysis also showed that the thermosensitive activity was reversible, that is, it was observed during both the heating and the cooling cycles. DSC measurements from other samples (and their sample fractions) aqueous solutions are listed in Tables 67, 68 and 69 at Appendix II (See section 10. Appendix II: Tables).

4.3. Synthesis and structural characterization of CMC-g-PNIPAAm graft copolymers

4.3.1. Amount and %yield

The synthesis of CMC-g-PNIPAAm graft copolymers was successfully performed and happened with low and medium %Yield (Tables 20, 21 and 22). Sample CCH-B5-3.40 presented the highest value with 60.26% and sample CCH-C2-1.40 the lowest value, with

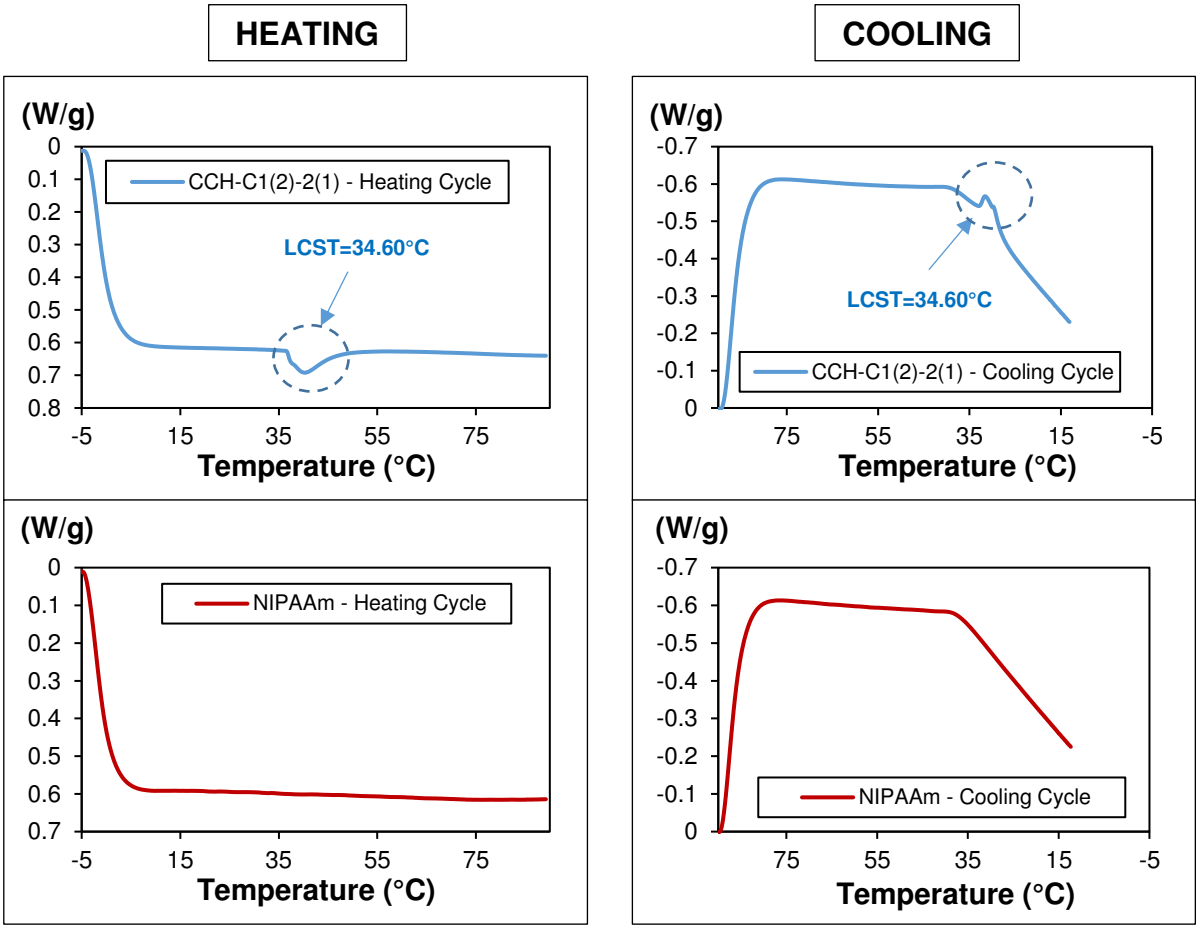

Figure 65. Reversibility of phase transition in water of aminoterminated PNIPAAm oligomers (sample fraction CCH-C1(2)-2(1)) versus NIPAAm monomers

9.73%. Due to the high amount of some reaction solutions to be purified, and the limited capacity of the dialysis membranes, some reaction solutions were purified in parts, therefore some samples were divided in fractions, giving as a result group of samples.

4.3.2. Elemental analysis

The results of the elemental analysis (Tables 23, 24 and 25) revealed that it was possible to obtain CMC-g-PNIPAAm graft copolymers with three different graft percentage values. The three groups of samples A, B and C had estimated graft percentages values that, in some cases, were close to the theoretical values chosen during the experimental design. Also the analysis allowed the estimation of the respective N° grafts per CMC Chain: Between 2-100 for group of samples A, around 1-60 for group of samples B and between 2-48 for group of samples C. The results observed are the average values calculated between the sample fractions of each sample. Results estimated during the elemental analysis of aminoterminated PNIPAAm oligomer samples were used in the calculation of the results correspondent to the

CMC-g-PNIPAAm graft copolymer samples. The results obtained by this analysis are absolute values.

Table 20

Amount and %Yield of Group of Samples A

(Mw(Graft)$_{(THEO)}$ = 5,000 g/mol)

Group of Samples A (Mw(Graft)$_{(THEO)}$ = 5,000 g/mol)			
Sub-Group A.1 (%Graft$_{(THEO)}$=40%)			
Sample	**N° of Sample Fractions**	**Amount (g)**	**%Yield (%)**
CCH-A27-1	5	1.1755	27.6
CCH-C2-1.40	1	0.0713	9.7
CCH-C2(2)-1.40	4	1.4183	35.3
Sub-Group A.2 (%Graft$_{(THEO)}$=50%)			
Sample	**N° of Sample Fractions**	**Amount (g)**	**%Yield (%)**
CCH-B5-1.50	1	0.5424	50.0
CCH-C2(2)-1.50	5	1.7109	34.1
Sub-Group A.3 (%Graft$_{(THEO)}$=80%)			
Sample	**N° of Sample Fractions**	**Amount (g)**	**%Yield (%)**
CCH-C2(2)-1.80	10	3.2724	28.1

Detailed measurement data from all samples, their samples, their sample fractions and their replicas are listed from Table 134 to Table 142 in Appendix II (See section 10. Appendix II: Tables).

4.3.3. FTIR

The FTIR spectrum of sample CCH-C2(2)-1.80 (Figure 66) confirms the structure of the CMC-g-PNIPAAm graft copolymers obtained. From this spectra are visible the characteristic peaks for PNIPAAm oligomers, at 1,649 cm^{-1} (group -N-C=O) and 1,546 cm^{-1} (group –NH-); and the characteristic ones for CMC polymers, at 1,460.0 and 1,063 cm^{-1} (group CH_2 and O atom

from the cellulose pyran ring) and at 3,434.4 cm^{-1} (group OH from the cellulose ring). As a complement, in Figure 66 are presented per separated, the spectra of aminoterminated PNIPAAm oligomers (Sample CCH-A15-1) and carboxymethyl cellulose (Sample NaCMC), showing their respective characteristic peaks. FTIR measurement data from other samples,

their sample fractions and their replicas are listed in Tables 70, 71 and 72 at Appendix II (See section 10. Appendix II: Tables).

4.3.4. DSC (Dry)

The DSC measurements (Figure 67 and 68) performed on dried samples of CMC-g-PNIPAAm graft copolymers, carboxymethyl cellulose (NaCMC) and aminoterminated PNIPAAm oligomers, confirmed that the grafting of the PNIPAAm oligomers on the CMC was successfully made. The analysis (Figure 67) showed a decrease of the melting temperature

Table 21
Amount and %Yield of Group of Samples B
($Mw(Graft)_{(THEO)}$ = 7,000 g/mol)

Group of Samples B ($Mw(Graft)_{(THEO)}$ = 7,000 g/mol)			
Sub-Group B.1 (%$Graft_{(THEO)}$=40%)			
Sample	**N° of Sample Fractions**	**Amount (g)**	**%Yield (%)**
CCH-B5-2.40	1	0.6823	52.1
CCH-C2(2)-2<1>.40	2	0.0838	15.6
CCH-C2(2)-2.40	5	0.8351	28.2
Sub-Group B.2 (%$Graft_{(THEO)}$=50%)			
Sample	**N° of Sample Fractions**	**Amount (g)**	**%Yield (%)**
CCH-B5-2.50	1	0.2637	24.8
CCH-C2(2)-2<1>.50	2	0.1455	22.4
CCH-C2(2)-2.50	4	1.4664	40.0
Sub-Group B.3 (%$Graft_{(THEO)}$=80%)			
Sample	**N° of Sample Fractions**	**Amount (g)**	**%Yield (%)**
CCH-C2(2)-2<1>.80	3	0.1578	10.2
CCH-C2(2)-2.80	7	3.4888	41.5

(T_m) from 185.6 °C for CMC to 174 °C for CMC-g-PNIPAAm graft copolymers (Sample CCH-C2(2)-1.80), which is close to the T_m of 175.2 °C from aminoterminated PNIPAAm oligomers (Sample fraction CCH-C1(2)-1(3)). The melting enthalpy of the 3 samples was also calculated: 102 J/g for aminoterminated PNIPAAm oligomers (Sample fraction CCH-C1(2)-1(3)), 138 J/g

for carboxymethyl cellulose (sample NaCMC) and 140 J/g for CMC-g-PNIPAAm graft copolymers (Sample CCH-C2(2)-1.80). Figure 68 shows, as another evidence of a successful grafting, that in the DSC curve is observed the presence of signals of CMC-g-PNIPAAm graft copolymers (Sample CCH-C2(2)-1.80), that correspond to glass transition temperatures (T_g) of aminoterminated PNIPAAm oligomers (146.6 °C) and CMC (53.9 °C). As a complement, in Figure 68 are presented separately, the curves of aminoterminated PNIPAAm oligomers (Sample fraction CCH-C1(2)-1(3)) and carboxymethyl cellulose (Sample NaCMC), showing their respective T_g. DSC measurements from other samples (and their sample fractions) are listed in Tables 73, 74 and 75 at Appendix II (See section 10. Appendix II: Tables).

Table 22

Amount and %Yield of Group of Samples C

($Mw(Graft)_{(THEO)}$ = 9,000 g/mol)

Group of Samples C ($Mw(Graft)_{(THEO)}$ = 9,000 g/mol)			
Sub-Group C.1 ($\%Graft_{(THEO)}$=40%)			
Sample	**N° of Sample Fractions**	**Amount (g)**	**%Yield (%)**
CCH-B5-3.40	1	0.4705	60.3
CCH-C2(2)-3.40	3	1.0651	37.3
Sub-Group C.2 ($\%Graft_{(THEO)}$=50%)			
Sample	**N° of Sample Fractions**	**Amount (g)**	**%Yield (%)**
CCH-B5-3.50	1	0.2930	46.6
CCH-C2(2)-3.50	3	1.0779	31.0
Sub-Group C.3 ($\%Graft_{(THEO)}$=80%)			
Sample	**N° of Sample Fractions**	**Amount (g)**	**%Yield (%)**
CCH-C2(2)-3.80	6	3.3153	44.9

Table 23

Mw(Total), %Graft(EXP) and N° Grafts per CMC Chain for Group of Samples A

(Mw(Graft)(THEO) = 5,000 g/mol)

Group of Samples A (Mw(Graft)(THEO) = 5,000 g/mol)						
Sub-Group A.1 (%Graft(THEO)=40%)						
Sample	**Mw(Total) (g/mol)**	**Mw(CMC)[a] (g/mol)**	**Mw(Graft)(EXP)[b] (g/mol)**	**%Graft(EXP) (%)**	**N° Grafts per CMC Chain**	**DP(Graft)[b]**
CCH-A27-1 Backbone: CMC Grafts: CCH-A15-1	1'016,283	700,000	5,101.340	31	60	44
CCH-C2-1.40 Backbone: CMC Grafts: CCH-C1-1	100,206	90,000	5,103.026	10	2	44
CCH-C2(2)-1.40 Backbone: CMC Grafts: CCH-A15-1, CCH-A15-2, CCH-A15-3, CCH-C1-1 and CCH-C1(2)-1	145,790	90,000	5,071.776	38	11	44

[a] Information provided by the supplier.

[b] Estimated in elemental analysis, corresponds to the molecular weight of grafts composed of either a unique aminoterminated PNIPAAM oligomer or different aminoterminated PNIPAAm oligomers, resulting in this case grafts with a molecular weight average value.

Table 23 (Cont.)

Group of Samples A (Mw(Graft)(THEO) = 5,000 g/mol)						
Sub-Group A.2 (%Graft(THEO)=50%)						
Sample	**Mw(Total) (g/mol)**	**Mw(CMC)[a] (g/mol)**	**Mw(Graft)(EXP)[b] (g/mol)**	**%Graft(EXP) (%)**	**N° Grafts per CMC Chain**	**DP(Graft)[b]**
CCH-B5-1.50 Backbone: CMC Grafts: CCH-A15-1	1‘210,134	700,000	5,101.340	42	100	44
CCH-C2(2)-1.50 Backbone: CMC Grafts: CCH-A15-1, CCH-A15-2, CCH-A15-3, CCH-C1-1 and CCH-C1(2)-1	176,220	90,000	5,071.776	49	17	44
Sub-Group A.3 (%Graft(THEO)=80%)						
Sample	**Mw(Total) (g/mol)**	**Mw(CMC)[a] (g/mol)**	**Mw(Graft)(EXP)[b] (g/mol)**	**%Graft(EXP) (%)**	**N° Grafts per CMC Chain**	**DP(Graft)[b]**
CCH-C2(2)-1.80 Backbone: CMC Grafts: CCH-A15-1, CCH-A15-2, CCH-A15-3, CCH-C1-1 and CCH-C1(2)-1	308,086	90,000	5,071.776	71	43	44

[a] Information provided by the supplier.

[b] Estimated in elemental analysis, corresponds to the molecular weight of grafts composed of either a unique aminoterminated PNIPAAM oligomer or different aminoterminated PNIPAAm oligomers, resulting in this case grafts with a molecular weight average value.

Table 24

Mw(Total), %Graft(EXP) and N° Grafts per CMC Chain for Group of Samples B

(Mw(Graft)(THEO) = 7,000 g/mol)

Group of Samples B (Mw(Graft)(THEO) = 7,000 g/mol)						
Sub-Group B.1 (%Graft(THEO)=40%)						
Sample	**Mw(Total) (g/mol)**	**Mw(CMC)[a] (g/mol)**	**Mw(Graft)(EXP)[b] (g/mol)**	**%Graft(EXP) (%)**	**N° Grafts per CMC Chain**	**DP(Graft)[c]**
CCH-B5-2.40 Backbone: CMC Grafts: CCH-B4-1	833,916	700,000	7,048.210	16	19	60
CCH-C2(2)-2<1>.40 Backbone: CMC Grafts: CCH-C1(2)-2(2)<1>	118,000	90,000	7,000.000	24	4	60
CCH-C2(2)-2.40 Backbone: CMC Grafts: CCH-B4-1, CCH-C1-2 and CCH-C1(2)-2	104,143	90,000	7,071.348	14	2	60

[a] Information provided by the supplier.

[b] Estimated in elemental analysis, corresponds to the molecular weight of grafts composed of either a unique aminoterminated PNIPAAM oligomer or different aminoterminated PNIPAAm oligomers, resulting in this case grafts with a molecular weight average value.

Table 24 (Cont.)

Group of Samples B (Mw(Graft)(THEO) = 7,000 g/mol)						
Sub-Group B.2 (%Graft(THEO)=50%)						
Sample	**Mw(Total) (g/mol)**	**Mw(CMC)[a] (g/mol)**	**Mw(Graft)(EXP)[b] (g/mol)**	**%Graft(EXP) (%)**	**N° Grafts per CMC Chain**	**DP(Graft)[b]**
CCH-B5-2.50 Backbone: CMC Grafts: CCH-B4-1	1‘136,989	700,000	7048.210	38	62	60
CCH-C2(2)-2<1>.50 Backbone: CMC Grafts: CCH-C1(2)-2(2)<1>	146,000	90,000	7000.000	38	8	60
CCH-C2(2)-2.50 Backbone: CMC Grafts: CCH-B4-1, CCH-C1-2 and CCH-C1(2)-2	167,785	90,000	7071.348	46	11	60

[a] Information provided by the supplier.

[b] Estimated in elemental analysis, corresponds to the molecular weight of grafts composed of either a unique aminoterminated PNIPAAM oligomer or different aminoterminated PNIPAAm oligomers, resulting in this case grafts with a molecular weight average value.

Table 24 (Cont.)

Group of Samples B (Mw(Graft)(THEO) = 7,000 g/mol)						
Sub-Group B.3 (%Graft(THEO)=80%)						
Sample	**Mw(Total) (g/mol)**	**Mw(CMC)[a] (g/mol)**	**Mw(Graft)(EXP)[b] (g/mol)**	**%Graft(EXP) (%)**	**N° Grafts per CMC Chain**	**DP(Graft)[b]**
CCH-C2(2)-2<1>.80 Backbone: CMC Grafts: CCH-C1(2)-2(2)<1>	181,000	90,000	7,000.000	50	13	60
Sample CCH-C2(2)-2.80 Backbone: CMC Grafts: CCH-B4-1, CCH-C1-2 and CCH-C1(2)-2	302,140	90,000	7,071.348	70	30	60

[a] Information provided by the supplier.

[b] Estimated in elemental analysis, corresponds to the molecular weight of grafts composed of either a unique aminoterminated PNIPAAM oligomer or different aminoterminated PNIPAAm oligomers, resulting in this case grafts with a molecular weight average value.

Table 25

Mw(Total), %Graft(EXP) and N° Grafts per CMC Chain

for Group of Samples C

(Mw(Graft)(THEO) = 9,000 g/mol)

Group of Samples C (Mw(Graft)(THEO) = 9,000 g/mol)						
Sub-Group C.1 (%Graft(THEO)=40%)						
Sample	**Mw(Total) (g/mol)**	**Mw(CMC)[a] (g/mol)**	**Mw(Graft)(EXP)[b] (g/mol)**	**%Graft(EXP) (%)**	**N° Grafts per CMC Chain**	**DP(Graft)[c]**
CCH-B5-3.40 Backbone: CMC Grafts: CCH-B4-2	929,229	700,000	9,169.140	25	25	78
CCH-C2(2)-3.40 Backbone: CMC Grafts: CCH-B4-2, CCH-C1-3, CCH-C1(2)-3, CCH-C1(2)-3.2 and CCH-C1(2)-3.3	108,161	90,000	9,080.610	17	2	78

[a] Information provided by the supplier.

[b] Estimated in elemental analysis, corresponds to the molecular weight of grafts composed of either a unique aminoterminated PNIPAAM oligomer or different aminoterminated PNIPAAm oligomers, resulting in this case grafts with a molecular weight average value.

Table 25 (Cont.)

Group of Samples C (Mw(Graft)(THEO) = 9,000 g/mol)						
Sub-Group C.2 (%Graft(THEO)=50%)						
Sample	**Mw(Total) (g/mol)**	**Mw(CMC)[a] (g/mol)**	**Mw(Graft)(EXP)[b] (g/mol)**	**%Graft(EXP) (%)**	**N° Grafts per CMC Chain**	**DP(Graft)[b]**
CCH-B5-3.50 Backbone: CMC Grafts: CCH-B4-2	1,149,288	700,000	9,169.140	39	49	78
CCH-C2(2)-3.50 Backbone: CMC Grafts: CCH-B4-2, CCH-C1-3, CCH-C1(2)-3, CCH-C1(2)-3.2 and CCH-C1(2)-3.3	162,645	90,000	9,080.610	45	8	78

[a] Information provided by the supplier.

[b] Estimated in elemental analysis, corresponds to the molecular weight of grafts composed of either a unique aminoterminated PNIPAAM oligomer or different aminoterminated PNIPAAm oligomers, resulting in this case grafts with a molecular weight average value.

Table 25 (Cont.)

Group of Samples C (Mw(Graft)(THEO) = 9,000 g/mol)						
Sub-Group C.3 (%Graft(THEO)=80%)						
Sample	**Mw(Total) (g/mol)**	**Mw(CMC)[a] (g/mol)**	**Mw(Graft)(EXP)[b] (g/mol)**	**%Graft(EXP) (%)**	**N° Grafts per CMC Chain**	**DP(Graft)[b]**
CCH-C2(2)-3.80 Backbone: CMC Grafts: CCH-B4-2, CCH-C1-3, CCH-C1(2)-3, CCH-C1(2)-3.2 and CCH-C1(2)-3.3	289,773	90,000	9,080.610	69	22	78

[a] Information provided by the supplier.

[b] Estimated in elemental analysis, corresponds to the molecular weight of grafts composed of either a unique aminoterminated PNIPAAM oligomer or different aminoterminated PNIPAAm oligomers, resulting in this case grafts with a molecular weight average value.

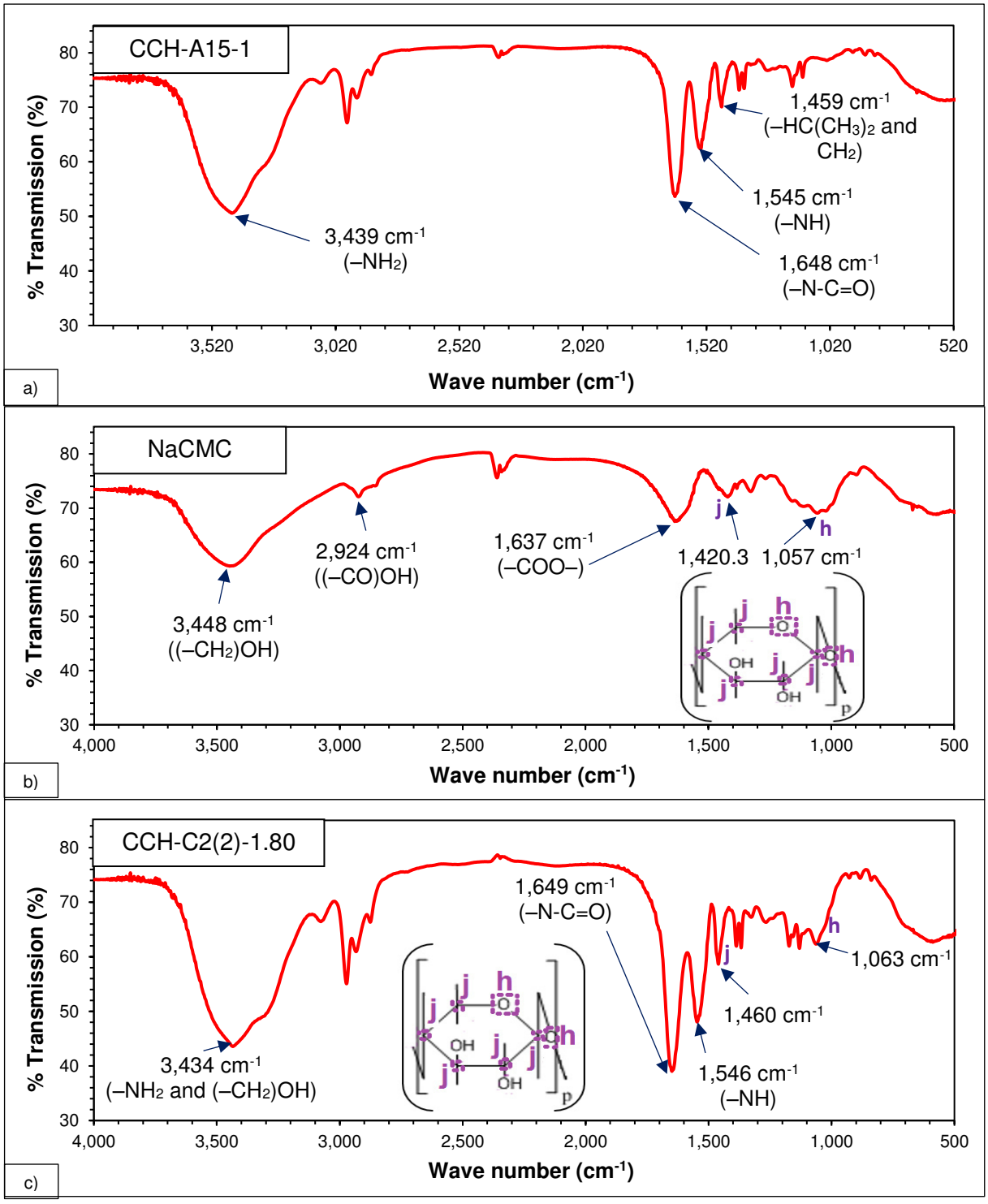

Figure 66. (a) FTIR Spectrum of CMC-g-PNIPAAm graft copolymers (Sample CCH-C2(2)-1.80) versus FTIR Spectra of (b) carboxymethyl cellulose (Sample NaCMC) and (c) amino-terminated PNIPAAm oligomers (Sample CCH-A15-1).

4.4. Characterization of Phase Transition Activity in CMC-g-PNIPAAm graft copolymers

4.4.1. Reversibility of Phase Transition in Water and in Buffer Solutions

The thermosensitive activity of aqueous solutions of CMC-g-PNIPAAm graft copolymers was revealed with DSC measurements (Figure 69) by showing a LCST peak signal, which was not visible in the measurements of carboxymethyl cellulose aqueous solutions. Low Critical Solution Temperatures (LCST) of around 33 °C (heating cycle) and 31 °C (cooling cycle) were estimated for the CMC-g-PNIPAAm graft copolymers. The analysis also showed that the thermosensitive activity was reversible during the heating and the cooling cycles. DSC measurements performed with buffer solutions of CMC-g-PNIPAAm graft copolymers, revealed also thermosensitive activity, noticeable by their respective LCST peak signal. DSC measurements from other samples (and their sample fractions) aqueous and buffer solutions are listed in Tables 76, 77, 78, 79, 80 and 81 at Appendix II (See section 10. Appendix II: Tables).

Finally, Figure 70 confirms that the thermosensitivity shown in aqueous and buffer solutions of CMC-g-PNIPAAm graft copolymers, was due the grafting of PNIPAAm oligomers to the CMC backbone, because the DSC measurements performed to aqueous and buffer solutions of carboxymethyl cellulose (CMC) with different molecular weights, exhibited no LCST signal. Therefore no thermosensitivity, neither during the heating cycles, nor during the cooling cycles occurred. (No hay Tabla en el apéndice)

4.5. Synthesis and Structural Characterization of comb-type graft hydrogels

4.5.1. FTIR

The FTIR spectra of sample CCH-C3(5)-2(35%) (Figure 71) confirmed the structure of the obtained CMC-g-PNIPAAm comb-type graft hydrogels. From this spectra, the crosslinking of the CMC-g-PNIPAAm graft copolymers, is represented by the characteristic peak of the crosslinker citric acid at 1,712 cm^{-1} (-COOH). This peak was not visible in the FTIR spectra of the CMC-g-PNIPAAm graft copolymers (Figure 66). The characteristic peaks of the CMC-g-PNIPAAm graft copolymers are also visible. FTIR measurement data from other samples (and their replicas) are listed in Table 82 at Appendix II (See section 10. Appendix II: Tables).

4.5.2. DSC (Dry)

The DSC measurements (Figure 72) performed on dried samples of CMC-g-PNIPAAm comb-type graft hydrogels crosslinked with citric acid, Al^{3+} Ions and CMC-g-PNIPAAm graft copolymers, confirmed that the crosslinking of the CMC-g-PNIPAAm graft copolymers was successfully made, because the analysis showed an increase of the melting temperature (T_m) from 174 °C for CMC-g-PNIPAAm graft copolymers (Sample CCH-C2(2)-1.80) to 196.5 °C for

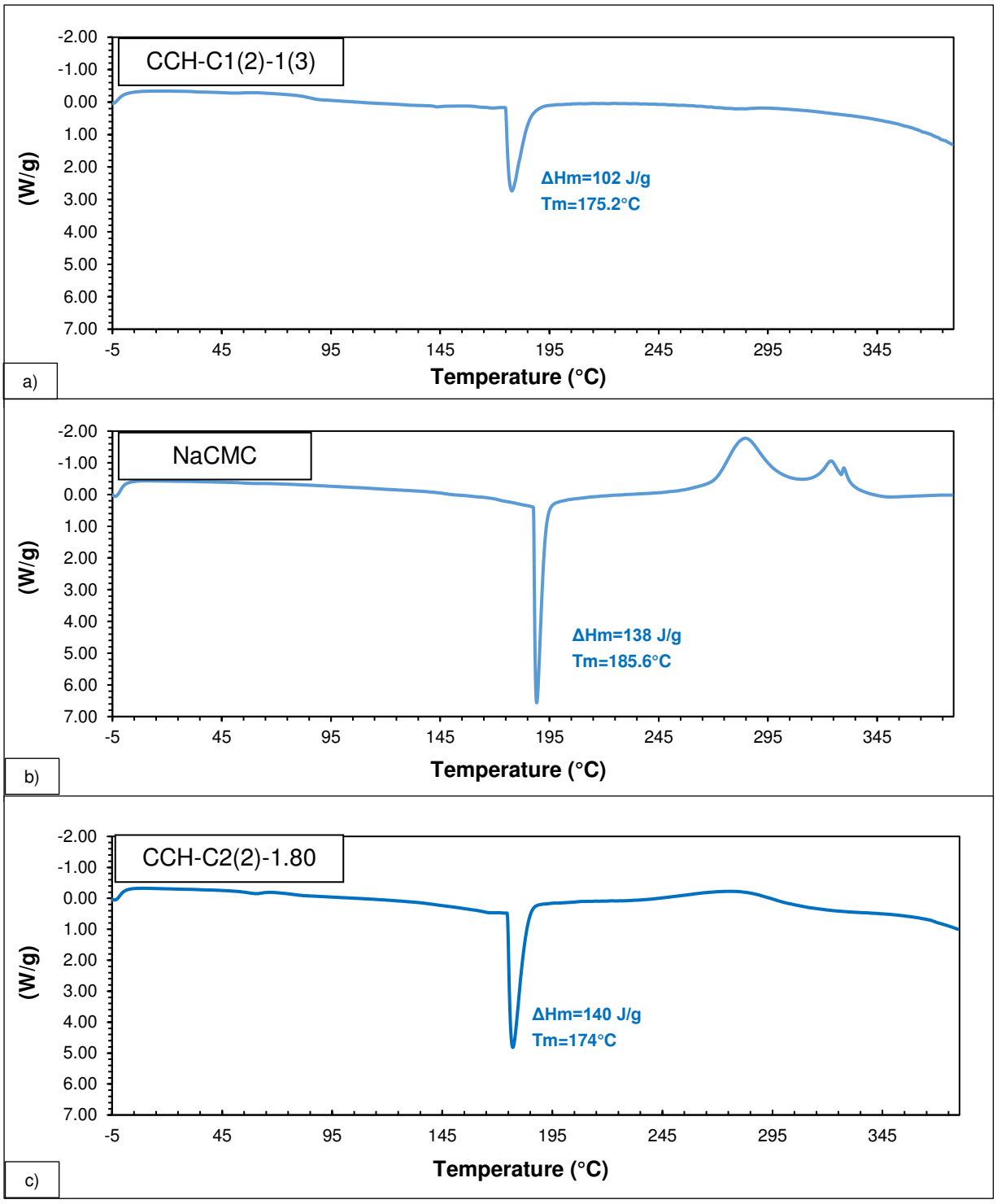

Figure 67. T_m and ΔH_m of (a) CMC-g-PNIPAAm graft copolymers (Sample CCH-C2(2)-1.80) versus (b) aminoterminated PNIPAAm oligomers (Sample fraction CCH-C1(2)-1(3)) and (c) carboxymethyl cellulose (Sample NaCMC)

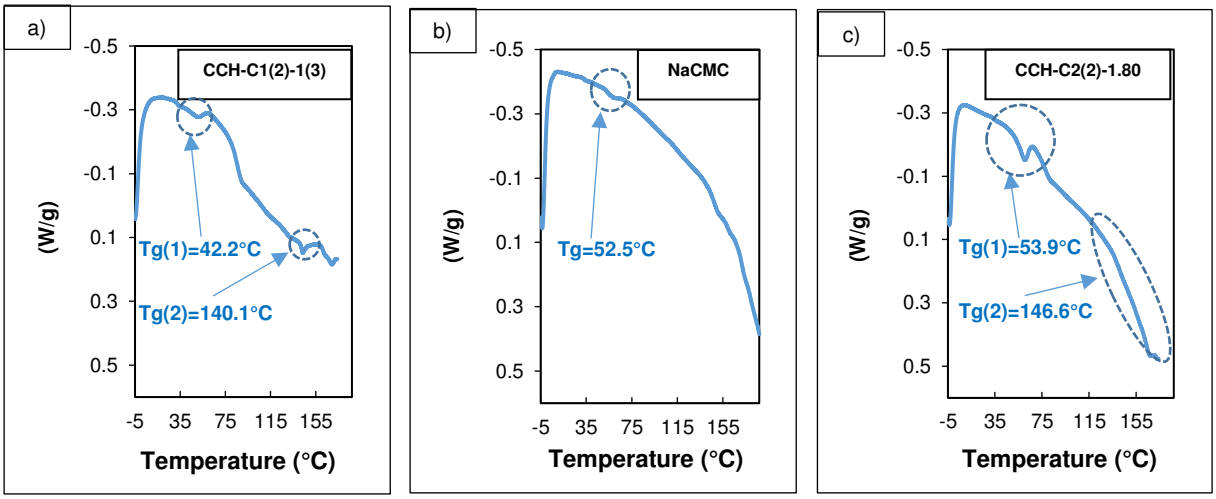

Figure 68. T_g of (a) aminoterminated PNIPAAm oligomers (Sample fraction CCH-C1(2)-1(3)) and (b) carboxymethyl Cellulose (Sample NaCMC) versus (c) CMC-g-PNIPAAm graft copolymers (Sample CCH-C2(2)-1.80)

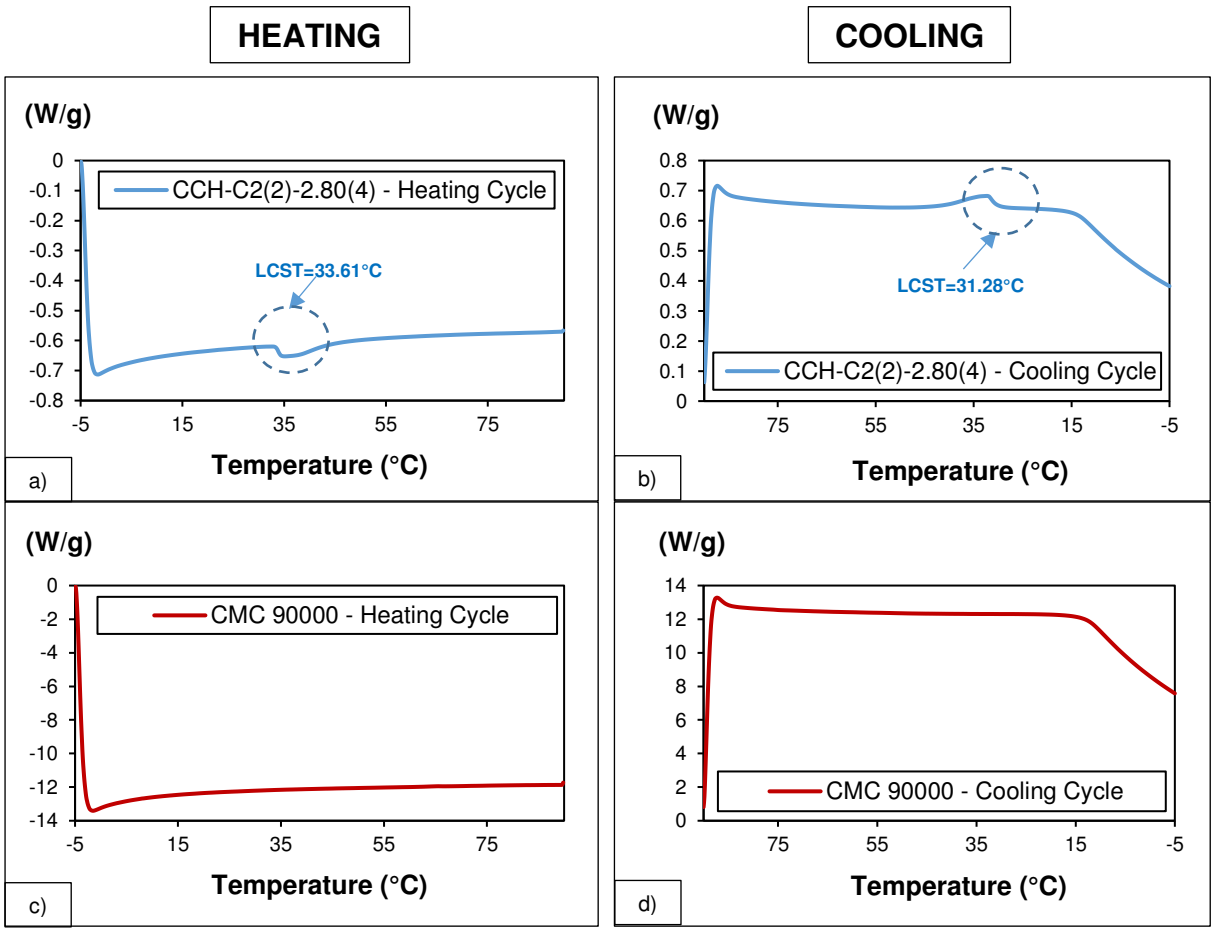

Figure 69. Reversibility of phase transition in water of (a and b) CMC-g-PNIPAAm graft copolymers (Sample fraction CCH-C2(2)-2.80(4)) versus (c and d) carboxymethyl cellulose (Sample CMC 90,000)

CMC-g-PNIPAAm comb-type graft hydrogels crosslinked with citric acid (sample CCH-C3(8)MONO-1(CA)) and 306.5 °C for the ones crosslinked with Al^{3+} Ions (sample CCH-C3(8)MONO-1(Al)). This result also revealed that the CMC-g-PNIPAAm comb-type graft hydrogels crosslinked with Al^{3+} Ions were more thermally stable than the ones crosslinked with citric acid.

4.5.3. Swelling Kinetics and Equilibrium Ratio

With the collected data, tendency lines were plotted (Figure 73). From the graphics presented, it can be deduced that CMC-g-PNIPAAm comb-type graft hydrogel samples crosslinked with Al^{3+} Ions, had a higher swelling degree (527%) than the ones crosslinked with citric acid (365%), and at the same time, this ones had a higher swelling degree than the CMC hydrogel samples crosslinked with Al^{3+} ions (258%). Also, even the samples crosslinked with citric acid, had lower swelling degree than the ones crosslinked with Al^{3+} ions, they achieved their maximum swelling degree in approximately 70 minutes, while the other ones required circa 100 minutes. Detailed measurement data from other samples (and their replicas) are listed in Tables 83 and 84 at Appendix II (See section 10. Appendix II: Tables).

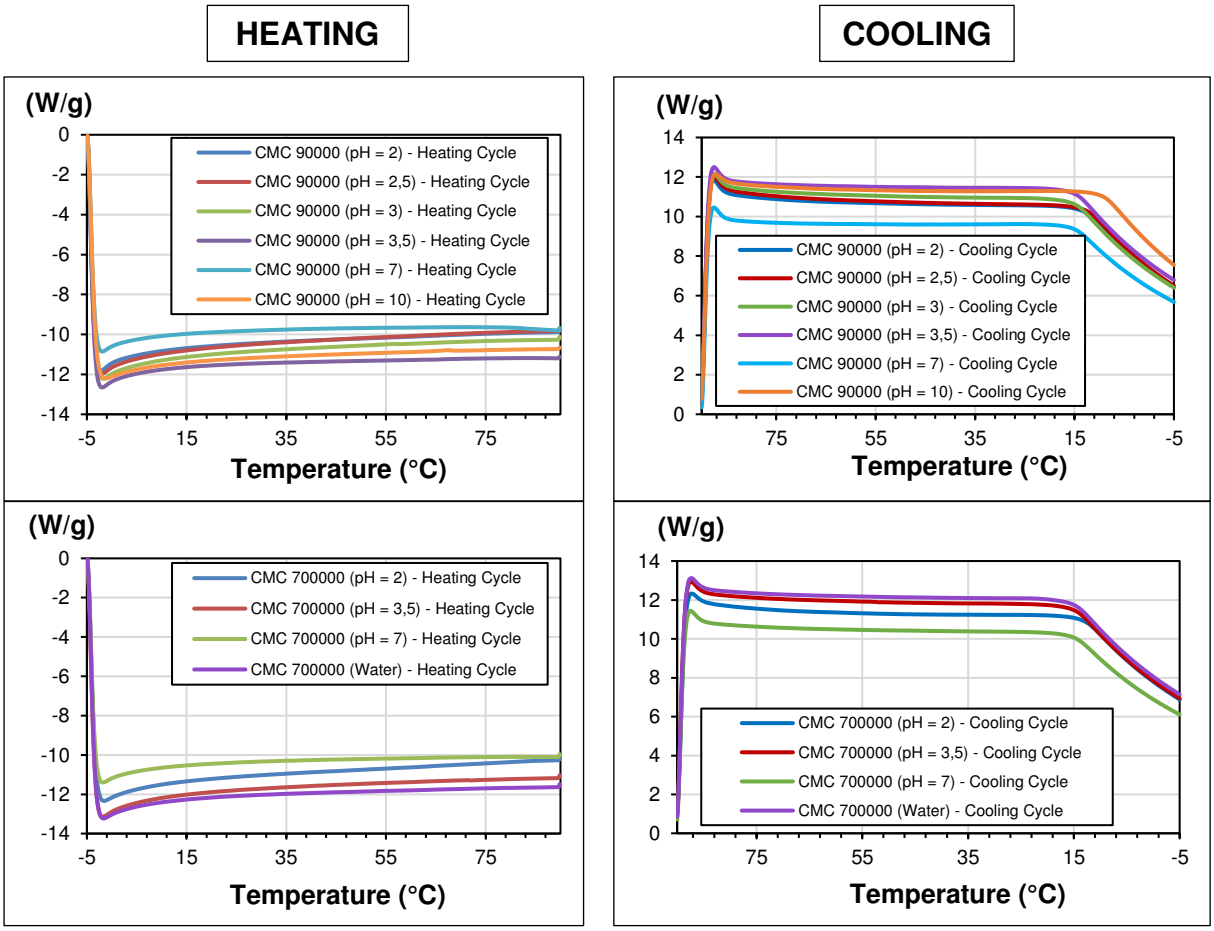

Figure 70. DSC of CMC in Water and Buffer Solutions

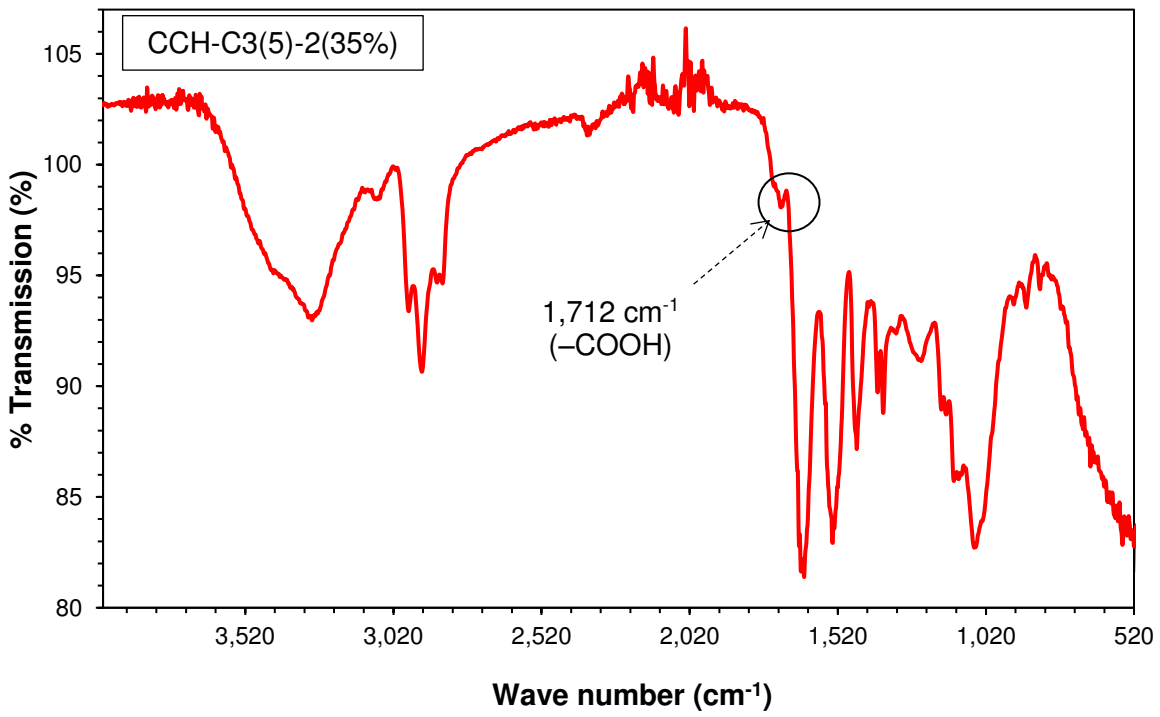

Figure 71. FTIR spectrum of CMC-g-PNIPAAm comb-type graft hydrogels (Sample CCH-C3(5)-2(35%))

4.6. Characterization of phase transition activity in comb-type graft hydrogels

4.6.1. Characterization of phase transition activity by digital photographs

Figure 72 shows that the swelling degree in water of CMC-g-PNIPAAm comb-type hydrogels, crosslinked either with citric acid or with Al^{3+} ions, can be tuned with temperature and time.

At 80 °C and after 5 minutes, the sample crosslinked with Al^{3+} ions presented a drastic reduction in its dimensions, in comparison with the same sample at 25 °C. The sample maintained these decreased dimensions for 50 minutes, then it presented a second shrinking event. Finally, a third shrinking was noticeable after 120 minutes of immersion.

In the case of the sample crosslinked with citric acid, a first shrinking is observed after 15 minutes. However, this shrinking was not as drastic as with the sample crosslinked with Al^{3+} ions. The shrinking occurred gradually with time, and between 50 and 120 minutes. A drastic reduction in its dimensions was visible in comparison with the same sample at 25 °C.

In order to demonstrate that the shrinking of the CMC-g-PNIPAAm comb-type graft hydrogels, was due to the grafting of PNIPAAm oligomers on the CMC polymer chain, complementary measurements were also performed with CMC hydrogels, crosslinked either with citric acid or with Al^{3+}. As it was expected, in both samples, no reduction of dimensions was observed with time. It is to note was that the CMC sample crosslinked with citric acid was not stable at 80 °C, and after 120 minutes, the sample dissolved in water.

Figure 75 showed that the swelling degree in buffer solutions (pH=2 and pH=3) of CMC-g-PNIPAAm comb-type hydrogels, crosslinked with citric acid can be tuned with temperature and time. These samples achieved a drastic reduction of their dimensions after 46 minutes, presenting a faster shrinking in comparison with the sample evaluated in water at 80 °C that reached its maximum shrinking after 120 minutes.

CMC-g-PNIPAAm comb-type graft hydrogels crosslinked with Al^{3+} ions were not stable at 80 °C and in buffer solutions, and the samples were dissolved after 25 minutes (buffer solution pH=2) and 46 minutes (buffer solution pH=3).

4.6.2. Deswelling kinetics in water and in buffer solution pH=3 at 80 °C

From the collected data, tendency lines were plotted (Figure 76 and 77). According to Figure 76, it can be shown that CMC-g-PNIPAAm comb-type graft hydrogel sample crosslinked with Al^{3+} Ions, had a higher thermosensible deswelling (from 480% until 81%) than the one crosslinked with citric acid (from 390% until 300%). Also, the sample crosslinked with citric acid showed a lower deswelling than the one crosslinked with Al^{3+} ions. This achieved its maximum deswelling degree in circa 20 minutes, while the other one required about 80 minutes. Measurements with a CMC hydrogel crosslinked with citric acid were also performed, and no thermosensible deswelling occurred. An influence of media pH on the thermosensible deswelling of CMC-g-PNIPAAm comb-type graft hydrogel samples crosslinked with citric acid was observed. Sample immersed in buffer solution pH=3 had a higher thermosensible deswelling (from 379% until 114%) than the one immersed in water (from 390% until 300%). Detailed measurement data from other samples (and their replicas) are listed in Tables 85, 86, 87 and 88 at Appendix II (See section 10. Appendix II: Tables).

4.6.3. Pulsatile temperature dependent kinetics in water and buffer solution pH=3 at 80 °C and 4 °C

Figure 78 shows the reversibility and cycling of the thermosensitive swelling behavior, besides the influence of media pH on the thermosensible pulsatile kinetics, of CMC-g-PNIPAAm comb-type graft hydrogel samples crosslinked with citric acid. Sample immersed in buffer solution pH=3 had thermosensible pulsatile kinetics, varying from 132% (at 80 °C) to 545% (at 4 °C). This values were higher than the ones corresponding to the sample immersed in water, with thermosensible pulsatile kinetics, varying from 285% (at 80 °C) to 101% (at 4 °C). Detailed measurement data from other samples (and their replicas) are listed in Tables 89, 90, 91 and 92 at Appendix II (See section 10. Appendix II: Tables).

4.7. Synthesis and structural characterization of functionalized PA6 substrates

4.7.1. EA until initial activation with glutaraldehyde

The results of the element analysis (Table 26) revealed that it was possible to initially activate PA6 substrates with glutaraldehyde. The activation implies the generation of pendant

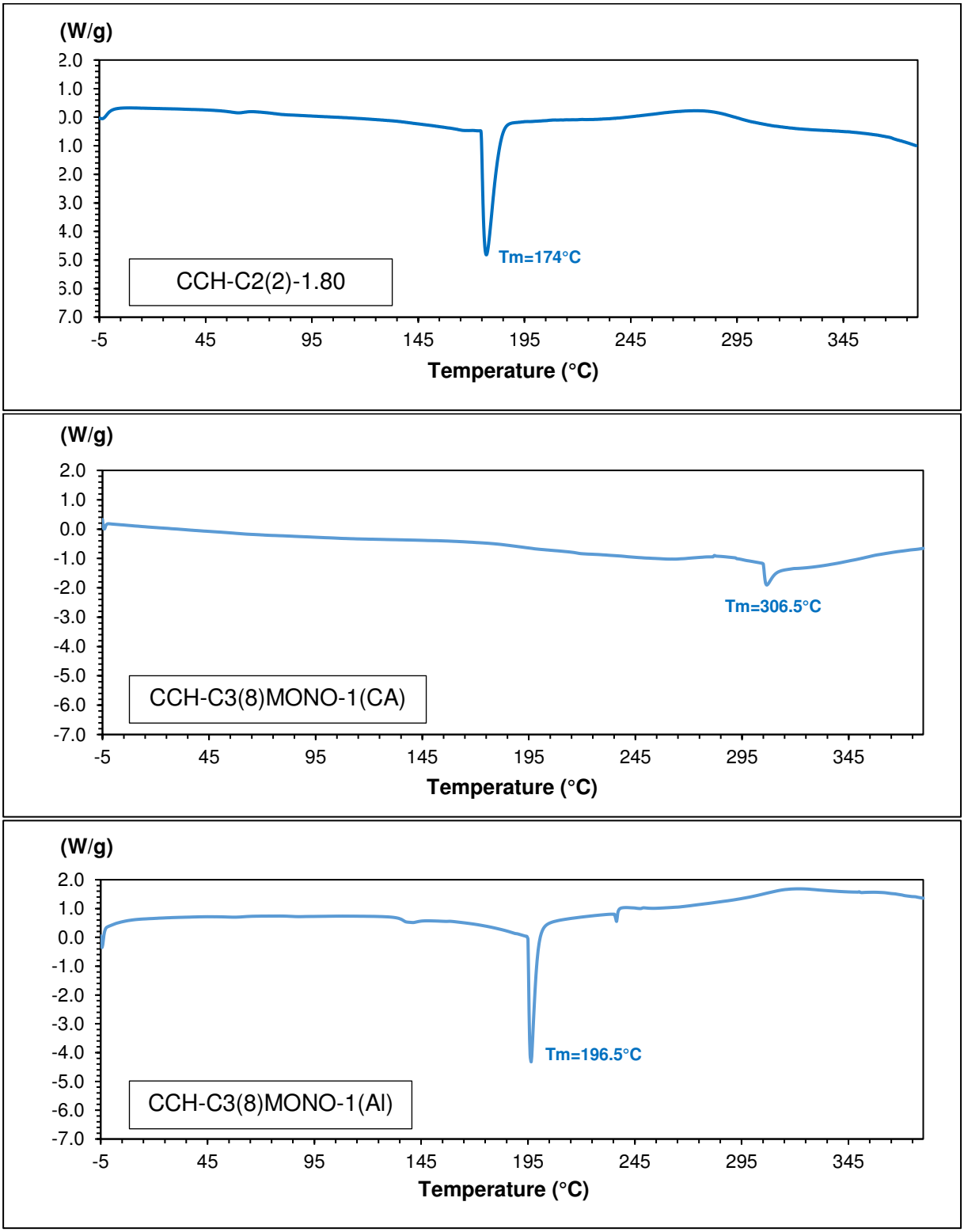

Figure 72. T_m of CMC-g-PNIPAAm comb-type graft hydrogels crosslinked with citric acid (Sample CCH-C3(8)MONO-1(CA)) and Al^{3+} ions (Sample CCH-C3(8)MONO-1(Al)) versus T_m of CMC-g-PNIPAAm graft copolymers (Sample CCH-C2(2)-1.80)

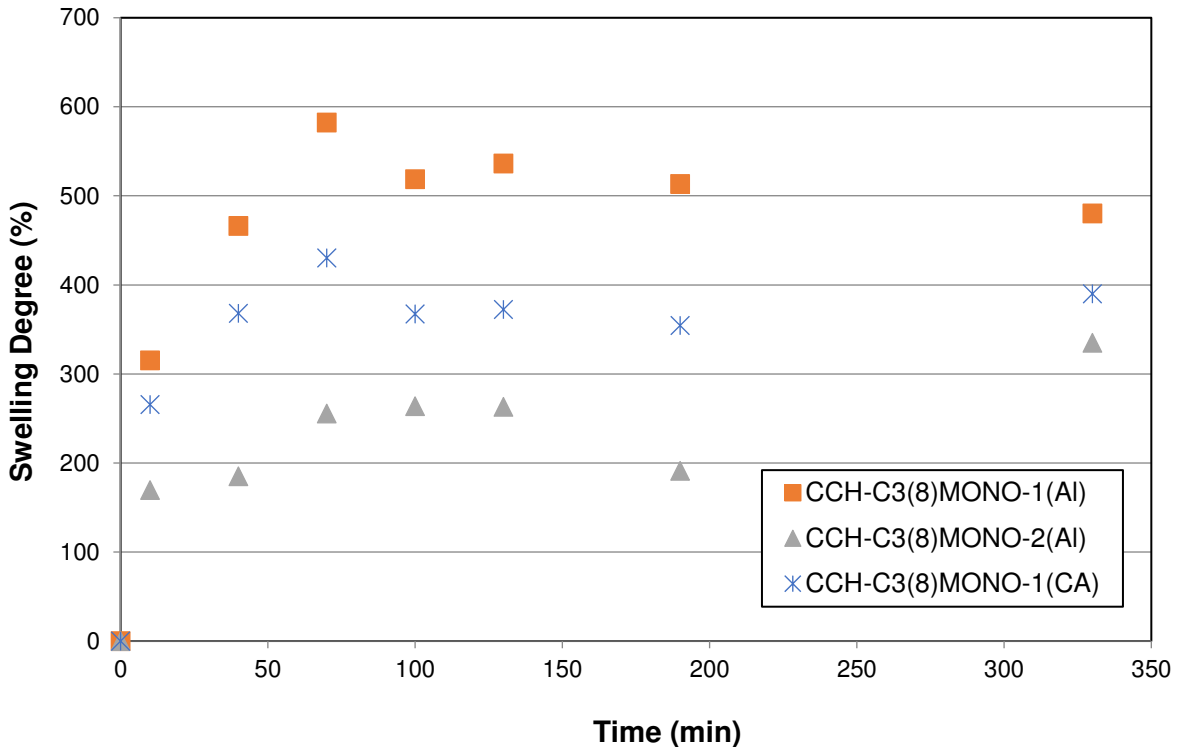

Figure 73. Swelling Degree in water of CMC-g-PNIPAAm comb-type graft hydrogels crosslinked with citric acid (Sample CCH-C3(8)MONO-1(CA)) and Al^{3+} Ions (Sample CCH-C3(8)MONO-1(Al)) versus Swelling Degree in water of CMC hydrogels crosslinked with Al^{3+} (Sample CCH-C3(8)MONO-2(Al))

aldehyde groups on the surface of the PA6 substrate, and this is supposed to be validated by element analysis by an increase on the carbon weight percentages (%C) present on each treated PA6 substrate, in relation with the untreated PA6 substrates.

In substrates treated with concentrated acidic hydrolysis (substrates CCH-C3(8)BI-PA6(1a) and CCH-C3(8)BI-PA6(1b)), there were a decrement and a low increment (-0.89 and 0.06%) on the %C, probably due to a degradation of the substrates caused by the concentrated HCl solution employed. Substrates treated with aqueous hydrolysis (substrates CCH-C3(8)BI-PA6(2a) and CCH-C3(8)BI-PA6(2b)) presented the highest %C increment (3.8 and 3.3%). Finally, the substrates treated with diluted acidic hydrolysis (substrates CCH-C3(8)BI-PA6(3a), CCH-C3(8)BI-PA6(3b) and CCH-C3(8)BI-PA6(3b.2)) presented intermediate %C increment (1.3, 1.3 and 1.5%).

4.7.2. FTIR until final activation with glutaraldehyde

The FTIR spectras of PA6 substrates before (and after) their respective hydrolysis treatment (Figure 79, 80 and 81), confirms that it was possible to activate PA6 substrates with glutaraldehyde by the generation of pendant aldehyde groups on the surface of the PA6

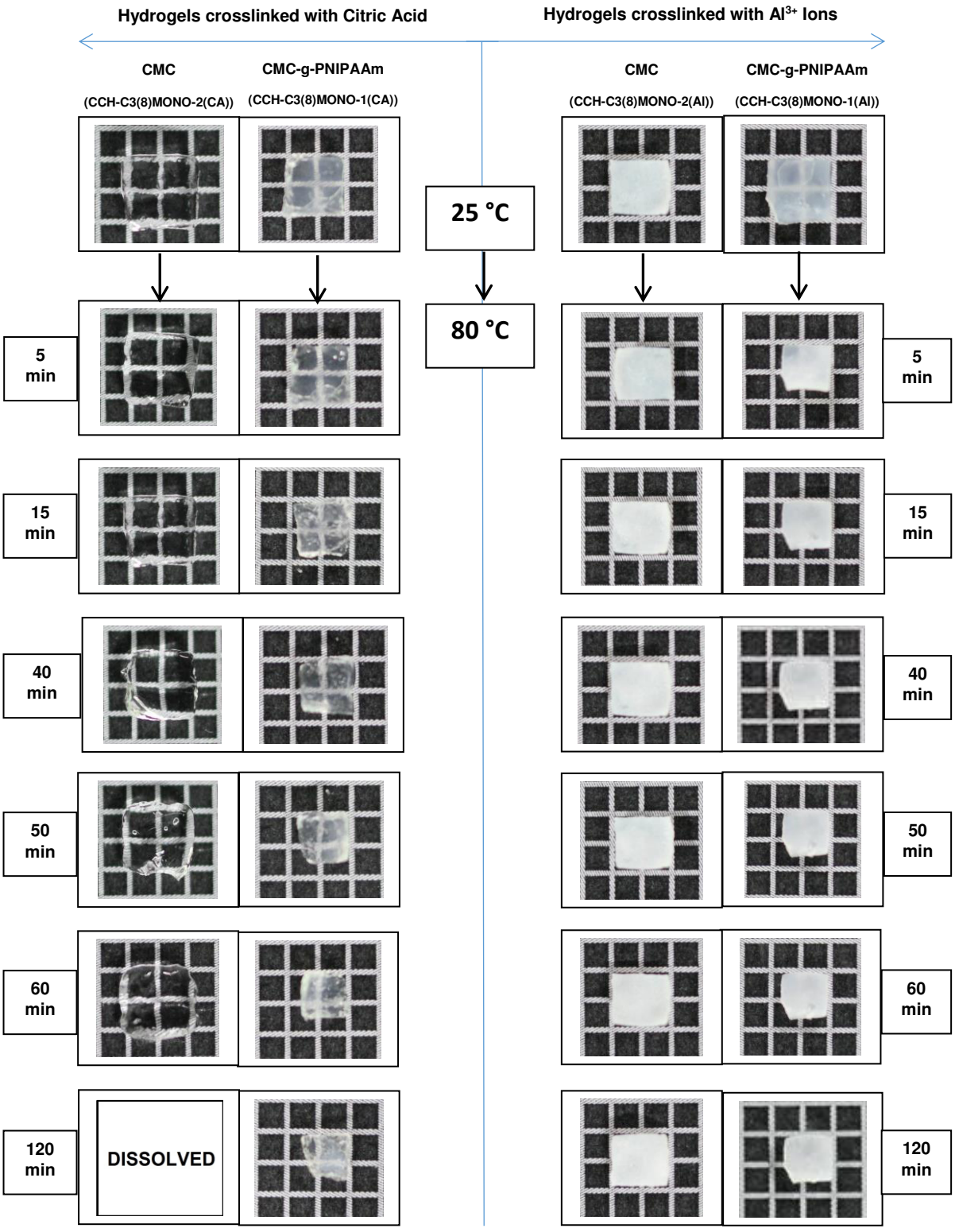

Figure 74. Photographs of the deswelling process in water of square-shape gel films of CMC and CMC grafted with poly(N-Isopropylacrylamide) (CMC-g-PNIPAAm) undergoing shrinking at 80 °C after elevated temperature from 25 °C.

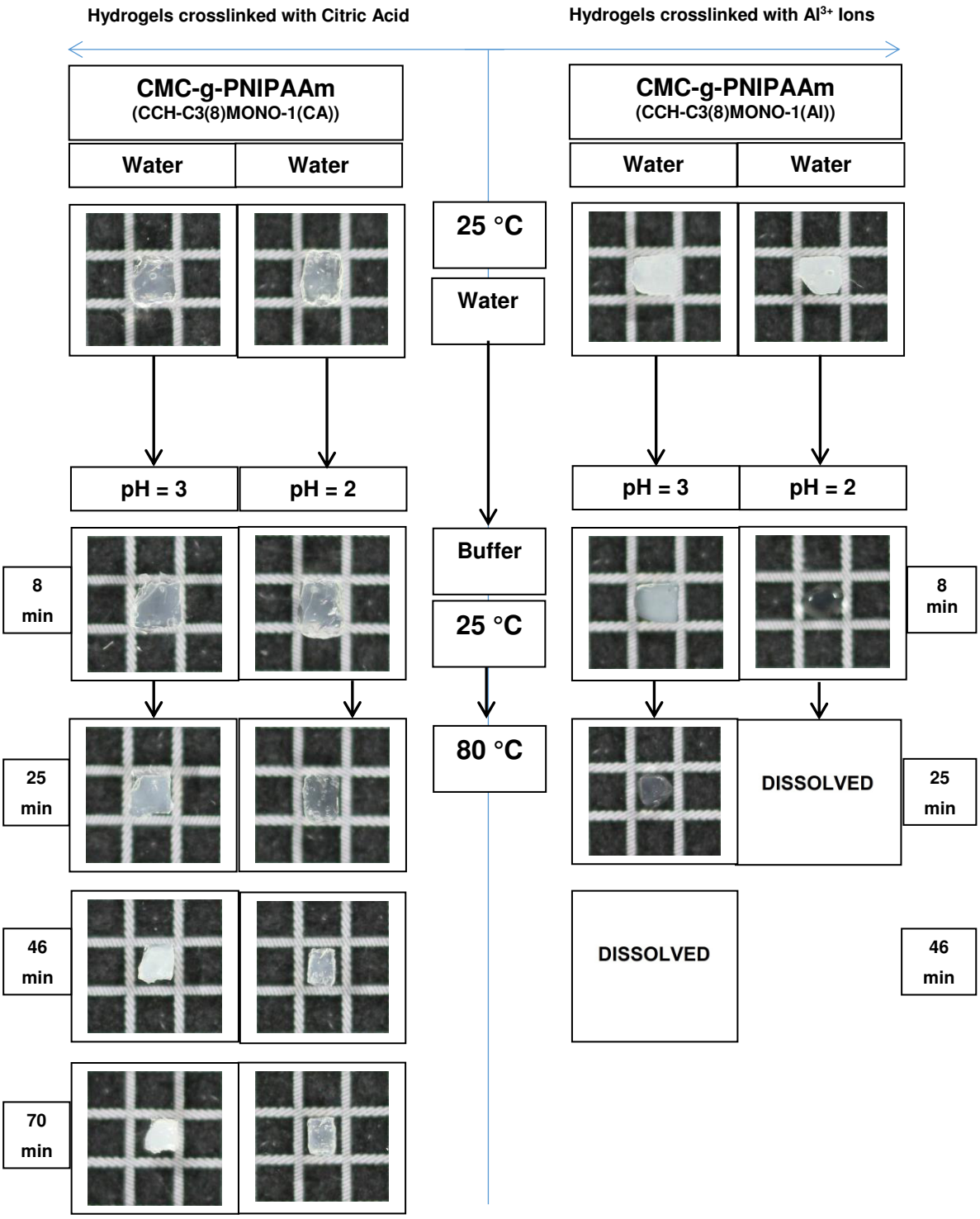

Figure 75. Photographs of the deswelling process in buffer solutions of square-shape gel films of carboxymethyl cellulose grafted with poly(N-Isopropylacrylamide) (CMC-g-PNIPAAm) undergoing shrinking in at 80 °C after elevated temperature from 25 °C and starting from water.

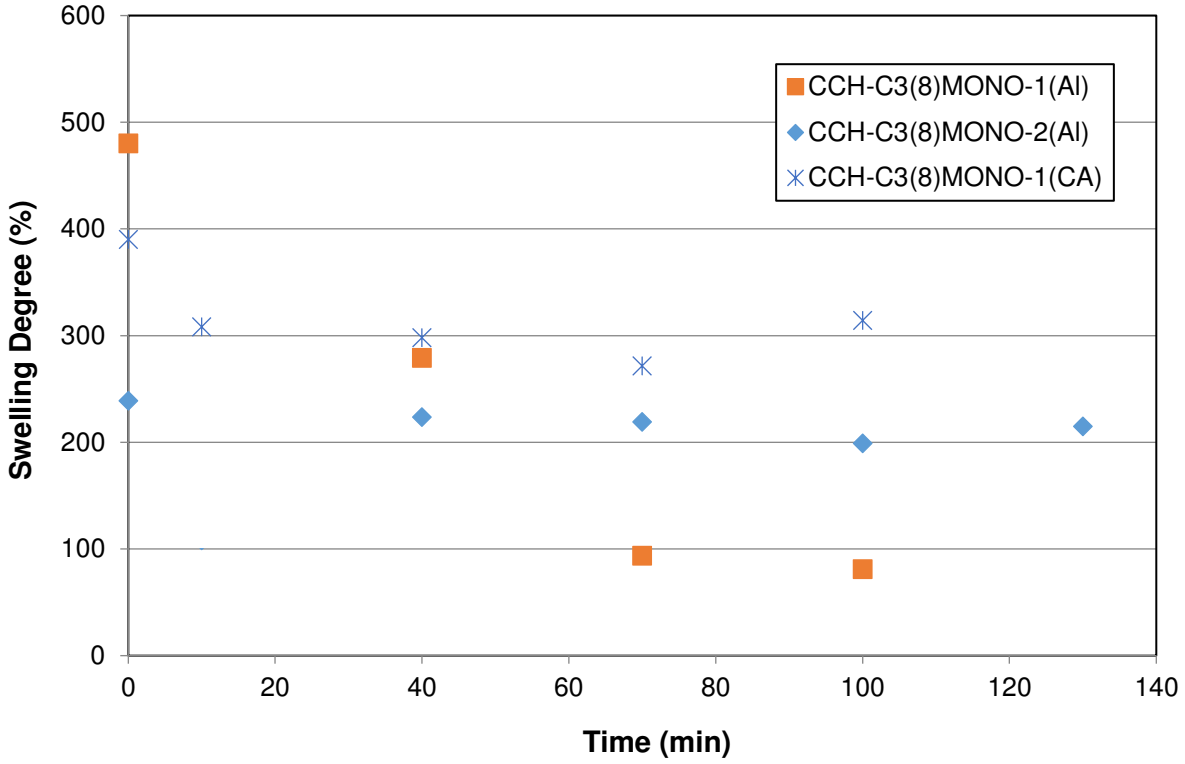

Figure 76. Deswelling in water at 80 °C of CMC-g-PNIPAAm comb-type graft hydrogels crosslinked with citric acid (Sample CCH-C3(8)MONO-1(CA)) and Al^{3+} ions (Sample CCH-C3(8)MONO-1(Al)) versus swelling degree in water of CMC hydrogels crosslinked with Al^{3+} (Sample CCH-C3(8)MONO-2(Al))

substrate, and this is validated by FTIR with spectra II. and III., that showed the characteristic peak of aldehyde group between 1,717 and 1,740 cm^{-1} (group -CHO). This peak was not visible in the FTIR spectra of the untreated PA6 substrates (Spectra I.). Detailed measurement data from other substrates (and their replicas) are listed in Tables 93, 94 and 95 at Appendix II (See section 10. Appendix II: Tables).

4.8. Synthesis and structural characterization of bilayer actuators based on CMC-g-PNIPAAm comb-type graft hydrogel films

4.8.1. FTIR

The FTIR spectra of sample CCH-C3(8)BI-3 (Figure 82) confirmed the structure of the obtained bilayer based on CMC-g-PNIPAAm comb-type graft hydrogel films. From this spectra, the interfacial crosslinking between the CMC-g-PNIPAAm comb-type graft hydrogel films and the functionalized PA6 substrate, is represented by the characteristic peak of the crosslinker citric acid at 1,718.0 cm^{-1} (group -COOH). The functionalized PA6 substrates (substrate CCH-C3(8)BI-PA6(2a)f) are represented by the characteristic peak of aldehyde

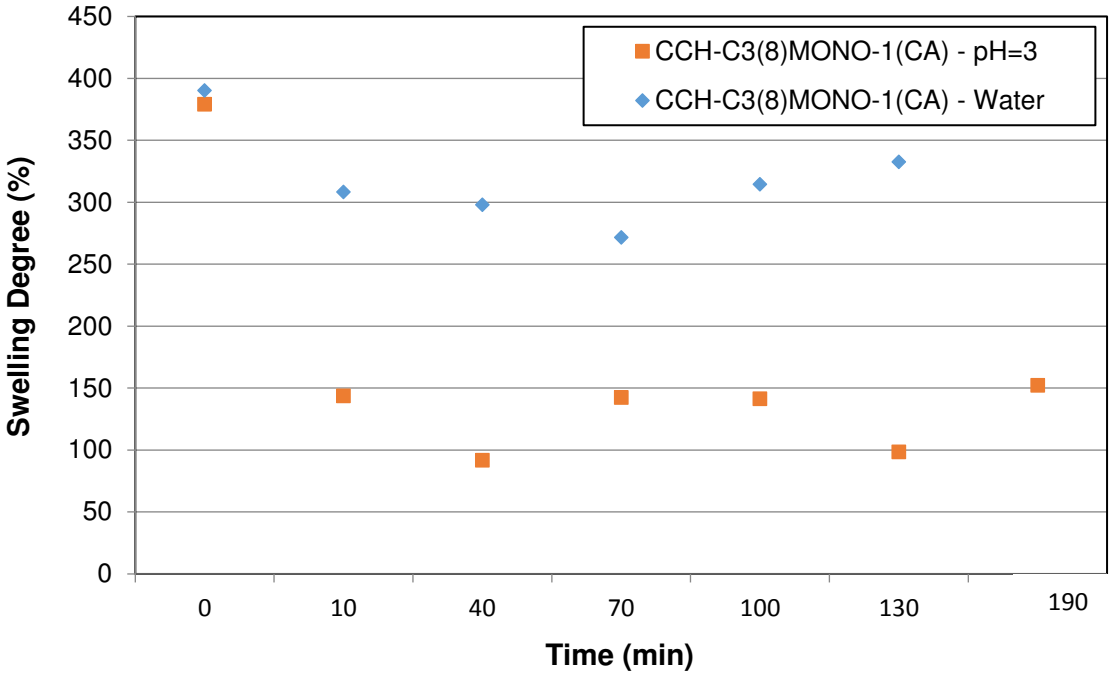

Figure 77. Deswelling in water and buffer solution pH=3 at 80 °C of CMC-g-PNIPAAm comb-type graft hydrogels crosslinked with citric acid (Sample CCH-C3(8)MONO-1(CA))

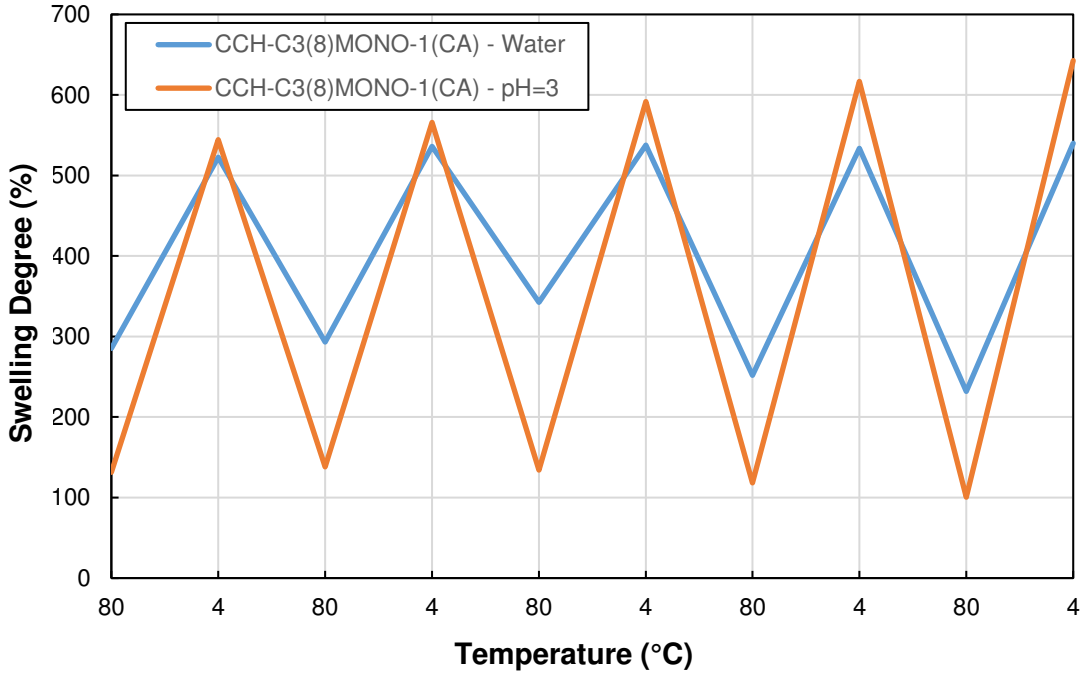

Figure 78. Pulsatile kinetics in water and buffer solution pH=3 between 4 and 80 °C of CMC-g-PNIPAAm comb-type graft hydrogels crosslinked with citric acid (Sample CCH-C3(8)MONO-1(CA))

group between 1,742 cm^{-1} (group -CHO) and also in sample CCH-C3(8)BI-3 by the peak 1,736 cm^{-1} (group -CHO).

Finally, in order to confirm that the interfacial crosslinking between the CMC-g- PNIPAAm comb-type graft hydrogel films and the functionalized PA6 substrate, was due to the presence of aldehyde pendant groups on the surface of the functionalized PA6 substrate, a sample was made with untreated PA6 and CMC-g-PNIPAAm comb-type graft hydrogel films and FTIR measurements were performed (Figure 83). The spectra of sample CCH-C3(8)BI-84 revealed no signal for the group –COOH of the citric acid crosslinker, then no interfacial crosslinking took place. Detailed measurement data from other samples (and their replicas) are listed from Table 96 to Table 103 in Appendix II (See section 10. Appendix II: Tables).

Table 26
Elemental Analysis after initial activation with glutaraldehyde

Substrate	%C (%)	% Dif. with PA6 (%)
PA6	62.17	0.00
CCH-C3(8)BI-PA6(1a)	61.61	-0.89
CCH-C3(8)BI-PA6(1b)	62.20	0.06
CCH-C3(8)BI-PA6(2a)	64.54	3.81
CCH-C3(8)BI-PA6(2b)	64.22	3.31
CCH-C3(8)BI-PA6(3a)	62.97	1.29
CCH-C3(8)BI-PA6(3b)	63.00	1.34
CCH-C3(8)BI-PA6(3b.2)	63.08	1.46

4.8.2. SEM

The SEM micrograph taken to a transversal section of sample CCH-C3(8)BI-56 (Figure 84), confirms the structure of the obtained bilayer based on CMC-g- PNIPAAm comb-type graft hydrogel films. The active layer of CMC-g-PNIPAAm comb-type graft hydrogel and the passive layer of PA6 are clearly visible.

4.9. Characterization of temperature dependent actuation property in bilayer actuators based on CMC-g-PNIPAAm comb-type graft hydrogel films

4.9.1. Photographs of actuation

Figure 85(c) confirmed that the thermosensitive actuation of a bilayer based on CMC-g-PNIPAAm comb-type graft hydrogel films (Sample CCH-C3(8)BI-56) was finally achieved. The actuation was quantified by using the gyration angle as a parameter. At the beginning of the

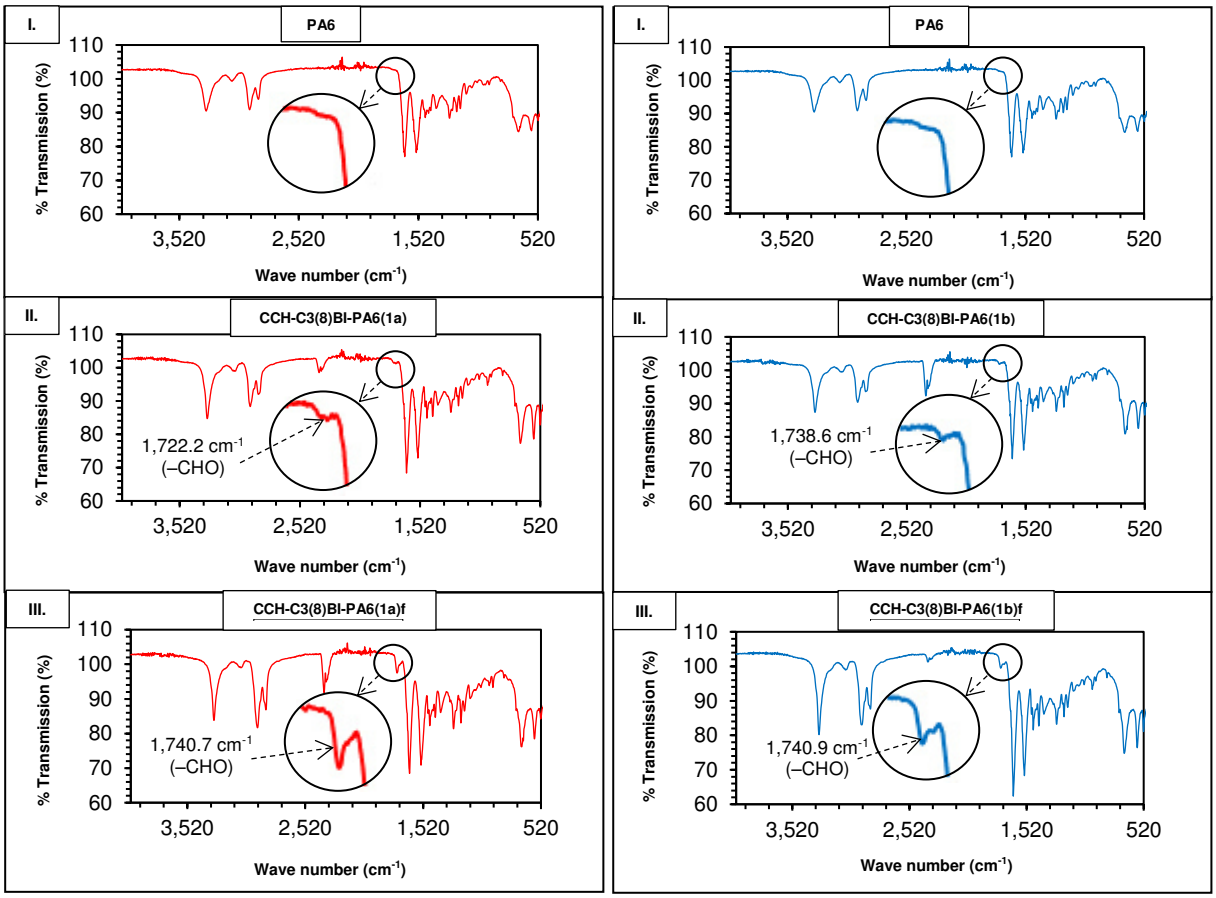

Figure 79. FTIR spectra of PA6 substrates before (and after) concentrated acidic hydrolysis: I. PA6 substrate untreated, II. after initial activation with glutaraldehyde and III. after final activation with glutaraldehyde.

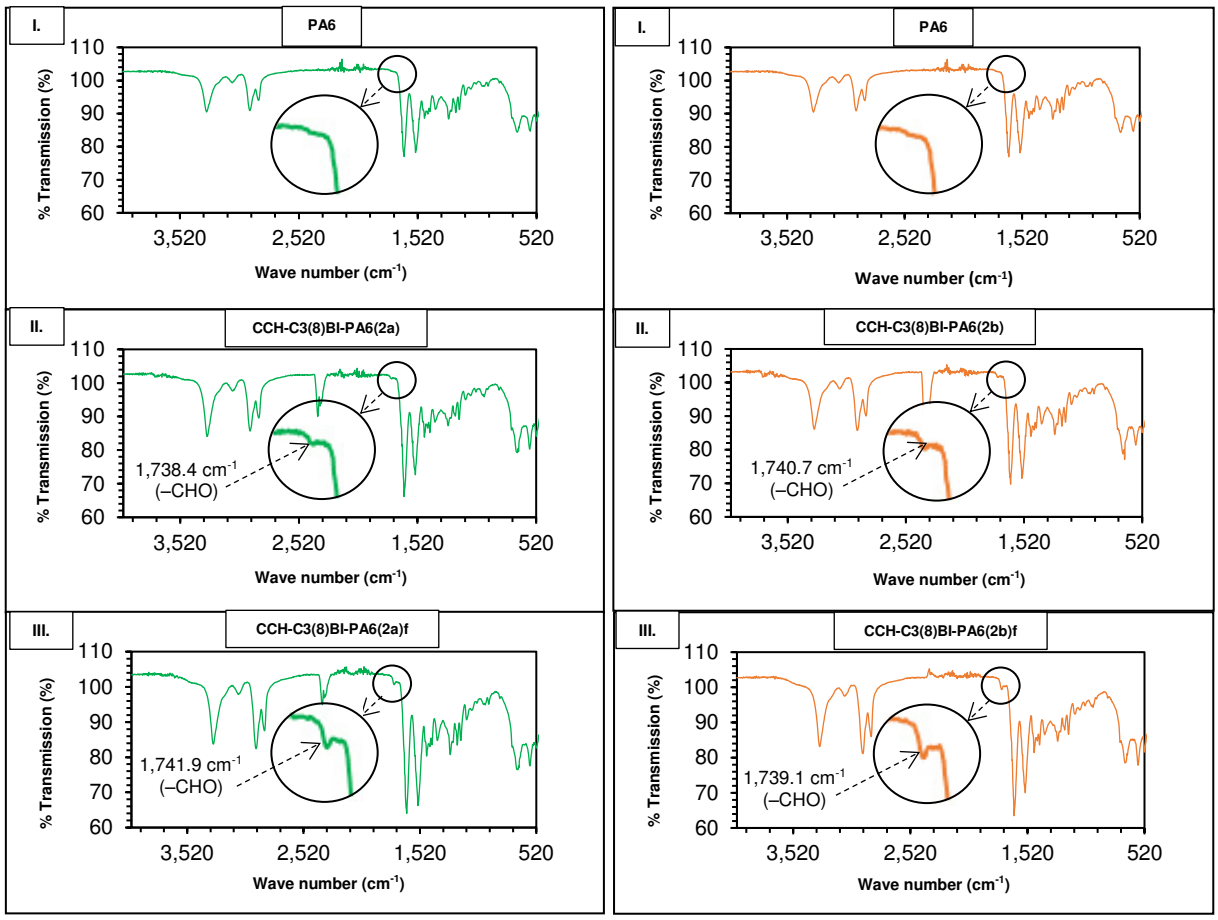

Figure 80. FTIR spectra of PA6 substrates before (and after) aqueous hydrolysis: I. PA6 substrate untreated, II. after initial activation with glutaraldehyde and III. after final activation with glutaraldehyde.

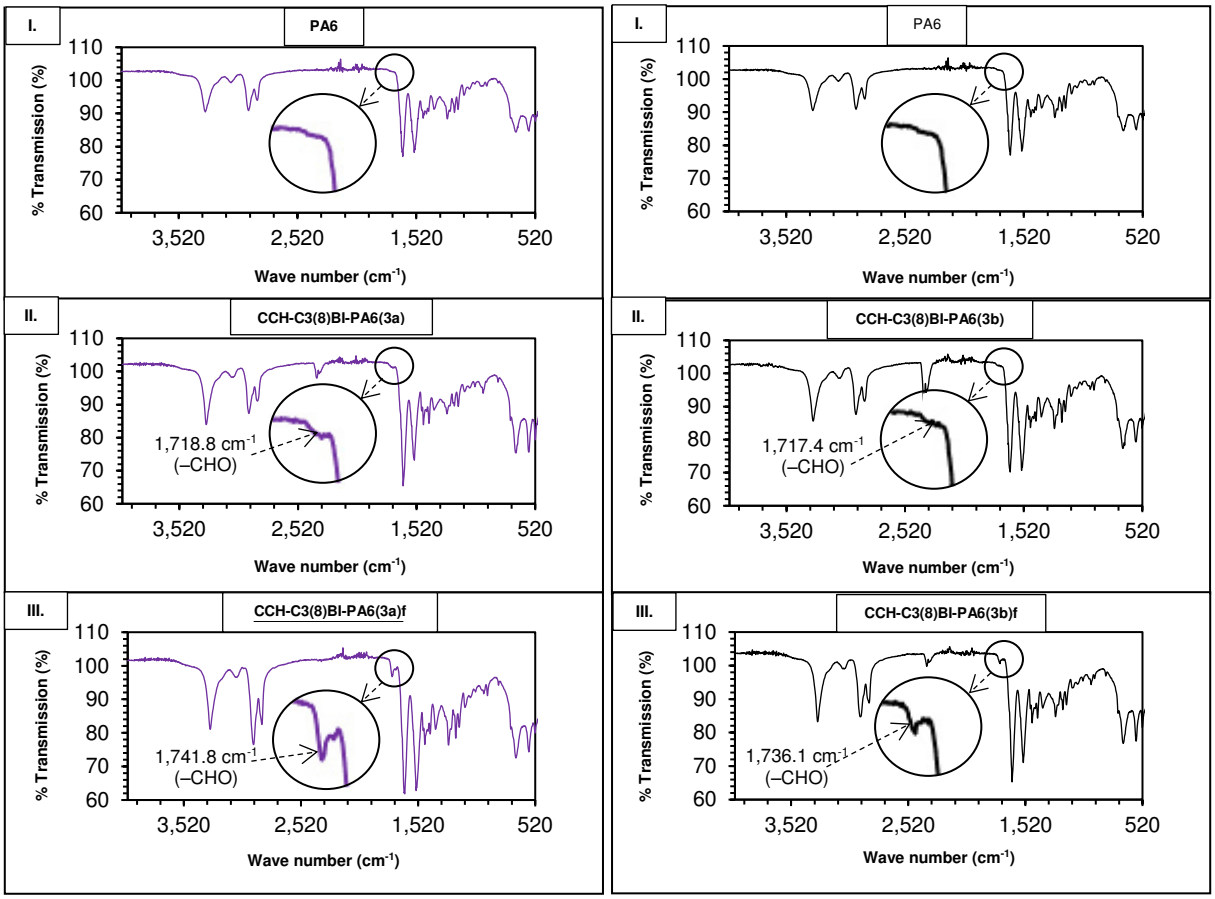

Figure 81. FTIR spectra of PA6 substrates before (and after) diluted acidic hydrolysis: I. PA6 substrate untreated, II. after initial activation with glutaraldehyde and III. after final activation with glutaraldehyde.

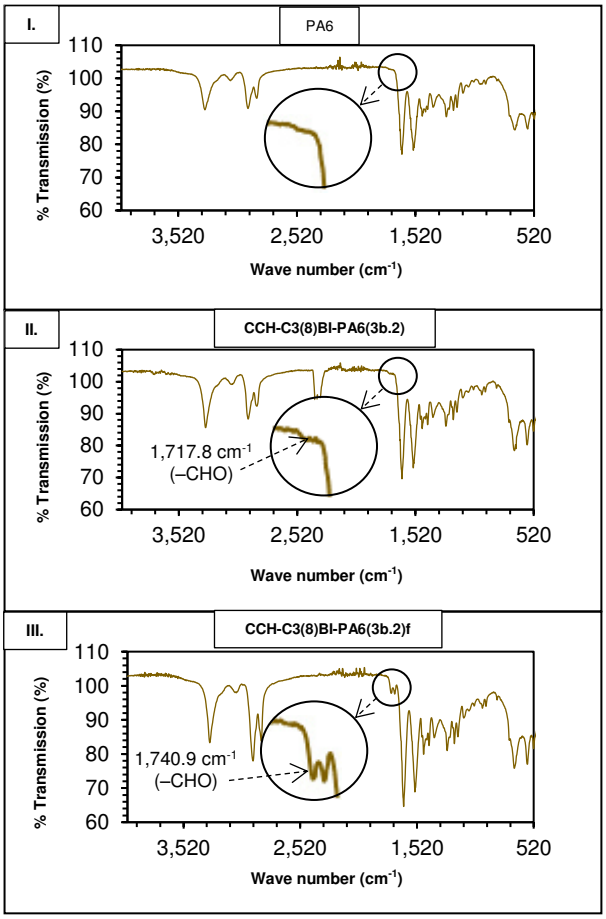

Figure 81 (Cont.)

experiment, when the temperature of water is 25 °C the gyration angle had a value of 10.1°, then when the temperature of water achieved a value of 60 °C and after 45 minutes, a displacement of circa 10° was observed and the final gyration angle of the bilayer was 20.6°.

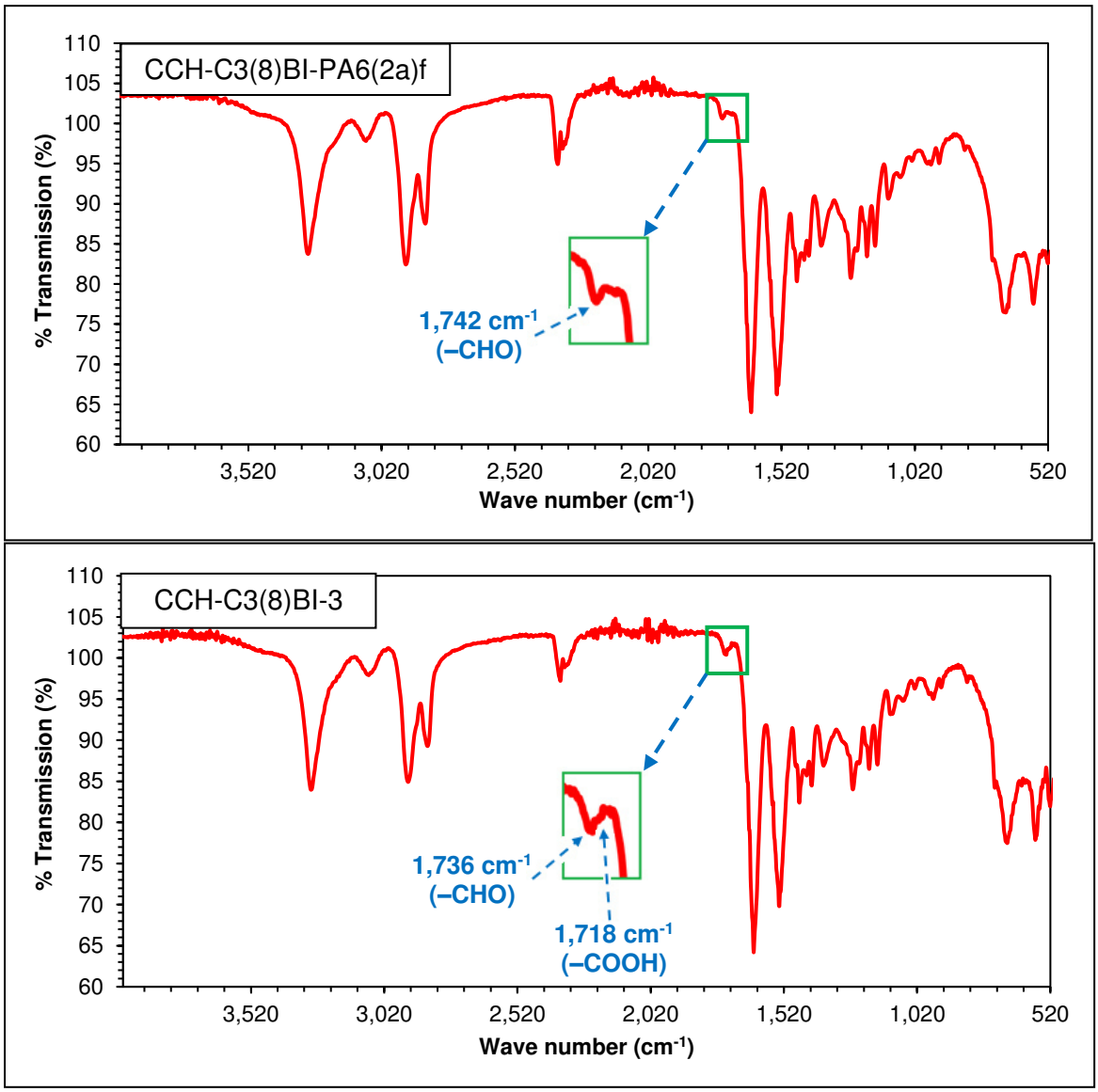

Figure 82. FTIR Spectra of bilayer based on CMC-g- PNIPAAm comb-type graft hydrogel films (Sample CCH-C3(8)BI-3) versus functionalized PA6 substrate (Substrate CCH-C3(8)BI-PA6(2a)f)

As a complement, the same measurements were made first, with a sample of untreated PA6 substrate (Sample CCH-C3(8)BI-Blanc(8)) and second, with a functionalized PA6 substrate (Sample CCH-C3(8)BI-Blanc(4)), this sample was the same used as passive layer in the bilayer sample CCH-C3(8)BI-56. In both cases, no thermosentive actuation was observed (Figure 85(a) and 85(b)). Then it was possible to confirm that the thermosensible actuation in

the bilayer was due to the presence of the active layer of CMC-g-PNIPAAm comb-type graft hydrogel films that was covalently attached to the PA6 passive layer;

Once the thermosensitive actuation of the bilayer samples was established, the next step was to determine the reversibility of this actuation. Figure 86 confirmed the reversibility of the

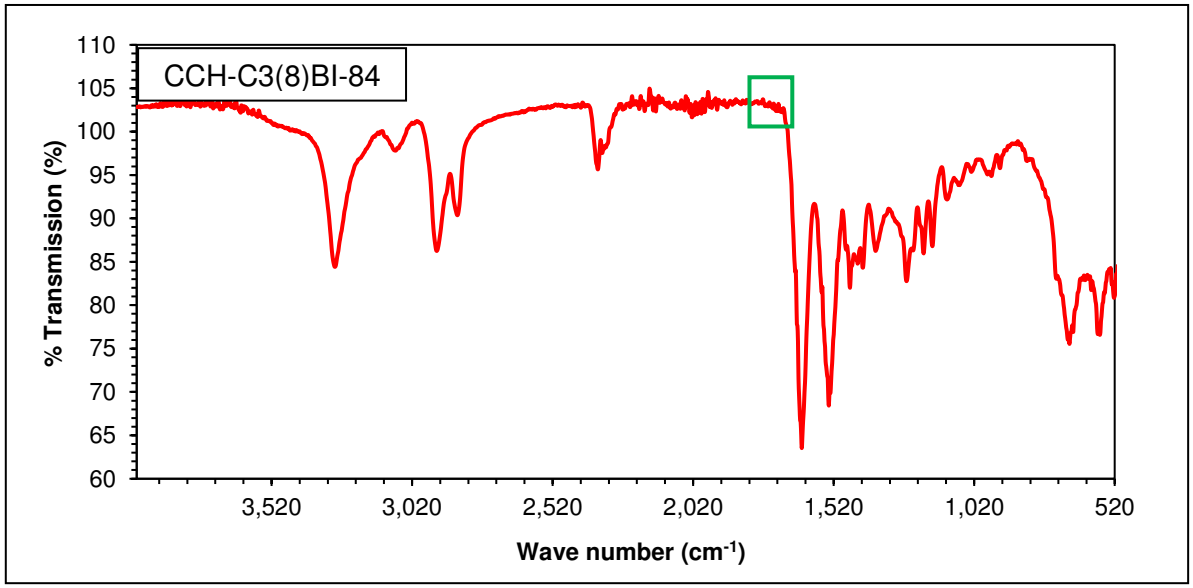

Figure 83. FTIR spectrum of bilayer based on CMC-g- PNIPAAm comb-type graft hydrogel films (sample CCH-C3(8)BI-84)

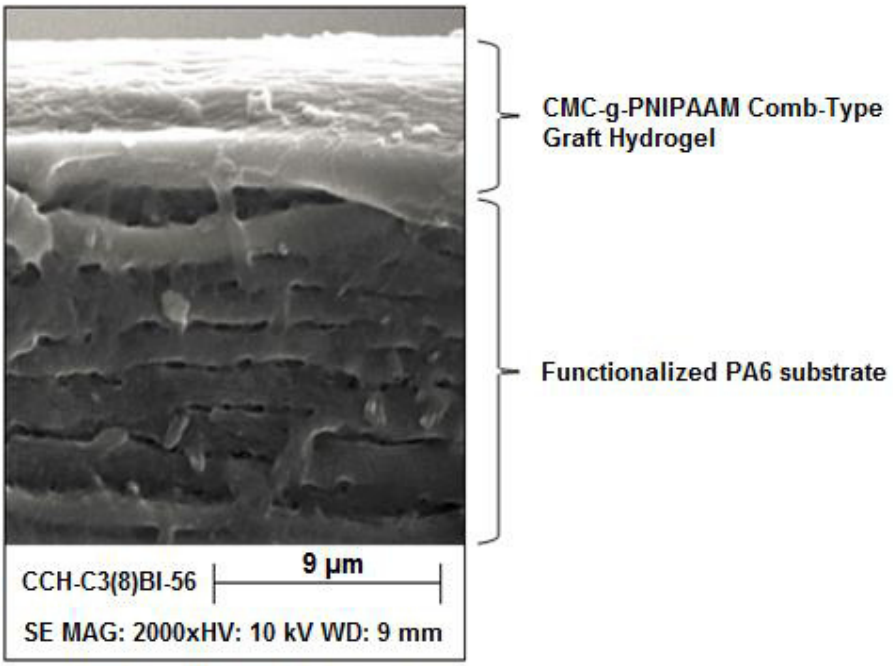

Figure 84. SEM micrograph of a bilayer based on CMC-g- PNIPAAm comb-type graft hydrogel films (sample CCH-C3(8)BI-56)

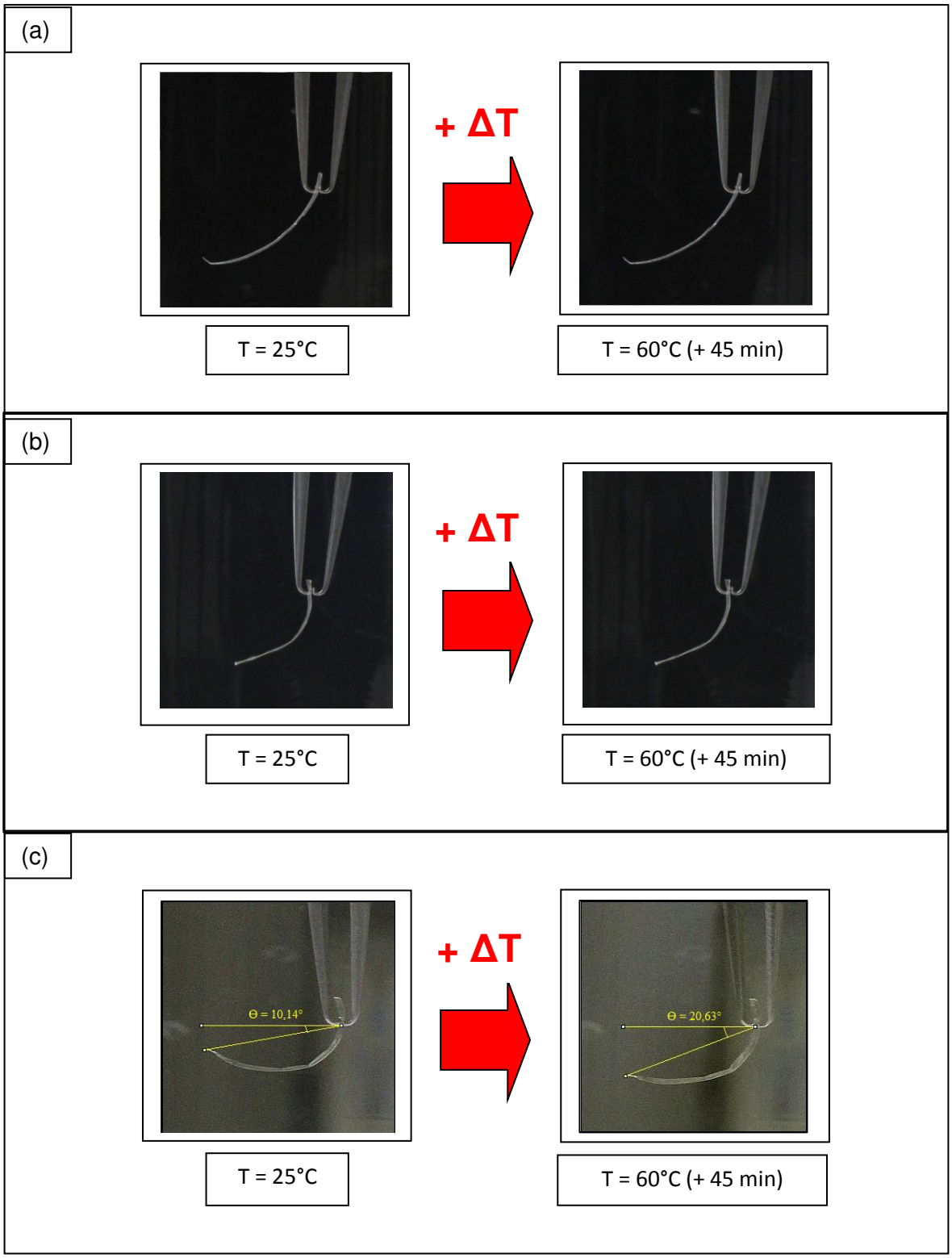

Figure 85. Thermosensitive actuation in Water of (a) untreated PA6 substrate (Sample CCH-C3(8)BI-Blanc(8)), (b) funtionalized PA6 substrate (Sample CCH-C3(8)BI-Blanc(4)) and (c) functionalized PA6 substrate covered with active layer – bilayer Film (Sample CCH-C3(8)BI-56).

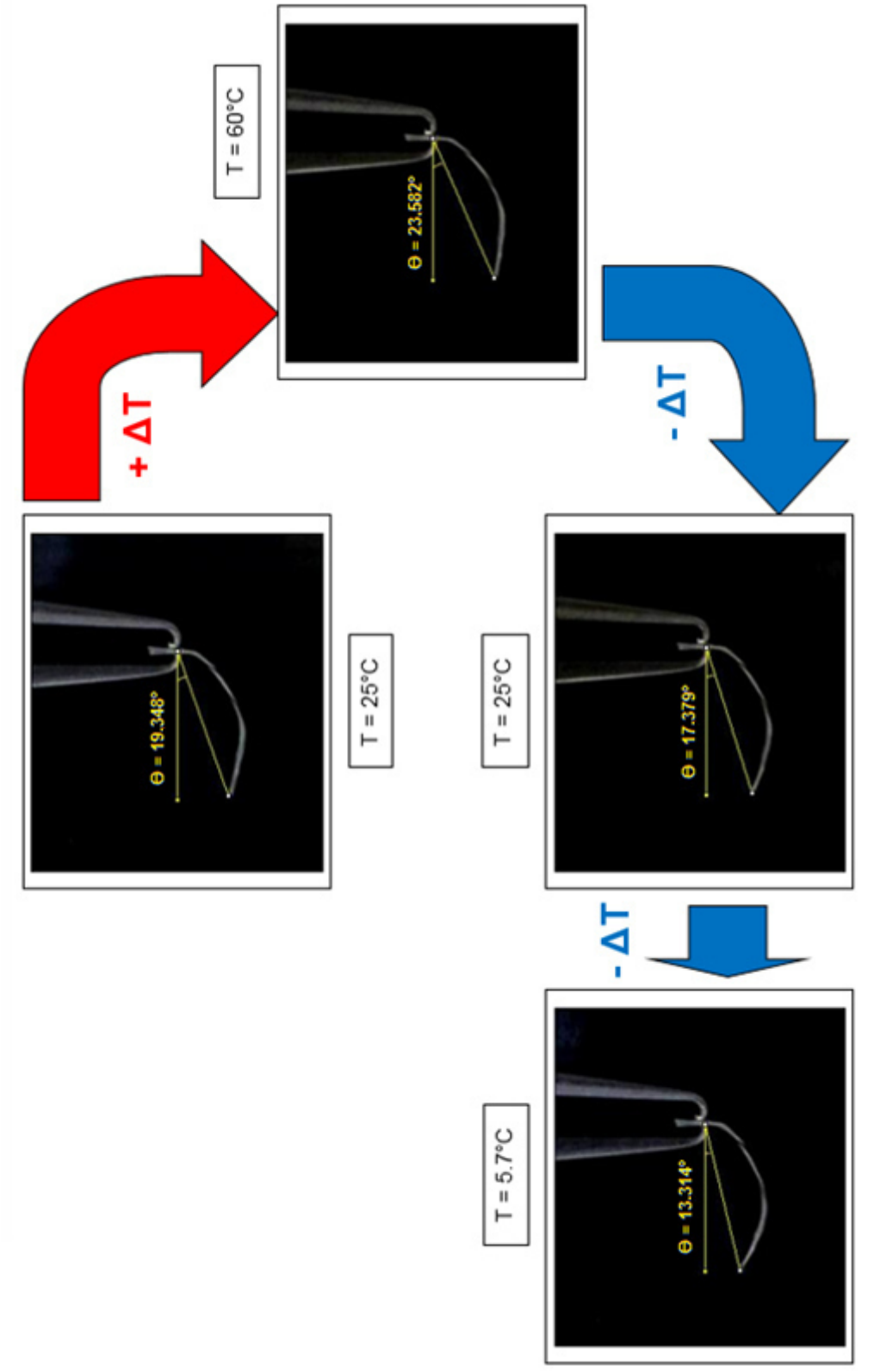

Figure 86. Thermosensitive actuation in water – reversibility (Sample: CCH-C3(8)BI-40)

thermosensitive actuation, for bilayers based on CMC-g-PNIPAAm comb-type graft hydrogel films (Sample CCH-C3(8)BI-40). First, the bilayer was heated in water from 25 °C (gyration angle of 19.3°) until 60 °C (gyration angle of 23.5°), then a thermosensitive actuation of almost 6° was observed. After that, the bilayer was left cooling down in water until 25 °C a gyration angle of 17.3° was attained, then a reversible thermosensitive actuation of almost 8° was observed and the bilayer returned to almost its initial gyration angle.

An additional measurement was made with the same sample in water: After the temperature of 25 °C was attained, then the sample was left cooling down in a fridge, until circa 5 °C (gyration angle of 13.3°) was reached, an extra reversible thermosensitive actuation of almost 4° was observed.

4.9.2. Gyration Angle

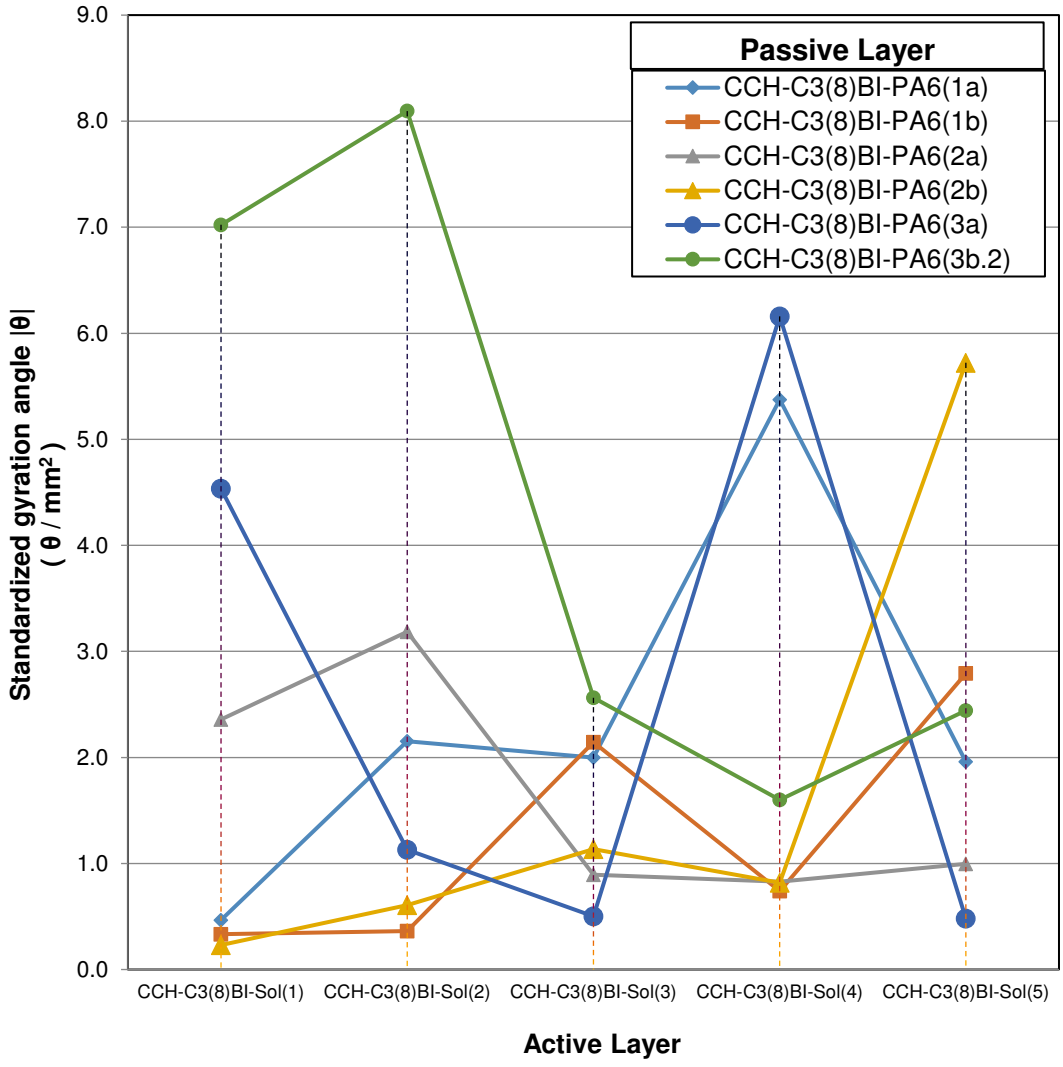

Figure 87. Evolution of standardized gyration angle (|θ|) with active and passive layer types

Figure 87 shows for the thermosensitive actuation performance of each bilayer sample, in terms of the standardsized gyration angle (|θ|) achieved at 60 °C, in water and after heating from 25 °C. We can conclude from the graph that, for an active layer made from low and medium pre-gel solution concentrations (solutions CCH-C3(8)BI-Sol(1)), CCH-C3(8)BI-Sol(2)) and CCH-C3(8)BI- Sol(3)), the best performance was achieved by a bilayer sample with a PA6 passive layer that had undergone a diluted acidic hydrolysis (Substrate CCH-C3(8)BI-PA6(3b.2)). For active layers made from high pre-gel solution concentrations (solutions CCH-C3(8)BI-Sol(4)) and CCH-C3(8)BI-Sol(5)), higher gyration angles were achieved by bilayer samples with PA6 passive layers, that had gone through aqueous, concentrated and diluted acidic hydrolysis (substrates CCH-C3(8)BI-PA6(2b)), CCH-C3(8)BI-PA6(1a)) and CCH-C3(8)BI-PA6(3a)). Detailed measurement data from other samples are listed from Table 104 to Table 110 at Appendix II (See section 10. Appendix II: Tables).

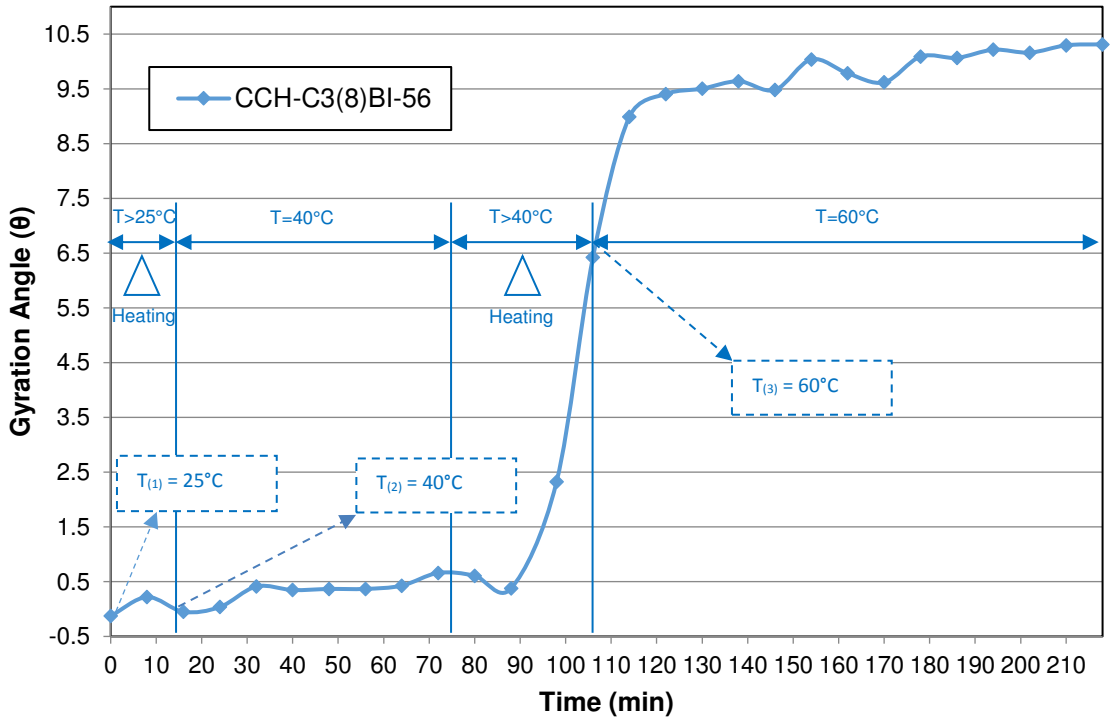

Figure 88. Gyration angle (θ) vs time

Figure 88 shows the evolution with time of thermosensitive actuation (gyration angle displacement) in water for bilayer sample CCH-C3(8)BI-56. At 40 °C, the amount of angular displacement achieved by this sample is minimum. However, when water is heated until 60 °C, the gyration angle displacement increments around 6°, and after 45 minutes at this same temperature, the angular displacement increases until a maximum value of around 10°.

Detailed measurement data from this sample is listed in Table 111 at Appendix II (See section 10. Appendix II: Tables).

5. Discussion of Results

5.1. Introduction

The following research question was tried to be answered in this thesis:

Is it possible to replicate the natural actuation mechanism "cell wall swelling (or shrinking)" (Burgert et al. (2009)) by developing a smart biomimetic actuator?

A possible answer (or main hypothesis) presented by this research was:

A biomimetic bilayer actuator based on thermosensitive CMC-g-PNIPAAm comb-type graft hydrogels would be able to replicate the natural actuation mechanism "cell wall swelling (or shrinking)" (Burgert et al. (2009)).

The main hypothesis is explained in detail:

The bilayer actuator proposed would perform thermosensitive actuation in aqueous solutions. It would have as passive layer an uniaxially stretched polyamide 6 (PA6) film, which according to Dai et al. (2013) is capable of allineate polymer networks, and an active layer made of a thermosensitive CMC-g-PNIPAAm comb-type graft hydrogel since according to Burgert et al. (2009) technical actuating devices based on gels are adequate as bioinspired representations of actuation, because of the swelling or shrinking of the gel cell walls. Adherence between passive and active layers would be achieved with an interfacial chemical bonding that would be possible with an aldehyde functionalization of the PA6 passive layer. The active layer would be a hydrogel, synthesized from CMC-g-PNIPAAm graft copolymers that would be crosslinked with citric acid. The CMC-g-PNIPAAm graft copolymers would be made from grafting onto copolymerization of CMC polymers with aminoterminated PNIPAAm semitelechelic oligomers and by using the coupling agent EDC. The aminoterminated PNIPAAm semitelechelic oligomers would be synthesized by telomerization in water of NIPAAm monomers with 2-aminoethanethiol.

Then, in order to develop this thesis, the main hypothesis was decomposed in the following secondary hypotheses:

1. Is it possible to develop aminoterminated poly(N-Isopropylacrylamide) semitelechelic oligomers by a telomerization reaction with 2-aminoethanethiol?

2. Is it possible to generate a thermo-modification of carboxymethyl cellulose polymers with amino-terminated PNIPAAm semitelechelic oligomers by coupling reaction with EDC?
3. Is it possible to synthesize CMC-g-PNIPAAm comb-type graft hydrogels?
4. Is it possible the aldehyde functionalization of PA6 unidirectional substrates by acidic (or aqueous) hydrolysis and a two-step glutaraldehyde activation?
5. Is it possible interfacial chemical bonding between active and passive layers, by reactions between the passive layer aldehyde groups and the active layer hydroxyl OH- moeities of their carboxylic groups (interfacial chemical crosslinking and interfacial reactions)?
6. Is it possible thermosensitive actuation in aqueous solutions from bilayer actuators based on CMC-g- PNIPAAm comb-type graft hydrogel films?

5.2. Synthesis of bilayer actuators based on CMC-g-PNIPAAm comb-type graft hydrogels

5.2.1. Aminoterminated poly(N-Isopropylacrylamide) semitelechelic oligomers as thermosensitive polymers

5.2.1.1. Antecedents and secondary hypothesis proposed

Poly(N-isopropylacrylamide) was chosen as the thermosensitive polymer that would provide thermosensitivity to CMC because of its thermal behavior in aqueous media, which consists in an inverse solubility during heating (Schild et al. (1992)).

For performing the grafting onto copolymerization of CMC with PNIPAAm, it was necessary to provide the PNIPAAm polymers with a functional end group that opens the possibility of a coupling reaction with the carboxylic groups of CMC. The end group chosen was an amino group. Then the first task, was to synthesize semitelechelic PNIPAAm oligomers with amino end groups. Literature has shown that this synthesis was possible by using telomerisation reactions with amines (Behr et al. (2009)), specifically with 2-aminoethanethiol (Yoshida et al. (1995), Durand et al. (1999), Bokias et al. (2001)) and with this the first secondary hypothesis was confirmed.

5.2.1.2. Amount and %yield

The telomerization reaction of Bokias et al. (2001) used for this synthesis is shown in **Figure 89**. The reaction temperature was 29 °C in order to avoid any possible phase separation due to a PNIPAAm phase transition that could occur around 30 °C (Bokias et al. (2001)). However, some phase separation was observed during the reaction and this limited the conversion of the polymerization (Bokias et al. (2001)), as it was evidenced by the medium and lower %yield values obtained (Table 17).

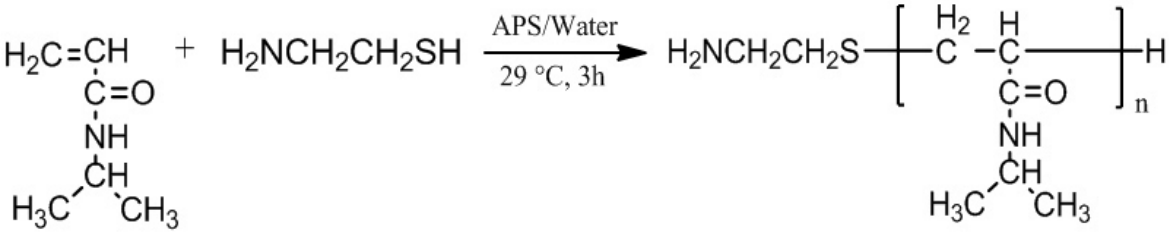

Figure 89. Telomerization reaction for N-isopropylacrylamide with 2-aminoethanothiol initiated with ammonium persulphate (APS) (Bokias et al. (2001)).

5.2.1.3. Gel permeation cromatography and elemental analysis

The development of aminoterminated poly(Isopropylacrylamide) oligomers with different molecular weights by manipulating the stoichiometry of the telomerization reaction with 2-aminoethanothiol was confirmed with GPC and Elemental Analysis measurements (Figure 60 and Tables 18 und 19). These conclusions agreed with the ones obtained by Yoshida et al. (1995), who also performed a synthesis of aminoterminated poly(Isopropylacrylamide) with the same telomerization reaction and demonstrated through GPC measurements the obtention of oligomers with two different molecular weight values (14,000 and 19,000 g/mol). Durand et al. (1999) confirmed with Size Exclusion Cromatography (SEC) the obtention (also through a telomerization reaction with 2-aminoethanothiol) of aminoterminated poly(Isopropylacrylamide) oligomers with four different molecular weigths (5,200, 9,800, 13,200 and 12,600 g/mol).

5.2.1.4. FTIR and NMR

The aminotermination and structure of PNIPAAm oligomers obtained by telomerization with 2-aminoethanothiol (and also the effectiveness of this reaction) was confirmed with FTIR and NMR measurements (Figure 61 and 62). Bokias et al. (2001) also confirmed through FTIR measurements the structure of PNIPAAm in aminoterminated PNIPAAm oligomers with a peak at 1650 cm^{-1} (group –CONH–). Durand et al. (1999) managed to demonstrate the amino end functionalization of aminoterminated oligomers (synthesized also through telomerization with 2-aminoethanothiol) with a quantitative potentiometric titration and a qualitative dye-partition test (he used disulfine blue as a dye).

5.2.1.5. DSC (Dry)

The glas transition temperature step measured in aminoterminated PNIPAAm oligomers with DSC (Figure 64) agrees with the one of 140 °C measured by Bokias et al. (2001) and confirms that the telomerization reaction was performed successfully and the NIPAAm monomer was polymerized.

5.2.1.6. DSC (in solution)

The phase transition behavior in water of the aminoterminated samples was also studied with DSC and the results were compared with measurements made with NIPAAm aqueous solutions (Figure 65). The phase transition in aqueous DSC measurements is represented by a broad peak, as it was shown by Otake et al. (1990), who stated that this signal was associated to the cloud point of PNIPAAm aqueous solutions, by comparing the onset temperature of the DSC peak with the temperature measured with light scattering techniques at an angle of 90 °.

Kano et al. (2009) described this phase transition as an endothermic peak and based on his observations, he considered the existence of three different segment-based interactions: “water with amide”, “amide with amide” and “water with hydrocarbon”. The first two interactions are based on hydrogen bonding (hydrophilic interactions) and the last one is a hydrophobic one. They assumed that the enthalpy depicted, was associated to the energy required for breaking the hydrogen bonding of the dissolved polymer in water and producing phase separation.

The increased LCST values (between 34-36 °C during the heating and 34-39 °C during the cooling cycles) could be a consequence of the amino end group attached to the PNIPAAm oligomers. This goes in coincidence with an increment in PNIPAAm LCST values because of the copolymerization of NIPAAm with hydrophilic monomers, as it was described by Dimitrov et al. (2007). In addition, according to Kokufuta et al. (2012) the LCST increment could be attributed to a restriction of the amide-water interactions, due to the inclusion of other molecules in the PNIPAAm chain. In their study, they included N-isopropylmethacrylamide (NiPMA) monomers in a PNIPAAm chain. The NiPMA isopropyl groups affected the amide-water interactions.

Duan et al. (2006) and Kujawa et al. (2006) also studied the effect, on the LCST temperature, of the inclusion of other molecules in the PNIPAAm chain. They described a decrease in the LCST values, due to the formation of aggregates between the end groups of the semitelechelic developed PNIPAAm molecules.

Figure 65 shows that the reversibility of the phase transition was also visible during the DSC measurements of the aminoterminated PNIPAAm aqueous solutions. The reversibility of phase transition was previously explained by Dimitrov et al. (2007) by the presence (and absence) of hydrogen bonds between the polymer an water molecules under (and over) the LCST temperature, going from a spiral (under the LCST) to a globular structure (over LCST), as it is showed in Figure 15.

The influence of molecular weight in PNIPAAm LCST values was also studied with DSC

analysis to aqueous PNIPAAm solutions and a moderate direct tendency of increment of the LCST with the molecular weight of the semitelechelic oligomers was observed. Kaneko et al. (1995) explained this direct tendency by stating that the attractive forces between dehydrated PNIPAAm chains increase with an increment of the molecular weight.

Therefore it could be said that after an increment of PNIPAAm molecular weight, a major amount of attractive forces between dehydrated PNIPAAm molecules is obtained. Then a higher LCST temperature will be needed in order to break a higher amount of hydrophilic bonds (between PNIPAAm and water molecules), producing PNIPAAm dehydration, attraction between dehydrated molecules and finally phase transition.

The moderate increase of LCST temperature with molecular weight could be due to the high polydispersity of the aminoterminated PNIPAAm samples, which implies that an important amount of molecules with molecular weights lower than the ones theoretically expected, were present, diminishing the increasing effect of the LCST with molecular weight because of a non-significant increment of the attractives forces between the dehydrated PNIPAAm molecules.

5.2.2. Thermal modification of carboxymethyl cellulose polymers with Aminoterminated PNIPAAm oligomers by coupling reaction with EDC

5.2.2.1. Antecedents and secondary hypothesis proposed

CMC is, due to its anionic nature and solubility in water (Cash et al. (2009)), suitable for many synthetic reactions performed in aqueous media. It was chosen as the cellulosic polymer that can be readily crosslinked with citric acid (Demitri et al. (2008)), in order to obtain a thermosensitive cellulosic hydrogel (used later as an active layer). However, CMC is not thermosensible, then in order to achieve this goal, a chemical modification with thermosensitive grafts was performed, by using grafting onto polymerization with thermosensitive PNIPAAm oligomers.

Literature showed that polymers can be turned into thermosensitive by grafting onto polymerization with thermosentive grafts. Grafting onto reactions between amino end groups from thermosentive grafts (like polyethylene oxide and PNIPAAm) and carboxylate groups from non-thermosensitive backbones (like acrylic acid and CMC polymers) were performed by using coupling agents like EDC, DCCI or NHS (L'Alloret et al. (1995), Hourdet et al. (1997), Durand et al. (1999), Bokias et al. (2001), Karakasyan et al. (2008)).

Then based on this information, the second secondary hypothesis was confirmed.

5.2.2.2. Amount and %yield

The reaction used for this polymerization, was a coupling between amino end groups (from previously synthesized aminoterminated PNIPAAM grafts) and carboxylate groups (from CMC polymer backbone), supported by the coupling agent EDC (Figure 90) (Bokias et al. (2001)).

The medium and low reaction yields showed in Tables 20, 21 and 22 are a consequence of the limited grafting conversion, probably because the viscosity of the CMC reaction solution could limit the mobility of the CMC, aminoterminated PNIPAAm and EDC molecules, making difficult the reaction between them. Another reason why the grafting reaction was limitedly performed could be, that not all of the PNIPAAm oligomers used had amino end groups, since the telomerization reaction was made by using the initiator ammonium persulphate, which is a redox initiator that can polymerize the NIPAAm monomer slowly (needs an accelerator, see Table 2) (Schild et al. (1992)) in a parallel reaction without a telomerization and therefore without providing the oligomers with an amino end groups. Also manipulation of the product mixture after the reaction and long dialysis times could contribute to a loss of product and therefore a decreasing in the reaction yields.

5.2.2.3. Elemental analysis and FTIR

The structure and graft percentage of the graft copolymers was confirmed by elemental analysis (Tables 23, 24 and 25) and FTIR analysis (Figure 66). On the one hand, Bokias et al. (2001) also showed through FTIR measurements (and with a –CONH– peak) the presence of PNIPAAm grafts and on the other hand, Haleem et al. (2014) demonstrated the presence of the CMC backbone with (–CH_2)OH, (–CO)OH and (–COO-) FTIR-peaks where the broad (–CH_2)OH peak corresponded to the -OH frequency of stretching, the overlapped (–CO)OH peak to stretching vibration of C-H and the also overlapped (–COO-) peak to the presence of carboxylate groups.

5.2.2.4. DSC (Dry)

The grafting of PNIPAAM grafts on the CMC backbone was confirmed through DSC measurements performed on CMC-g-PNIPAAm graft copolymer dried samples (Figure 68(c) - CCH-C2(2)-1.80). Bokias et al. (2001) also confirmed the grafting reaction on CMC-g-PNIPAAm graft copolymers with DSC measurements through the presence of a solid state microphase separation represented by two transition temperatures, which are similar to the glass transition temperatures of the pure CMC and PNIPAAm.

5.2.2.5. DSC (In solution)

Aqueous solutions of CMC-g-PNIPAAm graft copolymers were measured with DSC and the results were compared with those corresponding to CMC aqueous solutions (Figure 69).

Phase transition in graft copolymers aqueous solutions is represented by a broad peak, which is not visible in the CMC aqueous solution measurements, since cellulose does not take part on the phase transition of copolymers (Li et al. (2008)).

The representation of phase transition by a peak for aqueous solutions of CMC-g-PNIPAAm graft copolymers is expected. This is a similar result to the ones obtained by other researchers

(Li et al. (2008), Jin et al. (2013), Guo et al. (2015)) (See Figure 40, 42 and 43). The reversibility of phase transition for the graft copolymers is shown by broad peaks during the heating and cooling cycles (Figure 69), and it was confirmed also by Li et al. (2008) (Figure 40).

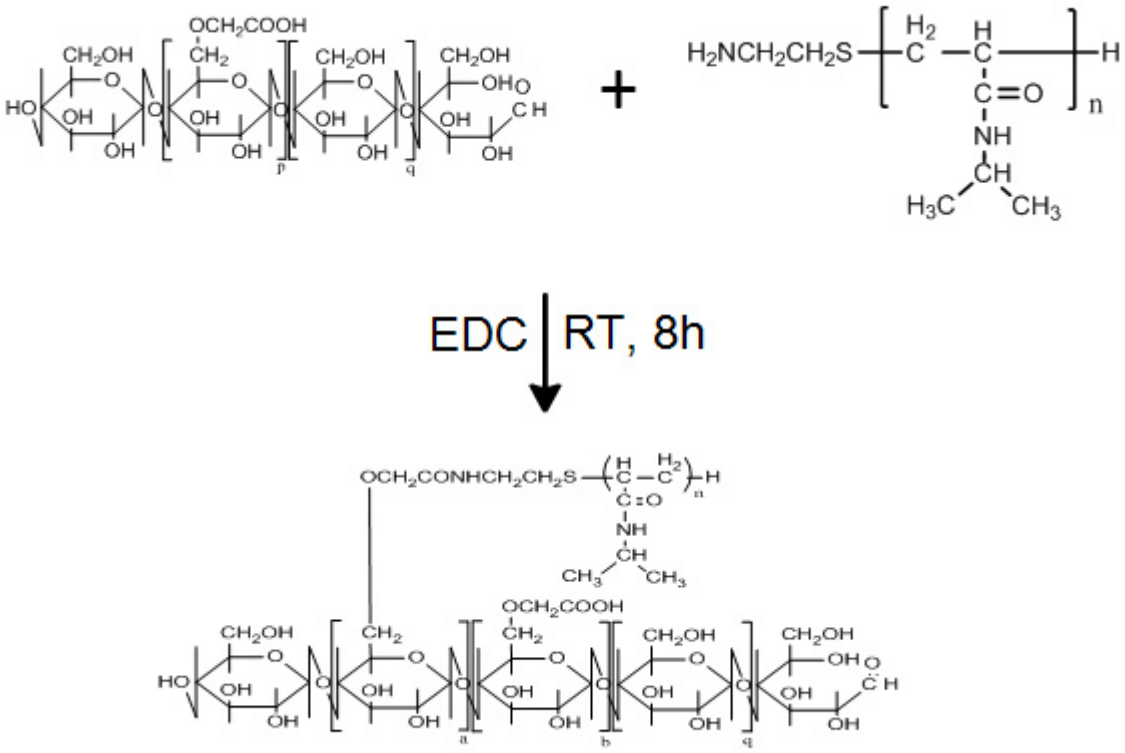

Figure 90. Grafting onto reaction between aminoterminated PNIPAAm and carboxymethyl cellulose (CMC) supported by EDC (Bokias et al. (2001)).

Guo et al. (2015) showed in their study that during phase transition, the association process between thermosensitive grafts (attached to a not thermosensitive backbone), is not favored when they are not close to each other (in a same backbone), then the phase transition enthalpy (peak area) is lower, in comparison to the one of graft copolymers with thermosensitive backbones (grafted with non-thermosensitive grafts). They explained that this decrease in phase transition enthalpy, could be due to an energetic impediment because of the steric obstacle derived from the hydrophilic backbone.

This was also complemented in DSC studies of the influence that thermosen-sitive grafts size performed in the LCST of graft copolymers (Figure 42) (Jin et al. (2013)). Their results showed that copolymers with short grafts and low graft densities, presented low LCST values since the grafts cannot interact with their neighbors and therefore they only stay as coils surrounding the backbone (Jin et al. (2013)). However, when the grafts are longer, they make intra-molecular associations by forming hydrogen bond between amide groups, and create a layer around the

backbones limiting water from leaving through the layer, therefore a higher energy would be needed for breaking the hydrogen bonds and therefore a higher LCST (Jin et al. (2013)).

5.2.3. CMC-g-PNIPAAm comb-type graft hydrogels

5.2.3.1. Antecedents and secondary hypothesis proposed

In order to obtain the thermosensitive hydrogel that would be used as active layer in the bilayers, it was necessary to crosslink the previously synthesized CMC-g-PNIPAAm graft copolymers. In literature, CMC (and cellulosic polymers) has been previously crosslinked chemically and ionically.

In one hand, chemically crosslinked CMC were possible by using the crosslinkers: Citric acid (Coma et al. (2003), Demitri et al. (2008)), divinyl sulfone (DVS) (Sannino et al. (2005)) and water soluble carbodiimide (WSC) 1-ethyl-3-(3-dimethylaminopropyl)carbodiimide hydrochloride (Sannino et al. (2006)). On the other hand, it was registered the ionic crosslinking of CMC with multicharged metal cations like Fe^{3+} (Heinze et al. (2005)), a mixture of Ca^{2+} (from $CaCl_2.2H_2O$) and Al^{3+} (from $AlCl_3.6H_2O$) (Saeedi et al. (2009)), Al^{3+} (from $Al(OH)_3$) (Kaushik et al. (2012)) and Al^{3+} ions (from aluminium sulfate octadecahydrate, $Al_2(SO_4)_3.18H_2O$) (Braihi et al. (2014)).

With all of these antecedents and taking into account that the PNIPAAm grafts only occupy some of the reaction sites in the copolymer, while leaving the other ones free, the third secondary hypothesis was confirmed.

5.2.3.2. Amount and %yield

In this research work, was achieved the chemical crosslinking of CMC with citric acid and the ionic crosslinking with $AlCl_3$ ions. For the citric acid chemical crosslinking of the CMC-g-PNIPAAm graft copolymers (Figure 91), the synthesis reaction was based on the one used by Demitri et al. (2008).

Hydroxypropyl cellulose (HEC) was added as an additive for promoting intermolecular crosslinking by avoiding intramolecular crosslinking (Demitri et al. (2008)), due to an electrostatic repulsion between macromolecular chains because of the highly substituted C6 with OH groups (Sannino et al. (2005)).

5.2.3.3. FTIR

FTIR measurements were performed on the chemically crosslinked hydrogels only to validate the chemical crosslinking with the citric acid (Figure 71), by showing a peak at 1711.9 cm^{-1} (group -COOH) which was absent in the CMC-g-PNIPAAm graft copolymer FTIR spectra (Figure 66). This peak corresponds to the carboxylic groups of the crosslinker citric acid (Demitri et al. (2008)), now part of the hydrogel structure. FTIR analysis was not used for

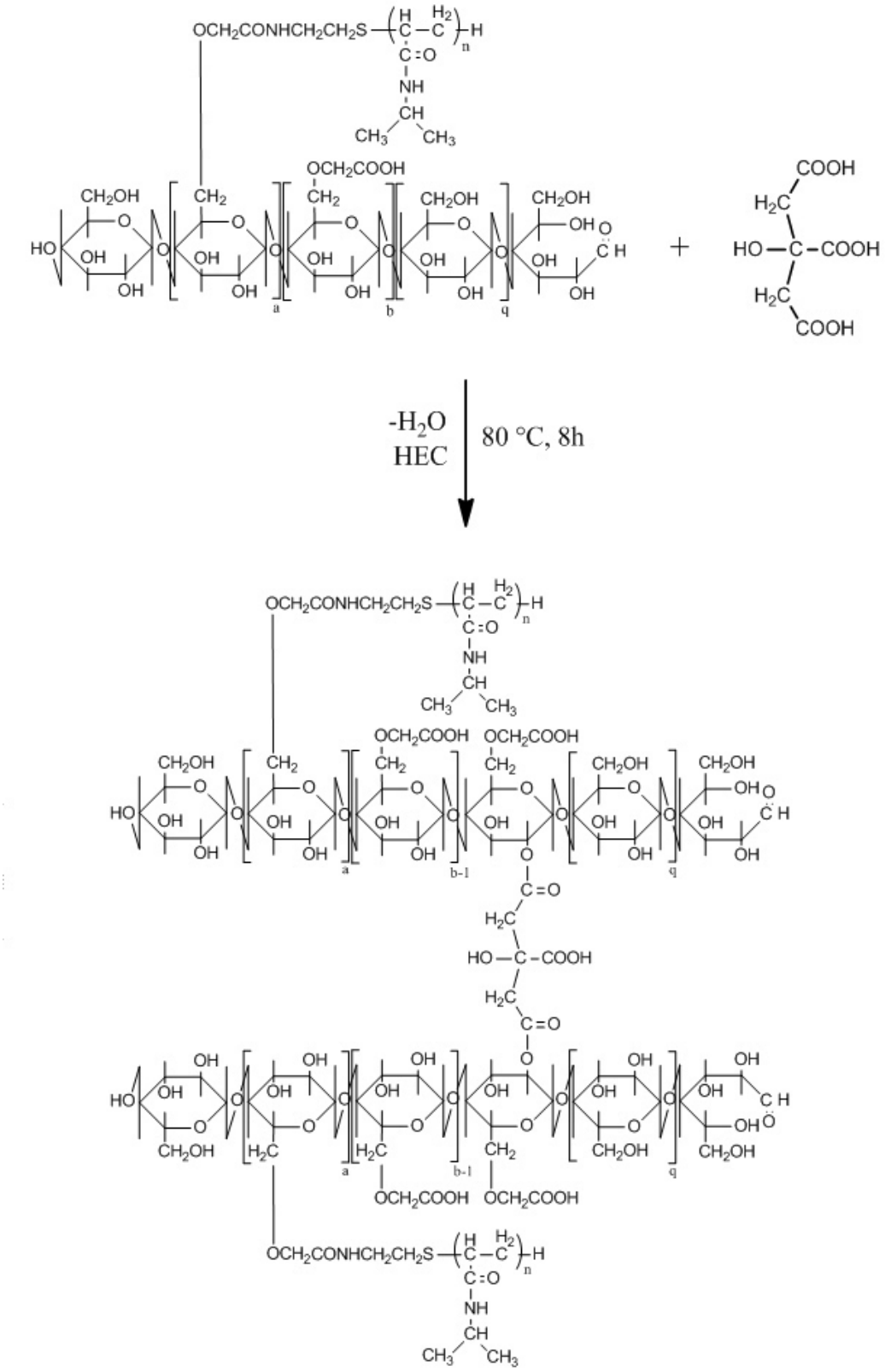

Figure 91. Chemical crosslinking of CMC-g-PNIPAAm graft copolymers with citric acid (Demitri et al. (2008)).

hydrogels the ionic crosslinking with Al^{3+} ions, since their type of crosslinking cannot be detected by FTIR measurements.

5.2.3.4. DSC (Dry)

Thermal stability studies made to dry samples with DSC were executed in order to validate the chemical (or physical) crosslinking of the CMC-g-PNIPAAm graft copolymers (Figure 72). The shifting of the melting point from 174 °C (non- crosslinked copolymer) to higher values like 196.5 °C (hydrogel covalently crosslinked with citric acid) and 306.5 °C (hydrogel ionically crosslinked with aluminium ions), was a confirmation that the hydrogels were successfully synthesized (Shah et al. (2014)). Also, the shifting to higher temperature values indicates that the thermal stability of the resulting hydrogels was improved (Distantina et al. (2013)) and affected (Hongbo et al. (2012)) by the crosslinking, in comparison with the one of graft copolymers.

5.2.3.5. Swelling kinetics and equilibrium ratio

Swelling kinetics and equilibrium ratio of hydrogels crosslinked with citric acid, were measured and compared with hydrogels crosslinked with Al^{3+} ions (Figure 73). Kaneko et al. (1995) summarized the observation of other researchers (Vrentas et al. (1975), Okuyama et al. (1993), Yoshida et al. (1994)) by describing the swelling process of gels with three steps: First, permeation of water molecules to the glassy hydrogel network; second, hydration of hydrogel polymer networks with a subsequent transition from a glassy state to a rubbery state and third, permeation of hydrogel polymer networks to neighboring water (expansion).

Kaneko et al. (1995) justified the long equilibrium swelling times (> 800 minutes) of their samples by stating that in comb-type graft hydrogels, hydration of grafts was not fast during the hydration and expansion stages, due to hydrophobic backbones that made difficult hydration and expansion of grafts. However, the comb-type grafts hydrogel samples synthesized during this research had relatively fast equilibrium swelling times, with circa 100 minutes for the ones crosslinked with citric acid and circa 70 minutes for the ones crosslinked with Al^{3+} ions. This rapid equilibrium swelling times could be explained because of the constituents of the backbone matrix (Ju et al. (2001)). Then rapid swelling kinetics was obtained because carboxymethyl cellulose have hydrophilic carboxylic groups and not hydrophobic isopropyl groups, like in the hydrogels from Kaneko et al. (1995) and Ju et al. (2001).

The difference between the swelling degree of hydrogels crosslinked with citric acid (365 %) with the ones crosslinked with Al^{3+} ions (527 %) could be explained because a covalent crosslinking (citric acid) exerted a higher restriction to polymer networks movement during the expansion state, in comparison to a ionic crosslinking (Al^{3+} ions).

It is interesting to point out that the presence of PNIPAAm grafts on CMC backbones increments the swelling degree of CMC hydrogels, this is evident in the comparison of CMC-g-PNIPAAm comb-type hydrogels crosslinked with Al^{3+} (527%) versus non-grafted CMC hydrogels also crosslinked with Al^{3+} (365%). This could be explained because the developed comb-type graft hydrogels did not maintain an homogenous structure (due to the hydrophilic CMC backbone) and therefore exhibited a porous structure, which is known to accelerate hydrogel swelling kinetics (Kaneko et al. (1995), Hirasa et al. (1991), Kabra et al. (1991), Wu et al. (1992)).

5.2.3.6. Phase transition activity by digital photographs

Thermosensitive swelling degree studies with digital photographs were performed in water (Figure 74) and in acidic media (pH=2 and pH=3) (Figure 75), to samples crosslinked either with citric acid or with Al^{3+} ions. In all of the tests, after specific times, it was observed that the hydrogel films became less transparent (or more opaque) after going abruptly from 25 to 80 °C. This could be related with a phase separation of the polymer network from the aqueous media (Kaneko et al. (1995)), probably due to a dehydration process.

In the studies performed in aqueous media, it was observed that hydrogel samples crosslinked with Al^{3+} ions contracted faster (first shrinking after 5 minutes) in comparison with samples crosslinked with citric acid (first shrinking after 15 minutes). This could be explained, as in the case of swelling kinetic analysis, because the restriction of movement produced to the polymer chain hydrogel networks by the covalent crosslinking with citric acid was higher in comparison with the samples crosslinked with Al^{3+} ions.

In acidic media (pH=2 and 3) and at 80 °C, hydrogel samples crosslinked with citric acid contracted faster (46 minutes) than in aqueous media (120 minutes). At very low pH values, the decomposition of the carboxylic groups at the CMC is enoughly inhibited, then it could be said that the polymer backbone is practically uncharged and a macroscopic phase separation can happen (Bokias et al. (2001)). At neutral or higher pH values, the dissociation of carboxylic groups makes the backbone more stable and inhibit partially phase separation, making the contraction of hydrogels slower than in acidic media (Bokias et al. (2001)).

The hydrogel samples did not present bubbles on their surfaces during deswelling, which differed with the results obtained by Kaneko et al. (1995) on their PNIPAAm comb-type graft hydrogels samples with short (2900 g/mol) and medium sizes grafts (4000 g/mol). These samples showed bubble formation on their surfaces (Kaneko et al. (1995), Matsuo et al. (1988), Okano et al. (1990), Kaneko et al. (1995)).

According to Kaneko et al. (1995) bubble formation was a consequence of accumulated hydrostatic internal pressure created inside the gels, because of a non-homogeneous

deswelling along them, generating temporal surface layers all over the samples (Kaneko et al. (1995), Matsuo et al. (1988), Kaneko et al. (1995), Yoshida et al. (1992)). These temporal surface layers constituted a barrier for the water desorption outside the gels and therefore bubbles were formed on their surfaces (Kaneko et al. (1995)).

The discrepance between our results with the ones of Kaneko et al. (1995) would be probably because the hydrogels synthesized during this research work had grafts with different sizes (5000, 7000 and 9000 g/mol), and it seems that this size mixture creates a synergistic effect, where no bubbles were observed since no deswelling of superficial layers was generated. The hypothesis that bubble formation is not observed because of the presence of longer grafts is valid, since this behavior was similar to one of the PNIPAAm comb-type graft hydrogels samples with long grafts (9000 g/mol) obtained also by Kaneko et al. (1995).

The absence of bubbles could be explained because of a strong chain collapse inside the gels (due to the presence of long grafts), which allowed an homogeneous deswelling along the samples, therefore no temporal superficial layers on the gels were formed that could produce bubbles during the water expulsion (Kaneko et al. (1995)).

5.2.3.7. Deswelling Kinetics in Water and in Buffer Solution pH=3 at 80 °C

Thermosensitive deswelling kinetics at 80 °C from CMC and CMC-g-PNIPAAm comb-type graft hydrogel samples crosslinked either with citric acid or with Al^{3+} were studied in water (Figure 76) and in buffer solution with pH=3 (Figure 77). In both types of CMC-g-PNIPAAm comb-type graft hydrogels, high and relatively fast volume variations with a visible bending was observed, which was an indicator that strong cohesive forces were present along the grafted gel (Kaneko et al. (1995)). The thermosensitive deswelling process was also evidenced by digital photographs (Figure 74 and 75).

The study revealed that CMC gels presented no thermosensitive deswelling in comparison with the CMC-g-PNIPAAm comb-type graft hydrogels. The hydrophilic thermosensitive PNIPAAm grafts had an influence in the thermosensitive deswelling of CMC-g-PNIPAAm gels, because over the LCST temperature probably water release conducts are generated along the polymeric matrix (Kaneko et al. (1999)). These water channels could be generated because of a hydrophobic aggregation of the graft chains that took place along the CMC backbone network, and as a result water was fast expelled out from the comb-type graft hydrogels (Kaneko et al. (1999)).

This hypothesis of Kaneko et al. (1999) was also validated by Ju et al. (2001). They stated that over the LCST temperature, PNIPAAm grafts are no more hydrated and they get aggregate due hydrophobic cohesive forces that happened between the graft chains (Ju et al. (2001)). As a result, the amount of voids along the gel network was incremented and a fast expulsion

of water took place (Ju et al. (2001)).

Figure 77 revealed the influence of pH over the deswelling of CMC-g-PNIPAAm comb-type graft hydrogels. At pH=3 the deswelling degree (from 379 until 114%) was higher than in water (from 390 until 300%). This result was also validated by the thermosentive deswelling kinetic studies made with digital photographs at pH=3 and water, where a higher dimensional reduction was observed with the samples submerged at buffer solution with pH=3.

This higher reduction at pH=3 could be associated to the formation of larger voids (Ju et al. (2001)) (or water release conducts (Kaneko et al. (1999))) because of a stronger aggregation of the graft chains at LCST temperatures, that happened because the CMC polymer backbone at low pH is expected to be stabilized with almost no dissociation of their carboxylic groups, facilitating graft chain aggregation (Bokias et al. (2001)). Higher voids allows the expulsing of higher amounts of water outside the gel, therefore higher deswelling degrees are obtained.

5.2.3.8. Pulsatile temperature dependent kinetics in water and buffer solution pH=3 at 80 °C and 4 °C

As shown in Figure 78, the thermosensitive swelling/deswelling behavior proved to be repeatable with cyclic temperature changes and the ionic strength in solution hat an influence on the swelling/deswelling behavior of the comb-type graft hydrogels in a similar way as happened with the alginate-g-PNIPAAm comb-type graft hydrogels prepared by Ju et al. (2001). The higher deswelling ratio at pH=3 in these cyclic experiments agrees with the results of the non-cyclic deswelling kinetics experiment performed at 80 °C. Similar results agreement between cyclic and no cyclic experiments was also observed by Ju et al. (2001). Than in order to explain the higher deswelling ratio at pH=3, is posible to extrapolate for these results the hypothesis of Ju et al. (2001) that at low pH values larger voids are formed and the hypothesis of Bokias et al. (2001) that high graft chain aggregation at low pH values happened due to no dissociation of the CMC polymer backbone.

5.2.4. Aldehyde functionalization of PA6 unidirectional substrates by acidic hydrolysis

5.2.4.1. Antecedents and secondary hypothesis proposed

In order to achieve the adhesion between the CMC-g-PNIPAAm comb-type graft hydrogel active layer and the PA6 passive layer, it was necessary to generate an interfacial chemical bonding between these two layers (Haldorai et al. (2014)). It was anticipated that this bonding would be between the carboxylic groups from the active layer (and the crosslinker citric acid) and the aldehyde groups from a previously functionalized PA6 passive layer.

Previous work in protein immobilization on PA6 substrates, showed that the immobilization (interfacial chemical bonding) was possible with aldehyde functionalization of the PA6 films (Isgrove et al. (2001), Vasileva et al. (2004), Pessoa de Amorim et al. (2014)). The

functionalization was achieved after a surface activation with glutaraldehyde, which possess aldehyde groups as pendant groups. While Vasileva et al. (2004) performed this activation in one step, Isgrove et al. (2001) and Pessoa de Amorim et al. (2014) required a two-step activation with a first glutaraldehyde activation before the final one (Figure 36).

Before Isgrove et al. (2001) and Pessoa de Amorim et al. (2014) could perform the first surface activation of PA6 passive layers with glutaraldehyde, they made an amino group activation, either by acidic hydrolysis or by aqueous hydrolysis. The generation of $–NH_2$ groups in PA6 was higher during the 24 h aqueous hydrolysis as with the diluted or the concentrated acidic hydrolysis, which agrees with the conclusions of Isgrove et al. (2001), where the more prolonged time and the not dissolution of the film in water, allowed to give rise to more $–NH_2$ groups.

In the subsequent first glutaraldehyde activation of the PA6 films, performed by Isgrove et al. (2001) and Pessoa de Amorim et al. (2014), Pessoa de Amorim et al. (2014) stated that the glutaraldehyde acted as a coupling agent for a PEI branched spacer, which Isgrove et al. (2001) and Andrews et al. (1991) used in order to increment the amount of active sites (in each pendant amino group of the PA6 films) that would react with glutaraldehyde during the second activation. Another advantange of the PEI branched spacer addressed by Isgrove et al. (2001) and Andrews et al (1991) was the reduction of surrounding effects coming from the matrix groups and the steric hindrance.

5.2.4.2. Elemental Analysis

This hypothesis of an aldehyde functionalization of PA6 unidirectional substrates by acidic (or aqueous) hydrolysis and a two-step glutaraldehyde activation was validated by assuming that after first activation with glutaraldehyde, increments in carbon weight percentages (%C) in hydrolyzed PA6 samples were taken as an indication of aldehyde group (-COH) presence on the PA6 substrates. Elemental analysis measurements performed to hydrolyzed PA6 samples after first glutaraldehyde activation (Table 26), revealed that the %C was higher in those samples hydrolyzed with water. This behavior was expected, since the prolonged time of aqueous hydrolysis (24 h) allowed the generation of more amino groups (Isgrove et al. (2001)).

5.2.5. Chemical bonding between active and passive layers in bilayer actuators

5.2.5.1. Antecedents and secondary hypothesis proposed

Once the aldehyde functionalization of the PA6 passive layer was confirmed and as it was stated before, the interfacial chemical bonding chosen would be reactions between the generated aldehyde groups from the functionalized PA6 passive layer and:

- The carboxylic groups from the crosslinker citric acid (interfacial chemical crosslinking).

- The hydroxyl OH- function from CMC carboxylic groups of the active layer (interfacial reactions).

The reaction between aldehyde groups and hydroxyl OH- function from carboxylic groups is believed to be possible, since in the past Buhus et al. (2009) proposed as a possible crosslinking reaction for the synthesis of gelatin hydrogels, the one between the aldehyde groups from the crosslinker glutaraldehyde and the OH-groups from gelatin chains (Figure 35).

It is important to add that when the aldehyde groups from the functionalized PA6 passive layer reacted with the hydroxyl OH- function from citric acid carboxylic groups, it was supposed that per each citric acid molecule, one carboxylic group would react with one aldehyde group while the other carboxylic group would react with the OH- from CMC carboxylic groups.

5.2.5.2. FTIR

This hypothesis was validated with a FTIR spectra performed to a bilayer sample (Figure 82): The interfacial chemical bonding is confirmed by the presence of an overlapped carboxylic group peak at 1718.0 cm^{-1} (-COOH), which would be part of the citric acid chemical structure. The presence of this peak is expected as a sign of successful crosslinking, since it was already registered in FTIR studies (Demitri et al. (2008)) the crosslinking reaction progress between the citric acid carboxylic groups and the OH- portion from CMC acid carboxylic groups.

This carboxylic group peak would be an unreacted group that remained in the citric acid after the crosslinking reaction was performed, as it was described in a possible crosslinking mechanism between CMC and citric acid (Figure 28) (Demitri et al. (2008)). This signal was not visible on the FTIR spectra of the aldehyde functionalized PA6 single passive layer.

It was inferred from these results, that if the reaction between a citric acid carboxylic group and the OH- from CMC carboxylic group was confirmed, then for the same citric acid molecule, its other carboxylic group had reacted with an aldehyde group from the functionalized PA6 passive layer. Otherwise the interfacial chemical crosslinking would not be produced and therefore the adherence between the active and passive layers would not be possible.

5.2.5.3. SEM

The adherence between the CMC-g-PNIPAAm comb-type graft hydrogel active layer and the aldehyde functionalized PA6 passive layer was also shown by SEM (Figure 84), confirming with this result the chemical bonding between active and passive layers was obtained. Interfacial chemical crosslinking promoted also a good adhesion between both layers, probably because of the formation of covalent bonds between the citric acid carboxylic groups with: First, the OH- from CMC carboxylic groups of the active layer (Demitri et al. (2008)) (Figure 84) and second, with the aldehyde groups (-COH) (Buhus et al. (2009)) (Figure 35) of the functionalized PA6 passive layer. Additionally, it was also assumed from the SEM investigation

that interfacial reactions between aldehyde groups (from the functionalized PA6 passive layer) and the hydroxyl OH- groups from CMC carboxylic groups of the active layer (Buhus et al. (2009)) (Figure 35) also contributed to the adherence between both layers.

5.3. Thermal and actuation properties from bilayer actuators based on CMC-g-PNIPAAm comb-type graft hydrogel films

5.3.1. Antecedents and secondary hypothesis proposed

A smart bilayer actuator reacts towards an external stimulus applied to its environment, such as example changes in acetone concentration (Hu et al. (1995)), humidity (Guan at al. (2005), Ma et al. (2011), Dai et al. (2013)), electricity applied (Feinberg et al. (2007)) or pH (Bassik et al. (2010), Haldorai et al. (2014)). The reaction is a mechanical bending of the structure. The mechanical bending is produced from a contraction of the active layer, which is sensitive to the external stimulus applied and reacts accordingly.

It is expected that the bilayer fabricated during this research work would be thermosensitive, which means that the active layer would be sensitive to temperature changes of its environment (external stimulus) (Hu et al. (1995), Simpson et al. (2010), LeMieux et al. (2006), Zhang et al. (2011), Stoychev et al. (2012), Stoychev et al. (2013), Yamamoto et al. (2015), Stroganov et al. (2015)). This means that, when heat is applied to the environment where the bilayer actuator is located and a temperature change happens, the active layer would be supposed to react towards this stimulus by contracting and therefore a bending of the bilayer would be observed.

The manufactured bilayer actuator consisted of an inert PA6 passive layer and an active layer made of CMC-g-PNIPAAm comb-type graft hydrogel film. In aqueous solutions, the PNIPAAm grafts from the active layer are thermosensitive polymers, which were supposed to provide thermosensitivity to the CMC hydrogel film. The thermosensitive property in aqueous solutions was provided to the CMC-g- PNIPAAm comb-type graft hydrogel films, as it was confirmed by the validation of the previous secondary hypotheses.

Once it was confirmed that thermosensitive active layer was obtained and also that it was possible to build a bilayer actuator by adhesion with a PA6 passive layer.

5.3.2. Photographs of actuation

This hypothesis was validated with digital photographs, where the influence of the active layer on the actuation was showed (Figure 85(c)) in contrast with functionalized (Figure 85(b)) and not-functionalized (Figure 85(a)) PA6 passive monolayers, which presented no bending. It was observed that the bilayer actuator took 45 minutes at 60 °C for bending circa 10° to the flank of the PA6 passive layer.

The bending observed at 60 °C was attributed to a thermosensitive contraction of the CMC-g-PNIPAAm comb-type graft hydrogel active layer. As it was stated before (See section 5.2.3.6.), the thermosensitive contraction from the CMC-g-PNIPAAm comb-type graft hydrogel active layer probably happened because over the LCST temperature the PNIPAAm grafts are dehydrated and therefore they aggregate producing water release conducts (Kaneko et al. (1999)) or voids (Ju et al. (2001)) along the hydrogel matrix, that facilitated the water expulsion and therefore the contraction of the active layer.

While the CMC-g-PNIPAAm comb-type graft hydrogel active layer was contracted, the PA6 passive layer stayed unchanged. This large difference in contraction is supposed to produce an interfacial stress between both layers (Ma et al. (2011)) then bending was generated. However, the bending movement was heterogeneous, which could be attribute to the clamp that could produce some end defects on the bilayer (Dai et al. (2013)).

5.3.3. Gyration angle

The curve gyration angle (Θ) versus time (Figure 88) was obtained from measurements to the bilayer actuator when it was submerged in water and heated from room temperature until 60 °C. The gyration angle was used to give a quantitative description of the thermosensitive bending actuation and is defined as a type of angular displacement.

An angular displacement is defined as the variation in the angular position from any point of a (or a complete) rotation segment. While an angular position is represented by the length (r) of an specific point to the origin (of a given axis of rotation) and the angle between a chosen reference axis (perpendicular to the axis of rotation) and the segment generated, by connecting the specific point with the origin Mc Lester et al. (2008).

In this case, the bilayer was considered as the rotation segment, the extreme attached with a clamp was taken as the origin, an horizontal line drawn perpendicular to a vertical line parallel to the clamp orientation, was taken as the reference axis and the free extreme of the bilayer (not attached by the clamp), was the specific point taken for measuring the angular displacement or gyration angle.

At 40 °C, which was over the LCST temperature of PNIPAAm, almost no thermosentive actuation was visible. However, after circa 15 minutes of heating from 40 °C to 60 °C, started the thermosensitive bending actuation of the bilayer until reaching a gyration angle displacement of circa 6°. It is assumed that before this point the collapse or aggregation of PNIPAAm grafts was not high enough for creating voids (Ju et al. (2001)) or water release conducts (Kaneko et al. (1999)) that could allow water expulsion of the gel, then the contraction of the active gel layer was still not possible and therefore no thermosensitive bending (actuation) was observed.

The gyration angle results presented in this work are quantitative representations of thermosensitive actuations and are comparable to the deflection angles from the (PAA/PAH)*30/NOA 63 bilayers developed by Ma et al. (2011), which were quantitative representations of humidity-sensitive actuations. Ma et al. (2011) performed on (PAA/PAH)*30/NOA 63 bilayers cyclic experiments by varying the relative humidity of the environment and obtained deflection angles of 57° after 4 seconds and after 8 seconds their bilayers were uncurved until a deflection angle of 0° was achieved (**Figure 57**).

Alternatively, Dai et al. (2013) und Haldorai et al. (2014) quantified humidity- and chemosensitive actuation, respectively by measuring the curvature of the bilayers they developed. While Dai et al. (2013) reported curvature results for PA6/LC bilayers related to relative humidity variations (**Figure 58**), Haldorai et al. (2014) presented curvatures for PA6/poly(PNIPAAm-co-PAA)-g-CMC obtained from pH and ionic strength environment variations (**Figure 59**).

6. Bibliography

Andrews A. T., Mbafor W., *Biochem Soc. Trans.*, 1991, **19**, 271S.

Arens J., *Bulletin Société Chimique de France*, 1968, **35**, 3037e44.

ASTM, *Annual Book of ASTM Standards, Part 21 (ASTM, Philadelphia)*, 1995, Designation: D 1439-94 “Standard Test Method for Sodium Carboxymethylcellulose”.

Balser K., Hoppe L., Eicher T., Wendel M., Astheimer A.-J., *Ullmann’s Encyclopedia of Industrial Chemistry, 5th ed. (Gerhartz W., Yamamoto Y. S., Champbell F. T., Pfefferkorn R., Rounsaville J. F., Eds., VCH, Weinheim, New York)*, 1986, **A5**, 419.

Bassik N., Abebe B. T., Laflin K. E., Gracias D. H., *Polymer*, 2010, **51**, 6093-6098.

Behr A., Urschey M., Brehme V. A., *Green Chemistry*, 2003, **5**, 198–204.

Behr A., Becker M., Beckmann T., Johnen L., Leschinski J., Reyer S., *Angewandte Chemie International Edition*, 2009, **48**, 3598 – 3614.

Billups W. E., Walker W. E., Shields T. C., *Chemical Communications*, 1971, 1067-1068.

Bokias G., Mylonas Y., Staikos G., Bumbu G. G., Vasile C., *Macromolecules*, 2001, **34**, 4958-4964.

Bontempo D., Li R. C., Ly T., Brubaker C. E., Maynard H. D., *Chemical Communications*, 2005, 4702–4704.

Braihi A. J., Salih S. I., Hashem F. A., Ahmed J. K., *International Journal of Materials Science and Applications*, 2014, **3**, 363-369.

Brand L., *Ullmann’s Encyclopedia of Industrial Chemistry, 5th ed. (Gerhartz W., Yamamoto Y. S., Champbell F. T., Pfefferkorn R., Rounsaville J. F., Eds., VCH, Weinheim, New York)*, 1986, **5**, 482.

Buhus G., Popa M., Desbrieres J., *Journal of Bioactive and Compatible Polymers*, 2009, **24**,

525-545.

Burgert I., Fratzl P., *Philosophical Transactions of the Royal Society of London, Series A: Mathematical, Physical and Engineering Sciences*, 2009, **367**, 1541-1557.

Cash M. J., Caputo S. J., *Food Stabilisers, Thickeners and Gelling Agents*, 2009, Chapter 6. Cellulose Derivatives, 95–115.

Clement N. D., Routaboul L., Grotevendt A., Jackstell R., Beller M., *Chemistry - A European Journal*, 2008, **14**, 7408 – 7420.

Collins Dictionaries, *Collins English Dictionary – Complete and Unabridged (HarperCollins Publishers), 12th Edition*, 2014.

Coma V., Sebti I., Pardon P., Pichavant F. H., Deschamps A., *Carbohydrate Polymers*, 2003, **51**, 265–271.

Dahlgren L., *Wood Cellulose (Kennedy J. F., Phillips G. O., Williams P. A., Eds, Horwood Publ. Chichester)*, 1987, 427.

Dai M., Picot O. T., Verjans J. M. N., de Haan L. T., Schenning A. P. H. J., Peijs T., Bastiaansen C. W. M., *ACS Applied Materials & Interfaces*, 2013, **5**, 4945−4950.

Dawson C., Vincent J. F. V., Rocca A. M., *Nature*, 1997, **390**, 668.

Demitri Ch., Del Sole R., Scalera F., Sannino A., Vasapollo G., Maffezzoli A., Ambrosio L., Nicolais L., *Journal of Applied Polymer Science*, 2008, **110**, 2453–2460.

Dimitrov I., Trzebicka B., Müller A. H. E., Dworak A., Tsvetanov C. B., *Progress in Polymer Science*, 2007, **32**, 1278-1317.

Dinjus E., Leitner W., *Applied Organometallic Chemistry*, 1995, **9**, 43-50.

Distantina S., Rochmadi, Fahrurrozi M., Wiratni, *Engineering Journal*, 2013, **17**, 57–66.

Duan Q., Miura Y., Narumi A., Shen X., Sato S.-I., Satoh T., Kakuchi T., *Journal of Polymer Science: Part A: Polymer Chemistry*, 2006, **44**, 1117–1124.

Durand A., Hourdet D., *Polymer*, 1999, **40**, 4941–4951.

Eyler R. W., Klug E. D., *Analytical Chemistry*, 1947, **19**, 24.

Feddersen R. L., Thorp S. N., *Industrial Gums, Polysaccharides and their Derivatives (Whistler R. L., BeMiller J. N., Eds, Academic Press Inc., San Diego, Boston, New York, 3rd ed)*, 1993, 537.

Feinberg A. W., Feigel A., Shevkoplyas S. S., Sheehy S., Whitesides G. M., Parker K. K., *Science*, 2007, **317**, 1366-1370.

Fischer F., Freitag R., *Journal of Chemical Education*, 2006, **83**, 447-450.

Forterre Y., Skotheim J. M., Dumais J., Mahadevan L., *Nature*, 2005, **433**, 421–425.

Fratzl P., Elbaum R., Burgert I., *Faraday Discussions*, 2008, **139**, 275–282.

Guan J., He H., Hansford D. J., Lee L. J., *Journal of Physical Chemistry B: Condensed Matter, Materials, Surfaces, Interfaces & Biophysical Chemistry*, 2005, **109**, 23134-23137.

Guo H., Brˆulet A., Rajamohanan P. R., Marcellan A., Sanson N., Hourdet D., *Polymer*, 2015, **60**, 164-175.

Haldorai Y., Shim J.-J., *New Journal of Chemistry*, 2014, **38**, 2653-2659.

Haleem N., Arshad M., Shahid M., Ashraf Tahir M., *Carbohydrate Polymers*, 2014, **113**, 249–255.

Haupt W., *Bewegungsphysiologie der Pflanzen (Stuttgart, Germany: Thieme Verlag)*, 1977, 406.

Heinze T., Klemm D., Loth F., Phillip B., *Acta Polymerica*, 1990, **41**, 259.

Heinze T., Helbig K., Klemm D., *Acta Polymerica*, 1993, **44**, 108.

Heinze T., Heinze U., *Macromolecular Rapid Communications*, 1997, **18**, 1033.

Heinze T., Liebert T., *Progress in Polymer Science*, 2001, **26**, 1689.

Heinze T., *Macromolecular Symposia*, 2005, **223**, 13 – 40.

Hirasa O., Ito S., Yamauchi A., Fujishige S., Ichijo H., *In Polymer Gels* (DeRossi D. et al., Eds., Plenum Press, New York), 1991, 247.

Hongbo T., Yanping L., Min S., Xiguang W., *Polymer Journal*, 2012, **44**, 211–216.

Hourdet D., L'AIloret F., Audebert R., *Polymer*, 1997, **38**, 2535-2547.

Hourdet D., L'Alloret F., Durand A., Lafuma F., Audebert R., Cotton J.-P., *Macromolecules*, 1998, **31**, 5323-5335.

Hoogendam C. W., de Keizer A., Cohen Stuart M. A., Bijsterbosch B. H., Smit J. A. M., van der Horst J. A. P. P., Batelaan J. G., *Macromolecules*, 1998, **31**, 6297.

Hu Z., Zhang X., Li Y., *Science*, 1995, **269**, 525-527.

Isgrove F. H., Williams R. J. H., Niven G. W., Andrews A. T., *Enzyme and Microbial Technology*, 2001, **28**, 225–232.

Jardeby K., Influence of pulp and wood properties on the unreacted residuals in carboxymethyl cellulose, Ph.D. thesis (University of Karlstad, Karlstad, Sweden) and Jardeby K., Lennholm H., Germgard U., *Cellulose*, 2004, **11**, 195-202.

Jin X., Kang H., Liu R., Huang Y., *Carbohydrate Polymers*, 2013, **95**, 155–160.

Ju H. K., Kim S. Y., Lee Y. M., *Polymer*, 2001, **42**, 6851-6857.

Kabra B. G., Gehrke S. H., *Polym. Commun.*, 1991, **32**, 322-323.

Kaneda K., Kurosaki H., Terasawa M., Imanaka T., Teranishi Sh., *The Journal of Organic Chemistry*, 1981, **46**, 2356-2362.

Kaneko Y., Sakai K., Kikuchi A., Yoshida R., Sakurai Y., Okano T., *Macromolecules*, 1995, **28**, 7717-7723.

Kaneko Y., Yoshida R., Sakai K., Sakurai Y., Okano T., *J. Membr. Sci.*, 1995, **101**, 13-22.

Kaneko Y., Nakamura S., Sakai K., Kikuchi A., Aoyagi T., Sakurai Y., Okano T., *Journal of Biomaterials Science, Polymer Edition*, 1999, **10**, 1079-1091.

Kano M., Kokufuta E., *Langmuir*, 2009, **25**, 8649–8655.

Käuper P., Kulicke W.-M., Horner S., Saake B., Puls J., Kunze J., Fink H.-P., Heinze T., Klohr E.-A., Thielking H., Koch W., *Die Angewandte Makromolekulare Chemie*, 1998, **260**, 53.

Karakasyan C., Lack S., Brunel F., Maingault P., Hourdet D., *Biomacromolecules*, 2008, **9**, 2419-2429.

Kaushik M., Tathagata K., Biswanath S., *Der Pharmacia Lettre*, 2012, **4**, 1633-1647.

Kirk-Othmer, Encyclopedia of Chemical Technology, John Wiley & Sons, 4ta edición, 1991, 107, 133 and 143.

Kötz J., Philipp B., Nehls I., Heinze T., Klemm D., *Acta Polymerica*, 1990, **41**, 333.

Kokufuta M. K., Sato S., Kokufuta E., *Colloid and Polymer Science*, 2012, **290**, 1671–1681.

Kujawa P., Segui F., Shaban Sh., Diab Ch., Okada Y., Tanaka F., Winnik F. M., *Macromolecules*, 2006, **39**, 341-348.

L'Alloret F., Hourdet D., Audebert R., *Colloid and Polymer Science*, 1995, **273**, 1163-1173.

Lazik W., Heinze T., Pfeiffer K., Albrecht G., Mischnick P., *Journal of Applied Polymer Science*, 2002, **86**, 743.

Lazutkin A. M., Lazutkina A. I., Yermakov Yu. I., *Reaction Kinetics, Mechanisms and Catalysis*, 1978, **8**, 353-357.

Leca F., Réau R., *Journal of Catalysis*, 2006, **238**, 425–429.

LeMieux M. C., McConney M. E., Lin Y. H., Singamaneni S., Jiang H., Bunning T. J., Tsukruk V. V., *Nano Letters*, 2006, **6**, 730-734.

Li Y., Liu R., Huang Y., *Journal of Applied Polymer Science*, 2008, **110**, 1797–1803.

Liu R. C. W., Cantin S., Perrot F., Winnik F. M., *Polymers for Advanced Technologies*, 2006, **17**, 798–803.

Lo Verso F., Likos C. N., *Polymer*, 2008, **49**, 1425-1434.

Lüttge U., Kluge M., Bauer G., *Botanik (Weinheim, Germany: Wiley-VCH)*, 2005.

Mc Lester J., St. Pierre P., *Applied Biomechanics: Concepts and Connections* (Thomson Wadsworth, Canada), 2008, 169.

Ma Y., Zhang Y., Wu B., Sun W., Li Zh., Sun J., *Angewandte Chemie International Edition*, 2011, **50**, 6254 –6257.

Masci G., Giacomelli L., Crescenzi V., *Macromolecular Rapid Communications*, 2004, **25**, 559–564.

Matsuo E. S., Tanaka T., *J. Chem. Phys*, 1988, **89**, 1695-1703.

Matthews L. A., Giurgiutiu V., *Smart structures and materials 2006: smart structures and integrated systems (ed. Y. Matsuzaki)*, 2006, **Proc. SPIE 6173**, O1–O10.

Monflier E., Bourdauducq P., Couturier J.-L., Kervennal J., Suisse I., Mortreux A., *Catalysis Letters*, 1995, **34**, 201-212.

Musco A., Perego C., Tartiari V., *Inorganica Chimica Acta*, 1978, **28**, L147-L148.

Nicholson M. D., Merrit F. M., *Cellulose Chemistry. Its Application (Nevell T., Zeronian P., Haig S., Eds, Hor-wood Publ. Chichester)*, 1989, 363.

Okano T., Bae Y. H., Jacobs H., Kim S. W., *J. Controlled Release*, 1990, **11**, 255-265.

Okuyama Y., Yoshida R., Sakai K., Okano T., Sakurai Y. J., *Biomater. Sci., Polym. Ed.*, 1993, **4**, 545-556.

Otake K., Inomata H., Konno M., Saito Sh., *Macromolecules*, 1990, **23**, 283-289.

Pessoa de Amorim M. T., Guimaraes H., Soares G. M., Miranda T. M. R., *ResearchGate*, 2014, “Study of the modification of polyamide membranes for laccase immobilization and application in degradation of reactive dye from textile industry”, 1-6. https://www.researchgate.net/publication/266883353_Study_of_the_modification_of_polyamide_membranes_for_laccase_immobilization_and_application_in_degradation_of_reactive_dye_from_textile_industry.

Ritter H., Cheng J., Tabatabai M., *Beilstein Journal of Organic Chemistry*, 2012, **8**, 1528–1535.

Rose D., Lepper H., *Journal of Organometallic Chemistry*, 1973, **49**, 473-476.

Saeedi M., Akbari J., Enayatifard R., Morteza-Semnani K., Tahernia M., Valizadeh H., *Iranian Journal of Pharmaceutical Research*, 2009, **8**, 241-249.

Salmi T., Valtakari D., Paatero E., Holmbom B., Sjöholm R., *Industrial and Engineering Chemistry Research*, 1994, **33**, 1454.

Sandas S. E., Salminen P. J., *Nordic Pulp & Paper Research Journal*, 1993, **1**, 184.

Sannino A., Nicolais L., *Polymer*, 2005, **46**, 4676–4685.

Sannino A., Madaghiele M., Lionetto M. G., Schettino T., Maffezzoli A., *Journal of Applied Polymer Science*, 2006, **102**, 1524–1530.

Schild H. G., Tirrel D. A., *The Journal of Physical Chemistry A*, 1990, **94**, 4352-4356.

Schild H. G., *Progress in Polymer Science*, 1992, **17**, 163-249.

Shah N., Patel K. R., *Journal of Pharmaceutical Science and Bioscientific Research*, 2014, **4**, 114–120.

Shahinpoor M., Thompson M. S., *Materials Science and Engineering C: Biomimetic and Supramolecular Systems*, 1995, **2**, 229–233.

Simpson B., Nunnery G., Tannenbaum R., Kalaitzidou K., *Journal of Materials Chemistry*, 2010, **20**, 3496–3501.

Skotheim J. M., Mahadevan L., *Science*, 2005, **308**, 1308–1310.

Sjostrom B., *Cellulose, Structural and Functional Aspects (Kennedy J. F., Philipps G. O., Williams P. A., Eds., E. Horwood Publ., Chichester)*, 1989, Characterization of carboxymethylcellulose by gas-liquid chromatography, 239.

Smithenry D. W., Kang M.-S., Gupta V. K., *Macromolecules*, 2001, **34**, 8503-8511.

Stigsson V., Kloow G., Germgard U., *Paper Asia*, 2001, **17**, 16-21.

Stoychev G., Zakharchenko S., Turcaud S., Dunlop J. W. C., Ionov L., *ACS Nano*, 2012, **6**, 3925–3934.

Stoychev G., Turcaud S., Dunlop J. W. C., Ionov L., *Advanced Functional Materials*, 2013, **23**, 2295–2300.

Stroganov V., Al-Hussein M., Sommer J. U., Janke A., Zakharchenko S., Ionov L., *Nano Letters*, 2015, **15**, 1786−1790.

Sungur S., Emregül E., *Macromolecular Reports*, 1996, **A33**, 319.

Taya M., *Smart structures and materials 2003: electroactive polymer actuators and devices (ed. Y. BarCohen)*, 2003, **Proc. SPIE 5051**, 54–65.

Thilarik K., Pastek M., *Chemical Papers*, 1987, **41**, 703.

Touzinsky G. F., Gordon Sh. H., *Carbohydrate Research*, 1979, **69**, 327-329

Vasileva N., Godjevargova Ts., *Journal of Membrane Science*, 2004, **239**, 157–161.

Vincent J. F. V., Bogatyreva O. A., Bogatyrev N. R., Bowyer A., Pahl A.-K., *Journal of the Royal Society Interface*, 2006, **3**, 471-482.

Volkov A. G., Adesina T., Markin V. S., Jovanov E., *Plant Physiology*, 2008, **146**, 694–702.

Vrentas J. S., Jarzebski C. M., Duda J. L., *AIChE J.*, 1975, **21**, 894-901.

Wu X. Sh., Hoffmann A. S., Yager P., *Journal of Polymer Science: Part A Polymer Chemistry*, 1992, **30**, 2121-2129.

Yamamoto Y., Kanao K., Arie T., Akita S., Takei K., *ACS Applied Materials & Interfaces*, 2015, **7**, 11002−11006.

Yoshida R., Sakai K., Okano T., Sakurai Y., *Ind. Eng. Chem. Res.*, 1992, **31**, 2339-2345.

Yoshida R., Okuyama Y., Sakai K., Okano T., Sakurai Y., *J. Membr. Sci.*, 1994, **89**, 267-277.

Yoshida R., Uchida K., Kaneko Y., Sakai K., Kikuchi A., Sakurai Y., Okano T., *Nature*, 1995, **374**, 240-242.

Zecher D., Gerrisch T., *Thickening and Gelling Agents for Food (Imeson A., Ed., Blackie Academic & Professional, London)*, 1997, Cellulose derivatives, 60-85.

Zhang X., Pint C. L., Lee M. H., Schubert B. E., Jamshidi A., Takei K., Ko H., Gillies A., Bardhan R., Urban J. J., Wu M., Fearing R., Javey A., *Nano Letters*, 2011, **11**, 3239–3244.

Zhou Y. J., Luner, P., Caluwe, P. J., *Journal of Applied Polymer Science*, 1995, **58**, 1523.

7. Index of Figures

Figure 1. Venus flytrap showing its closed and opened stages (Burgert et al. (2009)). The curve drawn was based from values obtained by Forterre et al. (2005). It shows a metastable path is produced going from a state with high elastic energy (opened stage) to a one with low elastic energy (closed stage) when external stimulation is applied to the plant (Burgert et al. (2009))... 3
Figure 2. Cross-section at different stages of annular cells which forms a ring around a fern container: a) Anullar cells completely full of water, b) decrease of ring perimeter due to dehydration, and c) return to initial state of the system after the surpassing of water cohesion forces (Burgert et al. (2009), Lüttge et al. (2005)) 4
Figure 3. Longitudinal section of a pine cone: a) Wet (closed state) and b) dry (opened state) (Burgert et al. (2009)). c) Sketch of one pine cone scale during the opened state, showing the cellulose fibril orientation inside the cell walls, at the top side of the scale (----------) and at the bottom side of the scale (Burgert et al. (2009), Dawson et al. (1997))..... 5
Figure 4. Thermo- and solvent-sensitive folding in a bilayer actuator: a) Drawing of the actuator displaying a PAAM gel (blank area) interpenetrated by one side with a NIPA gel, forming an interpenetrated PAAM-NIPA gel net (hatched area). Images showing the thermosensitive folding of the bilayer actuator at b) 30.0 °C and c) 37.8°C. For an optimum viewing sample was dyed with blue color. Reference sample located at the right side is a pure NIPA gel stripe. Images showing the acetone solvent concentration-sensitive folding of the bilayer actuator in an aqueous environment at d) 20% and e) 45% per weight of total solution mixture. Reference sample located at the right side is a pure PAAM gel stripe. Scale: 5 mm. (Hu et al. (1995)) 7
Figure 5. Micro photographs of hydrogel bilayers in water: a) Monolayer made of chitosan; b) monolayer made from the copolymer poly(PEGMA-co-PEGDMA) with 5:1 PEGMA:PEGDMA weight proportion; c), d), e) Bended bilayers of chitosan and copolymer poly(PEGMA-co-PEGDMA) with 5:1, 3:1 and 1:1 PEGMA:PEGDMA weight proportions. Scale: 100 µm (Guan at al. (2005)). 7
Figure 6. Representation of the actuation process for a PEODA/NIPAm-AAc hydrogel bilayer. a) Bilayer actuator is submerged in an aqueous solution (solution 1) with determined pH and ionic strength values. b) The bilayer actuator is translated to solution 2, which has different pH and ionic strength values. c) A differential swelling occurs as a consequence from changing the solution. d) Bilayer actuator is returned again to solution 1. e) Bilayer actuators deswells as a consequence of changing the pH and ionic strength (Bassik et al. (2010)).. 8

Figure 7. Thermosensitive and reversible folding of a PDMS/Au bilayer (Simpson et al. (2010)). 9
Figure 8. a) Graphical representation of the two-material cantilever during its flexing due to increment of temperature. b) Optical picture of the multilayer actuator flexing when temperature rises from 20 to 40 °C (LeMieux et al. (2006)).. 10
Figure 9. Comparison between the thermosensitive deflections of cantilevers made of silicon/PS, silicon/metal and only silicon during the heating interval (LeMieux et al. (2006))..... 10
Figure 10. a) Manufacture process for elaboration of SWNT-pNIPAM/LDPE bilayer actuators, including amplification of certain portion with optical photos. b) Response time for reaching a 90° bending versus SWNT concentration with photo images of the bilayer actuator at the left before and at the right after flexing (Zhang et al. (2011)). 11
Figure 11. Different possibilities of folding for a bilayer actuator: short-side, long-side and diagonal (Stoychev et al. (2012)). 12
Figure 12. Folding of a bilayer actuator: a) Graphic representation of the thermosensitive bending of a PMMA/P(NIPAM-AA) bilayer actuator (Stoychev et al. (2013)). Step by step actuation until pyramids of four shaft star bilayer actuators: b), c) Unactivated bilayer actuator. d), e) Shriveling of peripherical shaft region into pipes, during first part of bending (indicated by arrows). f) – h) Bending of shafts directing to pyramids formation. Scale bar = 200 µm each. i) Simulation of the bending of a four shaft star (Stoychev et al. (2013)). 13
Figure 13. PolyNIPAAM/PET thermosensitive bilayer actuator. a) Figures and photo-graphs of the bilayer actuator (with CNTs) over a heating plate at 50°C. b) Bilayer actuator at 50°C without CNTs. c) Bilayer actuator bending angle versus heating plate temperature. d) Reaction times of bilayer actuator at 50 and 22 °C. e) Bending force versus Width of pNIPAAM layer in bilayer actuators with and without CNTs (Yamamoto et al. (2015)). 14
Figure 14. a) Synthesis of N-isopropylacrylamide (Kirk-Othmer (1991)) b) Molecular structure of PNIPAAm (Schild et al. (1992)). 15
Figure 15. Temperature – induced phase transition of poly(N-isopropylacrylamide) (Dimitrov et al. (2007)). 17
Figure 16. Hydrogen bridge bond interactions proposed for aleatory NIPAAm – carboxylic acid copolymers (Dimitrov et al. (2007)). 19
Figure 17. Types of telechelic polymers: Top-left, diblock and triblock copolymers; top-center, graft copolymer with telechelic graft groups; top-right, a telechelic star polymer and down-center, a telechelic dendritic polymer (Lo Verso et al. (2008)). 21
Figure 18. Synthesis reaction used for telechelic PNIPAM (Smithenry et al. (2001)). 22
Figure 19. Synthesis of telechelic PNIPAAm polymers functionalized with pyrenyl end groups (Duan et al. (2006)). 23

Figure 20. Telomerization of PNIPAAm at a microwave oven and by using AIBN initiator and 3-mercaptopropionic acid chain-transfer agent (Fischer et al. (2006)). 24
Figure 21. Telomerization reaction and its components (Fischer et al. (2006)). 25
Figure 22. Telomerization reaction for 1,3-butadiene with methanol (Clement et al. (2008)). 26
Figure 23. Products obtained by the telomerization of butadiene with ethylene glycol (L: ligand of carbene of phosphine ligand) (Behr et al (2003)) 27
Figure 24. Theoretical chemical structure of CMC (Reproduced with permission of Hercules incorporated, a subsidiary of Ashland Inc.) (Cash et al. (2009)). 30
Figure 25. Synthesis reaction of 2-acrylamido-2-methyl propane sulfonic acid (AMPS) / acrylic acid (AA) linear copolymers (L'Alloret et al. (1995)). 34
Figure 26. Grafting reaction of aminoterminated O-(2-aminoethyl)-O'-methyl polyethylene oxide (PEO5) to 2-acrylamido-2-methyl propane sulfonic acid (AMPS) / acrylic acid (AA) linear copolymers (L'Alloret et al. (1995)).. 35
Figure 27. Synthesis reaction for CMC grafted with PNIPAAM (Bokias et al. (2001) 36
Figure 28. Possible mechanism proposed for the crosslinking reaction between CMC and citric acid (Demitri et al. (2008)). 38
Figure 29. Possible representation of structures of conventional and macroporous hydrogel (Wu et al. (1992)). 40
Figure 30. Configuration and thermosensitive deswelling of homopolymer and comb-type graft PNIPAAm hydrogel (Yoshida et al. (1995)). 41
Figure 31. Deswelling at LCST temperatures of conventional PNIPAAm hydrogels (NG) vs comb-type graft hydrogels (GG) (Kaneko et al. (1995))... 42
Figure 32. Influence of graft length in the deswelling at LCST temperatures of comb-type graft hydrogels (GG) vs conventional PNIPAAm hydrogels (NG) (Kaneko et al. (1995)).... 42
Figure 33. Representation of the structures for: (a) comb-type graft alginate with PNIPAAm grafts hydrogel and (b) PNIPAAm-alginate semi-interpenetrated network hydrogels (Ju et al. (2001)). 43
Figure 34. Reaction treatment of polyamide 6 PA6 films for generating aldehyde functional groups (Extracted from a Figure of Pessoa de Amorim (2014)). 45
Figure 35. Possible crosslinking reactions between OH groups from CMC, NH2 groups from gelatin chains and the aldehyde groups from the crosslinker glutaraldehyde (Buhus et al. (2009)) 46
Figure 36. Reaction between aldehyde (CHO) groups of modified PA6 film and amino (H_2N) groups of lacasse enzyme (Extracted from a Figure of Pessoa de Amorim (2014)) 46
Figure 37. Effect of type of salt and salt concentration shown from microcalorimetric endotherms from DSC measurements performed on aqueous solutions (0.40 mg/mL) of

PNIPAAm polymer sample A1: (a) Without salt, (b) with NaBr, (c) with Na_2SO_4 and (d) with NaSCN (Schild et al. (1990)). 48
Figure 38. LCST determination in a DSC thermogram embedded in a 90° light scattering analysis for LCST measurement of PNIPAAm linear homopolymer sample aqueous solution (7.8×10^{-5} mol PNIPAAm/g sol). The LCST values obtained for this sample (31.2 °C for DSC vs 31.1 °C for light scattering) are similar (Otake et al. (1990)). 48
Figure 39. LCST endotherms determined by DSC measurements of linear homopolymer aqueous solutions (Kano et al. (2009)). 49
Figure 40. Heating (A) and cooling (B) cycles from DSC measurements showing the variation of LCST temperatures by changing the PEG content in cellulose-g-PEG2k graft copolymers: (a) 100% PEG_{2k}, (b) 94% $PEG_{2k,}$ (c) 85% PEG_{2k} and (d) 50% PEG_{2k} (Li et al. (2008)). 50
Figure 41. LCST tunning of HPC-g-PNIPAAm by changing the length of the PNIPAAm grafts (Jin et al. (2013)). 51
Figure 42. LCST tunning demonstrated by DSC thermograms of HPC and HPC-g-PNIPAAm with different PNIPAAm graft lengths (150, 130, 114, 96 and 81). The graft length is represented by the numerical subindex written at the end of the polymer name (Jin et al. (2013)). 52
Figure 43. DSC measurements of PNIPAAm-g-PDMA (dash line) and PDMA-g-PNIPAAm (solid line) aqueous solutions. PNIPAAm-g-PDMA sample showed the lowest LCST (36°C) while PDMA-g-PNIPAAm, an LCST of 38 °C (Guo et al. (2015)). 53
Figure 44. a) Equilibrium swelling (swelling ratio) at different temperatures for the PNIPAAm homopolymer (○) and comb-type graft (●) gels. Swelling ratio is described as weight of absorbed water per weight of dried gel sample (M_w/M_p) (Yoshida et al. (1995)). b) Deswelling kinetics (measured as swelling ratio) at 40 °C (starting from an equilibrium swelling at 10 °C) of PNIPAAm homopolymer (○) and comb-type graft (●) gels (Yoshida et al. (1995)). 54
Figure 45. a) Deswelling kinetics (measured as swelling ratio) at different temperatures (starting from an equilibrium swelling at 10 °C) of PNIPAAm homopolymer (NG) and comb-type graft with 2900 g/mol graft chain length (GG2900), 4000 g/mol graft chain length (GG4000) and 9000 g/mol graft chain length (GG9000) hydrogels (Kaneko et al. (1995)). b) Swelling degree at 10 °C (starting from an equilibrium swelling at 10 °C) of PNIPAAm homopolymer (NG) and comb-type graft with 2900 g/mol graft chain length (GG2900), 4000 g/mol graft chain length (GG4000) and 9000 g/mol graft chain length (GG9000) hydrogels (Kaneko et al. (1995)). 55

Figure 46. Deswelling kinetics (measured as swelling degree) at: a) 30 and b) 40 °C (starting from an equilibrium swelling at 10 °C) of PNIPAAm homopolymer (NG) and comb-type graft with 2900 g/mol graft chain length (GG2900), 4000 g/mol graft chain length (GG4000) and 9000 g/mol graft chain length (GG9000) hydrogels (Kaneko et al. (1995)). c) Deswelling kinetics (measured as swelling ratio) at different temperatures (starting from an equilibrium swelling at 10 °C) of non-grafted (IP-NG and ID-NG) and comb-type graft (ID-GG and IP-GG) hydrogels (Kaneko et al. (1995)). 56
Figure 47. a) Deswelling kinetics (measured as swelling ratio) between 30 and 40 °C (starting from an equilibrium swelling at 10 °C) for non grafted ID-NG hydrogels (Kaneko et al. (1999)). b) Deswelling kinetics (measured as swelling ratio) between 30 and 40 °C (starting from an equilibrium swelling at 10 °C) for comb-type graft ID-GG hydrogels (Kaneko et al. (1999)). 57
Figure 48. Deswelling kinetics (measured as swelling ratio) between 30 and 40 °C (starting from an equilibrium swelling at 10 °C) for comb-type graft IP-GG hydrogels (Kaneko et al. (1999)). 58
Figure 49. Swelling kinetics (measured as swelling ratio) at 25 °C in pH=5.4 aqueous solutions of comb-type graft hydrogels (samples GAN28, GAN55 and GAN82) (Ju et al. (2001)). 59
Figure 50. Deswelling kinetics (measured as swelling ratio) in water at 40 °C (starting from an equilibrium swelling at 25 °C) of comb-type graft (samples GAN28, GAN55 and GAN82) and semi-IPN (sample IPN55) hydrogels (Ju et al. (2001)). 59
Figure 51. Thermosensitive pulsatile measurements in water and between 25 and 40 °C of comb-type graft (samples GAN28, GAN55 and GAN82) hydrogels (Ju et al. (2001)). 60
Figure 52. Bilayer actuators (robotic grippers) sensitive to electric pulses applied to the structure at different frequencies. (E) The robotic “gripper” was a rectangular PDMS thin film, provided on the concave side of it with longitudinally aligned myocardium tissue, the tips (yellow circunferences) of the gripper joined together during contraction of the muscle due to electric pulse. Scale: 1 mm (Extracted from a figure shown in Feinberg et al. (2007)). 61
Figure 53. a) Folding and unfolding of (PAA/PAH)*30/NOA 63 bilayer actuator (0.5 X 0.8 cm) measured time outlines versus different relative humidity (RH) values. Left column: Relative humidity decreased from 12 to 5% RH. Right column: Relative humidity increased from 5 to 12% RH. (Extracted from a figure shown in Ma et al. (2011)) 62
Figure 54. Humidity sensitive actuation of the PA6/LC bilayer after activation in basic solution and exposition to water vapor (Dai et al. (2013)). 62

Figure 55. (Rows b and c) photos during the folding in water of the bilayer actuator (Photos (i) to (vi) taken each 102 s) and in ethanol for the unfolding ((i) to (vi) taken each 66 s) (Extracted from a figure shown in Haldorai et al. (2014)). 63
Figure 56. Bilayer actuators (robotic grippers) sensitive to electric pulses applied to the structure at different frequencies. (F) Measurement of actuation expressed in terms of maximum tip separation and its correspondent contact time, for different frequencies (pacing rate) of applied electric pulses (pacing rate). The tips are the extremes of the bilayer presented as yellow circunferences in Figure 52 (Extracted from a figure shown in Feinberg et al. (2007)). 63
Figure 57. b) Bending angles (deflection angles) vs time of (PAA/PAH)*30/NOA 63 bilayer actuator (0.5 X 0.8 cm) measured when relative humidity decreased from 12 to 5% RH (top) and relative humidity increased from 5 to 12% RH (bottom). Measurements made from actuation photos of Figure 53. (Extracted from a figure shown in Ma et al. (2011))..... 64
Figure 58. Curvature of a PA6/LC bilayer versus relative humidity. Testing was done two times. First the relative humidity was incremented and then decremented in order to see the respective reactive actuation. The embedded figure shows the deflection radius r defined for the bilayer actuator (Extracted from a figure shown in Dai et al. (2013)). 64
Figure 59. (a) Determination of the R of curvature. Curvature (K=1/R) versus time measured during (d) the folding in water of the bilayer actuator (photos (i) to (vi) from Figure 55 taken each 102 s) and (e) in ethanol for the unfolding (photos (i) to (vi) from Figure 55 taken each 66 s) (Extracted from a figure shown in Haldorai et al. (2014)) 65
Figure 60. Gel Permeation Cromatography elugrams for group of samples A, B and C 86
Figure 61. FTIR Spectrum of aminoterminated PNIPAAm oligomer (Sample CCH-A15-1) 88
Figure 62. ^{1}H-NMR spectra of aminoterminated PNIPAAm oligomer (Sample CCH-A15-1). 88
Figure 63. T_m and ΔH_m of NIPAAm monomer versus aminoterminated PNIPAAm oligomer (Sample fraction CCH-C1(2)-1(3)) 89
Figure 64. Tg of NIPAAm monomer versus amino-terminated PNIPAAm oligomer (Sample fraction CCH-C1(2)-1(3)) 89
Figure 65. Reversibility of phase transition in water of aminoterminated PNIPAAm oligomers (sample fraction CCH-C1(2)-2(1)) versus NIPAAm monomer..... 91
Figure 66. (a) FTIR Spectrum of CMC-g-PNIPAAm graft copolymers (Sample CCH-C2(2)-1.80) versus FTIR Spectra of (b) carboxymethyl cellulose (Sample NaCMC) and (c) amino-terminated PNIPAAm oligomers (Sample CCH-A15-1)..... 103

Figure 67. T_m and ΔH_m of (a) CMC-g-PNIPAAm graft copolymers (Sample CCH-C2(2)-1.80) versus (b) aminoterminated PNIPAAm oligomers (Sample fraction CCH-C1(2)-1(3)) and (c) carboxymethyl cellulose (Sample NaCMC) 105
Figure 68. T_g of (a) aminoterminated PNIPAAm oligomers (Sample fraction CCH-C1(2)-1(3)) and (b) carboxymethyl Cellulose (Sample NaCMC) versus (c) CMC-g-PNIPAAm graft copolymers (Sample CCH-C2(2)-1.80) 106
Figure 69. Reversibility of phase transition in water of (a and b) CMC-g-PNIPAAm graft copolymers (Sample fraction CCH-C2(2)-2.80(4)) versus (c and d) carboxymethyl cellulose (Sample CMC 90,000) 106
Figure 70. DSC of CMC in Water and Buffer Solutions 107
Figure 71. FTIR spectrum of CMC-g-PNIPAAm comb-type graft hydrogels (Sample CCH-C3(5)-2(35%)) 108
Figure 72. T_m of CMC-g-PNIPAAm comb-type graft hydrogels crosslinked with citric acid (Sample CCH-C3(8)MONO-1(CA)) and Al^{3+} ions (Sample CCH-C3(8)MONO-1(Al)) versus T_m of CMC-g-PNIPAAm graft copolymers (Sample CCH-C2(2)- 1.80) 110
Figure 73. Swelling Degree in water of CMC-g-PNIPAAm comb-type graft hydrogels crosslinked with citric acid (Sample CCH-C3(8)MONO-1(CA)) and Al^{3+} Ions (Sample CCH-C3(8)MONO-1(Al)) versus Swelling Degree in water of CMC hydrogels crosslinked with Al^{3+} (Sample CCH-C3(8)MONO-2(Al)) 111
Figure 74. Photographs of the deswelling process in water of square-shape gel films of CMC and CMC grafted with poly(N-Isopropylacrylamide) (CMC-g-PNIPAAm) undergoing shrinking at 80 °C after elevated temperature from 25 °C. 112
Figure 75. Photographs of the deswelling process in buffer solutions of square-shape gel films of carboxymethyl cellulose grafted with poly(N-Isopropylacrylamide) (CMC-g-PNIPAAm) undergoing shrinking in at 80 °C after elevated temperature from 25 °C and starting from water 113
Figure 76. Deswelling in water at 80 °C of CMC-g-PNIPAAm comb-type graft hydrogels crosslinked with citric acid (Sample CCH-C3(8)MONO-1(CA)) and Al^{3+} ions (Sample CCH-C3(8)MONO-1(Al)) versus swelling degree in water of CMC hydrogels crosslinked with Al^{3+} (Sample CCH-C3(8)MONO-2(Al)) 114
Figure 77. Deswelling in water and buffer solution pH=3 at 80 °C of CMC-g-PNIPAAm comb-type graft hydrogels crosslinked with citric acid (Sample CCH-C3(8)MONO-1(CA)). 115
Figure 78. Pulsatile kinetics in water and buffer solution pH=3 between 4 and 80 °C of CMC-g-PNIPAAm comb-type graft hydrogels crosslinked with citric acid (Sample CCH-C3(8)MONO-1(CA)) 115

Figure 79. FTIR spectra of PA6 substrates before (and after) concentrated acidic hydrolysis: I. PA6 substrate untreated, II. after initial activation with glutaraldehyde and III. after final activation with glutaraldehyde. 117
Figure 80. FTIR spectra of PA6 substrates before (and after) aqueous hydrolysis: I. PA6 substrate untreated, II. after initial activation with glutaraldehyde and III. after final activation with glutaraldehyde. 118
Figure 81. FTIR spectra of PA6 substrates before (and after) diluted acidic hydrolysis: I. PA6 substrate untreated, II. after initial activation with glutaraldehyde and III. after final activation with glutaraldehyde. 119
Figure 82. FTIR Spectra of bilayer based on CMC-g- PNIPAAm comb-type graft hydrogel films (Sample CCH-C3(8)BI-3) versus functionalized PA6 substrate (Substrate CCH-C3(8)BI-PA6(2a)f) 121
Figure 83. FTIR spectrum of bilayer based on CMC-g- PNIPAAm comb-type graft hydrogel films (sample CCH-C3(8)BI-84) 122
Figure 84. SEM micrograph of a bilayer based on CMC-g- PNIPAAm comb-type graft hydrogel films (sample CCH-C3(8)BI-56). 122
Figure 85. Thermosensitive actuation in Water of (a) untreated PA6 substrate (Sample CCH-C3(8)BI-Blanc(8)), (b) funtionalized PA6 substrate (Sample CCH-C3(8)BI-Blanc(4)) and (c) func-tionalized PA6 substrate covered with active layer – bilayer Film (Sample CCH-C3(8)BI-56). 123
Figure 86. Thermosensitive actuation in water – reversibility (Sample: CCH-C3(8)BI-40) 124
Figure 87. Evolution of standardized gyration angle (|θ|) with active and passive layer types 125
Figure 88. Gyration angle (θ) vs time 126
Figure 89. Telomerization reaction for N-isopropylacrylamide with 2-aminoethanothiol initiated with ammonium persulphate (APS) (Bokias et al. (2001)) 130
Figure 90. Grafting onto reaction between aminoterminated PNIPAAm and carboxymethyl cellulose (CMC) supported by EDC (Bokias et al. (2001)). 134
Figure 91. Chemical crosslinking of CMC-g-PNIPAAm graft copolymers with citric acid (Demitri et al. (2008)) 136
Figure 92. Molecular structure of aminoterminated PNIPAAm 177

8. Index of Tables

Table 1. Free radical initiators and organic solvents for PNIPAAm synthesis (Schild (1992)). 16
Table 2. Redox initiators (and their accelerators) used in aqueous media for PNIPAAm synthesis (Schild (1992)). 16
Table 3. Various polysaccharides used for carboxymethylation (Heinze et al. (2005), Balser et al. (1986)). 29
Table 4. Molecular weight and degree of polymerization (DP) of more commercial CMC with a DS=0.7 (Cash et al. (2009)). 30
Table 5. Types and grades of CMC and its applications (Heinze et al. (2005), Stigsson et al. (2001)). 31
Table 6. PNIPAAm polymer samples and data obtained from measurements to their aqueous solutions (Schild et al. (1990)). 47
Table 7. LCST data obtained from DSC and transmittance measurements on aqueous solutions of PNIPAAm (PNiPA), other N-propylacrylamides and N-propylmethacrylamides (Kano et al. (2009)). 49
Table 8. Experimental Design for synthesis of aminoterminated PNIPAAm oligomers..... 71
Table 9. Experimental Design for synthesis of CMC-g-PNIPAAm graft copolymers..... 73
Table 10. Experimental Design for synthesis of CMC-g-PNIPAAm comb-type graft hydrogels crosslinked with Al ions. 75
Table 11. Experimental Design for synthesis of CMC-g-PNIPAAm comb-type graft hydrogels crosslinked with citric acid 77
Table 12. Experimental Design for synthesis and comparison between CMC-g-PNIPAAm comb-type graft hydrogels crosslinked with citric acid versus crosslinking with Al^{3+} 77
Table 13. Experimental design for preparation of CMC-g-PNIPAAm comb-type graft pre-gel solutions used in bilayers with hydrogel or PA6 substrates 79
Table 14. Experimental Design for functionalization of PA6 substrates 80
Table 15. Experimental Design for synthesis of bilayer actuators with PA6 substrates..... 81
Table 16. Experimental Design for synthesis of bilayer actuators with hydrogel substrates 82
Table 17. Amount and %Yield for Groups of Samples A, B and C 85
Table 18. Molecular Weight and Polydispersity values for Groups of Samples A, B and C 86
Table 19. Molecular Weight ($Mw_{(EXP)}$) and Experimental Degree of Polymerization (n_{exp}). 90
Table 20. Amount and %Yield of Group of Samples A ($Mw(Graft)_{(THEO)}$ = 5,000 g/mol) ... 92
Table 21. Amount and %Yield of Group of Samples B ($Mw(Graft)_{(THEO)}$ = 7,000 g/mol) ... 93
Table 22. Amount and %Yield of Group of Samples C ($Mw(Graft)_{(THEO)}$ = 9,000 g/mol) ... 94
Table 23. Mw(Total), $\%Graft_{(EXP)}$ and N° Grafts per CMC Chain for Group of Samples A ($Mw(Graft)_{(THEO)}$ = 5,000 g/mol) 95

Table 24. Mw(Total), %Graft(EXP) and N° Grafts per CMC Chain for Group of Samples B (Mw(Graft)(THEO) = 7,000 g/mol) 97
Table 25. Mw(Total), %Graft(EXP) and N° Grafts per CMC Chain for Group of Samples C (Mw(Graft)(THEO) = 9,000 g/mol) 100
Table 26. Elemental Analysis after initial activation with glutaraldehyde 116
Table 27. Elemental Analysis: Aminoterminated PNIPAAm oligomers Experimental Data - Part 1: Experimental weight percentages (%W) (Sample CCH-A15-1) 172
Table 28. Elemental Analysis: Aminoterminated PNIPAAm oligomers Experimental Data - Part 2: Experimental weights (Sample CCH-A15-1) 173
Table 29. Elemental Analysis: Aminoterminated PNIPAAm oligomers Experimental Data - Part 3: Experimental moles (mol_{exp}) (Sample CCH-A15-1) 174
Table 30. Elemental Analysis: Aminoterminated PNIPAAm oligomers Experimental Data - Part 4: Average experimental moles (mol_{avg}) (Sample CCH-A15-1) 175
Table 31. Elemental Analysis: Aminoterminated PNIPAAm oligomers Experimental Data - Part 5: Experimental mol percentages ($\%mol_{exp}$) (Sample CCH-A15-1) 176
Table 32. Elemental Analysis: Aminoterminated PNIPAAm oligomers Theoretical Data - Part 1: Theoretical moles (mol_{theo}) (Sample CCH-A15-1) 178
Table 33. Elemental Analysis: Aminoterminated PNIPAAm oligomers Theoretical Data - Part 2: Theoretical mol percentages ($\%mol_{theo}$) (Sample CCH-A15-1) 179
Table 34. Elemental Analysis: CMC-g-PNIPAAm graft copolymers Experimental Data - Part 1: Experimental weight percentages of N (%W - N) (Sample CCH-A27-1) 183
Table 35. Elemental Analysis: CMC-g-PNIPAAm graft copolymers Experimental Data - Part 2: Average experimental weight percentage of N ($\%W_{avg}$ - N) (Sample CCH-A27-1) 183
Table 36. Buffer solutions 187
Table 37. Aminoterminated PNIPAAm oligomers (NH_2-PNIPAAm) (Mw(THEO) = 5,000 g/mol) 189
Table 38. Aminoterminated PNIPAAm oligomers (NH_2-PNIPAAm) (Mw(THEO) = 7,000 g/mol) 190
Table 39. Aminoterminated PNIPAAm oligomers (NH_2-PNIPAAm) (Mw(THEO) = 9,000 g/mol) 191
Table 40. CMC-g-PNIPAAm graft copolymers (Mw(Graft)(THEO) = 5,000 g/mol – %Graft(THEO) = 40%) 192
Table 41. CMC-g-PNIPAAm graft copolymers (Mw(Graft)(THEO) = 5,000 g/mol – %Graft(THEO) = 50%) 193
Table 42. CMC-g-PNIPAAm graft copolymers (Mw(Graft)(THEO) = 5,000 g/mol – %Graft(THEO) = 80%) 195

Table 43. CMC-g-PNIPAAm graft copolymers ($Mw(Graft)_{(THEO)}$ = 7,000 g/mol – $\%Graft_{(THEO)}$ = 40%) 196
Table 44. CMC-g-PNIPAAm graft copolymers ($Mw(Graft)_{(THEO)}$ = 7,000 g/mol – $\%Graft_{(THEO)}$ = 50%) 197
Table 45. CMC-g-PNIPAAm graft copolymers ($Mw(Graft)_{(THEO)}$ = 7,000 g/mol – $\%Graft_{(THEO)}$ = 80%) 198
Table 46. CMC-g-PNIPAAm graft copolymers ($Mw(Graft)_{(THEO)}$ = 9,000 g/mol – $\%Graft_{(THEO)}$ = 40%) 199
Table 47. CMC-g-PNIPAAm graft copolymers ($Mw(Graft)_{(THEO)}$ = 9,000 g/mol – $\%Graft_{(THEO)}$ = 50%) 200
Table 48. CMC-g-PNIPAAm graft copolymers ($Mw(Graft)_{(THEO)}$ = 9,000 g/mol – $\%Graft_{(THEO)}$ = 80%) 201
Table 49. CCH-C3(4)-2(30%) pregel stock solution 202
Table 50. $AlCl_3$ aqueous solutions (Vsolution = 10 mL) 202
Table 51. Pregel stock solutions 203
Table 52. CCH-C3(8)-2.1(35%) pregel stock solution 207
Table 53. CCH-C3(8)-1a(35%) pregel stock solution 208
Table 54. CCH-C3(8)-2.2(35%) pregel stock solution 208
Table 55. CCH-C3(8)-2.3(35%) pregel stock solution 209
Table 56. CMC-g-PNIPAAm comb-type graft pre-gel solutions used for bilayers with hydrogel substrate 210
Table 57. Solutions used for functionalization of PA6 substrates by concentrated (and diluted) acidic and aqueous hydrolysis 211
Table 58. FTIR Measurements: Aminoterminated PNIPAAm oligomers (Group of Samples A ($Mw(Graft)_{(THEO)}$ = 5,000 g/mol)) 212
Table 59. FTIR Measurements: Aminoterminated PNIPAAm oligomers (Group of Samples B ($Mw(Graft)_{(THEO)}$ = 7,000 g/mol)) 214
Table 60. FTIR Measurements: Aminoterminated PNIPAAm oligomers (Group of Samples C ($Mw(Graft)_{(THEO)}$ = 9,000 g/mol)) 216
Table 61. NMR Measurements: Aminoterminated PNIPAAm oligomers (Group of Samples A ($Mw(Graft)_{(THEO)}$ = 5,000 g/mol)) 220
Table 62. NMR Measurements: Aminoterminated PNIPAAm oligomers (Group of Samples A ($Mw(Graft)_{(THEO)}$ = 7,000 g/mol)) 222
Table 63. NMR Measurements: Aminoterminated PNIPAAm oligomers (Group of Samples C ($Mw(Graft)_{(THEO)}$ = 9,000 g/mol)) 224
Table 64. DSC (Dry) Measurements: Aminoterminated PNIPAAm oligomers (Group of Samples A ($Mw(Graft)_{(THEO)}$ = 5,000 g/mol)) 228

Table 65. DSC (Dry) Measurements: Aminoterminated PNIPAAm oligomers (Group of Samples A ($Mw_{(THEO)}$ = 7,000 g/mol)) 228
Table 66. DSC (Dry) Measurements: Aminoterminated PNIPAAm oligomers (Group of Samples C ($Mw_{(THEO)}$ = 9,000 g/mol)) 229
Table 67. DSC (Aqueous) Measurements in water: Aminoterminated PNIPAAm oligomers (Group of Samples A ($Mw(Graft)_{(THEO)}$ = 5,000 g/mol)) 231
Table 68. DSC (Aqueous) Measurements in water: Aminoterminated PNIPAAm oligomers (Group of Samples A ($Mw(Graft)_{(THEO)}$ = 7,000 g/mol)) 232
Table 69. DSC (Aqueous) Measurements in water: Aminoterminated PNIPAAm oligomers (Group of Samples C ($Mw(Graft)_{(THEO)}$ = 9,000 g/mol)) 233
Table 70. FTIR Measurements: CMC-g-PNIPAAm graft copolymers (Group of Samples A ($Mw(Graft)_{(THEO)}$ = 5,000 g/mol)) 236
Table 71. FTIR Measurements: CMC-g-PNIPAAm graft copolymers (Group of Samples B ($Mw(Graft)_{(THEO)}$ = 7,000 g/mol)) 241
Table 72. FTIR Measurements: CMC-g-PNIPAAm graft copolymers (Group of Samples C ($Mw(Graft)_{(THEO)}$ = 9,000 g/mol)) 244
Table 73. DSC (Dry) Measurements: CMC-g-PNIPAAm graft copolymers (Group of Samples A ($Mw(Graft)_{(THEO)}$ = 5,000 g/mol)) 247
Table 74. DSC (Dry) Measurements: CMC-g-PNIPAAm graft copolymers (Group of Samples B ($Mw(Graft)_{(THEO)}$ = 7,000 g/mol)) 249
Table 75. DSC (Dry) Measurements: CMC-g-PNIPAAm graft copolymers (Group of Samples C ($Mw(Graft)_{(THEO)}$ = 9,000 g/mol)) 250
Table 76. DSC (Aqueous) Measurements in water: CMC-g-PNIPAAm graft copolymers (Group of Samples A ($Mw(Graft)_{(THEO)}$ = 5,000 g/mol)) 252
Table 77. DSC (Aqueous) Measurements in water: CMC-g-PNIPAAm graft copolymers (Group of Samples B ($Mw(Graft)_{(THEO)}$ = 7,000 g/mol)) 254
Table 78. DSC (Aqueous) Measurements in water: CMC-g-PNIPAAm graft copolymers (Group of Samples C ($Mw(Graft)_{(THEO)}$ = 9,000 g/mol)) 255
Table 79. DSC (Aqueous) Measurements in buffer solutions: CMC-g-PNIPAAm graft copolymers (Group of Samples A ($Mw(Graft)_{(THEO)}$ = 5,000 g/mol)) 256
Table 80. DSC (Aqueous) Measurements in buffer solutions: CMC-g-PNIPAAm graft copolymers (Group of Samples B ($Mw(Graft)_{(THEO)}$ = 7,000 g/mol)) 261
Table 81. DSC (Aqueous) Measurements in buffer solutions: CMC-g-PNIPAAm graft copolymers (Group of Samples C ($Mw(Graft)_{(THEO)}$ = 9,000 g/mol)). 264
Table 82. FTIR Measurements: CMC-g-PNIPAAm comb-type graft hydrogels (Group of Samples: Crosslinked with citric acid) 267

Table 83. Equilibrium Swelling Ratio Data (Part 1): Weight measurements from dried and swelled hydrogels in water 267
Table 84. Equilibrium Swelling Ratio Data (Part 2): Swelling degree measurements from dried and swelled hydrogels in water 268
Table 85. Equilibrium Temperature-Responsive Swelling Behavior (Part 1): Weight measurements from dried and swelled hydrogels in water at 80 °C 268
Table 86. Equilibrium Temperature-Responsive Swelling Behavior (Part 2): Swelling degree measurements from swelled hydrogels in water at 80 °C 269
Table 87. Equilibrium Temperature-Responsive Swelling Behavior (Part 1): Weight measurements from dried and swelled hydrogels in buffer pH=3 at 80 °C 269
Table 88. Equilibrium Temperature-Responsive Swelling Behavior (Part 2): Swelling degree measurements from swelled hydrogels in buffer pH=3 at 80 °C. 270
Table 89. Pulsatile Temperature-Responsive Swelling Behavior (Part 1): Weight measurements from dried and swelled hydrogels in water at 4 and 80 °C 270
Table 90. Pulsatile Temperature-Responsive Swelling Behavior (Part 2): Swelling degree measurements from swelled hydrogels in water at 4 and 80 °C 271
Table 91. Pulsatile Temperature-Responsive Swelling Behavior (Part 1): Weight measurements from dried and swelled hydrogels in buffer pH=3 at 4 and 80 °C 271
Table 92. Pulsatile Temperature-Responsive Swelling Behavior (Part 2): Swelling degree measurements from swelled hydrogels in buffer pH=3 at 4 and 80 °C 272
Table 93. FTIR Measurements: Functionalization of PA6 substrates (Group of Substrates: “Concentrated Acidic Hydrolysis” NH_2 Production Method) 272
Table 94. FTIR Measurements: Functionalization of PA6 substrates (Group of Substrates: “Aqueous Hydrolysis” NH_2 Production Method) 273
Table 95. FTIR Measurements: Functionalization of PA6 substrates (Group of Substrates: “Diluted Acidic Hydrolysis” NH_2 Production Method) 274
Table 96. FTIR Measurements: Bilayer actuators based on CMC-g-PNIPAAm comb-type graft hydrogel films on PA6 substrates (Group of Samples: Substrate CCH-C3(8)BI-PA6(1a)) 275
Table 97. FTIR Measurements: Bilayer actuators based on CMC-g-PNIPAAm comb-type graft hydrogel films on PA6 substrates (Group of Samples: Substrate CCH-C3(8)BI-PA6(1b)) 275
Table 98. FTIR Measurements: Bilayer actuators based on CMC-g-PNIPAAm comb-type graft hydrogel films on PA6 substrates (Group of Samples: Substrate CCH-C3(8)BI-PA6(2a)) 276

Table 99. FTIR Measurements: Bilayer actuators based on CMC-g-PNIPAAm comb-type graft hydrogel films on PA6 substrates (Group of Samples: Substrate CCH-C3(8)BI-PA6(2b)) 276
Table 100. FTIR Measurements: Bilayer actuators based on CMC-g-PNIPAAm comb-type graft hydrogel films on PA6 substrates (Group of Samples: Substrate CCH-C3(8)BI-PA6(3a)) 277
Table 101. FTIR Measurements: Bilayer actuators based on CMC-g-PNIPAAm comb-type graft hydrogel films on PA6 substrates (Group of Samples: Substrate CCH-C3(8)BI-PA6(3b)) 277
Table 102. FTIR Measurements: Bilayer actuators based on CMC-g-PNIPAAm comb-type graft hydrogel films on PA6 substrates (Group of Samples: Substrate CCH-C3(8)BI-PA6(3b.2)) 278
Table 103. FTIR Measurements: Bilayer actuators based on CMC-g-PNIPAAm comb-type graft hydrogel films on PA6 substrates (Group of Samples: Substrate PA6) 278
Table 104. Standardsized gyration angle (|θ|) versus active layer of bilayer actuators based on CMC-g-PNIPAAm comb-type graft hydrogel films on PA6 substrates (Group of Samples: Substrate CCH-C3(8)BI-PA6(1a))..... 279
Table 105. Standardsized gyration angle (|θ|) versus active layer of bilayer actuators based on CMC-g-PNIPAAm comb-type graft hydrogel films on PA6 substrates (Group of Samples: Substrate CCH-C3(8)BI-PA6(1b)) 280
Table 106. Standardsized gyration angle (|θ|) versus active layer of bilayer actuators based on CMC-g-PNIPAAm comb-type graft hydrogel films on PA6 substrates (Group of Samples: Substrate CCH-C3(8)BI-PA6(2a)) 281
Table 107. Standardsized gyration angle (|θ|) versus active layer of bilayer actuators based on CMC-g-PNIPAAm comb-type graft hydrogel films on PA6 substrates (Group of Samples: Substrate CCH-C3(8)BI-PA6(2b)) 282
Table 108. Standardsized gyration angle (|θ|) versus active layer of bilayer actuators based on CMC-g-PNIPAAm comb-type graft hydrogel films on PA6 substrates (Group of Samples: Substrate CCH-C3(8)BI-PA6(3a)) 283
Table 109. Standardsized gyration angle (|θ|) versus active layer of bilayer actuators based on CMC-g-PNIPAAm comb-type graft hydrogel films on PA6 substrates (Group of Samples: Substrate CCH-C3(8)BI-PA6(3b)) 284
Table 110. Standardsized gyration angle (|θ|) versus active layer of bilayer actuators based on CMC-g-PNIPAAm comb-type graft hydrogel films on PA6 substrates (Group of Samples: Substrate CCH-C3(8)BI-PA6(3b).2) 285
Table 111. Gyration Angle (θ) vs Time (Sample: CCH-C3(8)BI-56) 286

Table 112. Elemental Analysis: Aminoterminated PNIPAAm oligomers Experimental Data - Part 1: Experimental weight percentages (%W) (Group of Samples A ($Mw_{(THEO)}$ = 5,000 g/mol)) 288
Table 113. Elemental Analysis: Aminoterminated PNIPAAm oligomers Experimental Data - Part 1: Experimental weight percentages (%W) (Group of Samples B ($Mw_{(THEO)}$ = 7,000 g/mol)) 290
Table 114. Elemental Analysis: Aminoterminated PNIPAAm oligomers Experimental Data - Part 1: Experimental weight percentages (%W) (Group of Samples C ($Mw_{(THEO)}$ = 9,000 g/mol)) 291
Table 115. Elemental Analysis: Aminoterminated PNIPAAm oligomers Experimental Data - Part 2: Experimental weights (Group of Samples A ($Mw_{(THEO)}$ = 5,000 g/mol)) 294
Table 116. Elemental Analysis: Aminoterminated PNIPAAm oligomers Experimental Data - Part 2: Experimental weights (Group of Samples B ($Mw_{(THEO)}$ = 7,000 g/mol)) 296
Table 117. Elemental Analysis: Aminoterminated PNIPAAm oligomers Experimental Data - Part 2: Experimental weights (Group of Samples C ($Mw_{(THEO)}$ = 9,000 g/mol)) 397
Table 118. Elemental Analysis: Aminoterminated PNIPAAm oligomers Experimental Data - Part 3: Experimental moles (mol_{exp}) (Group of Samples A ($Mw_{(THEO)}$ = 5,000 g/mol)) 300
Table 119. Elemental Analysis: Aminoterminated PNIPAAm oligomers Experimental Data - Part 3: Experimental moles (mol_{exp}) (Group of Samples B ($Mw_{(THEO)}$ = 7,000 g/mol)) 302
Table 120. Elemental Analysis: Aminoterminated PNIPAAm oligomers Experimental Data - Part 3: Experimental moles (mol_{exp}) (Group of Samples C ($Mw_{(THEO)}$ = 9,000 g/mol)) 303
Table 121. Elemental Analysis: Aminoterminated PNIPAAm oligomers Experimental Data - Part 4: Average experimental moles (mol_{avg}) (Group of Samples A ($Mw_{(THEO)}$ = 5,000 g/mol)) 306
Table 122. Elemental Analysis: Aminoterminated PNIPAAm oligomers Experimental Data - Part 4: Average experimental moles (mol_{avg}) (Group of Samples B ($Mw_{(THEO)}$ = 7,000 g/mol))..... 306
Table 123. Elemental Analysis: Aminoterminated PNIPAAm oligomers Experimental Data - Part 4: Average experimental moles (mol_{avg}) (Group of Samples C ($Mw_{(THEO)}$ = 9,000 g/mol)) 307
Table 124. Elemental Analysis: Aminoterminated PNIPAAm oligomers

Experimental Data - Part 5: Experimental mol percentages ($\%mol_{exp}$) 307
Table 125. Elemental Analysis: Aminoterminated PNIPAAm oligomers
Experimental Data - Part 5: Experimental mol percentages ($\%mol_{exp}$) (Group of Samples B ($Mw_{(THEO)}$ = 7,000 g/mol)) 308
Table 126. Elemental Analysis: Aminoterminated PNIPAAm oligomers
Experimental Data - Part 5: Experimental mol percentages ($\%mol_{exp}$) (Group of Samples C ($Mw_{(THEO)}$ = 9,000 g/mol)) 308
Table 127. Elemental Analysis: Aminoterminated PNIPAAm oligomers
Theoretical Data - Part 1: Theoretical moles (mol_{theo}) (Group of Samples A ($Mw_{(THEO)}$ = 5,000 g/mol)) 309
Table 128. Elemental Analysis: Aminoterminated PNIPAAm oligomers
Theoretical Data - Part 1: Theoretical moles (mol_{theo}) (Group of Samples B ($Mw_{(THEO)}$ = 7,000 g/mol)) 310
Table 129. Elemental Analysis: Aminoterminated PNIPAAm oligomers
Theoretical Data - Part 1: Theoretical moles (mol_{theo}) (Group of Samples C ($Mw_{(THEO)}$ = 9,000 g/mol)) 311
Table 130. Elemental Analysis: Aminoterminated PNIPAAm oligomers Theoretical Data - Part 2: Theoretical mol percentages ($\%mol_{theo}$) (Group of Samples A ($Mw_{(THEO)}$ = 5,000 g/mol)) 312
Table 131. Elemental Analysis: Aminoterminated PNIPAAm oligomers Theoretical Data - Part 2: Theoretical mol percentages ($\%mol_{theo}$) (Group of Samples B ($Mw_{(THEO)}$ = 7,000 g/mol)) 312
Table 132. Elemental Analysis: Aminoterminated PNIPAAm oligomers
Theoretical Data - Part 2: Theoretical mol percentages ($\%mol_{theo}$) (Group of Samples C ($Mw_{(THEO)}$ = 9,000 g/mol)) 313
Table 133. Elemental Analysis: CMC-g-PNIPAAm graft copolymers
Experimental Data - Part 1: Experimental weight percentages of N (%W - N) (Group of Samples A ($Mw(Graft)_{(THEO)}$ = 5,000 g/mol)) 314
Table 134. Elemental Analysis: CMC-g-PNIPAAm graft copolymers
Experimental Data - Part 1: Experimental weight percentages of N (%W-N) (Group of Samples B ($Mw(Graft)_{(THEO)}$ = 7,000 g/mol)) 317
Table 135. Elemental Analysis: CMC-g-PNIPAAm graft copolymers
Experimental Data - Part 1: Experimental weight percentages of N (%W-N) (Group of Samples C ($Mw(Graft)_{(THEO)}$ = 9,000 g/mol)) 320
Table 136. Elemental Analysis: CMC-g-PNIPAAm graft copolymers
Experimental Data - Part 2: Average experimental weight percentage of N ($\%W_{avg}$ - N) (Group of Samples A ($Mw(Graft)_{(THEO)}$ = 5,000 g/mol)) 323

Table 137. Elemental Analysis: CMC-g-PNIPAAm graft copolymers Experimental Data - Part 2: Average experimental weight percentage of N (%W_{avg} - N) (Group of Samples B (Mw(Graft)$_{(THEO)}$ = 7,000 g/mol)) 324
Table 138. Elemental Analysis: CMC-g-PNIPAAm graft copolymers Experimental Data - Part 2: Average experimental weight percentage of N (%W_{avg} - N) (Group of Samples C (Mw(Graft)$_{(THEO)}$ = 9,000 g/mol)) 325
Table 139. Elemental Analysis: CMC-g-PNIPAAm graft copolymers Experimental Data - Part 3: Degree of substitution of PNIPAAm grafts per anhydroglucose unit (AGU) in CMC (DS) (Group of Samples A (Mw(Graft)$_{(THEO)}$ = 5,000 g/mol)) 326
Table 140. Elemental Analysis: CMC-g-PNIPAAm graft copolymers Experimental Data - Part 3: Degree of substitution of PNIPAAm grafts per anhydroglucose unit (AGU) in CMC (DS) (Group of Samples B (Mw(Graft)$_{(THEO)}$ = 7,000 g/mol)) 328
Table 141. Elemental Analysis: CMC-g-PNIPAAm graft copolymers Experimental Data - Part 3: Degree of substitution of PNIPAAm grafts per anhydroglucose unit (AGU) in CMC (DS) (Group of Samples C (Mw(Graft)$_{(THEO)}$ = 9,000 g/mol)) 330

9. Appendix I: Protocols

9.1. Elemental analysis protocol

For determination of molecular weight and degree of polymerization for aminoterminated PNIPAAm oligomers, the following procedure was followed:

a) First, experimental mol values (mol_{exp}) of O, N, C, H and S were calculated from the measured experimental weight percentages of O, N, C, H and S:

Example: Sample CCH-A15-1 ($Mw_{(THEO)}$ = 5,000 g/mol)

Sample CCH-A15-1 was measured twice with the replicas CCH-A15-1a and CCH-A15-1b (Table 27): (Detailed measurement data from this and other samples (and their replicas) are listed in Tables 113, 114 and 115 at Appendix II (See section 12. Appendix II: Tables)).

Table 27

Elemental Analysis: Aminoterminated PNIPAAm oligomers

Experimental Data - Part 1: Experimental weight percentages (%W)

(Sample CCH-A15-1)

Sample	Replica	Weight (g)	% W – O (%)	% W – N (%)	% W – C (%)	% W – H (%)	% W – S (%)
CCH-A15-1	CCH-A15-1a	2.0750	16.347	11.556	59.759	9.812	0.114
	CCH-A15-1b	2.1080	16.563	11.467	58.890	9.750	0.089

Where:

Weight : Weight of sample (or replica)

% W – O: Experimental weight percentage of O, measured by elemental analysis.

% W – N: Experimental weight percentage of N, measured by elemental analysis.

% W – C: Experimental weight percentage of C, measured by elemental analysis.

% W – H: Experimental weight percentage of H, measured by elemental analysis.

% W – S: Experimental weight percentage of S, measured by elemental analysis.

From these values and the weight of each replica, experimental weights of O, N, C, H and S were calculated (Table 28): (Detailed measurement data from this and other samples (and their replicas) are listed in Tables 116, 117 and 118 at Appendix II (See section 12. Appendix II: Tables)).

Table 28

Elemental Analysis: Aminoterminated PNIPAAm oligomers

Experimental Data - Part 2: Experimental weights

(Sample CCH-A15-1)

Sample	Replica	Weight (g)	Weight – O (g)	Weight – N (g)	Weight – C (g)	Weight – H (g)	Weight – S (g)
CCH-A15-1	CCH-A15-1a	2.0750	0.3392	0.2398	1.2400	0.2036	0.0024
	CCH-A15-1b	2.1080	0.3491	0.2417	1.2414	0.2055	0.0019

Where:

Weight : Weight of sample (or replica)

Weight – O: Experimental weight of O.

Weight – N: Experimental weight of N.

Weight – C: Experimental weight of C.

Weight – H: Experimental weight of H.

Weight – S: Experimental weight of S.

Detailed calculation:

For CCH-A15-1a:

Weight – O = % W – O x Weight = 16.347% x 2.0750 g = 0.3392 g

Weight – N = % W – N x Weight = 11.556% x 2.0750 g = 0.2398 g

Weight – C = % W – C x Weight = 59.759% x 2.0750 g = 1.2400 g

Weight – H = % W – H x Weight = 9.812% x 2.0750 g = 0.2036 g

Weight – S = % W – S x Weight = 0.114% x 2.0750 g = 0.0024 g

For CCH-A15-1b:

Weight – O = % W – O x Weight = 16.563% x 2.1080 g = 0.3491 g

Weight – N = % W – N x Weight = 11.467% x 2.1080 g = 0.2417 g

Weight – C = % W – C x Weight = 58.890% x 2.1080 g = 1.2414 g

Weight – H = % W – H x Weight = 9.750% x 2.1080 g = 0.2055 g

Weight – S = % W – S x Weight = 0.089% x 2.1080 g = 0.0019 g

With the calculated experimental weights and molecular weights of 15.999 g/mol for O, 14.007 g/mol for N, 12.011 g/mol for C, 1.008 g/mol for H and 32.060 g/mol for S, experimental moles (mol_{exp}) of O, N, C, H and S were calculated (Table 29): (Detailed measurement data from this

and other samples (and their replicas) are listed in Tables 119, 120 and 121 at Appendix II (See section 12. Appendix II: Tables)).

Table 29

Elemental Analysis: Aminoterminated PNIPAAm oligomers

Experimental Data - Part 3: Experimental moles (mol_{exp})

(Sample CCH-A15-1)

Sample	Replica	mol_{exp} – O (mol)	mol_{exp} – N (mol)	mol_{exp} – C (mol)	mol_{exp} – H (mol)	mol_{exp} – S (mol)
CCH-A15-1	CCH-A15-1a	0.0212	0.0171	0.1032	0.2020	$7.38x10^{-5}$
	CCH-A15-1b	0.0218	0.0173	0.1034	0.2039	$5.85x10^{-5}$

Where:

mol_{exp} – O: Experimental moles of O.

mol_{exp} – N: Experimental moles of N.

mol_{exp} – C: Experimental moles of C.

mol_{exp} – H: Experimental moles of H.

mol_{exp} – S: Experimental moles of S.

Detailed calculation:

For CCH-A15-1a:

mol_{exp} – O = Weight – O / 15.999 g/mol = 0.3392 g / 15.999 g/mol = 0.0212 mol

mol_{exp} – N = Weight – N / 14.007 g/mol = 0.2398 g / 14.007 g/mol = 0.0171 mol

mol_{exp} – C = Weight – C / 12.011 g/mol = 1.2400 g / 12.011 g/mol = 0.1032 mol

mol_{exp} – H = Weight – H / 1.008 g/mol = 0.2036 g / 1.008 g/mol = 0.2020 mol

mol_{exp} – S = Weight – S / 32.060 g/mol = 0.0024 g / 32.060 g/mol = $7.38x10^{-5}$ mol

For CCH-A15-1b:

mol_{exp} – O = Weight – O / 15.999 g/mol = 0.3491 g / 15.999 g/mol = 0.0218 mol

mol_{exp} – N = Weight – N / 14.007 g/mol = 0.2417 g / 14.007 g/mol = 0.0173 mol

mol_{exp} – C = Weight – C / 12.011 g/mol = 1.2414 g / 12.011 g/mol = 0.1034 mol

mol_{exp} – H = Weight – H / 1.008 g/mol = 0.2055 g / 1.008 g/mol = 0.2039 mol

mol_{exp} – S = Weight – S / 32.060 g/mol = 0.0019 g / 32.060 g/mol = $5.85x10^{-5}$ mol

Then with these experimental moles, average experimental moles (mol_{avg}) for each sample were calculated (Table 30): (Detailed measurement data from this and other samples are listed in Tables 122, 123 and 124 at Appendix II (See section 12. Appendix II: Tables)).

Table 30

Elemental Analysis: Aminoterminated PNIPAAm oligomers

Experimental Data - Part 4: Average experimental moles (mol_{avg})

(Sample CCH-A15-1)

Sample	mol_{avg} – O (mol)	mol_{avg} – N (mol)	mol_{avg} – C (mol)	mol_{avg} – H (mol)	mol_{avg} – S (mol)
CCH-A15-1	0.0215	0.0172	0.1033	0.2029	$6.62x10^{-5}$

Where:

mol_{avg} – O: Average experimental moles of O.

mol_{avg} – N: Average experimental moles of N.

mol_{avg} – C: Average experimental moles of C.

mol_{avg} – H: Average experimental moles of H.

mol_{avg} – S: Average experimental moles of S.

Detailed calculation:

For CCH-A15-1:

$mol_{avg} - O = [(mol_{exp} - O)_{CCH\text{-}A15\text{-}1a} + (mol_{exp} - O)_{CCH\text{-}A15\text{-}1b}] / 2$

$mol_{avg} - O = [0.0212 \text{ mol} + 0.0218 \text{ mol}] / 2$

$\boxed{mol_{avg} - O = 0.0215 \text{ mol}}$

$mol_{avg} - N = [(mol_{exp} - N)_{CCH\text{-}A15\text{-}1a} + (mol_{exp} - N)_{CCH\text{-}A15\text{-}1b}] / 2$

$mol_{avg} - N = [0.0171 \text{ mol} + 0.0173 \text{ mol}] / 2$

$\boxed{mol_{avg} - N = 0.0172 \text{ mol}}$

$mol_{avg} - C = [(mol_{exp} - C)_{CCH\text{-}A15\text{-}1a} + (mol_{exp} - C)_{CCH\text{-}A15\text{-}1b}] / 2$

$mol_{avg} - C = [0.1032 \text{ mol} + 0.1034 \text{ mol}] / 2$

$\boxed{mol_{avg} - C = 0.1033 \text{ mol}}$

$mol_{avg} - H = [(mol_{exp} - H)_{CCH\text{-}A15\text{-}1a} + (mol_{exp} - H)_{CCH\text{-}A15\text{-}1b}] / 2$

$mol_{avg} - H = [0.2020 \text{ mol} + 0.2039 \text{ mol}] / 2$

$\boxed{mol_{avg} - H = 0.2029 \text{ mol}}$

$mol_{avg} - S = [(mol_{exp} - S)_{CCH\text{-}A15\text{-}1a} + (mol_{exp} - S)_{CCH\text{-}A15\text{-}1b}] / 2$

$mol_{avg} - S = [7.38x10^{-05} \text{ mol} + 5.85x10^{-05} \text{ mol}] / 2$

$\boxed{mol_{avg} - S = 6.62x10^{-05} \text{ mol}}$

b) Second, from the obtained average experimental moles, experimental mol percentages ($\%mol_{exp}$) of O, N, C, H and S were calculated (Table 31). (Complete data from this and other samples are listed in Tables 125, 126 and 127 at Appendix II (See section 12. Appendix II: Tables)).

Example: Sample CCH-A15-1 ($Mw_{(THEO)}$ = 5,000 g/mol)

Table 31

Elemental Analysis: Aminoterminated PNIPAAm oligomers

Experimental Data - Part 5: Experimental mol percentages ($\%mol_{exp}$)

(Sample CCH-A15-1)

Sample	$\%mol_{exp}$–O (mol)	$\%mol_{exp}$–N (mol)	$\%mol_{exp}$–C (mol)	$\%mol_{exp}$–H (mol)	$\%mol_{exp}$–S (mol)
CCH-A15-1	6.2353	4.9820	29.9408	58.8227	0.0192

Where

$\%mol_{exp}$–O: Experimental mol percentage of O.

$\%mol_{exp}$–N: Experimental mol percentage of N.

$\%mol_{exp}$–C: Experimental mol percentage of C.

$\%mol_{exp}$–H: Experimental mol percentage of H.

$\%mol_{exp}$–S: Experimental mol percentage of S.

Detailed calculation:

For CCH-A15-1:

$$\%mol_{exp}\text{–}O = [(mol_{avg} - O)/(mol_{avg} - O + mol_{avg} - N + mol_{avg} - C + mol_{avg} - H + mol_{avg} - S)]x100$$

$$\%mol_{exp}\text{–}O = [(0.0212mol)/(0.0215mol+0.0172mol+0.1033mol+0.2029mol +6.62x10^{-05}mol)]x100$$

$$\boxed{\%mol_{exp}\text{–}O = 6.2353\ \%}$$

$$\%mol_{exp}\text{–}N = [(mol_{avg} - N)/(mol_{avg} - O + mol_{avg} - N + mol_{avg} - C + mol_{avg} - H + mol_{avg} - S)]x100$$

$$\%mol_{exp}\text{–}N = [(0.0212mol)/(0.0215mol+0.0172mol+0.1033mol+0.2029mol +6.62x10^{-05}mol)]x100$$

$$\boxed{\%mol_{exp}\text{–}N = 4.9820\ \%}$$

$$\%mol_{exp}\text{–}C = [(mol_{avg} - C)/(mol_{avg} - O + mol_{avg} - N + mol_{avg} - C + mol_{avg} - H + mol_{avg} - S)]x100$$

$\%mol_{exp}–C = [(0.0212mol)/(0.0215mol+0.0172mol+0.1033mol+0.2029mol +6.62x10^{-05}mol)]x100$

$\boxed{\%mol_{exp}–C = 29.9408\ \%}$

$\%mol_{exp}–H = [(mol_{avg} – H)/(mol_{avg} – O + mol_{avg} – N + mol_{avg} – C + mol_{avg} – H + mol_{avg} – S)]x100$

$\%mol_{exp}–H = [(0.0212mol)/(0.0215mol+0.0172mol+0.1033mol+0.2029mol +6.62x10^{-05}mol)]x100$

$\boxed{\%mol_{exp}–H = 58.8227\ \%}$

$\%mol_{exp}–S = [(mol_{avg} – S)/(mol_{avg} – O + mol_{avg} – N + mol_{avg} – C + mol_{avg} – H + mol_{avg} – S)]x100$

$\%mol_{exp}–S = [(0.0212mol)/(0.0215mol+0.0172mol+0.1033mol+0.2029mol +6.62x10^{-05}mol)]x100$

$\boxed{\%mol_{exp}–S = 1.92x10^{-02}\ \%}$

c) Third, based on a theoretical structural formula of an aminoterminated PNIPAAm oligomer and the theoretical molecular weights (5,000, 7,000 and 9,000 g/mol) used for the oligomer synthesis, theoretical number of atoms or mol values (mol_{theo}) of O, N, C, H, S and the oligomer were calculated.

Example: Sample CCH-A15-1 ($Mw_{(THEO)}$ = 5,000 g/mol)

The aminoterminated PNIPAAm oligomer hat the following structural formula:

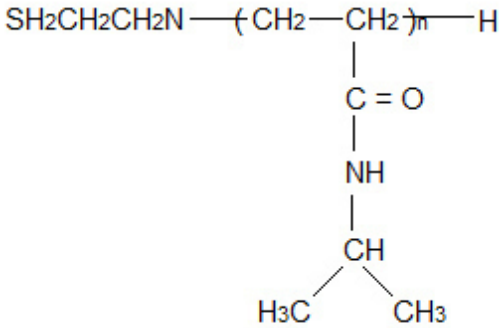

Figure 92. Molecular structure of aminoterminated PNIPAAm

From this formula we can obtain the global formula:

$\boxed{C_{6n+2}H_{11n+7}N_{n+1}SO_n}$

With the global formula, the molecular weights of 5,000 g/mol for CCH-A15-1, 15.999 g/mol for O, 14.007 g/mol for N, 12.011 g/mol for C, 1.008 g/mol for H and 32.060 g/mol for S, the theoretical degree of polymerization (n) was calculated:

$$5{,}000 = (n)x15.999 + (n+1)x14.007 + (6n+2)x12.011 + (11n+7)x1.008 + (1)x32.060$$

$$\boxed{n = 45}$$

d) Then, with the calculated n value, the theoretical moles (mol_{theo}) for the atoms and the oligomer for this sample were calculated (Table 32): (Complete data from this and other samples are listed in Tables 128, 129 and 130 at Appendix II (See section 12. Appendix II: Tables)).

Example: Sample CCH-A15-1 ($Mw_{(THEO)}$ = 5,000 g/mol)

Table 32

Elemental Analysis: Aminoterminated PNIPAAm oligomers

Theoretical Data - Part 1: Theoretical moles (mol_{theo})

(Sample CCH-A15-1)

Sample	mol_{theo} – olig. (mol)	mol_{theo} - O (mol)	mol_{theo} - N (mol)	mol_{theo} - C (mol)	mol_{theo} - H (mol)	mol_{theo} - S (mol)
CCH-A15-1	866	45	46	272	502	1

Where:

mol_{theo} – olig.: Theoretical moles of the oligomer.

mol_{theo} – O: Theoretical moles of O.

mol_{theo} – N: Theoretical moles of N.

mol_{theo} – C: Theoretical moles of C.

mol_{theo} – H: Theoretical moles of H.

mol_{theo} – S: Theoretical moles of S.

Detailed calculation:

For CCH-A15-1: (n=45)

mol_{theo} – olig. = (mol_{theo} – O) + (mol_{theo} – N) + (mol_{theo} – C) + (mol_{theo} – H) + (mol_{theo} – S)

mol_{theo} – olig. = (n) + (n+1) + (6n+2) + (11n+7) + (1)

mol_{theo} – olig. = (45) + (45+1) + (6x45+2) + (11x45+7) + (1)

$\boxed{mol_{theo} \text{ – olig. = 866 moles}}$

mol_{theo} – O = (n)

mol_{theo} – O = 45 moles

mol_{theo} – N = (n+1)

mol_{theo} – N = (45+1)

mol_{theo} – N = 46 moles

mol_{theo} – C = (6n+2)

mol_{theo} – C = (6x45+2)

mol_{theo} – C = 272 moles

mol_{theo} – H = (11n+7)

mol_{theo} – H = (11x45+7)

mol_{theo} – H = 502 moles

mol_{theo} – S = (1)

mol_{theo} – S = 1 mol

e) Fourth, from the theoretical moles, theoretical mol percentages ($\%mol_{theo}$) of O, N, C, H and S were calculated (Table 33): (Complete data from this and other samples are listed in Tables 131, 132 and 133 at Appendix II (See section 12. Appendix II: Tables)).

Example: Sample CCH-A15-1 ($Mw_{(THEO)}$ = 5,000 g/mol)

Table 33

Elemental Analysis: Aminoterminated PNIPAAm oligomers

Theoretical Data - Part 2: Theoretical mol percentages ($\%mol_{theo}$)

(Sample CCH-A15-1)

Sample	$\%mol_{theo}$ – O (mol)	$\%mol_{theo}$– N (mol)	$\%mol_{theo}$– C (mol)	$\%mol_{theo}$– H (mol)	$\%mol_{theo}$ – S (mol)
CCH-A15-1	5.1963	5.3118	31.4088	57.9677	0.1155

Where

$\%mol_{theo}$ – O: Theoretical mol percentage of O.

$\%mol_{theo}$ – N: Theoretical mol percentage of N.

$\%mol_{theo}$ – C: Theoretical mol percentage of C.

$\%mol_{theo}$ – H: Theoretical mol percentage of H.

$\%mol_{theo}$ – S: Theoretical mol percentage of S.

Detailed calculation:

$\%mol_{theo} – O = [(mol_{theo} – O)/(mol_{theo} – O + mol_{theo} – N + mol_{theo} – C + mol_{theo} – H + mol_{theo} – S)] x100$

$\%mol_{theo} – O = [(45 \text{ moles})/(45 \text{ moles} + 46 \text{ moles} + 272 \text{ moles} + 502 \text{ moles} + 1 \text{ mol})] x100$

$\boxed{\%mol_{theo} – O = 5.1963 \%}$

$\%mol_{theo} – N = [(mol_{theo} – N)/(mol_{theo} – O + mol_{theo} – N + mol_{theo} – C + mol_{theo} – H + mol_{theo} – S)] x100$

$\%mol_{theo} – N = [(46 \text{ moles})/(45 \text{ moles} + 46 \text{ moles} + 272 \text{ moles} + 502 \text{ moles} + 1 \text{ mol})] x100$

$\boxed{\%mol_{theo} – N = 5.3118 \%}$

$\%mol_{theo} – C = [(mol_{theo} – C)/(mol_{theo} – O + mol_{theo} – N + mol_{theo} – C + mol_{theo} – H + mol_{theo} – S)] x100$

$\%mol_{theo} – C = [(272 \text{ moles})/(45 \text{ moles} + 46 \text{ moles} + 272 \text{ moles} + 502 \text{ moles} + 1 \text{ mol})]x100$

$\boxed{\%mol_{theo} – C = 31.4088 \%}$

$\%mol_{theo} – H = [(mol_{theo} – H)/(mol_{theo} – O + mol_{theo} – N + mol_{theo} – C + mol_{theo} – H + mol_{theo} – S)] x100$

$\%mol_{theo} – H = [(502 \text{ moles})/(45 \text{ moles} + 46 \text{ moles} + 272 \text{ moles} + 502 \text{ moles} + 1 \text{ mol})]x100$

$\boxed{\%mol_{theo} – H = 57.9677 \%}$

$\%mol_{theo} – S = [(mol_{theo} – S)/(mol_{theo} – O + mol_{theo} – N + mol_{theo} – C + mol_{theo} – H + mol_{theo} – S)] x100$

$\%mol_{theo} – S = [(1 \text{ moles})/(45 \text{ moles} + 46 \text{ moles} + 272 \text{ moles} + 502 \text{ moles} + 1 \text{ mol})] x100$

$\boxed{\%mol_{theo} – S = 0.1155 \%}$

f) Fifth, the experimental molecular weight of aminoterminated PNIPAAm oligomers were calculated from the ratio $\%mol_{exp}$:$\%mol_{theo}$, the theoretical moles mol_{theo} and molecular weights of 15.999 g/mol for O, 14.007 g/mol for N, 12.011 g/mol for C, 1.008 g/mol for H and 32.060 g/mol for S: (Complete data from this and other samples are listed in Table 19 at the Results).

Example: Sample CCH-A15-1 ($Mw_{(THEO)}$ = 5,000 g/mol)

$Mw_{(EXP)} = (\%mol_{exp} – O / \%mol_{theo} – O) x (mol_{theo} – O) x (15.999 \text{ g/mol}) + (\%mol_{exp} – N / \%mol_{theo} – N) x (mol_{theo} – N) x (14.007 \text{ g/mol})$

$+ (\%mol_{exp} - C / \%mol_{theo} - C) \times (mol_{theo} - C) \times (12.011\ g/mol)$

$+ (\%mol_{exp} - H / \%mol_{theo} - H) \times (mol_{theo} - H) \times (1.008\ g/mol)$

$+ (\%mol_{exp} - S / \%mol_{theo} - S) \times (mol_{theo} - S) \times (32.060\ g/mol)$

$Mw_{(EXP)} = (6.2353\ \% / 5.1963\ \%) \times (45) \times (15.999\ g/mol)$

$+ (4.9820\ \% / 5.3118\ \%) \times (46) \times (14.007\ g/mol)$

$+ (29.9408\ \% / 31.4088\ \%) \times (272) \times (12.011\ g/mol)$

$+ (58.8227\ \% / 57.9677\ \%) \times (502) \times (1.008\ g/mol)$

$+ (1.92 \times 10^{-2}\ \% / 0.1155\ \%) \times (1) \times (32.060\ g/mol)$

$\boxed{Mw_{(EXP)} = 5{,}101.34\ g/mol}$

g) Finally, with the global formula, the experimental molecular weight of 5,101.34 g/mol for CCH-A15-1 and the molecular weights of 15.999 g/mol for O, 14.007 g/mol for N, 12.011 g/mol for C, 1.008 g/mol for H and 32.060 g/mol for S, the experimental degree of polymerization (n_{exp} = DP(Graft)) was calculated: (Complete data from this and other samples are listed in Table 19 at the Results).

Example: Sample CCH-A15-1 ($Mw_{(THEO)}$ = 5,000 g/mol)

$5{,}101.34 = n_{exp} \times 15.999 + (n_{exp}+1) \times 14.007 + (6n_{exp}+2) \times 12.011 + (11n_{exp}+7) \times 1.008$

$+ (1) \times 32.060$

$5{,}101.34 = 15.999n_{exp} + 14.007n_{exp} + 14.007 + 72.066n_{exp} + 24.022 + 11.088n_{exp} + 7.616$

$+ 32.060$

$5{,}101.34 = 113.16n_{exp} + 77.705$

$n_{exp} = (5{,}101.34 - 77.705)/113.16$

$\boxed{n_{exp} = 44.39 = DP(Graft)}$

For determination of molecular weight and degree of polymerization for CMC-g-PNIPAAm graft copolymers, the following procedure was followed:

First, degree of substitution (DS) of PNIPAAm grafts per anhydroglucose unit (AGU) in CMC was estimated with the following equation:

$$DS = (n)(d.s_1)$$

Where:

n = Degree of substitution of the carboxymethyl groups in the cellulose polymer

$d.s_1$ = Degree of substitution of PNIPAAm grafts per carboxymethyl group saturated anhydroglucose unit in CMC.

n has a value of 0.9 for CMC with molecular weight of 700,000 g/mol and a value of 0.7 for CMC with molecular weight of 90,000 g/mol.

The degree of substitution ($d.s_1$) was calculated by using a correlation formulated by Touzinsky et al. (1979):

$$\frac{PC_1}{100} = \frac{(d.s_1)(MW_1)(N_1)}{(MWU) + (d.s_1)(MWG_1)}$$

Where:

$d.s_1$: Degree of substitution of substituent group 1

PC_1: Weight percent of measurable component in substituent group 1

MW_1: Molecular weight of the measured component

N_1: Number of measurable components in the substituent

MWU: Molecular weight of the basic repeating-unit, the glucosyl residue

MWG_1: Molecular weight added for each substituent group

Example: Sample CCH-A27-1

Sample CCH-A27-1 is a CMC ($Mw_{(THEO)}$ = 700,000 g/mol) grafted with the PNIPAAm graft oligomers CCH-A15-1 ($Mw_{(THEO)}$ = 5,000 g/mol). The experimental molecular weight of the grafts was previously estimated with elemental analysis ($Mw_{(EXP)}$ = 5,101.34 g/mol). For the $d.s_1$ calculation the experimental molecular weight value will be used.

The degree of substitution ($d.s_1$) will be calculated from the correlation proposed by Touzinsky et al. (1979):

$$\frac{PC_1}{100} = \frac{(d.s_1)(MW_1)(N_1)}{(MWU) + (d.s_1)(MWG_1)}$$

$$PC_1(MWU) + PC_1(d.s_1)(MWG_1) = 100(d.s_1)(MW_1)(N_1)$$

$$PC_1(MWU) = 100(d.s_1)(MW_1)(N_1) - PC_1(d.s_1)(MWG_1)$$

$$d.s_1 = \frac{PC_1(MWU)}{100(MW_1)(N_1) - PC_1(MWG_1)}$$

PC_1, the weight percentage of N (from the PNIPAAm grafts), will be taken as the average experimental weight percentage of N ($\%W_{avg}$ - N) from sample CCH-A27-1, calculated from its experimental weight percentages of N (%W-N), which were measured with elemental analysis

in 5 fractions: CCH-A27-1(1), CCH-A27-1(2) (with between 4 and 7 replicas), CCH-A27-1(3), CCH-A27-1(4) and CCH-A27-1(5) (Table 34): (Detailed measurement data from this and other samples (and their fractions and replicas) are listed in Tables 134, 135 and 136 at Appendix II (See section 12. Appendix II: Tables)).

Table 34

Elemental Analysis: CMC-g-PNIPAAm graft copolymers

Experimental Data - Part 1: Experimental weight percentages of N (%W - N)

(Sample CCH-A27-1)

Sample	Sample Fraction	Replica	Weight (g)	% W – N (%)
CCH-A27-1	CCH-A27-1(1)	CCH-A27-1(1)	1.2440	3.659
	CCH-A27-1(2)	CCH-A27-1(2)	1.1230	3.706
		CCH-A27-1(2).1ASE	1.7740	3.672
		CCH-A27-1(2).2ASE	1.1870	3.757
		CCH-A27-1(2).3ASE	0.5820	3.790
	CCH-A27-1(3)	CCH-A27-1(3)	1.0380	3.583
	CCH-A27-1(4)	CCH-A27-1(4)	1.4750	3.527
	CCH-A27-1(5)	CCH-A27-1(5)	1.7930	3.533

Where:

Weight : Weight of sample (or replica)

% W – N: Experimental weight percentage of N, measured by elemental analysis.

Then with these experimental weights percentages of N (%W - N), the average experimental weight percentage of N (%W_{avg} - N) from sample CCH-A27-1 was calculated (Table 35): (Detailed measurement data from this and other samples are listed in Tables 137, 138 and 139 at Appendix II (See section 12. Appendix II: Tables)).

Table 35

Elemental Analysis: CMC-g-PNIPAAm graft copolymers

Experimental Data - Part 2: Average experimental weight percentage of N (%W_{avg} - N)

(Sample CCH-A27-1)

Sample	% W_{avg} – N (%)
CCH-A27-1	3.653

Where:

% W_{avg} – N: Average experimental weight percentage of N, measured by elemental analysis.

Detailed calculation:

For sample CCH-A27-1:

$$\%\ W_{avg} - N = [(\%\ W - N)_{CCH\text{-}A27\text{-}1(1)} + (\%\ W - N)_{CCH\text{-}A27\text{-}1(2)} + (\%\ W - N)_{CCH\text{-}A27\text{-}1(2).1ASE} + (\%\ W - N)_{CCH\text{-}A27\text{-}1(2).2ASE} + (\%\ W - N)_{CCH\text{-}A27\text{-}1(2).3ASE} + (\%\ W - N)_{CCH\text{-}A27\text{-}1(3)} + (\%\ W - N)_{CCH\text{-}A27\text{-}1(4)} + (\%\ W - N)_{CCH\text{-}A27\text{-}1(5)}] / 8$$

$$\%\ W_{avg} - N = [3.659 + 3.706 + 3.672 + 3.757 + 3.790 + 3.583 + 3.527 + 3.533] / 8$$

$$\boxed{\%\ W_{avg} - N = 3.653\ \%}$$

Then:

$\boxed{PC_1 = 3.653\ \%}$ (The N atom from PNIPAAm grafts will be used as measurable component)

The rest of parameters will adopt the following values:

$\boxed{MW_1: 14.007\ g/mol}$ (Molecular weight of the N atom from PNIPAAm grafts)

$\boxed{N_1: 44\ mol}$ (Number of N atoms per PNIPAAm graft)

$\boxed{MWU: 223\ g/mol}$ (It will be assumed as basic repeating unit a carboxymethyl group saturated anhydroglucose unit).

$\boxed{MWG_1\ (=Mw(Graft)_{(EXP)}): 5{,}101.34\ g/mol}$ (Molecular weight added of the PNIPAAm graft)

(Detailed calculated data from this and other samples are listed in Tables 140, 141 and 142 at Appendix II (See section 12. Appendix II: Tables)).

And from the equation proposed by Touzinsky et al. (1979) degree of substitution ($d.s_1$) of PNIPAAm grafts per carboxymethyl group saturated anhydroglucose unit in CMC is estimated:

$$d.s_1 = \frac{PC_1(MWU)}{100(MW_1)(N_1) - PC_1(MWG_1)}$$

$$d.s_1 = \frac{(3.653)(223)}{100(14.007)(44) - 3.653(5{,}101.34)}$$

$$\boxed{d.s_1 = 0.0189}$$

(Detailed calculated data from this and other samples are listed in Tables 140, 141 and 142 at Appendix II (See section 12. Appendix II: Tables)).

Then with the value of $d.s_1$ degree of substitution (DS) of PNIPAAm grafts per anhydroglucose unit (AGU) in CMC can be calculated as follows:

$$DS = (n)(d.s_1)$$

$$DS = (0.9)(0.0189)$$

$$\boxed{DS = 0.0171}$$

(Detailed calculated data from this and other samples are listed in Tables 140, 141 and 142 at Appendix II (See section 12. Appendix II: Tables)).

Finally with the calculated degree of substitution (DS) is possible to estimate:

1) Number of Grafts per CMC Chain (N° Grafts per CMC Chain)

$$N° \text{ Grafts per CMC Chain} = (DS)(\text{Number of AGU in CMC})$$

Where:

Number of AGU in CMC = (Mw(CMC))/(Mw(AGU)) = (Mw(CMC))/192.5 g/mol

For: Mw(CMC) = 700,000 g/mol => Number of AGU in CMC = 3,636.36

For: Mw(CMC) = 90,000 g/mol => Number of AGU in CMC = 467.53

Then:

For: Mw(CMC) = 700,000 g/mol => N° Grafts per CMC Chain = (DS)(3,636.36)

For: Mw(CMC) = 90,000 g/mol => N° Grafts per CMC Chain = (DS)(467.53)

For sample CCH-A27-1:

N° Grafts per CMC Chain = (DS)(3,636.36) = (0.0171)(3,636.36)

$$\boxed{N° \text{ Grafts per CMC Chain} = 62}$$

(Detailed data from this and other samples are listed in Table 23, 24 and 25 at the Results).

2) Molecular Weight of the CMC grafted with aminoterminated PNIPAAm oligomers (Mw(Total))

$$Mw(Total) = Mw(CMC) + (N° \text{ Grafts per CMC Chain})(Mw(Graft)_{(EXP)})$$

Where:

$Mw(Graft)_{(EXP)}$ = Estimated in elemental analysis (Tables 23, 24 and 25 from Results), corresponds to the molecular weight of grafts composed of either a unique aminoterminated PNIPAAM oligomer or different aminoterminated PNIPAAm oligomers, resulting in this case grafts with a molecular weight average value.

For sample CCH-A27-1:

Backbone: CMC (Mw(CMC) = 700,000 g/mol)
Grafts: CCH-A15-1 ($Mw(Graft)_{(EXP)}$ = 5,101.34 g/mol)
N° Grafts per CMC Chain: 62

Mw(Total) = 700,000 + (62)(5,101.34)
Mw(Total) = 1'016,283 g/mol

(Detailed data from this and other samples are listed in Table 23, 24 and 25 at the Results)

3) Graft Weight Percentage per Carboxymethyl Cellulose Chain ($\%Graft_{(EXP)}$)

$$\%Graft_{(EXP)} = ((N° \text{ Grafts per CMC Chain})(Mw(Graft)_{(EXP)}))x100 / (Mw(Total))$$

For sample CCH-A27-1:

Backbone: CMC (Mw(CMC) = 700,000 g/mol)
Grafts: CCH-A15-1 ($Mw(Graft)_{(EXP)}$ = 5,101.34 g/mol)
N° Grafts per CMC Chain: 62

$\%Graft_{(EXP)}$ = ((62)(5,101.34)x100 / (1'016,283)
$\%Graft_{(EXP)}$ = 31%

(Detailed data from this and other samples are listed in Table 23, 24 and 25 at the Results)

10. Appendix II: Tables

Table 36

Buffer solutions

pH = 2 Buffer Solution ($V_{solution}$ = 250 mL)	
Ingredients:	
-0.2 M Potasium Chloride Solution.....	62.5 mL
-0.2 M HCl Solution.....	16.3 mL
-Deionized Water.....	Until 250 mL of solution was achieved
Where:	
1) 0.2 M Potasium Chloride Solution ($V_{solution}$ = 250 mL):	
-Potasium Chloride.....	3.7281 g
-Deionized Water.....	Until 250 mL of solution was achieved
2) 0.2 M HCl Solution ($V_{solution}$ = 500 mL)	
-6 M HCl.....	16.7 mL
-Deionized Water.....	Until 500 mL of solution was achieved
pH = 2,5 Buffer Solution ($V_{solution}$ = 250 mL)	
Ingredients:	
-0.1 M Potasium Hydrogen Phthalate.....	125 mL
-0.1 M HCl Solution.....	97 mL
-Deionized Water.....	Until 250 mL of solution was achieved
Where:	
1) 0.1 M Potasium Hydrogen Phthalate ($V_{solution}$ = 1 L)	
-Potasium Hydrogen Phthalate.....	20.4221 g
-Deionized Water.....	Until 1 L of solution was achieved
2) 0.1 M HCl Solution ($V_{solution}$ = 500 mL)	
-6 M HCl.....	8.3 mL
-Deionized Water.....	Until 500 mL of solution was achieved
pH = 3 Buffer Solution (Vsolution = 250 mL)	
Ingredients:	
-0.1 M Potasium Hydrogen Phthalate.....	100 mL
-0.1 M HCl Solution.....	44.6 mL
-Deionized Water.....	Until 250 mL of solution was achieved
pH = 3,5 Buffer Solution (Vsolution = 250 mL)	
Ingredients:	
-0.1 M Potasium Hydrogen Phthalate.....	125 mL
-0.1 M HCl Solution.....	20.5 mL
-Deionized Water.....	Until 250 mL of solution was achieved

Table 36

(Cont.)

pH = 7 Buffer Solution (Vsolution = 250 mL)	
Ingredients:	
-0.1 M KH_2PO_4.....	125 mL
-0.1 M NaOH Solution.....	72.75 mL
-Deionized Water.....	Until 250 mL of solution was achieved
Where:	
1) 0.1 M KH_2PO_4 (Vsolution = 1 L)	
-KH_2PO_4.....	13.6084 g
-Deionized Water.....	Until 1 L of solution was achieved
2) 0.1 M NaOH Solution (Vsolution = 1 L)	
-NaOH.....	4.0009 g
-Deionized Water.....	Until 1 L of solution was achieved
pH = 10 Buffer Solution (Vsolution = 200 mL)	
Ingredients:	
-0.05 M $NaHCO_3$.....	100 mL
-0.1 M NaOH Solution.....	21.4 mL
-Deionized Water.....	Until 200 mL of solution was achieved
Where:	
1) 0.05 M $NaHCO_3$ (Vsolution = 500 mL)	
-$NaHCO_3$.....	2.1002 g
-Deionized Water.....	Until 500 mL of solution was achieved
2) 0.1 M NaOH Solution (Vsolution = 1 L)	
-NaOH.....	4.0009 g
-Deionized Water.....	Until 1 L of solution was achieved
pH = 12 Buffer Solution (Vsolution = 200 mL)	
Ingredients:	
-0.2 M Potasium Chloride Solution.....	50 mL
-0.2 M NaOH Solution.....	12 mL
-Deionized Water.....	Until 200 mL of solution was achieved
Where:	
1) 0.2 M Potasium Chloride Solution (Vsolution = 250 mL):	
-Potasium Chloride.....	3.7281 g
-Deionized Water.....	Until 250 mL of solution was achieved
2) 0.2 M NaOH Solution (Vsolution = 500 mL)	
-NaOH.....	4.0000 g
-Deionized Water.....	Until 500 mL of solution was achieved

Table 37

Aminoterminated PNIPAAm oligomers (NH_2-PNIPAAm)

($Mw_{(THEO)}$ = 5,000 g/mol)

Reagent	Sample CCH-A15-1	
	Quantity (g or mL)	**Moles (mol)**
N-Isopropyl-acrylamide (NIPAAm)	11.3163 g	0.1 mol
Ammonium Persulfate (APS)	0.2282 g	$1.1x10^{-3}$ mol
Cysteamine Hydrochloride (AET.HCl)	0.2502 g	$2.2x10^{-3}$ mol
Millipored Water	80 mL (for NIPAAm)	4.44 mol (for NIPAAm)
	10 mL (for APS)	0.55 mol (for APS)
	10 mL (for AET.HCl)	0.55 mol (for AET.HCl)
Reagent	**Sample CCH-A15-2**	
	Quantity (g or mL)	**Quantity (g or mL)**
N-Isopropyl-acrylamide (NIPAAm)	2.8292 g	2.8292 g
Ammonium Persulfate (APS)	0.0628 g	0.0628 g
Cysteamine Hydrochloride (AET.HCl)	0.0625 g	0.0625 g
Millipored Water	20 mL (for NIPAAm)	20 mL (for NIPAAm)
	2.5 mL (for APS)	2.5 mL (for APS)
	2.5 mL (for AET.HCl)	2.5 mL (for AET.HCl)
Reagent	**Sample CCH-A15-3**	
	Quantity (g or mL)	**Moles (mol)**
N-Isopropyl-acrylamide (NIPAAm)	2.8299 g	0.025 mol
Ammonium Persulfate (APS)	0.0632 g	$2.75x10^{-4}$ mol
Cysteamine Hydrochloride (AET.HCl)	0.0628 g	$5.50x10^{-4}$ mol
Millipored Water	20 mL (for NIPAAm)	1.11 mol (for NIPAAm)
	2.5 mL (for APS)	0.14 mol (for APS)
	2.5 mL (for AET.HCl)	0.14 mol (for AET.HCl)
Reagent	**Sample CCH-C1-1**	
	Quantity (g or mL)	**Moles (mol)**
N-Isopropyl-acrylamide (NIPAAm)	8.3071 g	0.07341 mol
Ammonium Persulfate (APS)	0.1686 g	$7.39x10^{-4}$ mol
Cysteamine Hydrochloride (AET.HCl)	0.1851 g	$1.63x10^{-3}$ mol
Millipored Water	60 mL (for NIPAAm)	3.33 mol (for NIPAAm)
	10 mL (for APS)	0.55 mol (for APS)
	10 mL (for AET.HCl)	0.55 mol (for AET.HCl)
Reagent	**Sample CCH-C1(2)-1**	
	Quantity (g or mL)	**Moles (mol)**
N-Isopropylacrylamide (NIPAAm)	25.6423 g	0.2266 mol
Ammonium Persulfate (APS)	0.5088 g	$2.23x10^{-3}$ mol
Cysteamine Hydrochloride (AET.HCl)	0.5538 g	$4.87x10^{-3}$ mol
Millipored Water	181 mL (for NIPAAm)	10.05 mol (for NIPAAm)
	30 mL (for APS)	1.67 mol (for APS)
	30 mL (for AET.HCl)	1.67 mol (for AET.HCl)

Table 38

Aminoterminated PNIPAAm oligomers (NH_2-PNIPAAm)

($Mw_{(THEO)}$ = 7,000 g/mol)

Reagent	Sample CCH-B4-1	
	Quantity (g or mL)	**Moles (mol)**
N-Isopropyl-acrylamide (NIPAAm)	3.4979 g	0.03091 mol
Ammonium Persulfate (APS)	0.0571 g	2.5×10^{-4} mol
Cysteamine Hydrochloride (AET.HCl)	0.0568 g	5.0×10^{-4} mol
Millipored Water	24.7 mL (for NIPAAm)	1.37 mol (for NIPAAm)
	2.3 mL (for APS)	0.13 mol (for APS)
	2.3 mL (for AET.HCl)	0.13 mol (for AET.HCl)
Reagent	**Sample CCH-C1-2**	
	Quantity (g or mL)	**Quantity (g or mL)**
N-Isopropyl-acrylamide (NIPAAm)	8.3065 g	8.3065 g
Ammonium Persulfate (APS)	0.1375 g	0.1375 g
Cysteamine Hydrochloride (AET.HCl)	0.1361 g	0.1361 g
Millipored Water	60 mL (for NIPAAm)	60 mL (for NIPAAm)
	10 mL (for APS)	10 mL (for APS)
	10 mL (for AET.HCl)	10 mL (for AET.HCl)
Reagent	**Sample CCH-C1(2)-1**	
	Quantity (g or mL)	**Moles (mol)**
N-Isopropyl-acrylamide (NIPAAm)	25.4463 g	0.2249 mol
Ammonium Persulfate (APS)	0.4088 g	1.79×10^{-3} mol
Cysteamine Hydrochloride (AET.HCl)	0.4065 g	3.58×10^{-3} mol
Millipored Water	181 mL (for NIPAAm)	10.05 mol (for NIPAAm)
	30 mL (for APS)	1.67 mol (for APS)
	30 mL (for AET.HCl)	1.67 mol (for AET.HCl)

Table 39

Aminoterminated PNIPAAm oligomers (NH_2-PNIPAAm)

($Mw_{(THEO)}$ = 9,000 g/mol)

Reagent	Sample CCH-B4-2	
	Quantity (g or mL)	**Moles (mol)**
N-Isopropyl-acrylamide (NIPAAm)	4.5084 g	0.03977 mol
Ammonium Persulfate (APS)	0.0571 g	$2.5x10^{-4}$ mol
Cysteamine Hydrochloride (AET.HCl)	0.0569 g	$5.0x10^{-4}$ mol
Millipored Water	31.8 mL (for NIPAAm)	1.77 mol (for NIPAAm)
	2.3 mL (for APS)	0.13 mol (for APS)
	2.3 mL (for AET.HCl)	0.13 mol (for AET.HCl)
Reagent	**Sample CCH-C1-3**	
	Quantity (g or mL)	**Quantity (g or mL)**
N-Isopropyl-acrylamide (NIPAAm)	8.3184 g	8.3184 g
Ammonium Persulfate (APS)	0.1071 g	0.1071 g
Cysteamine Hydrochloride (AET.HCl)	0.1063 g	0.1063 g
Millipored Water	60 mL (for NIPAAm)	60 mL (for NIPAAm)
	10 mL (for APS)	10 mL (for APS)
	10 mL (for AET.HCl)	10 mL (for AET.HCl)
Reagent	**Sample CCH-C1(2)-3**	
	Quantity (g or mL)	**Moles (mol)**
N-Isopropyl-acrylamide (NIPAAm)	25.0663 g	0.2215 mol
Ammonium Persulfate (APS)	0.3177 g	$1.39x10^{-3}$ mol
Cysteamine Hydrochloride (AET.HCl)	0.3182 g	$2.8x10^{-3}$ mol
Millipored Water	181 mL (for NIPAAm)	10.05 mol (for NIPAAm)
	31 mL (for APS)	1.72 mol (for APS)
	31 mL (for AET.HCl)	1.72 mol (for AET.HCl)
Reagent	**Sample CCH-C1(2)-3.2**	
	Quantity (g or mL)	**Quantity (g or mL)**
N-Isopropyl-acrylamide (NIPAAm)	25.2357 g	25.2357 g
Ammonium Persulfate (APS)	0.3169 g	0.3169 g
Cysteamine Hydrochloride (AET.HCl)	0.3164 g	0.3164 g
Millipored Water	181 mL (for NIPAAm)	181 mL (for NIPAAm)
	31 mL (for APS)	31 mL (for APS)
	31 mL (for AET.HCl)	31 mL (for AET.HCl)
Reagent	**Sample CCH-C1(2)-3.3**	
	Quantity (g or mL)	**Moles (mol)**
N-Isopropylacrylamide (NIPAAm)	25.0926 g	0.2217 mol
Ammonium Persulfate (APS)	0.3174 g	$1.39x10^{-3}$ mol
Cysteamine Hydrochloride (AET.HCl)	0.3166 g	$2.8x10^{-3}$ mol
Millipored Water	181 mL (for NIPAAm)	10.05 mol (for NIPAAm)
	31 mL (for APS)	1.72 mol (for APS)
	31 mL (for AET.HCl)	1.72 mol (for AET.HCl)

Table 40

CMC-g-PNIPAAm graft copolymers

($Mw(Graft)_{(THEO)}$ = 5,000 g/mol – $\%Graft_{(THEO)}$ = 40%)

Reagent	Sample CCH-A27-1	
	Quantity (g or mL)	**Moles (mol)**
CMC (Mw = 700,000 g/mol)	2.7049 g	3.86×10^{-6} mol
NH_2-PNIPAAm	1.3515 g	2.65×10^{-4} mol
NH_2-PNIPAAm is composed by:		
Sample CCH-A15-1*	.....1.3515 g	……2.65×10^{-4} mol
TOTAL (NH_2-PNIPAAm)	……..…**1.3515 g**	……**2.65×10^{-4} mol**
EDC	0.2013 g	1.05×10^{-3} mol
Millipored Water	160 mL (for CMC)	8.89 mol (for CMC)
	35 mL (for NH_2-PNIPAAm)	1.95 mol (for NH_2-PNIPAAm)
	10 mL (for EDC)	0.55 mol (for EDC)
Reagent	**Sample CCH-C2-1.40**	
	Quantity (g or mL)	**Moles (mol)**
CMC (Mw = 90,000 g/mol)	0.4126 g	4.58×10^{-6} mol
NH_2-PNIPAAm	0.2765 g	5.37×10^{-5} mol
NH_2-PNIPAAm is composed by:		
Sample Fraction CCH-C1-1(1)*	.....0.1816 g	……3.53×10^{-5} mol
Sample Fraction CCH-C1-1(2)*	……..…0.0949 g	……1.84×10^{-5} mol
TOTAL (NH_2-PNIPAAm)	……..…**0.2765 g**	……**5.37×10^{-5} mol**
EDC	0.0417 g	2.18×10^{-4} mol
Millipored Water	25 mL (for CMC)	1.39 mol (for CMC)
	7 mL (for NH_2-PNIPAAm)	0.39 mol (for NH_2-PNIPAAm)
	5 mL (for EDC)	0.28 mol (for EDC)

* Molecular weight of aminoterminated PNIPAAm used for mol calculation, was obtained from Elemental Analysis measurements (see Table 23 in Results).

Table 40

(Cont.)

Reagent	Sample CCH-C2(2)-1.40	
	Quantity (g or mL)	**Moles (mol)**
CMC (Mw = 90,000 g/mol)	2.0418 g	2.27×10^{-5} mol
NH_2-PNIPAAm	1.3620 g	2.69×10^{-4} mol
NH_2-PNIPAAm is composed by:		
Sample CCH-A15-1*	.....0.0361 g	.....7.08×10^{-6} mol
Sample CCH-A15-2*	.....0.0080 g	.....1.58×10^{-6} mol
Sample CCH-A15-3*	.....0.0749 g	.....1.49×10^{-5} mol
Sample Fraction CCH-C1-1(1)*	.....0.0903 g	.....1.75×10^{-5} mol
Sample Fraction CCH-C1-1(2)*	.....0.0545 g	.....1.06×10^{-5} mol
Sample Fraction CCH-C1(2)-1(1)*	.....0.1765 g	.....3.49×10^{-5} mol
Sample Fraction CCH-C1(2)-1(2)*	.....0.2633 g	.....5.20×10^{-5} mol
Sample Fraction CCH-C1(2)-1(3)*	.....0.0859 g	.....1.70×10^{-5} mol
Sample Fraction CCH-C1(2)-1(4)*	.....0.2446 g	.....4.83×10^{-5} mol
Sample Fraction CCH-C1(2)-1(5)*	.....0.2098 g	.....4.14×10^{-5} mol
Sample Fraction CCH-C1(2)-1(6)*	.....0.1181 g	.....2.33×10^{-5} mol
TOTAL (NH_2-PNIPAAm)	.....**1.3620 g**	.....**2.69×10^{-4} mol**
EDC	0.6195 g	0.0032 mol
Millipored Water	121 mL (for CMC)	6.72 mol (for CMC)
	35 mL (for NH_2-PNIPAAm)	1.94 mol (for NH_2-PNIPAAm)
	15 mL (for EDC)	0.83 mol (for EDC)

* Molecular weight of aminoterminated PNIPAAm used for mol calculation, was obtained from Elemental Analysis measurements (see Table 23 in Results).

Table 41

CMC-g-PNIPAAm graft copolymers

($Mw(Graft)_{(THEO)}$ = 5,000 g/mol – $\%Graft_{(THEO)}$ = 50%)

Reagent	Sample CCH-B5-1.50	
	Quantity (g or mL)	**Moles (mol)**
CMC (Mw = 700,000 g/mol)	0.5064 g	7.23×10^{-7} mol
NH_2-PNIPAAm	0.5035 g	9.87×10^{-5} mol
NH_2-PNIPAAm is composed by:		
Sample CCH-A15-1*	.....0.5035 g	.....9.87×10^{-5} mol
TOTAL (NH_2-PNIPAAm)	.....**0.5035 g**	.....**9.87×10^{-5} mol**
EDC	0.0747 g	3.90×10^{-4} mol
Millipored Water	30 mL (for CMC)	1.67 mol (for CMC)
	13 mL (for NH_2-PNIPAAm)	0.72 mol (for NH_2-PNIPAAm)
	2 mL (for EDC)	0.11 mol (for EDC)

* Molecular weight of aminoterminated PNIPAAm used for mol calculation, was obtained from Elemental Analysis measurements (see Table 23 in Results).

Table 41

(Cont.)

Reagent	Sample CCH-C2(2)-1.50	
	Quantity (g or mL)	**Moles (mol)**
CMC (Mw = 90,000 g/mol)	2.0418 g	2.27×10^{-5} mol
NH_2-PNIPAAm	2.0419 g	4.03×10^{-4} mol
NH_2-PNIPAAm is composed by:		
Sample CCH-A15-1*	.....0.0542 g	….....1.06×10^{-5} mol
Sample CCH-A15-2*	.....0.0120 g	….....2.37×10^{-6} mol
Sample CCH-A15-3*	.....0.1123 g	….....2.23×10^{-5} mol
Sample Fraction CCH-C1-1(1)*	.....0.1354 g	….....2.63×10^{-5} mol
Sample Fraction CCH-C1-1(2)*	.....0.0816 g	….....1.59×10^{-5} mol
Sample Fraction CCH-C1(2)-1(1)*	.....0.2647 g	….....5.23×10^{-5} mol
Sample Fraction CCH-C1(2)-1(2)*	.....0.3946 g	….....7.79×10^{-5} mol
Sample Fraction CCH-C1(2)-1(3)*	.....0.1286 g	….....2.54×10^{-5} mol
Sample Fraction CCH-C1(2)-1(4)*	.....0.3664 g	….....7.24×10^{-5} mol
Sample Fraction CCH-C1(2)-1(5)*	.....0.3148 g	….....6.22×10^{-5} mol
Sample Fraction CCH-C1(2)-1(6)*	.....0.1773 g	.....3.50×10^{-5} mol
TOTAL (NH_2-PNIPAAm)	.....**2.0419 g**	…..**4.03×10^{-4} mol**
EDC	0.9296 g	0.0048 mol
Millipored Water	121 mL (for CMC)	6.72 mol (for CMC)
	53 mL (for NH_2-PNIPAAm)	2.94 mol (for NH_2-PNIPAAm)
	23 mL (for EDC)	1.28 mol (for EDC)

* Molecular weight of aminoterminated PNIPAAm used for mol calculation, was obtained from Elemental Analysis measurements (see Table 23 in Results).

Table 42

CMC-g-PNIPAAm graft copolymers

($Mw(Graft)_{(THEO)}$ = 5,000 g/mol – $\%Graft_{(THEO)}$ = 80%)

Reagent	Sample CCH-C2(2)-1.80	
	Quantity (g or mL)	**Moles (mol)**
CMC (Mw = 90,000 g/mol)	1.7081 g	1.90×10^{-5} mol
NH_2-PNIPAAm	6.8282 g	1.35×10^{-3} mol
NH_2-PNIPAAm is composed by:		
Sample CCH-A15-1*	.....0.1470 g	.....2.88×10^{-5} mol
Sample CCH-A15-2*	.....0.0415 g	.....8.21×10^{-6} mol
Sample CCH-A15-3*	.....0.3545 g	.....7.04×10^{-5} mol
Sample Fraction CCH-C1-1(1)*	.....0.3249 g	.....6.31×10^{-5} mol
Sample Fraction CCH-C1-1(2)*	.....0.1673 g	.....3.25×10^{-5} mol
Sample Fraction CCH-C1(2)-1(1)*	.....0.9187 g	.....1.81×10^{-4} mol
Sample Fraction CCH-C1(2)-1(2)*	.....1.5625 g	.....3.09×10^{-4} mol
Sample Fraction CCH-C1(2)-1(3)*	.....0.3913 g	.....7.73×10^{-5} mol
Sample Fraction CCH-C1(2)-1(4)*	.....1.3022 g	.....2.57×10^{-4} mol
Sample Fraction CCH-C1(2)-1(5)*	.....1.0652 g	.....2.10×10^{-4} mol
Sample Fraction CCH-C1(2)-1(6)*	.....0.5531 g	.....1.09×10^{-4} mol
TOTAL (NH_2-PNIPAAm)	.....**6.8282 g**	.....**1.35×10^{-3} mol**
EDC	3.1069 g	0.0162 mol
Millipored Water	121 mL (for CMC)	6.72 mol (for CMC)
	212 mL (for NH_2-PNIPAAm)	11.78 mol (for NH_2-PNIPAAm)
	93 mL (for EDC)	5.17 mol (for EDC)

* Molecular weight of aminoterminated PNIPAAm used for mol calculation, was obtained from Elemental Analysis measurements (see Table 23 in Results).

Table 43

CMC-g-PNIPAAm graft copolymers

($Mw(Graft)_{(THEO)}$ = 7,000 g/mol – $\%Graft_{(THEO)}$ = 40%)

Reagent	Sample CCH-B5-2.40	
	Quantity (g or mL)	**Moles (mol)**
CMC (Mw = 700,000 g/mol)	0.7544 g	1.08×10^{-6} mol
NH_2-PNIPAAm	0.5011 g	7.11×10^{-5} mol
NH_2-PNIPAAm is composed by:		
Sample CCH-B4-1**	.....0.5011 g	.....7.11×10^{-5} mol
TOTAL (NH_2-PNIPAAm)	.....**0.5011 g**	.....**7.11×10^{-5} mol**
EDC	0.0542 g	2.83×10^{-4} mol
Millipored Water	45 mL (for CMC)	2.50 mol (for CMC)
	10 mL (for NH_2-PNIPAAm)	0.55 mol (for NH_2-PNIPAAm)
	2 mL (for EDC)	0.11 mol (for EDC)
Reagent	**Sample CCH-C2(2)-2.40**	
	Quantity (g or mL)	**Moles (mol)**
CMC (Mw = 90,000 g/mol)	1.5426 g	1.71×10^{-5} mol
NH_2-PNIPAAm	1.0274 g	1.46×10^{-4} mol
NH_2-PNIPAAm is composed by:		
Sample CCH-B4-1**	.....0.0166 g	.....2.36×10^{-6} mol
Sample Fraction CCH-C1-2(1)**	.....0.0340 g	.....4.79×10^{-6} mol
Sample Fraction CCH-C1-2(2)**	.....0.0236 g	.....3.32×10^{-6} mol
Sample Fraction CCH-C1(2)-2(1)**	.....0.2025 g	.....2.87×10^{-5} mol
Sample Fraction CCH-C1(2)-2(3)**	.....0.1311 g	.....1.86×10^{-5} mol
Sample Fraction CCH-C1(2)-2(4)**	.....0.1956 g	.....2.77×10^{-5} mol
Sample Fraction CCH-C1(2)-2(5)**	.....0.3122 g	.....4.43×10^{-5} mol
Sample Fraction CCH-C1(2)-2(6)**	.....0.1118 g	.....1.58×10^{-5} mol
TOTAL (NH_2-PNIPAAm)	.....**1.0274 g**	.....**1.46×10^{-4} mol**
EDC	0.3868 g	0.0020 mol
Millipored Water	91 mL (for CMC)	5.05 mol (for CMC)
	27 mL (for NH_2-PNIPAAm)	1.50 mol (for NH_2-PNIPAAm)
	10 mL (for EDC)	0.55 mol (for EDC)

* Molecular weight of aminoterminated PNIPAAm used for mol calculation, was obtained from Elemental Analysis measurements (see Table 24 in Results).

Table 44

CMC-g-PNIPAAm graft copolymers

($Mw(Graft)_{(THEO)}$ = 7,000 g/mol – $\%Graft_{(THEO)}$ = 50%)

Reagent	Sample CCH-B5-2.50	
	Quantity (g or mL)	**Moles (mol)**
CMC (Mw = 700,000 g/mol)	0.5026 g	$7.18x10^{-7}$ mol
NH_2-PNIPAAm	0.5063 g	$7.18x10^{-5}$ mol
NH_2-PNIPAAm is composed by:		
Sample CCH-B4-1**	0.5063 g	$7.18x10^{-5}$ mol
TOTAL (NH_2-PNIPAAm)	**0.5063 g**	**$7.18x10^{-5}$ mol**
EDC	0.0541 g	$2.82x10^{-4}$ mol
Millipored Water	30 mL (for CMC)	1.67 mol (for CMC)
	10 mL (for NH_2-PNIPAAm)	0.55 mol (for NH_2-PNIPAAm)
	2 mL (for EDC)	0.11 mol (for EDC)
Reagent	**Sample CCH-C2(2)-2.50**	
	Quantity (g or mL)	**Moles (mol)**
CMC (Mw = 90,000 g/mol)	1.5445 g	$9.06x10^{-5}$ mol
NH_2-PNIPAAm	1.5405 g	$2.18x10^{-4}$ mol
NH_2-PNIPAAm is composed by:		
Sample CCH-B4-1**	0.0242 g	$3.43x10^{-6}$ mol
Sample Fraction CCH-C1-2(1)**	0.0511 g	$7.19x10^{-6}$ mol
Sample Fraction CCH-C1-2(2)**	0.0352 g	$4.96x10^{-6}$ mol
Sample Fraction CCH-C1(2)-2(1)**	0.3012 g	$4.27x10^{-5}$ mol
Sample Fraction CCH-C1(2)-2(3)**	0.1968 g	$2.79x10^{-5}$ mol
Sample Fraction CCH-C1(2)-2(4)**	0.2938 g	$4.16x10^{-5}$ mol
Sample Fraction CCH-C1(2)-2(5)**	0.4689 g	$6.65x10^{-5}$ mol
Sample Fraction CCH-C1(2)-2(6)**	0.1693 g	$2.40x10^{-5}$ mol
TOTAL (NH_2-PNIPAAm)	**1.5405 g**	**$2.18x10^{-4}$ mol**
EDC	0.5789 g	0.0002 mol
Millipored Water	91 mL (for CMC)	5.05 mol (for CMC)
	40 mL (for NH_2-PNIPAAm)	2.22 mol (for NH_2-PNIPAAm)
	14 mL (for EDC)	0.78 mol (for EDC)

** Molecular weight of aminoterminated PNIPAAm used for mol calculation, was obtained from Elemental Analysis measurements (see Table 24 in Results).

Table 45

CMC-g-PNIPAAm graft copolymers

($Mw(Graft)_{(THEO)}$ = 7,000 g/mol – $\%Graft_{(THEO)}$ = 80%)

Reagent	Sample CCH-C2(2)-2.80	
	Quantity (g or mL)	**Moles (mol)**
CMC (Mw = 90,000 g/mol)	1.2936 g	$1.44x10^{-5}$ mol
NH_2-PNIPAAm	5.1806 g	$7.34x10^{-4}$ mol
NH_2-PNIPAAm is composed by:		
Sample CCH-B4-1**	.....0.0417 g	.....$5.92x10^{-6}$ mol
Sample Fraction CCH-C1-2(1)**	.....0.1202 g	.....$1.69x10^{-5}$ mol
Sample Fraction CCH-C1-2(2)**	.....0.0618 g	.....$8.70x10^{-6}$ mol
Sample Fraction CCH-C1(2)-2(1)**	.....1.0512 g	.....$1.49x10^{-4}$ mol
Sample Fraction CCH-C1(2)-2(3)**	.....0.5954 g	.....$8.44x10^{-5}$ mol
Sample Fraction CCH-C1(2)-2(4)**	.....1.0136 g	.....$1.44x10^{-4}$ mol
Sample Fraction CCH-C1(2)-2(5)**	.....1.7885 g	.....$2.54x10^{-4}$ mol
Sample Fraction CCH-C1(2)-2(6)**	.....0.5082 g	.....$7.20x10^{-5}$ mol
TOTAL (NH_2-PNIPAAm)	.....**5.1806 g**	.....**$7.34x10^{-4}$ mol**
EDC	1.9433 g	0.0101 mol
Millipored Water	91 mL (for CMC)	5.05 mol (for CMC)
	160 mL (for NH_2-PNIPAAm)	8.89 mol (for NH_2-PNIPAAm)
	58 mL (for EDC)	3.22 mol (for EDC)

** Molecular weight of aminoterminated PNIPAAm used for mol calculation, was obtained from Elemental Analysis measurements (see Table 24 in Results).

Table 46

CMC-g-PNIPAAm graft copolymers

($Mw(Graft)_{(THEO)}$ = 9,000 g/mol – $\%Graft_{(THEO)}$ = 40%)

Reagent	Sample CCH-B5-3.40	
	Quantity (g or mL)	**Moles (mol)**
CMC (Mw = 700,000 g/mol)	0.4533 g	6.48×10^{-7} mol
NH_2-PNIPAAm	0.3017 g	3.29×10^{-5} mol
NH_2-PNIPAAm is composed by:		
Sample CCH-B4-2***	.....0.3017 g	.....3.29×10^{-5} mol
TOTAL (NH_2-PNIPAAm)	.....**0.3017 g**	.....**3.29×10^{-5} mol**
EDC	0.0258 g	1.35×10^{-4} mol
Millipored Water	27 mL (for CMC)	1.50 mol (for CMC)
	6 mL (for NH_2-PNIPAAm)	0.33 mol (for NH_2-PNIPAAm)
	1 mL (for EDC)	0.05 mol (for EDC)
Reagent	**Sample CCH-C2(2)-3.40**	
	Quantity (g or mL)	**Moles (mol)**
CMC (Mw = 90,000 g/mol)	1.5655 g	1.74×10^{-5} mol
NH_2-PNIPAAm	1.0443 g	1.15×10^{-4} mol
NH_2-PNIPAAm is composed by:		
Sample CCH-B4-2***	.....0.0049 g	.....5.34×10^{-7} mol
Sample Fraction CCH-C1-3(1)***	.....0.0881 g	.....9.75×10^{-6} mol
Sample Fraction CCH-C1-3(2)***	.....0.1400 g	.....1.55×10^{-5} mol
Sample Fraction CCH-C1(2)-3(1)***	.....0.0554 g	.....6.15×10^{-6} mol
Sample Fraction CCH-C1(2)-3(2)***	.....0.0905 g	.....1.00×10^{-5} mol
Sample Fraction CCH-C1(2)-3(4)***	.....0.1800 g	.....2.00×10^{-5} mol
Sample Fraction CCH-C1(2)-3(5)***	.....0.1938 g	.....2.15×10^{-5} mol
Sample Fraction CCH-C1(2)-3(6)***	.....0.0630 g	.....6.99×10^{-6} mol
Sample Fraction CCH-C1(2)-3.2(1)***	.....0.0255 g	.....2.82×10^{-6} mol
Sample Fraction CCH-C1(2)-3.2(2)***	.....0.0263 g	.....2.91×10^{-6} mol
Sample Fraction CCH-C1(2)-3.2(3)***	.....0.0100 g	.....1.11×10^{-6} mol
Sample Fraction CCH-C1(2)-3.2(4)***	.....0.0317 g	.....3.50×10^{-6} mol
Sample Fraction CCH-C1(2)-3.2(6)***	.....0.0002 g	.....2.21×10^{-8} mol
Sample Fraction CCH-C1(2)-3.3(1)***	.....0.0785 g	.....8.53×10^{-6} mol
Sample Fraction CCH-C1(2)-3.3(2)***	.....0.0197 g	.....2.14×10^{-6} mol
Sample Fraction CCH-C1(2)-3.3(4)***	.....0.0264 g	.....2.87×10^{-6} mol
Sample Fraction CCH-C1(2)-3.3(5)***	.....0.0089 g	.....9.67×10^{-7} mol
Sample Fraction CCH-C1(2)-3.3(6)***	.....0.0014 g	.....1.52×10^{-7} mol
TOTAL (NH_2-PNIPAAm)	.....**1.0443 g**	.....**1.15×10^{-4} mol**
EDC	0.2465 g	0.0013 mol
Millipored Water	93 mL (for CMC)	5.17 mol (for CMC)
	27 mL (for NH_2-PNIPAAm)	1.50 mol (for NH_2-PNIPAAm)
	6 mL (for EDC)	0.33 mol (for EDC)

*** Molecular weight of aminoterminated PNIPAAm used for mol calculation, was obtained from Elemental Analysis measurements (see Table 25 in Results).

Table 47

CMC-g-PNIPAAm graft copolymers

(Mw(Graft) $_{(THEO)}$ = 9,000 g/mol – %Graft$_{(THEO)}$ = 50%)

Reagent	Sample CCH-B5-3.50	
	Quantity (g or mL)	**Moles (mol)**
CMC (Mw = 700,000 g/mol)	0.3012 g	4.30×10^{-7} mol
NH_2-PNIPAAm	0.3017 g	3.29×10^{-5} mol
NH_2-PNIPAAm is composed by:		
Sample CCH-B4-2***	.....0.3017 g	.....3.29×10^{-5} mol
TOTAL (NH_2-PNIPAAm)	.....**0.3017 g**	.....**3.29×10^{-5} mol**
EDC	0.0258 g	1.35×10^{-4} mol
Millipored Water	18 mL (for CMC)	1 mol (for CMC)
	6 mL (for NH_2-PNIPAAm)	0.33 mol (for NH_2-PNIPAAm)
	1 mL (for EDC)	0.05 mol (for EDC)
Reagent	**Sample CCH-C2(2)-3.50**	
	Quantity (g or mL)	**Moles (mol)**
CMC (Mw = 90,000 g/mol)	1.5555 g	1.73×10^{-5} mol
NH_2-PNIPAAm	1.5639 g	1.73×10^{-4} mol
NH_2-PNIPAAm is composed by:		
Sample CCH-B4-2***	.....0.0070 g	.....7.63×10^{-7} mol
Sample Fraction CCH-C1-3(1)***	.....0.1329 g	.....1.47×10^{-5} mol
Sample Fraction CCH-C1-3(2)***	.....0.2102 g	.....2.33×10^{-5} mol
Sample Fraction CCH-C1(2)-3(1)***	.....0.0820 g	.....9.10×10^{-6} mol
Sample Fraction CCH-C1(2)-3(2)***	.....0.1355 g	.....1.50×10^{-5} mol
Sample Fraction CCH-C1(2)-3(4)***	.....0.2692 g	.....2.99×10^{-5} mol
Sample Fraction CCH-C1(2)-3(5)***	.....0.2917 g	.....3.24×10^{-5} mol
Sample Fraction CCH-C1(2)-3(6)***	.....0.0956 g	.....1.06×10^{-5} mol
Sample Fraction CCH-C1(2)-3.2(1)***	.....0.0380 g	.....4.20×10^{-6} mol
Sample Fraction CCH-C1(2)-3.2(2)***	.....0.0388 g	.....4.29×10^{-6} mol
Sample Fraction CCH-C1(2)-3.2(3)***	.....0.0150 g	.....1.66×10^{-6} mol
Sample Fraction CCH-C1(2)-3.2(4)***	.....0.0478 g	.....5.28×10^{-6} mol
Sample Fraction CCH-C1(2)-3.2(6)***	.....0.0002 g	.....2.21×10^{-8} mol
Sample Fraction CCH-C1(2)-3.3(1)***	.....0.1171 g	.....1.27×10^{-5} mol
Sample Fraction CCH-C1(2)-3.3(2)***	.....0.0297 g	.....3.23×10^{-6} mol
Sample Fraction CCH-C1(2)-3.3(3)***	.....0.0050 g	.....5.43×10^{-7} mol
Sample Fraction CCH-C1(2)-3.3(4)***	.....0.0392 g	.....4.26×10^{-6} mol
Sample Fraction CCH-C1(2)-3.3(5)***	.....0.0086 g	.....9.34×10^{-7} mol
Sample Fraction CCH-C1(2)-3.3(6)***	.....0.0004 g	.....4.34×10^{-8} mol
TOTAL (NH_2-PNIPAAm)	.....**1.5639 g**	.....**1.73×10^{-4} mol**
EDC	0.3684 g	0.0019 mol
Millipored Water	93 mL (for CMC)	5.17 mol (for CMC)
	41 mL (for NH_2-PNIPAAm)	2.28 mol (for NH_2-PNIPAAm)
	9 mL (for EDC)	0.50 mol (for EDC)

*** Molecular weight of aminoterminated PNIPAAm used for mol calculation, was obtained from Elemental Analysis measurements (see Table 25 in Results).

Table 48

CMC-g-PNIPAAm graft copolymers

($Mw(Graft)_{(THEO)}$ = 9,000 g/mol – $\%Graft_{(THEO)}$ = 80%)

Reagent	Sample CCH-C2(2)-3.80	
	Quantity (g or mL)	**Moles (mol)**
CMC (Mw = 90,000 g/mol)	1.2431 g	1.38×10^{-5} mol
NH_2-PNIPAAm	4.9704 g	5.50×10^{-4} mol
NH_2-PNIPAAm is composed by:		
Sample CCH-B4-2***	.....0.0018 g	.....1.96×10^{-7} mol
Sample Fraction CCH-C1-3(1)***	.....0.4261 g	.....4.71×10^{-5} mol
Sample Fraction CCH-C1-3(2)***	.....0.6900 g	.....7.63×10^{-5} mol
Sample Fraction CCH-C1(2)-3(1)***	.....0.2100 g	.....2.33×10^{-5} mol
Sample Fraction CCH-C1(2)-3(2)***	.....0.4136 g	.....4.59×10^{-5} mol
Sample Fraction CCH-C1(2)-3(4)***	.....0.9545 g	.....1.06×10^{-4} mol
Sample Fraction CCH-C1(2)-3(5)***	.....1.0570 g	.....1.17×10^{-4} mol
Sample Fraction CCH-C1(2)-3(6)***	.....0.3125 g	.....3.47×10^{-5} mol
Sample Fraction CCH-C1(2)-3.2(1)***	.....0.0925 g	.....1.02×10^{-5} mol
Sample Fraction CCH-C1(2)-3.2(2)***	.....0.1359 g	.....1.50×10^{-5} mol
Sample Fraction CCH-C1(2)-3.2(3)***	.....0.0302 g	.....3.34×10^{-6} mol
Sample Fraction CCH-C1(2)-3.2(4)***	.....0.1399 g	.....1.55×10^{-5} mol
Sample Fraction CCH-C1(2)-3.3(1)***	.....0.3422 g	.....3.72×10^{-5} mol
Sample Fraction CCH-C1(2)-3.3(2)***	.....0.0950 g	.....1.03×10^{-5} mol
Sample Fraction CCH-C1(2)-3.3(4)***	.....0.0692 g	.....7.52×10^{-6} mol
TOTAL (NH_2-PNIPAAm)	**.....4.9704 g**	**.....5.50×10^{-4} mol**
EDC	1.1730 g	0.0061 mol
Millipored Water	93 mL (for CMC)	5.17 mol (for CMC)
	162 mL (for NH_2-PNIPAAm)	9 mol (for NH_2-PNIPAAm)
	37 mL (for EDC)	2.50 mol (for EDC)

*** Molecular weight of aminoterminated PNIPAAm used for mol calculation, was obtained from Elemental Analysis measurements (see Table 25 in Results).

Table 49

CCH-C3(4)-2(30%) pregel stock solution

Reagent	Quantity (g or mL)	Moles (mol)
Millipore Water	1.0000 mL	5.55×10^{-2} mol
CMC-g-PNIPAAm + HEC	0.3000 g	2.01×10^{-6} mol
Where:		
1)CMC-g-PNIPAAm..... .....0.2250 g….. …….1.18x10^{-6} mol		
CMC-g-PNIPAAm is composed by:		
Sample Fraction CCH-C2(2)-2.80(3)[a]	……...0.0144 g	……..4.97×10^{-8} mol
Sample Fraction CCH-C2(2)-2.80(6)[b]	……...0.0598 g	……..2.07×10^{-7} mol
Sample Fraction CCH-C2(2)-3.40(1)[c]	……...0.0715 g	……..6.52×10^{-7} mol
Sample Fraction CCH-C2(2)-3.80(2)[d]	……...0.0793 g	……..2.70×10^{-7} mol
TOTAL (CMC-g-PNIPAAm)	**……..0.2250 g**	**…….1.18x10^{-6} mol**
2)HEC[e]..... .....0.0750 g..… …….8.33x10^{-7} mol		
TOTAL (CMC-g-PNIPAAm + HEC)	**.....0.3000 g..… …….2.01x10^{-6} mol**	

[a] Molecular weight of Sample Fraction CCH-C2(2)-2.80(3) used for mol calculation, was obtained from Elemental Analysis measurements (see sample CCH-C2(2)-2.80 of Table 30 in Results).

[b] Molecular weight of Sample Fraction CCH-C2(2)-2.80(6) used for mol calculation, was obtained from Elemental Analysis measurements (see sample CCH-C2(2)-2.80 of Table 30 in Results).

[c] Molecular weight of Sample Fraction CCH-C2(2)-3.40(1) used for mol calculation, was obtained from Elemental Analysis measurements (see sample CCH-C2(2)-3.40 of Table 31 in Results).

[d] Molecular weight of Sample Fraction CCH-C2(2)-3.80(2) used for mol calculation, was obtained from Elemental Analysis measurements (see sample CCH-C2(2)-3.80 of Table 31 in Results).

[e] Molecular weight of HEC = 90,000 g/mol.

Table 50

$AlCl_3$ aqueous solutions ($V_{solution}$ = 10 mL)

Aqueous Solution	W_{AlCl_3} (g)
1 % $AlCl_3$	0.1013 g
1.5 % $AlCl_3$	0.1512 g
2 % $AlCl_3$	0.2014 g
2.5 % $AlCl_3$	0.2510 g
3 % $AlCl_3$	0.3025 g
3.5 % $AlCl_3$	0.3523 g
3.75 % $AlCl_3$	0.3785 g
15 % $AlCl_3$	1.5072 g

Table 51

Pregel stock solutions

Reagent	Sample CCH-C3(5)-1(15%)	
	Quantity (g)	**Moles (mol)**
Millipore Water	1.0000 g	5.56×10^{-2} mol
CMC + HEC	0.1501 g	1.67×10^{-6} mol
Where:		
1) CMC*	0.1125 g	1.25×10^{-6} mol
2) HEC**	0.0376 g	4.18×10^{-7} mol
TOTAL (CMC + HEC)	**0.1501 g**	**1.67×10^{-6} mol**
Citric Acid	0.0056 g	2.91×10^{-5} mol

Reagent	Sample CCH-C3(5)-1(20%)	
	Quantity (g)	**Moles (mol)**
Millipore Water	1.0000 g	5.56×10^{-2} mol
CMC + HEC	0.2002 g	2.22×10^{-6} mol
Where:		
1) CMC*	0.1501 g	1.67×10^{-6} mol
2) HEC**	0.0501 g	5.57×10^{-7} mol
TOTAL (CMC + HEC)	**0.2002 g**	**2.22×10^{-6} mol**
Citric Acid	0.0075 g	3.90×10^{-5} mol

Reagent	Sample CCH-C3(5)-1(25%)	
	Quantity (g)	**Moles (mol)**
Millipore Water	1.0000 g	5.56×10^{-2} mol
CMC + HEC	0.2501 g	2.78×10^{-6} mol
Where:		
1) CMC*	0.1876 g	2.08×10^{-6} mol
2) HEC**	0.0625 g	6.94×10^{-7} mol
TOTAL (CMC + HEC)	**0.2501 g**	**2.78×10^{-6} mol**
Citric Acid	0.0094 g	4.89×10^{-5} mol

Reagent	Sample CCH-C3(5)-1(30%)	
	Quantity (g)	**Moles (mol)**
Millipore Water	1.0000 g	5.56×10^{-2} mol
CMC + HEC	0.3002 g	3.34×10^{-6} mol
Where:		
1) CMC*	0.2250 g	2.50×10^{-6} mol
2) HEC**	0.0752 g	8.35×10^{-7} mol
TOTAL (CMC + HEC)	**0.3002 g**	**3.34×10^{-6} mol**
Citric Acid	0.0113 g	5.88×10^{-5} mol

Table 51

(Cont.)

Reagent	Sample CCH-C3(5)-1(35%)	
	Quantity (g)	**Moles (mol)**
Millipore Water	1.0000 g	5.56×10^{-2} mol
CMC + HEC	0.3500 g	3.89×10^{-6} mol
Where:		
1) CMC*.....	.....0.2625 g.....	.....2.92×10^{-6} mol
2) HEC**.....	.....0.0875 g.....	.....9.72×10^{-7} mol
**TOTAL (CMC + HEC).....	**.....0.3500 g.....	**.....3.89×10^{-6} mol**
Citric Acid	0.0131 g	6.82×10^{-5} mol
Reagent	**Sample CCH-C3(5)-1(40%)**	
	Quantity (g)	**Moles (mol)**
Millipore Water	1.0000 g	5.56×10^{-2} mol
CMC + HEC	0.4003 g	4.45×10^{-6} mol
Where:		
1) CMC*.....	.....0.3001 g.....	.....3.33×10^{-6} mol
2) HEC**.....	.....0.1002 g.....	.....1.11×10^{-6} mol
**TOTAL (CMC + HEC).....	**.....0.4003 g.....	**.....4.45×10^{-6} mol**
Citric Acid	0.0150 g	7.81×10^{-5} mol
Reagent	**Sample CCH-C3(5)-2(15%)**	
	Quantity (g)	**Moles (mol)**
Millipore Water	1.0000 g	5.56×10^{-2} mol
CMC-g-PNIPAAm + HEC	0.1502 g	8.08×10^{-7} mol
Where:		
**1) CMC-g-PNIPAAm.....	**.....0.1125 g.....	**.....3.89×10^{-7} mol**
CMC-g-PNIPAAm is composed by:		
Sample Fraction CCH-C2(2)-2.80(1)[a]	.....0.1125 g	.....3.89×10^{-7} mol
TOTAL (CMC-g-PNIPAAm)	**.....0.1125 g**	**.....3.89×10^{-7} mol**
2) HEC.....	**.....0.0377 g.....	**.....4.19×10^{-7} mol**
**TOTAL (CMC-g-PNIPAAm + HEC)....	**.....0.1502 g.....	**.....8.08×10^{-7} mol**
Citric Acid	0.0056 g	2.91×10^{-5} mol
Reagent	**Sample CCH-C3(5)-2(20%)**	
	Quantity (g)	**Quantity (g)**
Millipore Water	1.0000 g	5.56×10^{-2} mol
CMC-g-PNIPAAm + HEC	0.2001 g	1.07×10^{-6} mol
Where:		
**1) CMC-g-PNIPAAm.....	**.....0.1500 g.....	**.....5.18×10^{-7} mol**
CMC-g-PNIPAAm is composed by:		
Sample Fraction CCH-C2(2)-2.80(1)[a]	.....0.1500 g	.....5.18×10^{-7} mol
TOTAL (CMC-g-PNIPAAm)	**.....0.1500 g**	**.....5.18×10^{-7} mol**
2) HEC.....	**.....0.0501 g.....	**.....5.57×10^{-7} mol**
**TOTAL (CMC-g-PNIPAAm + HEC)....	**.....0.2001 g.....	**.....1.07×10^{-6} mol**
Citric Acid	0.0075 g	3.90×10^{-5} mol

Table 51

(Cont.)

Reagent	Sample CCH-C3(5)-2(25%)	
	Quantity (g)	Moles (mol)
Millipore Water	1.0000 g	5.56×10^{-2} mol
CMC-g-PNIPAAm + HEC	0.2500 g	1.34×10^{-6} mol
Where:		
1)CMC-g-PNIPAAm	**0.1875 g**	**6.48×10^{-7} mol**
CMC-g-PNIPAAm is composed by:		
Sample Fraction CCH-C2(2)-2.80(1)[a]	0.0427 g	1.48×10^{-7} mol
Sample Fraction CCH-C2(2)-2.80(3)[b]	0.1448 g	5.00×10^{-7} mol
TOTAL (CMC-g-PNIPAAm)	**0.1875 g**	**6.48×10^{-7} mol**
2)HEC**	**0.0625 g**	**6.94×10^{-7} mol**
TOTAL (CMC-g-PNIPAAm + HEC)	**0.2500 g**	**1.34×10^{-6} mol**
Citric Acid	0.0094 g	4.89×10^{-5} mol

Reagent	Sample CCH-C3(5)-2(30%)	
	Quantity (g)	Moles (mol)
Millipore Water	1.0000 g	5.56×10^{-2} mol
CMC-g-PNIPAAm + HEC	0.3002 g	1.61×10^{-6} mol
Where:		
1)CMC-g-PNIPAAm	**0.2251 g**	**7.78×10^{-7} mol**
CMC-g-PNIPAAm is composed by:		
Sample Fraction CCH-C2(2)-2.80(3)[b]	0.1076 g	3.72×10^{-7} mol
Sample Fraction CCH-C2(2)-2.80(4)[c]	0.1175 g	4.06×10^{-7} mol
TOTAL (CMC-g-PNIPAAm)	**0.2251 g**	**7.78×10^{-7} mol**
2)HEC**	**0.0751 g**	**8.34×10^{-7} mol**
TOTAL (CMC-g-PNIPAAm + HEC)	**0.3002 g**	**1.61×10^{-6} mol**
Citric Acid	0.0113 g	5.88×10^{-5} mol

Reagent	Sample CCH-C3(5)-2(35%)	
	Quantity (g)	Moles (mol)
Millipore Water	1.0000 g	5.56×10^{-2} mol
CMC-g-PNIPAAm + HEC	0.3502 g	1.88×10^{-6} mol
Where:		
1)CMC-g-PNIPAAm	**0.2625 g**	**9.07×10^{-7} mol**
CMC-g-PNIPAAm is composed by:		
Sample Fraction CCH-C2(2)-2.80(4)[c]	0.2625 g	9.07×10^{-7} mol
TOTAL (CMC-g-PNIPAAm)	**0.2625 g**	**9.07×10^{-7} mol**
2)HEC**	**0.0877 g**	**9.74×10^{-7} mol**
TOTAL (CMC-g-PNIPAAm + HEC)	**0.3502 g**	**1.88×10^{-6} mol**
Citric Acid	0.0131 g	6.82×10^{-5} mol

Table 51

(Cont.)

Reagent	Sample CCH-C3(5)-2(40%)	
	Quantity (g)	**Moles (mol)**
Millipore Water	1.0000 g	5.56×10^{-2} mol
CMC-g-PNIPAAm + HEC	0.4000 g	2.27×10^{-6} mol
Where:		
1) CMC-g-PNIPAAm	**0.3000 g**	**1.16×10^{-6} mol**
CMC-g-PNIPAAm is composed by:		
Sample Fraction CCH-C2(2)-2.80(4)[c]	0.2516 g	8.69×10^{-7} mol
Sample Fraction CCH-C2(2)-3.50(1)[d]	0.0484 g	2.90×10^{-7} mol
TOTAL (CMC-g-PNIPAAm)	**0.3000 g**	**1.16×10^{-6} mol**
2) HEC**	**0.1000 g**	**1.11×10^{-6} mol**
TOTAL (CMC-g-PNIPAAm + HEC)	**0.4000 g**	**2.27×10^{-6} mol**
Citric Acid	0.0150 g	7.81×10^{-5} mol

* Molecular weight of CMC = 90,000 g/mol.

** Molecular weight of HEC = 90,000 g/mol.

[a] Molecular weight of Sample Fraction CCH-C2(2)-2.80(1) used for mol calculation, was obtained from Elemental Analysis measurements (see sample CCH-C2(2)-2.80 of Table 30 in Results).

[b] Molecular weight of Sample Fraction CCH-C2(2)-2.80(3) used for mol calculation, was obtained from Elemental Analysis measurements (see sample CCH-C2(2)-2.80 of Table 30 in Results).

[c] Molecular weight of Sample Fraction CCH-C2(2)-2.80(4) used for mol calculation, was obtained from Elemental Analysis measurements (see sample CCH-C2(2)-2.80 of Table 30 in Results).

[d] Molecular weight of Sample Fraction CCH-C2(2)-3.50(1) used for mol calculation, was obtained from Elemental Analysis measurements (see sample CCH-C2(2)-3.50 of Table 31 in Results).

Table 52

CCH-C3(8)-2.1(35%) pregel stock solution

Reagent	Stock Solution CCH-C3(8)-2.1(35%)	
	Quantity (g)	**Moles (mol)**
Millipore Water	4.0000 g	2.22×10^{-1} mol
CMC-g-PNIPAAm + HEC	1.4117 g	9.03×10^{-6} mol
Where:		
1) CMC-g-PNIPAAm	**1.0603 g**	**5.12×10^{-6} mol**
CMC-g-PNIPAAm is composed by:		
Sample Fraction CCH-C2(2)-3.80(5)[a]	0.1840 g	6.27×10^{-7} mol
Sample Fraction CCH-C2(2)-3.80(4)[b]	0.0987 g	3.36×10^{-7} mol
Sample Fraction CCH-C2(2)-3.50(3)[c]	0.1331 g	7.97×10^{-7} mol
Sample Fraction CCH-C2(2)-2.50(4)[d]	0.1714 g	1.04×10^{-6} mol
Sample Fraction CCH-C2(2)-2.50(1)[e]	0.0962 g	5.83×10^{-7} mol
Sample Fraction CCH-C2(2)-2.40(2)[f]	0.0678 g	6.74×10^{-7} mol
Sample Fraction CCH-C2(2)-2.80(5)[g] + Sample Fraction CCH-C2(2)-2.80(7)[h]	0.3091 g	1.07×10^{-6} mol
TOTAL (CMC-g-PNIPAAm)	**1.0603 g**	**5.12×10^{-6} mol**
2) HEC*	**0.3514 g**	**3.90×10^{-6} mol**
TOTAL (CMC-g-PNIPAAm + HEC)	**1.4117 g**	**9.03×10^{-6} mol**
Citric Acid**	0.0525 g	2.73×10^{-4} mol

[a] Molecular weight of Sample Fraction CCH-C2(2)-3.80(5) used for mol calculation, was obtained from Elemental Analysis measurements (see sample CCH-C2(2)-3.80 of Table 31 in Results).

[b] Molecular weight of Sample Fraction CCH-C2(2)-3.80(4) used for mol calculation, was obtained from Elemental Analysis measurements (see sample CCH-C2(2)-3.80 of Table 31 in Results).

[c] Molecular weight of Sample Fraction CCH-C2(2)-3.50(3) used for mol calculation, was obtained from Elemental Analysis measurements (see sample CCH-C2(2)-3.50 of Table 31 in Results).

[d] Molecular weight of Sample Fraction CCH-C2(2)-2.50(4) used for mol calculation, was obtained from Elemental Analysis measurements (see sample CCH-C2(2)-2.50 of Table 30 in Results).

[e] Molecular weight of Sample Fraction CCH-C2(2)-2.50(1) used for mol calculation, was obtained from Elemental Analysis measurements (see sample CCH-C2(2)-2.50 of Table 30 in Results).

[f] Molecular weight of Sample Fraction CCH-C2(2)-2.40(2) used for mol calculation, was obtained from Elemental Analysis measurements (see sample CCH-C2(2)-2.40 of Table 30 in Results).

[g] Molecular weight of Sample Fraction CCH-C2(2)-2.80(5) used for mol calculation, was obtained from Elemental Analysis measurements (see sample CCH-C2(2)-2.80 of Table 30 in Results).

[h] Molecular weight of Sample Fraction CCH-C2(2)-2.80(7) used for mol calculation, was obtained from Elemental Analysis measurements (see sample CCH-C2(2)-2.80 of Table 30 in Results).

* Molecular weight of HEC = 90,000 g/mol.

** Only added in Sample CCH-C3(8)MONO-1(CA). Concentration = 3.75% weight percentage, respect of the weight of the polymer.

Table 53

CCH-C3(8)-1a(35%) pregel stock solution

Reagent	Stock Solution CCH-C3(8)-1a(35%)	
	Quantity (g)	Moles (mol)
Millipore Water	1.0000 g	5.56×10^{-2} mol
CMC + HEC	0.1002 g	1.11×10^{-6} mol
Where:		
1) CMC*.....	.....0.0751 g.....	.....8.34×10^{-7} mol
2) HEC**.....	.....0.0251 g.....	.....2.79×10^{-7} mol
**TOTAL (CMC+HEC).....	**.....0.1002 g.....**	**.....1.11×10^{-6} mol**

* Molecular weight of CMC = 90,000 g/mol.

** Molecular weight of HEC = 90,000 g/mol.

Table 54

CCH-C3(8)-2.2(35%) pregel stock solution

Reagent	Stock Solution CCH-C3(8)-2.2(35%)	
	Quantity (g)	Moles (mol)
Millipore Water	4.0000 g	2.22×10^{-1} mol
CMC-g-PNIPAAm + HEC	1.3786 g	8.88×10^{-6} mol
Where:		
**1) CMC-g-PNIPAAm.....	**.....1.0281 g.....**	**.....4.98×10^{-6} mol**
CMC-g-PNIPAAm is composed by:		
Sample Fraction CCH-C2(2)-3.80(5)[a]	.....0.1758 g	.....5.99×10^{-7} mol
Sample Fraction CCH-C2(2)-3.80(4)[b]	.....0.0942 g	.....3.21×10^{-7} mol
Sample Fraction CCH-C2(2)-3.50(3)[c]	.....0.1298 g	.....7.77×10^{-7} mol
Sample Fraction CCH-C2(2)-2.50(4)[d]	.....0.1670 g	.....1.01×10^{-6} mol
Sample Fraction CCH-C2(2)-2.50(1)[e]	.....0.0936 g	.....5.67×10^{-7} mol
Sample Fraction CCH-C2(2)-2.40(2)[f]	.....0.0675 g	.....6.71×10^{-7} mol
Sample Fraction CCH-C2(2)-2.80(5)[g] + Sample Fraction CCH-C2(2)-2.80(7)[h]	.....0.3002 g	.....1.04×10^{-6} mol
TOTAL (CMC-g-PNIPAAm)	**.....1.0281 g**	**.....4.98×10^{-6} mol**
**2) HEC*.....	**.....0.3505 g.....**	**.....3.89×10^{-6} mol**
**TOTAL (CMC-g-PNIPAAm + HEC).....	**.....1.3786 g.....**	**.....8.88×10^{-6} mol**

[a] Molecular weight of Sample Fraction CCH-C2(2)-3.80(5) used for mol calculation, was obtained from Elemental Analysis measurements (see sample CCH-C2(2)-3.80 of Table 31 in Results).

[b] Molecular weight of Sample Fraction CCH-C2(2)-3.80(4) used for mol calculation, was obtained from Elemental Analysis measurements (see sample CCH-C2(2)-3.80 of Table 31 in Results).

[c] Molecular weight of Sample Fraction CCH-C2(2)-3.50(3) used for mol calculation, was obtained from Elemental Analysis measurements (see sample CCH-C2(2)-3.50 of Table 31 in Results).

[d] Molecular weight of Sample Fraction CCH-C2(2)-2.50(4) used for mol calculation, was obtained from Elemental Analysis measurements (see sample CCH-C2(2)-2.50 of Table 30 in Results).

[e] Molecular weight of Sample Fraction CCH-C2(2)-2.50(1) used for mol calculation, was obtained from Elemental Analysis measurements (see sample CCH-C2(2)-2.50 of Table 30 in Results).

[f] Molecular weight of Sample Fraction CCH-C2(2)-2.40(2) used for mol calculation, was obtained from Elemental Analysis measurements (see sample CCH-C2(2)-2.40 of Table 30 in Results).

[g] Molecular weight of Sample Fraction CCH-C2(2)-2.80(5) used for mol calculation, was obtained from Elemental Analysis measurements (see sample CCH-C2(2)-2.80 of Table 30 in Results).

[h] Molecular weight of Sample Fraction CCH-C2(2)-2.80(7) used for mol calculation, was obtained from Elemental Analysis measurements (see sample CCH-C2(2)-2.80 of Table 30 in Results).

* Molecular weight of HEC = 90,000 g/mol.

Table 55

CCH-C3(8)-2.3(35%) pregel stock solution

Reagent	**Stock Solution CCH-C3(8)-2.3(35%)**	
	Quantity (g)	**Moles (mol)**
Millipore Water	4.0000 g	2.22×10^{-1} mol
CMC-g-PNIPAAm + HEC	1.4018 g	9.17×10^{-6} mol
Where:		
1) CMC-g-PNIPAAm	**1.0500 g**	**5.26×10^{-6} mol**
CMC-g-PNIPAAm is composed by:		
Sample Fraction CCH-C2(2)-1.50(1)[a]	0.1222 g	6.95×10^{-7} mol
Sample Fraction CCH-C2(2)-1.50(3)[b]	0.1962 g	1.12×10^{-6} mol
Sample Fraction CCH-C2(2)-1.40(4)[c]	0.1608 g	1.09×10^{-6} mol
Sample Fraction CCH-C2(2)-2.80(2)[d] + Sample Fraction CCH-C2(2)-2.80(5)[e]	0.2705 g	9.34×10^{-7} mol
Sample Fraction CCH-C2(2)-1.50(5)[f]	0.1800 g	1.02×10^{-6} mol
Sample Fraction CCH-C2(2)-1.80(1)[g]	0.0755 g	2.46×10^{-7} mol
Sample Fraction CCH-C2(2)-2.80(7)[h]	0.0448 g	1.55×10^{-7} mol
TOTAL (CMC-g-PNIPAAm)	**1.0500 g**	**5.26×10^{-6} mol**
2) HEC*	**0.3518 g**	**3.91×10^{-6} mol**
TOTAL (CMC-g-PNIPAAm + HEC)	**1.4018 g**	**9.17×10^{-6} mol**

[a] Molecular weight of Sample Fraction CCH-C2(2)-1.50(1) used for mol calculation, was obtained from Elemental Analysis measurements (see sample CCH-C2(2)-1.50 of Table 29 in Results).

[b] Molecular weight of Sample Fraction CCH-C2(2)-1.50(3) used for mol calculation, was obtained from Elemental Analysis measurements (see sample CCH-C2(2)-1.50 of Table 29 in Results).

[c] Molecular weight of Sample Fraction CCH-C2(2)-1.40(4) used for mol calculation, was obtained from Elemental Analysis measurements (see sample CCH-C2(2)-1.40 of Table 29 in Results).

[d] Molecular weight of Sample Fraction CCH-C2(2)-2.80(2) used for mol calculation, was obtained from Elemental Analysis measurements (see sample CCH-C2(2)-2.80 of Table 30 in Results).

[e] Molecular weight of Sample Fraction CCH-C2(2)-2.80(5) used for mol calculation, was obtained from Elemental Analysis measurements (see sample CCH-C2(2)-2.80 of Table 30 in Results).

[f] Molecular weight of Sample Fraction CCH-C2(2)-1.50(5) used for mol calculation, was obtained from Elemental Analysis measurements (see sample CCH-C2(2)-1.50 of Table 29 in Results).

[g] Molecular weight of Sample Fraction CCH-C2(2)-1.80(1) used for mol calculation, was obtained from Elemental Analysis measurements (see sample CCH-C2(2)-1.80 of Table 29 in Results).

[h] Molecular weight of Sample Fraction CCH-C2(2)-2.80(7) used for mol calculation, was obtained from Elemental Analysis measurements (see sample CCH-C2(2)-2.80 of Table 30 in Results).

* Molecular weight of HEC = 90,000 g/mol.

Table 56

CMC-g-PNIPAAm comb-type graft pre-gel solutions

Solution CCH-C3(8)BI-Sol(1)[a]	
Reagent	**Quantity (g)**
Stock Solution CCH-C3(8)-2.2(35%)	0.0842 g
Citric Acid*	0.0011 g
Deionized Water	1.9147 g
Solution CCH-C3(8)BI-Sol(2)[b]	
Reagent	**Quantity (g)**
Stock Solution CCH-C3(8)-2.2(35%)	0.1200 g
Citric Acid*	0.0016 g
Deionized Water	1.8784 g
Solution CCH-C3(8)BI-Sol(3)[c]	
Reagent	**Quantity (g)**
Stock Solution CCH-C3(8)-2.2(35%)	0.1665 g
Citric Acid*	0.0022 g
Deionized Water	1.8313 g
Solution CCH-C3(8)BI-Sol(4)[d]	
Reagent	**Quantity (g)**
Stock Solution CCH-C3(8)-2.2(35%)	0.2072 g
Citric Acid*	0.0027 g
Deionized Water	1.7901 g
Solution CCH-C3(8)BI-Sol(5)[e]	
Reagent	**Quantity (g)**
Stock Solution CCH-C3(8)-2.2(35%)	0.2451 g
Citric Acid*	0.0032 g
Deionized Water	1.7517 g
Solution CCH-C3(8)BI-Sol(6)[f,g,i]	
Reagent	**Quantity (g)**
Stock Solution CCH-C3(8)-2.2(35%)	0.2417 g
Stock Solution CCH-C3(8)-2.3(35%)	0.2417 g
Citric Acid*	0.0064 g

* Citric acid concentration: 3,75% $W_{CMC\text{-}g\text{-}PNIPAAm + HEC}$

[a] $CC_{pre\text{-}gel\ stock\ solution}$[h] = 4% / $W_{pre\text{-}gel\ solution}$ = 2 g

[b] $CC_{pre\text{-}gel\ stock\ solution}$[h] = 6% / $W_{pre\text{-}gel\ solution}$ = 2 g

[c] $CC_{pre\text{-}gel\ stock\ solution}$[h] = 8% / $W_{pre\text{-}gel\ solution}$ = 2 g

[d] $CC_{pre\text{-}gel\ stock\ solution}$[h] = 10% / $W_{pre\text{-}gel\ solution}$ = 2 g

[e] $CC_{pre\text{-}gel\ stock\ solution}$[h] = 12% / $W_{pre\text{-}gel\ solution}$ = 2 g

[f] $CC_{pre\text{-}gel\ stock\ solution}$[h] = 35% / $W_{pre\text{-}gel\ solution}$ = 0.4898 g

[g] Used for preparation of active layers in bilayers with hydrogel and PA6 substrates.

[h] Concentration of pre-gel stock solution in pre-gel solution.

[i] Used for preparation of passive layers in bilayers with hydrogel substrates.

Table 57

Solutions used for functionalization of PA6 substrates by concentrated (and diluted) acidic and aqueous hydrolysis

25 %Wt Glutaraldehyde Solution ($V_{solution}$ = 250 mL)	
Ingredients:	
-50 %Wt Glutaraldehyde	125 mL
-Deionized Water.....	Until 250 mL of solution was achieved
1 V/V% Polyethyleneimine (PEI) in 0.1 M Sodium Phosphate pH=8 solution ($V_{solution}$ = 250 mL)	
Ingredients:	
-Polyethyleneimine.....	2.5 mL
-0.1 M Sodium Phosphate Buffer pH=8.....	Until 250 mL of solution was achieved
Where:	
1) 0.1 M Sodium Phosphate Buffer pH=8 ($V_{solution}$ = 250 mL)	
-1 M Sodium Phosphate Buffer pH=8.....	25 mL
-Deionized Water.....	Until 250 mL of solution was achieved
2) 1 M Sodium Phosphate Buffer pH=8 ($V_{solution}$ = 100 mL)	
-1 M Disodium Hydrogene Phosphate Solution.....	93.2 mL
-1 M Sodium Phosphate Monobasic Solution.....	6.8 mL
3) 1 M Disodium Hydrogene Phosphate Solution ($V_{solution}$ = 100 mL)	
-Disodium Hydrogene Phosphate.....	14.1958 g
-Deionized Water.....	Until 100 mL of solution was achieved
4) 1 M Sodium Phosphate Monobasic Solution ($V_{solution}$ = 50 mL)	
-Sodium Phosphate Monobasic Solution.....	6.0079 g
-Deionized Water.....	Until 50 mL of solution was achieved
6 %Wt HCl Solution ($V_{solution}$ = 250 mL)	
Ingredients:	
-6 N HCl.....	82.28 mL
-Deionized Water.....	Until 250 mL of solution was achieved
10 V/V% Diethylamine Solution ($V_{solution}$ = 250 mL)	
Ingredients:	
-99.5 V/V% Diethylamine Solution.....	25.13 mL
-Deionized Water.....	Until 250 mL of solution was achieved

Table 58

FTIR Measurements: Aminoterminated PNIPAAm oligomers

(Group of Samples A (Mw(Graft)(THEO) = 5,000 g/mol))

Group of Samples A (Mw(THEO) = 5,000 g/mol)									
Sample	**Sample Fraction**	**Wave number NH (cm^{-1})**	**Wave number CH_3 (cm^{-1})**	**Wave number CH_2 (cm^{-1})**	**Wave number C=O (cm^{-1})**	**Wave number NH (cm^{-1})**	**Wave number $CH(CH_3)_2$ und CH_2 (cm^{-1})**	**Wave number $CH(CH_3)_2$ (cm^{-1})**	**Wave number CN (cm^{-1})**
CCH-A15-1	CCH-A15-1	3,439.2	2,973.8	2,934.1	1,647.6	1,545.0	1,458.8	1,387.7 and 1,367.8	1,172.5
CCH-A15-2	CCH-A15-2	3,442.2	2,975.7	2,936.6	1,654.4	1,550.8	1,459.5	1,388.3 and 1,368.4	1,172.6
CCH-A15-3	CCH-A15-3	3,483.0	2,975.9	2,936.9	1,654.4	1,551.0	1,459.4	1,388.3 and 1,368.5	1,172.7
CCH-C1-1	CCH-C1-1(1)	3,438.3	2,972.5	2,934.1	1,649.1	1,541.7	1,458.9	1,386.8 and 1,367.0	1,172.8
	CCH-C1-1(2)	No Data	No Data	No Data	No Data	No Data	No Data	No Data	No Data

Table 58

(Cont.)

Group of Samples A (Mw(THEO) = 5,000 g/mol)									
Sample	**Sample Fraction**	**Wave number NH (cm^{-1})**	**Wave number CH_3 (cm^{-1})**	**Wave number CH_2 (cm^{-1})**	**Wave number C=O (cm^{-1})**	**Wave number NH (cm^{-1})**	**Wave number $CH(CH_3)_2$ und CH_2 (cm^{-1})**	**Wave number $CH(CH_3)_2$ (cm^{-1})**	**Wave number CN (cm^{-1})**
CCH-C1(2)-1	CCH-C1(2)-1(1)	No Data	No Data	No Data	No Data	No Data	No Data	No Data	No Data
	CCH-C1(2)-1(2)	No Data	No Data	No Data	No Data	No Data	No Data	No Data	No Data
	CCH-C1(2)-1(3)	3,438.2	2,973.9	2,935.0	1,648.9	1,547.7	1,459.5	1,387.7 and 1,367.8	1,172.6
	CCH-C1(2)-1(4)	No Data	No Data	No Data	No Data	No Data	No Data	No Data	No Data
	CCH-C1(2)-1(5)	No Data	No Data	No Data	No Data	No Data	No Data	No Data	No Data
	CCH-C1(2)-1(6)	No Data	No Data	No Data	No Data	No Data	No Data	No Data	No Data

Table 59

FTIR Measurements: Aminoterminated PNIPAAm oligomers

(Group of Samples B ($M_{w(Graft)(THEO)}$ = 7,000 g/mol))

Group of Samples B (Mw(THEO) = 7,000 g/mol)									
Sample	**Sample Fraction**	**Wave number NH (cm^{-1})**	**Wave number CH_3 (cm^{-1})**	**Wave number CH_2 (cm^{-1})**	**Wave number C=O (cm^{-1})**	**Wave number NH (cm^{-1})**	**Wave number $CH(CH_3)_2$ und CH_2 (cm^{-1})**	**Wave number $CH(CH_3)_2$ (cm^{-1})**	**Wave number CN (cm^{-1})**
CCH-B4-1	CCH-B4-1	3,436.4	2,973.9	2,935.3	1,649.1	1,548.0	1,459.6	1,387.8 and 1,367.9	1,172.4
CCH-C1-2	CCH-C1-2(1)	3,436.9	2,972.4	2,934.1	1,649.7	1,542.0	1,458.9	1,386.8 and 1,367.0	1,172.8
	CCH-C1-2(2)	No Data	No Data	No Data	No Data	No Data	No Data	No Data	No Data

Table 59
(Cont.)

Group of Samples B (Mw(THEO) = 7,000 g/mol)									
Sample	**Sample Fraction**	**Wave number NH (cm^{-1})**	**Wave number CH_3 (cm^{-1})**	**Wave number CH_2 (cm^{-1})**	**Wave number C=O (cm^{-1})**	**Wave number NH (cm^{-1})**	**Wave number $CH(CH_3)_2$ und CH_2 (cm^{-1})**	**Wave number $CH(CH_3)_2$ (cm^{-1})**	**Wave number CN (cm^{-1})**
CCH-C1(2)-2	CCH-C1(2)-2(1)	No Data	No Data	No Data	No Data	No Data	No Data	No Data	No Data
	CCH-C1(2)-2(2)	3,438.0	2,973.2	2,934.3	1,647.8	1,544.6	1,459.0	1,386.7 and 1,367.3	1,172.6
	CCH-C1(2)-2(3)	No Data	No Data	No Data	No Data	No Data	No Data	No Data	No Data
	CCH-C1(2)-2(4)	No Data	No Data	No Data	No Data	No Data	No Data	No Data	No Data
	CCH-C1(2)-2(5)	No Data	No Data	No Data	No Data	No Data	No Data	No Data	No Data
	CCH-C1(2)-2(6)	No Data	No Data	No Data	No Data	No Data	No Data	No Data	No Data

Table 60

FTIR Measurements: Aminoterminated PNIPAAm oligomers

(Group of Samples C (Mw(Graft)$_{(THEO)}$ = 9,000 g/mol))

Group of Samples C (Mw(THEO) = 9,000 g/mol)								
Sample	**Sample Fraction**	**Wave number NH (cm^{-1})**	**Wave number CH_3 (cm^{-1})**	**Wave number CH_2 (cm^{-1})**	**Wave number C=O (cm^{-1})**	**Wave number NH (cm^{-1})**	**Wave number $CH(CH_3)_2$ und CH_2 (cm^{-1})**	**Wave number $CH(CH_3)_2$ (cm^{-1})**	**Wave number CN (cm^{-1})**
CCH-B4-2	CCH-B4-2	3,438.1	2,973.9	2,935.4	1,649.1	1,548.3	1,459.6	1,387.8 and 1,367.9	1,172.5
CCH-C1-3	CCH-C1-3(1)	No Data	No Data	No Data	No Data	No Data	No Data	No Data	No Data
	CCH-C1-3(2)	3,438.4	2,972.9	2,934.7	1,649.2	1,542.1	1,459.0	1,386.7 and 1,366.9	1,172.9

Table 60
(Cont.)

Group of Samples C (Mw(THEO) = 9,000 g/mol)									
Sample	**Sample Fraction**	**Wave number NH (cm^{-1})**	**Wave number CH_3 (cm^{-1})**	**Wave number CH_2 (cm^{-1})**	**Wave number C=O (cm^{-1})**	**Wave number NH (cm^{-1})**	**Wave number $CH(CH_3)_2$ und CH_2 (cm^{-1})**	**Wave number $CH(CH_3)_2$ (cm^{-1})**	**Wave number CN (cm^{-1})**
CCH-C1(2)-3	CCH-C1(2)-3(1)	3,439.3	2,974.5	2,935.8	1,649.2	1,549.5	1,459.9	1,387.7 and 1,368.1	1,172.4
	CCH-C1(2)-3(2)	No Data	No Data	No Data	No Data	No Data	No Data	No Data	No Data
	CCH-C1(2)-3(3)	No Data	No Data	No Data	No Data	No Data	No Data	No Data	No Data
	CCH-C1(2)-3(4)	No Data	No Data	No Data	No Data	No Data	No Data	No Data	No Data
	CCH-C1(2)-3(5)	No Data	No Data	No Data	No Data	No Data	No Data	No Data	No Data
	CCH-C1(2)-3(6)	No Data	No Data	No Data	No Data	No Data	No Data	No Data	No Data

Table 60
(Cont.)

Group of Samples C (Mw(THEO) = 9,000 g/mol)									
Sample	**Sample Fraction**	**Wave number NH (cm^{-1})**	**Wave number CH_3 (cm^{-1})**	**Wave number CH_2 (cm^{-1})**	**Wave number C=O (cm^{-1})**	**Wave number NH (cm^{-1})**	**Wave number $CH(CH_3)_2$ und CH_2 (cm^{-1})**	**Wave number $CH(CH_3)_2$ (cm^{-1})**	**Wave number CN (cm^{-1})**
CCH-C1(2)-3.2	CCH-C1(2)-3.2(1)	3,436.2	2,972.3	2,934.0	1,649.1	1,541.5	1,458.8	1,386.9 and 1,367.1	1,172.9
	CCH-C1(2)-3.2(2)	No Data	No Data	No Data	No Data	No Data	No Data	No Data	No Data
	CCH-C1(2)-3.2(3)	No Data	No Data	No Data	No Data	No Data	No Data	No Data	No Data
	CCH-C1(2)-3.2(4)	No Data	No Data	No Data	No Data	No Data	No Data	No Data	No Data
	CCH-C1(2)-3.2(5)	No Data	No Data	No Data	No Data	No Data	No Data	No Data	No Data
	CCH-C1(2)-3.2(6)	No Data	No Data	No Data	No Data	No Data	No Data	No Data	No Data

Table 60
(Cont.)

Group of Samples C (Mw(THEO) = 9,000 g/mol)									
Sample	**Sample Fraction**	**Wave number NH (cm^{-1})**	**Wave number CH_3 (cm^{-1})**	**Wave number CH_2 (cm^{-1})**	**Wave number C=O (cm^{-1})**	**Wave number NH (cm^{-1})**	**Wave number $CH(CH_3)_2$ und CH_2 (cm^{-1})**	**Wave number $CH(CH_3)_2$ (cm^{-1})**	**Wave number CN (cm^{-1})**
CCH-C1(2)-3.3	CCH-C1(2)-3.3(1)	No Data	No Data	No Data	No Data	No Data	No Data	No Data	No Data
	CCH-C1(2)-3.3(2)	No Data	No Data	No Data	No Data	No Data	No Data	No Data	No Data
	CCH-C1(2)-3.3(3)	No Data	No Data	No Data	No Data	No Data	No Data	No Data	No Data
	CCH-C1(2)-3.3(4)	No Data	No Data	No Data	No Data	No Data	No Data	No Data	No Data
	CCH-C1(2)-3.3(5)	No Data	No Data	No Data	No Data	No Data	No Data	No Data	No Data
	CCH-C1(2)-3.3(6)	3,437.5	2,972.1	2,933.9	1,649.0	1,540.8	1,458.6	1,386.7 and 1,366.8	1,172.9

Table 61

NMR Measurements: Aminoterminated PNIPAAm oligomers

(Group of Samples A ($Mw_{(THEO)}$ = 5,000 g/mol))

Group of Samples A ($Mw_{(THEO)}$ = 5,000 g/mol)							
Sample	**Sample Fraction**	**Chemical Shift (δ) CHNH (cm^{-1})**	**Chemical Shift (δ) CHCO (cm^{-1})**	**Chemical Shift (δ) SCH_2CH (cm^{-1})**	**Chemical Shift (δ) CH (cm^{-1})**	**Chemical Shift (δ) CH_2 (cm^{-1})**	**Chemical Shift (δ) CH_3 (cm^{-1})**
CCH-A15-1	CCH-A15-1	3.983	2.474	2.121	1.801	1.626	1.124
CCH-A15-2	CCH-A15-2	3.970	3.086	2.113	1.787	1.612	1.113
CCH-A15-3	CCH-A15-3	3.973	2.982	2.108	1.787	1.611	1.115
CCH-C1-1	CCH-C1-1(1)	3.975	2.836	2.109	1.791	1.612	1.117
	CCH-C1-1(2)	3.977	2.839	2.112	1.797	1.613	1.117

Table 61
(Cont.)

Group of Samples A (Mw(THEO) = 5,000 g/mol)							
Sample	**Sample Fraction**	**Chemical Shift (δ) CHNH (cm^{-1})**	**Chemical Shift (δ) CHCO (cm^{-1})**	**Chemical Shift (δ) SCH_2CH (cm^{-1})**	**Chemical Shift (δ) CH (cm^{-1})**	**Chemical Shift (δ) CH_2 (cm^{-1})**	**Chemical Shift (δ) CH_3 (cm^{-1})**
CCH-C1(2)-1	CCH-C1(2)-1(1)	3.986	2.225	2.225	1.819	1.626	1.125
	CCH-C1(2)-1(2)	3.986	2.332	2.127	1.823	1.617	1.124
	CCH-C1(2)-1(3)	3.973	2.880	2.110	1.793	1.613	1.116
	CCH-C1(2)-1(4)	3.973	3.005	2.098	1.790	1.611	1.115
	CCH-C1(2)-1(5)	3.978	2.823	2.113	1.799	1.617	1.119
	CCH-C1(2)-1(6)	3.980	2.719	2.120	1.805	1.616	1.121

Table 62

NMR Measurements: Aminoterminated PNIPAAm oligomers

(Group of Samples A (Mw(Graft)$_{(THEO)}$ = 7,000 g/mol))

Group of Samples B (Mw(THEO) = 7,000 g/mol)							
Sample	**Sample Fraction**	**Chemical Shift (δ) CHNH (cm^{-1})**	**Chemical Shift (δ) CHCO (cm^{-1})**	**Chemical Shift (δ) SCH_2CH (cm^{-1})**	**Chemical Shift (δ) CH (cm^{-1})**	**Chemical Shift (δ) CH_2 (cm^{-1})**	**Chemical Shift (δ) CH_3 (cm^{-1})**
CCH-B4-1	CCH-B4-1	3.978	2.697	2.107	1.795	1.614	1.119
CCH-C1-2	CCH-C1-2(1)	3.985	2.169	2.169	1.807	1.619	1.125
	CCH-C1-2(2)	3.978	2.690	2.112	1.810	1.616	1.119

Table 62
(Cont.)

Group of Samples B (Mw(THEO) = 7,000 g/mol)								
Sample	**Sample Fraction**	**Chemical Shift (δ) CHNH (cm^{-1})**	**Chemical Shift (δ) CHCO (cm^{-1})**	**Chemical Shift (δ) SCH_2CH (cm^{-1})**	**Chemical Shift (δ) CH (cm^{-1})**	**Chemical Shift (δ) CH_2 (cm^{-1})**	**Chemical Shift (δ) CH_3 (cm^{-1})**
CCH-C1(2)-2	CCH-C1(2)-2(1)	3.971	3.041	2.104	1.789	1.612	1.113
	CCH-C1(2)-2(2)	No Data	No Data	No Data	No Data	No Data	No Data
	CCH-C1(2)-2(3)	3.980	2.798	2.112	1.794	1.613	1.118
	CCH-C1(2)-2(4)	3.972	2.933	2.108	1.789	1.613	1.115
	CCH-C1(2)-2(5)	3.979	2.757	2.112	1.797	1.613	1.118
	CCH-C1(2)-2(6)	3.970	3.077	2.106	1.787	1.613	1.113

Table 63

NMR Measurements: Aminoterminated PNIPAAm oligomers

(Group of Samples C (Mw(Graft)$_{(THEO)}$ = 9,000 g/mol))

Group of Samples C (Mw(THEO) = 9,000 g/mol)							
Sample	**Sample Fraction**	**Chemical Shift (δ) CHNH (cm^{-1})**	**Chemical Shift (δ) CHCO (cm^{-1})**	**Chemical Shift (δ) SCH_2CH (cm^{-1})**	**Chemical Shift (δ) CH (cm^{-1})**	**Chemical Shift (δ) CH_2 (cm^{-1})**	**Chemical Shift (δ) CH_3 (cm^{-1})**
CCH-B4-2	CCH-B4-2	3.979	2.715	2.114	1.800	1.616	1.119
CCH-C1-3	CCH-C1-3(1)	3.977	2.668	2.114	1.795	1.618	1.118
	CCH-C1-3(2)	3.977	2.762	2.112	1.795	1.617	1.117

Table 63
(Cont.)

Group of Samples C (Mw(THEO) = 9,000 g/mol)							
Sample	**Sample Fraction**	**Chemical Shift (δ) CHNH (cm^{-1})**	**Chemical Shift (δ) CHCO (cm^{-1})**	**Chemical Shift (δ) SCH_2CH (cm^{-1})**	**Chemical Shift (δ) CH (cm^{-1})**	**Chemical Shift (δ) CH_2 (cm^{-1})**	**Chemical Shift (δ) CH_3 (cm^{-1})**
CCH-C1(2)-3	CCH-C1(2)-3(1)	3.981	2.550	2.109	1.799	1.618	1.122
	CCH-C1(2)-3(2)	3.978	2.636	2.113	1.800	1.616	1.119
	CCH-C1(2)-3(3)	No Data	No Data	No Data	No Data	No Data	No Data
	CCH-C1(2)-3(4)	3.983	2.578	2.116	1.807	1.618	1.122
	CCH-C1(2)-3(5)	3.980	2.584	2.097	1.802	1.613	1.121
	CCH-C1(2)-3(6)	3.980	2.576	2.107	1.800	1.622	1.121

Table 63
(Cont.)

Group of Samples C (Mw(THEO) = 9,000 g/mol)								
Sample	**Sample Fraction**	**Chemical Shift (δ) CHNH (cm^{-1})**	**Chemical Shift (δ) CHCO (cm^{-1})**	**Chemical Shift (δ) SCH_2CH (cm^{-1})**	**Chemical Shift (δ) CH (cm^{-1})**	**Chemical Shift (δ) CH_2 (cm^{-1})**	**Chemical Shift (δ) CH_3 (cm^{-1})**
CCH-C1(2)-3.2	CCH-C1(2)-3.2(1)	3.984	2.279	2.110	1.816	1.620	1.124
	CCH-C1(2)-3.2(2)	3.981	2.393	2.104	1.808	1.622	1.123
	CCH-C1(2)-3.2(3)	3.983	2.481	2.115	1.807	1.619	1.122
	CCH-C1(2)-3.2(4)	3.980	2.400	2.104	1.802	1.622	1.123
	CCH-C1(2)-3.2(5)	3.987	2.503	2.107	1.805	1.620	1.123
	CCH-C1(2)-3.2(6)	3.983	2.262	2.120	1.839	1.622	1.124

Table 63
(Cont.)

Group of Samples C (Mw(THEO) = 9,000 g/mol)							
Sample	**Sample Fraction**	**Chemical Shift (δ) CHNH (cm^{-1})**	**Chemical Shift (δ) CHCO (cm^{-1})**	**Chemical Shift (δ) SCH_2CH (cm^{-1})**	**Chemical Shift (δ) CH (cm^{-1})**	**Chemical Shift (δ) CH_2 (cm^{-1})**	**Chemical Shift (δ) CH_3 (cm^{-1})**
CCH-C1(2)-3.3	CCH-C1(2)-3.3(1)	3.983	2.426	2.109	1.805	1.618	1.123
	CCH-C1(2)-3.3(2)	3.981	2.552	2.099	1.806	1.621	1.121
	CCH-C1(2)-3.3(3)	3.981	2.416	2.127	1.806	1.619	1.123
	CCH-C1(2)-3.3(4)	3.979	2.776	2.104	1.796	1.613	1.118
	CCH-C1(2)-3.3(5)	3.984	2.379	2.102	1.808	1.620	1.123
	CCH-C1(2)-3.3(6)	3.984	2.431	2.116	1.801	1.621	1.122

Table 64

DSC (Dry) Measurements: Aminoterminated PNIPAAm oligomers

(Group of Samples A (Mw(Graft)(THEO) = 5,000 g/mol))

Group of Samples A (Mw(THEO) = 5,000 g/mol)				
Sample	**Sample Fraction**	**Tm (°C)**	**ΔHm (J/g)**	**Tg (°C)**
CCH-A15-1	CCH-A15-1	191	Not measured	94.5
CCH-A15-2	CCH-A15-2	No Data	No Data	No Data
CCH-A15-3	CCH-A15-3	209.5	Not measured	103
CCH-C1-1	CCH-C1-1(1)	No Data	No Data	No Data
	CCH-C1-1(2)	No Data	No Data	No Data
CCH-C1(2)-1	CCH-C1(2)-1(1)	No Data	No Data	No Data
	CCH-C1(2)-1(2)	No Data	No Data	No Data
	CCH-C1(2)-1(3)	175.2	159	82.9
	CCH-C1(2)-1(4)	No Data	No Data	No Data
	CCH-C1(2)-1(5)	No Data	No Data	No Data
	CCH-C1(2)-1(6)	No Data	No Data	No Data

Table 65

DSC (Dry) Measurements: Aminoterminated PNIPAAm oligomers

(Group of Samples A (Mw(THEO) = 7,000 g/mol))

Group of Samples B (Mw(THEO) = 7,000 g/mol)				
Sample	**Sample Fraction**	**Tm (°C)**	**ΔHm (J/g)**	**Tg (°C)**
CCH-B4-1	CCH-B4-1	187	Not measured	98
CCH-C1-2	CCH-C1-2(1)	No Data	No Data	No Data
	CCH-C1-2(2)	No Data	No Data	No Data

Table 65

(Cont.)

Group of Samples B (Mw(THEO) = 7,000 g/mol)				
Sample	**Sample Fraction**	**Tm (°C)**	**ΔHm (J/g)**	**Tg (°C)**
CCH-C1(2)-2	CCH-C1(2)-2(1)	No Data	No Data	No Data
	CCH-C1(2)-2(2)	217.1	150	99.8
	CCH-C1(2)-2(3)	No Data	No Data	No Data
	CCH-C1(2)-2(4)	No Data	No Data	No Data
	CCH-C1(2)-2(5)	No Data	No Data	No Data
	CCH-C1(2)-2(6)	No Data	No Data	No Data

Table 66

DSC (Dry) Measurements: Aminoterminated PNIPAAm oligomers

(Group of Samples C ($Mw_{(THEO)}$ = 9,000 g/mol))

Group of Samples C (Mw(THEO) = 9,000 g/mol)				
Sample	**Sample Fraction**	**Tm (°C)**	**ΔHm (J/g)**	**Tg (°C)**
CCH-B4-2	CCH-B4-2	172	Not measured	88
CCH-C1-3	CCH-C1-3(1)	No Data	No Data	No Data
	CCH-C1-3(2)	No Data	No Data	No Data

Table 66

(Cont.)

Group of Samples C (Mw(THEO) = 9,000 g/mol)				
Sample	**Sample Fraction**	**Tm (°C)**	**ΔHm (J/g)**	**Tg (°C)**
CCH-C1(2)-3	CCH-C1(2)-3(1)	202.6	159	95.3
	CCH-C1(2)-3(2)	168.5	244	70.4
	CCH-C1(2)-3(3)	No Data	No Data	No Data
	CCH-C1(2)-3(4)	No Data	No Data	No Data
	CCH-C1(2)-3(5)	No Data	No Data	No Data
	CCH-C1(2)-3(6)	No Data	No Data	No Data
CCH-C1(2)-3.2	CCH-C1(2)-3.2(1)	No Data	No Data	No Data
	CCH-C1(2)-3.2(2)	No Data	No Data	No Data
	CCH-C1(2)-3.2(3)	No Data	No Data	No Data
	CCH-C1(2)-3.2(4)	No Data	No Data	No Data
	CCH-C1(2)-3.2(5)	No Data	No Data	No Data
	CCH-C1(2)-3.2(6)	No Data	No Data	No Data

Table 66

(Cont.)

Group of Samples C (Mw(THEO) = 9,000 g/mol)				
Sample	**Sample Fraction**	**Tm (°C)**	**ΔHm (J/g)**	**Tg (°C)**
CCH-C1(2)-3.3	CCH-C1(2)-3.3(1)	No Data	No Data	No Data
	CCH-C1(2)-3.3(2)	No Data	No Data	No Data
	CCH-C1(2)-3.3(3)	No Data	No Data	No Data
	CCH-C1(2)-3.3(4)	No Data	No Data	No Data
	CCH-C1(2)-3.3(5)	No Data	No Data	No Data
	CCH-C1(2)-3.3(6)	No Data	No Data	No Data

Table 67

DSC (Aqueous) Measurements in water: Aminoterminated PNIPAAm oligomers

(Group of Samples A (Mw(Graft)(THEO) = 5,000 g/mol))

Group of Samples A (Mw(THEO) = 5,000 g/mol)			
Sample	**Sample Fraction**	**LCST Heating Cycle (°C)**	**LCST Cooling Cycle (°C)**
CCH-A15-1	CCH-A15-1	38.5	39
CCH-A15-2	CCH-A15-2	40	40
CCH-A15-3	CCH-A15-3	38	39
CCH-C1-1	CCH-C1-1(1)	38	41
	CCH-C1-1(2)	38	39

Table 67

(Cont.)

Group of Samples A (Mw(THEO) = 5,000 g/mol)			
Sample	**Sample Fraction**	**LCST Heating Cycle (°C)**	**LCST Cooling Cycle (°C)**
CCH-C1(2)-1	CCH-C1(2)-1(1)	39	40
	CCH-C1(2)-1(2)	39	40
	CCH-C1(2)-1(3)	No Data	No Data
	CCH-C1(2)-1(4)	38	38
	CCH-C1(2)-1(5)	37.5	37.8
	CCH-C1(2)-1(6)	38	40

Table 68

DSC (Aqueous) Measurements in water: Aminoterminated PNIPAAm oligomers

(Group of Samples A (Mw(Graft)$_{(THEO)}$ = 7,000 g/mol))

Group of Samples B (Mw(THEO) = 7,000 g/mol)			
Sample	**Sample Fraction**	**LCST Heating Cycle (°C)**	**LCST Cooling Cycle (°C)**
CCH-B4-1	CCH-B4-1	40.5	38
CCH-C1-2	CCH-C1-2(1)	38	32
	CCH-C1-2(2)	39	38

Table 68

(Cont.)

Group of Samples B (Mw(THEO) = 7,000 g/mol)			
Sample	**Sample Fraction**	**LCST Heating Cycle (°C)**	**LCST Cooling Cycle (°C)**
CCH-C1(2)-2	CCH-C1(2)-2(1)	37	37
	CCH-C1(2)-2(2)	No Data	No Data
	CCH-C1(2)-2(3)	38	39
	CCH-C1(2)-2(4)	37.4	36.8
	CCH-C1(2)-2(5)	37	38
	CCH-C1(2)-2(6)	37	37

Table 69

DSC (Aqueous) Measurements in water: Aminoterminated PNIPAAm oligomers

(Group of Samples C (Mw(Graft)$_{(THEO)}$ = 9,000 g/mol))

Group of Samples C (Mw(THEO) = 9,000 g/mol)			
Sample	**Sample Fraction**	**LCST Heating Cycle (°C)**	**LCST Cooling Cycle (°C)**
CCH-B4-2	CCH-B4-2	38	38.5
CCH-C1-3	CCH-C1-3(1)	38	37
	CCH-C1-3(2)	37	35

Table 69

(Cont.)

Group of Samples C (Mw(THEO) = 9,000 g/mol)			
Sample	**Sample Fraction**	**LCST Heating Cycle (°C)**	**LCST Cooling Cycle (°C)**
CCH-C1(2)-3	CCH-C1(2)-3(1)	No Data	No Data
	CCH-C1(2)-3(2)	No Data	No Data
	CCH-C1(2)-3(3)	No Data	No Data
	CCH-C1(2)-3(4)	39	34.5
	CCH-C1(2)-3(5)	36	39
	CCH-C1(2)-3(6)	38	40
CCH-C1(2)-3.2	CCH-C1(2)-3.2(1)	38.5	38
	CCH-C1(2)-3.2(2)	37.5	39
	CCH-C1(2)-3.2(3)	38	39
	CCH-C1(2)-3.2(4)	38	40.5
	CCH-C1(2)-3.2(5)	37	40.5
	CCH-C1(2)-3.2(6)	38	35

Table 69

(Cont.)

Group of Samples C (Mw(THEO) = 9,000 g/mol)			
Sample	**Sample Fraction**	**LCST Heating Cycle (°C)**	**LCST Cooling Cycle (°C)**
CCH-C1(2)-3.3	CCH-C1(2)-3.3(1)	38	35
	CCH-C1(2)-3.3(2)	38	40
	CCH-C1(2)-3.3(3)	38	40
	CCH-C1(2)-3.3(4)	38	38
	CCH-C1(2)-3.3(5)	35.4	39.1
	CCH-C1(2)-3.3(6)	37	40

Table 70

FTIR Measurements: CMC-g-PNIPAAm graft copolymers

(Group of Samples A (Mw(Graft)$_{(THEO)}$ = 5,000 g/mol))

Group of Samples A (Mw(Graft)(THEO) = 5,000 g/mol)											
Sub-Group A.1 (%Graft(THEO)=40%)											
Sample	**Sample Fraction**	**Wave number NH und OH (cm^{-1})**	**Wave number CH_3 (cm^{-1})**	**Wave number CH_2 (cm^{-1})**	**Wave number C=O (cm^{-1})**	**Wave number NH (cm^{-1})**	**Wave number $CH(CH_3)_2$ und CH_2 (cm^{-1})**	**Wave number CH_2 (cm^{-1})**	**Wave number $CH(CH_3)_2$ (cm^{-1})**	**Wave number CN (cm^{-1})**	**Wave number –O– (cm^{-1})**
CCH-A27-1	CCH-A27-1(1)	3,442.4	2,973.1	2,931.7	1,647.1	1,570.0	1,460.0	1,419.8	1,395.0	1,160.0	1,061.1
	CCH-A27-1(2)	3,448.3	2,973.4	2,932.5	1,637.7	1,565.0	1,462.0	1,420.0	1,390.0	1,160.0	1,060.6
	CCH-A27-1(3)	3,449.1	2,973.6	2,940.0	1,637.7	1,570.0	1,465.0	1,420.2	1,390.0	1,160.0	1,061.9
	CCH-A27-1(4)	3,442.1	2,972.8	2,930.6	1,637.8	1,560.0	1,463.0	1,419.8	1,380.0	1,170.0	1,061.4
	CCH-A27-1(5)	3,448.9	2,973.2	2,932.4	1,637.6	1,570.0	1,465.0	1,420.0	1,390.0	1,160.0	1,061.8
CCH-C2-1.40	CCH-C2-1.40	3,442.5	2,971.0	2,940.0	1,629.9	Not detected	Not detected	Not detected	1,384.1	1,170.0	1,061.4

Table 70
(Cont.)

Group of Samples A (Mw(Graft)(THEO) = 5,000 g/mol)											
Sub-Group A.1 (%Graft(THEO)=40%)											
Sample	Sample Fraction	Wave number NH und OH (cm^{-1})	Wave number CH_3 (cm^{-1})	Wave number CH_2 (cm^{-1})	Wave number C=O (cm^{-1})	Wave number NH (cm^{-1})	Wave number $CH(CH_3)_2$ und CH_2 (cm^{-1})	Wave number CH_2 (cm^{-1})	Wave number $CH(CH_3)_2$ (cm^{-1})	Wave number CN (cm^{-1})	Wave number –O– (cm^{-1})
CCH-C2(2)-1.40	CCH-C2(2)-1.40(1)	3,442.2	2,972.6	2,935.0	1,631.2	1,550.0	1,470.0	1,420.0	1,384.2	1,170.0	1,058.5
	CCH-C2(2)-1.40(2)	3,434.3	2,972.4	2,949.0	1,632.7	1,560.0	1,465.0	1,413.7	1,385.0	1,170.0	1,061.6
	CCH-C2(2)-1.40(3)	3,434.2	2,972.1	2,928.3	1,644.7	1,557.6	1,455.7	1,425.0	1,385.0	1,170.0	1,057.5
	CCH-C2(2)-1.40(4)	3,433.6	2,972.3	2,930.9	1,638.1	1,560.8	1,459.5	1,413.0	1,385.0	1,170.0	1,060.9

Table 70

(Cont.)

Group of Samples A (Mw(Graft)(THEO) = 5,000 g/mol)											
Sub-Group A.2 (%Graft(THEO)=50%)											
Sample	**Sample Fraction**	**Wave number NH und OH (cm^{-1})**	**Wave number CH_3 (cm^{-1})**	**Wave number CH_2 (cm^{-1})**	**Wave number C=O (cm^{-1})**	**Wave number NH (cm^{-1})**	**Wave number $CH(CH_3)_2$ und CH_2 (cm^{-1})**	**Wave number CH_2 (cm^{-1})**	**Wave number $CH(CH_3)_2$ (cm^{-1})**	**Wave number CN (cm^{-1})**	**Wave number –O– (cm^{-1})**
CCH-B5-1.50	CCH-B5-1.50	3,441.9	2,971.9	2,940.0	1,637.3	1,570.0	1,465.0	Not detected	1,384.4	1,170.0	1,059.2
CCH-C2(2)-1.50	CCH-C2(2)-1.50(1)	3,433.6	2,972.3	2,930.0	1,640.8	1,547.1	1,460.5	1,420.0	1,385.2	1,170.0	1,060.9
	CCH-C2(2)-1.50(2)	3,442.4	2,973.5	2,929.7	1,637.6	1,560.4	1,458.9	Not detected	1,387.5	1,170.0	1,061.3
	CCH-C2(2)-1.50(3)	3,434.9	2,972.9	2,930.7	1,640.3	1,551.0	1,459.5	Not detected	1,386.7	1,156.5	1,060.2
	CCH-C2(2)-1.50(4)	3,433.2	2,972.2	2,932.3	1,642.5	1,547.6	1,460.2	1,420.0	1,386.9	1,170.0	1,061.3
	CCH-C2(2)-1.50(5)	3,433.9	2,972.6	2,931.0	1,639.0	1,547.0	1,460.5	Not detected	1,385.1	1,170.0	1,061.9

Table 70

(Cont.)

Group of Samples A (Mw(Graft)(THEO) = 5,000 g/mol)											
Sub-Group A.3 (%Graft(THEO)=80%)											
Sample	**Sample Fraction**	**Wave number NH und OH (cm^{-1})**	**Wave number CH_3 (cm^{-1})**	**Wave number CH_2 (cm^{-1})**	**Wave number C=O (cm^{-1})**	**Wave number NH (cm^{-1})**	**Wave number $CH(CH_3)_2$ und CH_2 (cm^{-1})**	**Wave number CH_2 (cm^{-1})**	**Wave number $CH(CH_3)_2$ (cm^{-1})**	**Wave number CN (cm^{-1})**	**Wave number –O– (cm^{-1})**
CCH-C2(2)-1.80	CCH-C2(2)-1.80(1)	3,441.6	2,973.1	2,929.6	1,637.5	1,545.8	1,458.8	Not detected	1,386.4	1,172.5	1,061.6
	CCH-C2(2)-1.80(2)	3,434.6	2,972.2	2,932.9	1,649.1	1,544.2	1,459.4	Not detected	1,387.0	1,172.3	1,062.5
	CCH-C2(2)-1.80(3)	3,435.6	2,974.0	2,934.8	1,647.6	1,550.6	1,459.5	Not detected	1,387.9	1,172.1	1,062.6
	CCH-C2(2)-1.80(4)	3,457.8	2,974.5	2,933.0	1,646.9	1,551.7	1,460.1	Not detected	1,387.8	1,172.3	1,062.6
	CCH-C2(2)-1.80(5)	3,434.6	2,972.4	2,933.6	1,649.0	1,546.4	1,460.0	Not detected	1,387.2	1,172.2	1,062.7

Table 70

(Cont.)

Group of Samples A (Mw(Graft)(THEO) = 5,000 g/mol)											
Sub-Group A.3 (%Graft(THEO)=80%)											
Sample	**Sample Fraction**	**Wave number NH und OH (cm^{-1})**	**Wave number CH_3 (cm^{-1})**	**Wave number CH_2 (cm^{-1})**	**Wave number C=O (cm^{-1})**	**Wave number NH (cm^{-1})**	**Wave number $CH(CH_3)_2$ und CH_2 (cm^{-1})**	**Wave number CH_2 (cm^{-1})**	**Wave number $CH(CH_3)_2$ (cm^{-1})**	**Wave number CN (cm^{-1})**	**Wave number –O– (cm^{-1})**
CCH-C2(2)-1.80	CCH-C2(2)-1.80(6)	3,435.5	2,973.2	2,934.2	1,641.8	1,546.7	1,460.2	Not detected	1,387.7	1,172.3	1,062.0
	CCH-C2(2)-1.80(7)	3,433.4	2,972.2	2,933.3	1,642.2	1,546.7	1,460.3	Not detected	1,386.5	1,172.2	1,061.9
	CCH-C2(2)-1.80(8)	3,442.1	2,973.9	2,933.0	1,647.5	1,550.7	1,459.3	Not detected	1,387.4	1,172.2	1,060.0
	CCH-C2(2)-1.80(9)	3,442.0	2,974.1	2,934.8	1,640.7	1,550.7	1,459.7	Not detected	1,386.5	1,172.4	1,062.9
	CCH-C2(2)-1.80(10)	No Data	No Data	No Data	No Data	No Data	No Data	No Data	No Data	No Data	No Data

Table 71

FTIR Measurements: CMC-g-PNIPAAm graft copolymers

(Group of Samples B (Mw(Graft)$_{(THEO)}$ = 7,000 g/mol))

Group of Samples B (Mw(Graft)$_{(THEO)}$ = 7,000 g/mol)											
Sub-Group B.1 (%Graft(THEO)=40%)											
Sample	**Sample Fraction**	**Wave number NH und OH (cm^{-1})**	**Wave number CH_3 (cm^{-1})**	**Wave number CH_2 (cm^{-1})**	**Wave number C=O (cm^{-1})**	**Wave number NH (cm^{-1})**	**Wave number $CH(CH_3)_2$ und CH_2 (cm^{-1})**	**Wave number CH_2 (cm^{-1})**	**Wave number $CH(CH_3)_2$ (cm^{-1})**	**Wave number CN (cm^{-1})**	**Wave number –O– (cm^{-1})**
CCH-B5-2.40	CCH-B5-2.40	3,434.3	2,970.0	2,927.6	1,630.0	1,550.0	1,465.0	Not detected	1,384.4	1,165.0	1,062.2
CCH-C2(2)-2.40	CCH-C2(2)-2.40(1)	3,433.4	2,971.6	2,929.4	1,637.3	1,546.0	1,458.9	1,420.0	1,385.6	1,165.0	1,060.4
	CCH-C2(2)-2.40(2)	3,434.3	2,972.3	2,925.0	1,637.2	1,570.0	1,458.4	1,420.0	1,385.0	1,165.0	1,055.9
	CCH-C2(2)-2.40(3)	3,433.0	2,972.4	2,930.9	1,640.4	1,547.2	1,460.1	1,413.5	1,388.0	1,165.0	1,061.7
	CCH-C2(2)-2.40(4)	No Data	No Data	No Data	No Data	No Data	No Data	No Data	No Data	No Data	No Data
	CCH-C2(2)-2.40(5)	No Data	No Data	No Data	No Data	No Data	No Data	No Data	No Data	No Data	No Data

Table 71
(Cont.)

Group of Samples B (Mw(Graft)(THEO) = 7,000 g/mol)											
		Sub-Group B.2 (%Graft(THEO)=50%)									
Sample	Sample Fraction	Wave number NH und OH (cm^{-1})	Wave number CH_3 (cm^{-1})	Wave number CH_2 (cm^{-1})	Wave number C=O (cm^{-1})	Wave number NH (cm^{-1})	Wave number $CH(CH_3)_2$ und CH_2 (cm^{-1})	Wave number CH_2 (cm^{-1})	Wave number $CH(CH_3)_2$ (cm^{-1})	Wave number CN (cm^{-1})	Wave number –O– (cm^{-1})
CCH-B5-2.50	CCH-B5-2.50	3,449.0	2,972.7	2,930.0	1,641.6	1,560.0	1,460.0	1,420.0	1,384.7	1,165.0	1,060.5
CCH-C2(2)-2.50	CCH-C2(2)-2.50(1)	3,433.7	2,972.4	2,932.3	1,642.3	1,547.3	1,460.1	1,420.0	1,386.9	1,165.0	1,060.6
	CCH-C2(2)-2.50(2)	3,448.6	2,973.4	2,935.0	1,637.6	1,565.0	1,458.7	1,420.0	1,390.0	1,165.0	1,061.8
	CCH-C2(2)-2.50(3)	3,433.2	2,972.0	2,932.0	1,640.6	1,546.4	1,459.6	1,420.0	1,387.2	1,165.0	1,061.7
	CCH-C2(2)-2.50(4)	3,432.8	2,971.5	2,940.0	1,639.4	1,546.8	1,460.0	1,425.0	1,385.3	1,165.0	1,061.0

Table 71

(Cont.)

Group of Samples B (Mw(Graft)(THEO) = 7,000 g/mol)											
Sub-Group B.3 (%Graft(THEO)=80%)											
Sample	**Sample Fraction**	**Wave number NH und OH (cm^{-1})**	**Wave number CH_3 (cm^{-1})**	**Wave number CH_2 (cm^{-1})**	**Wave number C=O (cm^{-1})**	**Wave number NH (cm^{-1})**	**Wave number $CH(CH_3)_2$ und CH_2 (cm^{-1})**	**Wave number CH_2 (cm^{-1})**	**Wave number $CH(CH_3)_2$ (cm^{-1})**	**Wave number CN (cm^{-1})**	**Wave number –O– (cm^{-1})**
CCH-C2(2)-2.80	CCH-C2(2)-2.80(1)	3,434.5	2,972.6	2,933.3	1,642.7	1,546.7	1,459.9	Not detected	1,387.2	1,172.4	1,062.6
	CCH-C2(2)-2.80(2)	3,434.8	2,972.2	2,931.9	1,648.0	1,544.9	1,459.4	Not detected	1,387.0	1,172.4	1,062.2
	CCH-C2(2)-2.80(3)	3,434.7	2,972.3	2,933.5	1,642.3	1,547.0	1,460.6	Not detected	1,386.8	1,172.4	1,062.0
	CCH-C2(2)-2.80(4)	3,434.7	2,972.4	2,933.8	1,642.3	1,547.0	1,460.4	Not detected	1,387.0	1,172.5	1,062.6
	CCH-C2(2)-2.80(5)	3,434.2	2,972.3	2,931.3	1,641.9	1,545.0	1,459.2	Not detected	1,386.6	1,172.5	1,062.4
	CCH-C2(2)-2.80(6)	3,434.9	2,972.9	2,935.0	1,637.6	1,546.4	1,459.3	Not detected	1,385.7	1,172.3	1,061.7
	CCH-C2(2)-2.80(7)	3,435.0	2,972.4	2,933.4	1,641.5	1,547.0	1,460.3	Not detected	1,386.6	1,172.3	1,061.8

Table 72

FTIR Measurements: CMC-g-PNIPAAm graft copolymers

(Group of Samples C (Mw(Graft)(THEO) = 9,000 g/mol))

Group of Samples C (Mw(Graft)(THEO) = 9,000 g/mol)											
Sub-Group C.1 (%Graft(THEO)=40%)											
Sample	**Sample Fraction**	**Wave number NH und OH (cm^{-1})**	**Wave number CH_3 (cm^{-1})**	**Wave number CH_2 (cm^{-1})**	**Wave number C=O (cm^{-1})**	**Wave number NH (cm^{-1})**	**Wave number $CH(CH_3)_2$ und CH_2 (cm^{-1})**	**Wave number CH_2 (cm^{-1})**	**Wave number $CH(CH_3)_2$ (cm^{-1})**	**Wave number CN (cm^{-1})**	**Wave number –O– (cm^{-1})**
CCH-B5-3.40	CCH-B5-3.40	3,433.8	2,970.0	2,923.8	1,631.1	1,550.0	1,465.0	1,425.0	1,384.3	1,165.0	1,059.8
CCH-C2(2)-3.40	CCH-C2(2)-3.40(1)	3,433.1	2,972.1	2,930.0	1,637.8	1,546.0	1,459.4	1,420.7	1,380.0	1,165.0	1,061.8
	CCH-C2(2)-3.40(2)	3,434.5	2,971.6	2,930.0	1,636.6	1,545.8	1,458.5	1,420.0	1,385.9	1,170.0	1,060.3
	CCH-C2(2)-3.40(3)	3,433.3	2,971.8	2,928.6	1,638.6	1,546.7	1,460.0	1,420.0	1,384.8	1,165.0	1,059.1

Table 72

(Cont.)

Group of Samples C (Mw(Graft)(THEO) = 9,000 g/mol)											
Sub-Group C.2 (%Graft(THEO)=50%)											
Sample	**Sample Fraction**	**Wave number NH und OH (cm^{-1})**	**Wave number CH_3 (cm^{-1})**	**Wave number CH_2 (cm^{-1})**	**Wave number C=O (cm^{-1})**	**Wave number NH (cm^{-1})**	**Wave number $CH(CH_3)_2$ und CH_2 (cm^{-1})**	**Wave number CH_2 (cm^{-1})**	**Wave number $CH(CH_3)_2$ (cm^{-1})**	**Wave number CN (cm^{-1})**	**Wave number –O– (cm^{-1})**
CCH-B5-3.50	CCH-B5-3.50	3,448.8	2,972.7	2,925.0	1,637.8	1,570.0	1,459.5	1,420.0	1,385.0	1,165.0	1,061.6
CCH-C2(2)-3.50	CCH-C2(2)-3.50(1)	3,434.5	2,972.2	2,929.0	1,641.4	1,547.6	1,460.1	1,420.0	1,385.4	1,170.0	1,061.0
	CCH-C2(2)-3.50(2)	3,433.6	2,971.2	2,928.0	1,637.4	1,560.5	1,458.8	Not detected	1,385.0	1,170.0	1,060.2
	CCH-C2(2)-3.50(3)	3,434.7	2,972.2	2,928.7	1,637.6	1,545.5	1,458.9	1,425.0	1,386.3	1,170.0	1,060.4

Table 72

(Cont.)

Group of Samples C (Mw(Graft)(THEO) = 9,000 g/mol)											
Sub-Group C.3 (%Graft(THEO)=80%)											
Sample	**Sample Fraction**	**Wave number NH und OH (cm^{-1})**	**Wave number CH_3 (cm^{-1})**	**Wave number CH_2 (cm^{-1})**	**Wave number C=O (cm^{-1})**	**Wave number NH (cm^{-1})**	**Wave number $CH(CH_3)_2$ und CH_2 (cm^{-1})**	**Wave number $CH(CH_3)_2$ (cm^{-1})**	**Wave number CH_2 (cm^{-1})**	**Wave number CN (cm^{-1})**	**Wave number –O– (cm^{-1})**
CCH-C2(2)-3.80	CCH-C2(2)-3.80(1)	3,433.0	2,970.0	2,918.7	1,637.5	1,560.4	1,458.7	Not detected	1,385.6	1,173.6	1,064.2
	CCH-C2(2)-3.80(2)	3,438.1	2,973.2	2,935.0	1,640.6	1,546.0	1,459.4	Not detected	1,387.4	1,172.5	1,061.7
	CCH-C2(2)-3.80(3)	3,434.8	2,974.4	2,935.0	1,647.6	1,559.9	1,458.8	Not detected	1,387.8	1,172.5	1,062.0
	CCH-C2(2)-3.80(4)	3,435.2	2,973.7	2,934.5	1,648.2	1,549.6	1,459.7	Not detected	1,387.7	1,172.3	1,062.2
	CCH-C2(2)-3.80(5)	3,435.3	2,973.1	2,933.5	1,638.2	1,546.1	1,459.7	Not detected	1,387.9	1,172.4	1,063.6
	CCH-C2(2)-3.80(6)	3,448.7	2,974.2	2,935.0	1,637.8	1,560.3	1,458.9	Not detected	1,388.0	1,172.5	1,070.0

Table 73

DSC (Dry) Measurements: CMC-g-PNIPAAm graft copolymers

(Group of Samples A (Mw(Graft)$_{(THEO)}$ = 5,000 g/mol))

Group of Samples A (Mw(Graft)(THEO) = 5,000 g/mol)					
Sub-Group A.1 (%Graft(THEO)=40%)					
Sample	**Sample Fraction**	**Tm (°C)**	**ΔHm (J/g)**	**Tg1 (°C)**	**Tg2 (°C)**
CCH-A27-1	CCH-A27-1(1)	172	Not measured	43	134
	CCH-A27-1(2)	163	Not measured	46	143
	CCH-A27-1(3)	170	Not measured	46	146
	CCH-A27-1(4)	150	Not measured	46	115
	CCH-A27-1(5)	165	Not measured	43	146
CCH-C2-1.40	CCH-C2-1.40	No Data	No Data	No Data	No Data
CCH-C2(2)-1.40	CCH-C2(2)-1.40(1)	No Data	No Data	No Data	No Data
	CCH-C2(2)-1.40(2)	No Data	No Data	No Data	No Data
	CCH-C2(2)-1.40(3)	No Data	No Data	No Data	No Data
	CCH-C2(2)-1.40(4)	No Data	No Data	No Data	No Data
CCH-B5-1.50	CCH-B5-1.50	No Data	No Data	No Data	No Data
CCH-C2(2)-1.50	CCH-C2(2)-1.50(1)	No Data	No Data	No Data	No Data
	CCH-C2(2)-1.50(2)	No Data	No Data	No Data	No Data
	CCH-C2(2)-1.50(3)	No Data	No Data	No Data	No Data
	CCH-C2(2)-1.50(4)	No Data	No Data	No Data	No Data
	CCH-C2(2)-1.50(5)	No Data	No Data	No Data	No Data

Table 73

(Cont.)

Group of Samples A (Mw(Graft)(THEO) = 5,000 g/mol)					
Sub-Group A.3 (%Graft(THEO)=80%)					
Sample	**Sample Fraction**	**Tm (°C)**	**ΔHm (J/g)**	**Tg1 (°C)**	**Tg2 (°C)**
CCH-C2(2)-1.80	CCH-C2(2)-1.80(1)	No Data	No Data	No Data	No Data
	CCH-C2(2)-1.80(2)	No Data	No Data	No Data	No Data
	CCH-C2(2)-1.80(3)	No Data	No Data	No Data	No Data
	CCH-C2(2)-1.80(4)	No Data	No Data	No Data	No Data
	CCH-C2(2)-1.80(5)	No Data	No Data	No Data	No Data
CCH-C2(2)-1.80	CCH-C2(2)-1.80(6)	No Data	No Data	No Data	No Data
	CCH-C2(2)-1.80(7)	No Data	No Data	No Data	No Data
	CCH-C2(2)-1.80(8)	No Data	No Data	No Data	No Data
	CCH-C2(2)-1.80(9)	No Data	No Data	No Data	No Data
	CCH-C2(2)-1.80(10)	No Data	No Data	No Data	No Data

Table 74

DSC (Dry) Measurements: CMC-g-PNIPAAm graft copolymers

(Group of Samples B (Mw(Graft)$_{(THEO)}$ = 7,000 g/mol))

Group of Samples B (Mw(Graft)(THEO) = 7,000 g/mol)					
Sub-Group B.1 (%Graft(THEO)=40%)					
Sample	**Sample Fraction**	**Tm (°C)**	**ΔHm (J/g)**	**Tg1 (°C)**	**Tg2 (°C)**
CCH-B5-2.40	CCH-B5-2.40	No Data	No Data	No Data	No Data
CCH-C2(2)-2.40	CCH-C2(2)-2.40(1)	No Data	No Data	No Data	No Data
	CCH-C2(2)-2.40(2)	No Data	No Data	No Data	No Data
	CCH-C2(2)-2.40(3)	No Data	No Data	No Data	No Data
	CCH-C2(2)-2.40(4)	No Data	No Data	No Data	No Data
	CCH-C2(2)-2.40(5)	No Data	No Data	No Data	No Data
CCH-B5-2.50	CCH-B5-2.50	No Data	No Data	No Data	No Data
CCH-C2(2)-2.50	CCH-C2(2)-2.50(1)	No Data	No Data	No Data	No Data
	CCH-C2(2)-2.50(2)	172	Not measured	57	162.5
	CCH-C2(2)-2.50(3)	No Data	No Data	No Data	No Data
	CCH-C2(2)-2.50(4)	No Data	No Data	No Data	No Data

Table 74

(Cont.)

Group of Samples B (Mw(Graft)(THEO) = 7,000 g/mol)					
Sub-Group B.3 (%Graft(THEO)=80%)					
Sample	**Sample Fraction**	**Tm (°C)**	**ΔHm (J/g)**	**Tg1 (°C)**	**Tg2 (°C)**
CCH-C2(2)-2.80	CCH-C2(2)-2.80(1)	No Data	No Data	No Data	No Data
	CCH-C2(2)-2.80(2)	No Data	No Data	No Data	No Data
	CCH-C2(2)-2.80(3)	No Data	No Data	No Data	No Data
	CCH-C2(2)-2.80(4)	174	Not measured	52	164
	CCH-C2(2)-2.80(5)	No Data	No Data	No Data	No Data
	CCH-C2(2)-2.80(6)	No Data	No Data	No Data	No Data
	CCH-C2(2)-2.80(7)	No Data	No Data	No Data	No Data

Table 75

DSC (Dry) Measurements: CMC-g-PNIPAAm graft copolymers

(Group of Samples C (Mw(Graft)$_{(THEO)}$ = 9,000 g/mol))

Group of Samples C (Mw(Graft)(THEO) = 9,000 g/mol)					
Sub-Group C.1 (%Graft(THEO)=40%)					
Sample	**Sample Fraction**	**Tm (°C)**	**ΔHm (J/g)**	**Tg1 (°C)**	**Tg2 (°C)**
CCH-B5-3.40	CCH-B5-3.40	168	Not measured	50	163
CCH-C2(2)-3.40	CCH-C2(2)-3.40(1)	No Data	No Data	No Data	No Data
	CCH-C2(2)-3.40(2)	178	Not measured	53	167
	CCH-C2(2)-3.40(3)	No Data	No Data	No Data	No Data

Table 75

(Cont.)

Group of Samples C (Mw(Graft)(THEO) = 9,000 g/mol)					
Sub-Group C.2 (%Graft(THEO)=50%)					
Sample	**Sample Fraction**	**Tm (°C)**	**ΔHm (J/g)**	**Tg1 (°C)**	**Tg2 (°C)**
CCH-B5-3.50	CCH-B5-3.50	163	Not measured	50	150
CCH-C2(2)-3.50	CCH-C2(2)-3.50(1)	No Data	No Data	No Data	No Data
	CCH-C2(2)-3.50(2)	No Data	No Data	No Data	No Data
	CCH-C2(2)-3.50(3)	180	Not measured	56	165
CCH-C2(2)-3.80	CCH-C2(2)-3.80(1)	No Data	No Data	No Data	No Data
	CCH-C2(2)-3.80(2)	No Data	No Data	No Data	No Data
	CCH-C2(2)-3.80(3)	184	Not measured	58.5	167
	CCH-C2(2)-3.80(4)	No Data	No Data	No Data	No Data
	CCH-C2(2)-3.80(5)	No Data	No Data	No Data	No Data
	CCH-C2(2)-3.80(6)	No Data	No Data	No Data	No Data

Table 76

DSC (Aqueous) Measurements in water: CMC-g-PNIPAAm graft copolymers

(Group of Samples A (Mw(Graft)(THEO) = 5,000 g/mol))

Group of Samples A (Mw(Graft)(THEO) = 5,000 g/mol)			
Sub-Group A.1 (%Graft(THEO)=40%)			
Sample	**Sample Fraction**	**LCST Heating Cycle (°C)**	**LCST Cooling Cycle (°C)**
CCH-A27-1	CCH-A27-1(1)	No Data	No Data
	CCH-A27-1(2)	No Data	No Data
	CCH-A27-1(3)	No Data	No Data
	CCH-A27-1(4)	No Data	No Data
	CCH-A27-1(5)	No Data	No Data
CCH-C2-1.40	CCH-C2-1.40	No Data	No Data
CCH-C2(2)-1.40	CCH-C2(2)-1.40(1)	No Data	No Data
	CCH-C2(2)-1.40(2)	35.28	28.91
	CCH-C2(2)-1.40(3)	No Data	No Data
	CCH-C2(2)-1.40(4)	No Data	No Data
CCH-B5-1.50	CCH-B5-1.50	No Data	No Data
CCH-C2(2)-1.50	CCH-C2(2)-1.50(1)	No Data	No Data
	CCH-C2(2)-1.50(2)	29.29	26.54
	CCH-C2(2)-1.50(3)	No Data	No Data
	CCH-C2(2)-1.50(4)	No Data	No Data
	CCH-C2(2)-1.50(5)	No Data	No Data

Table 76

(Cont.)

Group of Samples A (Mw(Graft)(THEO) = 5,000 g/mol)			
Sub-Group A.3 (%Graft(THEO)=80%)			
Sample	**Sample Fraction**	**LCST Heating Cycle (°C)**	**LCST Cooling Cycle (°C)**
CCH-C2(2)-1.80	CCH-C2(2)-1.80(1)	No Data	No Data
	CCH-C2(2)-1.80(2)	No Data	No Data
	CCH-C2(2)-1.80(3)	No Data	No Data
	CCH-C2(2)-1.80(4)	No Data	No Data
	CCH-C2(2)-1.80(5)	36.61	34.03
	CCH-C2(2)-1.80(6)	No Data	No Data
	CCH-C2(2)-1.80(7)	No Data	No Data
	CCH-C2(2)-1.80(8)	No Data	No Data
	CCH-C2(2)-1.80(9)	No Data	No Data
	CCH-C2(2)-1.80(10)	No Data	No Data

Table 77

DSC (Aqueous) Measurements in water: CMC-g-PNIPAAm graft copolymers

(Group of Samples B (Mw(Graft)$_{(THEO)}$ = 7,000 g/mol))

Group of Samples B (Mw(Graft)(THEO) = 7,000 g/mol)			
Sub-Group B.1 (%Graft(THEO)=40%)			
Sample	**Sample Fraction**	**LCST Heating Cycle (°C)**	**LCST Cooling Cycle (°C)**
CCH-B5-2.40	CCH-B5-2.40	No Data	No Data
CCH-C2(2)-2.40	CCH-C2(2)-2.40(1)	No Data	No Data
	CCH-C2(2)-2.40(2)	No Data	No Data
	CCH-C2(2)-2.40(3)	30.76	29.01
	CCH-C2(2)-2.40(4)	No Data	No Data
	CCH-C2(2)-2.40(5)	No Data	No Data
CCH-B5-2.50	CCH-B5-2.50	No Data	No Data
CCH-C2(2)-2.50	CCH-C2(2)-2.50(1)	No Data	No Data
	CCH-C2(2)-2.50(2)	31.73	29.73
	CCH-C2(2)-2.50(3)	No Data	No Data
	CCH-C2(2)-2.50(4)	No Data	No Data
CCH-C2(2)-2.80	CCH-C2(2)-2.80(1)	No Data	No Data
	CCH-C2(2)-2.80(2)	No Data	No Data
	CCH-C2(2)-2.80(3)	No Data	No Data
	CCH-C2(2)-2.80(4)	33.60	31.24
	CCH-C2(2)-2.80(5)	No Data	No Data
	CCH-C2(2)-2.80(6)	No Data	No Data
	CCH-C2(2)-2.80(7)	No Data	No Data

Table 78

DSC (Aqueous) Measurements in water: CMC-g-PNIPAAm graft copolymers

(Group of Samples C (Mw(Graft)$_{(THEO)}$ = 9,000 g/mol))

Group of Samples C (Mw(Graft)(THEO) = 9,000 g/mol)			
Sub-Group C.1 (%Graft(THEO)=40%)			
Sample	**Sample Fraction**	**LCST Heating Cycle (°C)**	**LCST Cooling Cycle (°C)**
CCH-B5-3.40	CCH-B5-3.40	No Data	No Data
CCH-C2(2)-3.40	CCH-C2(2)-3.40(1)	No Data	No Data
	CCH-C2(2)-3.40(2)	31.81	29.49
	CCH-C2(2)-3.40(3)	No Data	No Data
CCH-B5-3.50	CCH-B5-3.50	No Data	No Data
CCH-C2(2)-3.50	CCH-C2(2)-3.50(1)	No Data	No Data
	CCH-C2(2)-3.50(2)	No Data	No Data
	CCH-C2(2)-3.50(3)	33.09	30.88
CCH-C2(2)-3.80	CCH-C2(2)-3.80(1)	No Data	No Data
	CCH-C2(2)-3.80(2)	No Data	No Data
	CCH-C2(2)-3.80(3)	33.93	32.16
	CCH-C2(2)-3.80(4)	No Data	No Data
	CCH-C2(2)-3.80(5)	No Data	No Data
	CCH-C2(2)-3.80(6)	No Data	No Data

Table 79

DSC (Aqueous) Measurements in buffer solutions: CMC-g-PNIPAAm graft copolymers

(Group of Samples A (Mw(Graft)$_{(THEO)}$ = 5,000 g/mol))

Group of Samples A (Mw(Graft)(THEO) = 5,000 g/mol)															
Sub-Group A.1 (%Graft(THEO)=40%)															
Sample	Sample Fraction	LCST Heating Cycle (°C)							LCST Cooling Cycle (°C)						
		pH							pH						
		2	2.5	3	3.5	7	10	12	2	2.5	3	3.5	7	10	12
CCH-A27-1	CCH-A27-1(1)	No Data	No Data	No Data	No Data	No Data	No Data	No Data	No Data	No Data	No Data	No Data	No Data	No Data	No Data
	CCH-A27-1(2)	No Data	No Data	No Data	No Data	No Data	No Data	No Data	No Data	No Data	No Data	No Data	No Data	No Data	No Data
	CCH-A27-1(3)	No Data	No Data	No Data	No Data	No Data	No Data	No Data	No Data	No Data	No Data	No Data	No Data	No Data	No Data
	CCH-A27-1(4)	No Data	No Data	No Data	No Data	No Data	No Data	No Data	No Data	No Data	No Data	No Data	No Data	No Data	No Data
	CCH-A27-1(5)	No Data	No Data	No Data	No Data	No Data	No Data	No Data	No Data	No Data	No Data	No Data	No Data	No Data	No Data
CCH-C2-1.40	CCH-C2-1.40	No Data	No Data	No Data	No Data	No Data	No Data	No Data	No Data	No Data	No Data	No Data	No Data	No Data	No Data

Table 79

(Cont.)

Group of Samples A (Mw(Graft)(THEO) = 5,000 g/mol)															
Sub-Group A.1 (%Graft(THEO)=40%)															
Sample	Sample Fraction	LCST Heating Cycle (°C)							LCST Cooling Cycle (°C)						
		pH							pH						
		2	2.5	3	3.5	7	10	12	2	2.5	3	3.5	7	10	12
CCH-C2(2)-1.40	CCH-C2(2)-1.40(1)	No Data	No Data	No Data	No Data	No Data	No Data	No Data	No Data	No Data	No Data	No Data	No Data	No Data	No Data
	CCH-C2(2)-1.40(2)	31.09	32.75	33.36	30.71	33.51	No Data	No Data	29.41	31.15	31.63	28.69	31.40	No Data	No Data
	CCH-C2(2)-1.40(3)	No Data	No Data	No Data	No Data	No Data	34.44	26.23	No Data	No Data	No Data	No Data	No Data	32.54	24.36
	CCH-C2(2)-1.40(4)	No Data	No Data	No Data	No Data	No Data	No Data	No Data	No Data	No Data	No Data	No Data	No Data	No Data	No Data

Table 79

(Cont.)

Group of Samples A (Mw(Graft)(THEO) = 5,000 g/mol)															
Sub-Group A.2 (%Graft(THEO)=50%)															
Sample	Sample Fraction	LCST Heating Cycle (°C)							LCST Cooling Cycle (°C)						
		pH							pH						
		2	2.5	3	3.5	7	10	12	2	2.5	3	3.5	7	10	12
CCH-B5-1.50	CCH-B5-1.50	No Data	No Data	No Data	No Data	No Data	No Data	No Data	No Data	No Data	No Data	No Data	No Data	No Data	No Data
CCH-C2(2)-1.50	CCH-C2(2)-1.50(1)	No Data	No Data	No Data	No Data	No Data	No Data	No Data	No Data	No Data	No Data	No Data	No Data	No Data	No Data
	CCH-C2(2)-1.50(2)	31.58	32.43	33.03	34.23	32.95	No Data	No Data	29.87	30.37	31.39	32.54	30.92	No Data	No Data
	CCH-C2(2)-1.50(3)	No Data	No Data	No Data	No Data	No Data	No Data	No Data	No Data	No Data	No Data	No Data	No Data	No Data	No Data
	CCH-C2(2)-1.50(4)	No Data	No Data	No Data	No Data	No Data	35.57	35.30	No Data	No Data	No Data	No Data	No Data	33.60	33.31
	CCH-C2(2)-1.50(5)	No Data	No Data	No Data	No Data	No Data	No Data	No Data	No Data	No Data	No Data	No Data	No Data	No Data	No Data

Table 79

(Cont.)

Group of Samples A (Mw(Graft)(THEO) = 5,000 g/mol)

Sub-Group A.3 (%Graft(THEO)=80%)

Sample	Sample Fraction	LCST Heating Cycle (°C) pH							LCST Cooling Cycle (°C) pH						
		2	2.5	3	3.5	7	10	12	2	2.5	3	3.5	7	10	12
CCH-C2(2)-1.80	CCH-C2(2)-1.80(1)	No Data	No Data	No Data	No Data	No Data	No Data	No Data	No Data	No Data	No Data	No Data	No Data	No Data	No Data
	CCH-C2(2)-1.80(2)	No Data	No Data	No Data	No Data	No Data	No Data	No Data	No Data	No Data	No Data	No Data	No Data	No Data	No Data
	CCH-C2(2)-1.80(3)	No Data	No Data	No Data	No Data	No Data	No Data	No Data	No Data	No Data	No Data	No Data	No Data	No Data	No Data
	CCH-C2(2)-1.80(4)	No Data	No Data	No Data	No Data	No Data	36.52	36.55	No Data	No Data	No Data	No Data	No Data	34.65	34.06
	CCH-C2(2)-1.80(5)	No Data	No Data	No Data	34.84	34.61	No Data	No Data	No Data	No Data	No Data	32.64	32.90	No Data	No Data

Table 79

(Cont.)

Group of Samples A (Mw(Graft)(THEO) = 5,000 g/mol)															
Sub-Group A.3 (%Graft(THEO)=80%)															
Sample	Sample Fraction	LCST Heating Cycle (°C)							LCST Cooling Cycle (°C)						
		pH							pH						
		2	2.5	3	3.5	7	10	12	2	2.5	3	3.5	7	10	12
CCH-C2(2)-1.80	CCH-C2(2)-1.80(6)	No Data	No Data	No Data	No Data	No Data	No Data	No Data	No Data	No Data	No Data	No Data	No Data	No Data	No Data
	CCH-C2(2)-1.80(7)	No Data	No Data	No Data	No Data	No Data	No Data	No Data	No Data	No Data	No Data	No Data	No Data	No Data	No Data
	CCH-C2(2)-1.80(8)	No Data	No Data	No Data	No Data	No Data	No Data	No Data	No Data	No Data	No Data	No Data	No Data	No Data	No Data
	CCH-C2(2)-1.80(9)	No Data	No Data	No Data	No Data	No Data	No Data	No Data	No Data	No Data	No Data	No Data	No Data	No Data	No Data
	CCH-C2(2)-1.80(10)	No Data	No Data	No Data	No Data	No Data	No Data	No Data	No Data	No Data	No Data	No Data	No Data	No Data	No Data

Table 80

DSC (Aqueous) Measurements in buffer solutions: CMC-g-PNIPAAm graft copolymers

(Group of Samples B (Mw(Graft)(THEO) = 7,000 g/mol))

Group of Samples B (Mw(Graft)(THEO) = 7,000 g/mol)															
Sub-Group B.1 (%Graft(THEO)=40%)															
Sample	Sample Fraction	LCST Heating Cycle (°C)							LCST Cooling Cycle (°C)						
		pH							pH						
		2	2.5	3	3.5	7	10	12	2	2.5	3	3.5	7	10	12
CCH-B5-2.40	CCH-B5-2.40	No Data	No Data	No Data	No Data	No Data	No Data	No Data	No Data	No Data	No Data	No Data	No Data	No Data	No Data
CCH-C2(2)-2.40	CCH-C2(2)-2.40(1)	No Data	No Data	No Data	No Data	No Data	30.89	31.19	No Data	No Data	No Data	No Data	No Data	29.21	29.86
	CCH-C2(2)-2.40(2)	No Data	No Data	No Data	No Data	No Data	No Data	No Data	No Data	No Data	No Data	No Data	No Data	No Data	No Data
	CCH-C2(2)-2.40(3)	29.89	28.76	28.44	No Data	No Data	No Data	No Data	28.34	27.40	26.44	No Data	No Data	No Data	No Data
	CCH-C2(2)-2.40(4)	No Data	No Data	No Data	No Data	No Data	No Data	No Data	No Data	No Data	No Data	No Data	No Data	No Data	No Data
	CCH-C2(2)-2.40(5)	No Data	No Data	No Data	No Data	No Data	No Data	No Data	No Data	No Data	No Data	No Data	No Data	No Data	No Data

Table 80

(Cont.)

Group of Samples B (Mw(Graft)(THEO) = 7,000 g/mol)															
Sub-Group B.2 (%Graft(THEO)=50%)															
Sample	**Sample Fraction**	**LCST Heating Cycle (°C)**							**LCST Cooling Cycle (°C)**						
		pH							**pH**						
		2	**2.5**	**3**	**3.5**	**7**	**10**	**12**	**2**	**2.5**	**3**	**3.5**	**7**	**10**	**12**
CCH-B5-2.50	CCH-B5-2.50	No Data	No Data	No Data	No Data	No Data	No Data	No Data	No Data	No Data	No Data	No Data	No Data	No Data	No Data
CCH-C2(2)-2.50	CCH-C2(2)-2.50(1)	No Data	No Data	No Data	No Data	No Data	No Data	No Data	No Data	No Data	No Data	No Data	No Data	No Data	No Data
	CCH-C2(2)-2.50(2)	30.93	27.67	29.95	No Data	29.04	No Data	No Data	29.21	26.56	27.85	No Data	27.04	No Data	No Data
	CCH-C2(2)-2.50(3)	No Data	No Data	No Data	No Data	No Data	No Data	No Data	No Data	No Data	No Data	No Data	No Data	No Data	No Data
	CCH-C2(2)-2.50(4)	No Data	No Data	No Data	No Data	No Data	35.46	31.63	No Data	No Data	No Data	No Data	No Data	33.64	29.85

Table 80

(Cont.)

Group of Samples B (Mw(Graft)(THEO) = 7,000 g/mol)														
Sub-Group B.3 (%Graft(THEO)=80%)														
Sample	Sample Fraction	LCST Heating Cycle (°C)							LCST Cooling Cycle (°C)					
		pH							pH					
		2	2.5	3	3.5	7	10	12	2	2.5	3	3.5	7	10	12
CCH-C2(2)-2.80	CCH-C2(2)-2.80(1)	No Data	No Data	No Data	No Data	No Data	No Data	No Data	No Data	No Data	No Data	No Data	No Data	No Data	No Data
	CCH-C2(2)-2.80(2)	No Data	No Data	No Data	No Data	No Data	No Data	No Data	No Data	No Data	No Data	No Data	No Data	No Data	No Data
	CCH-C2(2)-2.80(3)	No Data	No Data	No Data	No Data	No Data	33.11	33.01	No Data	No Data	No Data	No Data	No Data	30.51	30.42
	CCH-C2(2)-2.80(4)	31.98	No Data	30.83	31.60	31.32	No Data	No Data	30.09	No Data	27.98	30.03	28.82	No Data	No Data
	CCH-C2(2)-2.80(5)	No Data	No Data	No Data	No Data	No Data	No Data	No Data	No Data	No Data	No Data	No Data	No Data	No Data	No Data
	CCH-C2(2)-2.80(6)	No Data	No Data	No Data	No Data	No Data	No Data	No Data	No Data	No Data	No Data	No Data	No Data	No Data	No Data
	CCH-C2(2)-2.80(7)	No Data	No Data	No Data	No Data	No Data	No Data	No Data	No Data	No Data	No Data	No Data	No Data	No Data	No Data

Table 81

DSC (Aqueous) Measurements in buffer solutions: CMC-g-PNIPAAm graft copolymers

(Group of Samples C (Mw(Graft)(THEO) = 9,000 g/mol))

Group of Samples C (Mw(Graft)(THEO) = 9,000 g/mol)															
Sub-Group C.1 (%Graft(THEO)=40%)															
Sample	Sample Fraction	LCST Heating Cycle (°C)							LCST Cooling Cycle (°C)						
		pH							pH						
		2	2.5	3	3.5	7	10	12	2	2.5	3	3.5	7	10	12
CCH-B5-3.40	CCH-B5-3.40	No Data	No Data	No Data	No Data	No Data	No Data	No Data	No Data	No Data	No Data	No Data	No Data	No Data	No Data
CCH-C2(2)-3.40	CCH-C2(2)-3.40(1)	No Data	No Data	No Data	No Data	No Data	No Data	32.14	No Data	No Data	No Data	No Data	No Data	No Data	30.20
	CCH-C2(2)-3.40(2)	31.37	30.60	30.61	30.85	30.84	No Data	No Data	29.73	28.77	28.89	28.94	28.00	No Data	No Data
	CCH-C2(2)-3.40(3)	No Data	No Data	No Data	No Data	No Data	No Data	No Data	No Data	No Data	No Data	No Data	No Data	No Data	No Data

Table 81

(Cont.)

Group of Samples C (Mw(Graft)(THEO) = 9,000 g/mol)															
Sub-Group C.2 (%Graft(THEO)=50%)															
Sample	Sample Fraction	LCST Heating Cycle (°C)							LCST Cooling Cycle (°C)						
		pH							pH						
		2	2.5	3	3.5	7	10	12	2	2.5	3	3.5	7	10	12
CCH-B5-3.50	CCH-B5-3.50	No Data	No Data	No Data	No Data	No Data	No Data	No Data	No Data	No Data	No Data	No Data	No Data	No Data	No Data
CCH-C2(2)-3.50	CCH-C2(2)-3.50(1)	No Data	No Data	No Data	No Data	No Data	33.57	No Data	No Data	No Data	No Data	No Data	No Data	29.64	No Data
	CCH-C2(2)-3.50(2)	No Data	No Data	No Data	No Data	No Data	No Data	No Data	No Data	No Data	No Data	No Data	No Data	No Data	No Data
	CCH-C2(2)-3.50(3)	32.08	31.26	32.50	31.61	31.81	No Data	No Data	30.26	29.41	29.61	29.54	28.30	No Data	No Data

Table 81

(Cont.)

Group of Samples C (Mw(Graft)(THEO) = 9,000 g/mol)															
Sub-Group C.3 (%Graft(THEO)=80%)															
Sample	Sample Fraction	LCST Heating Cycle (°C)							LCST Cooling Cycle (°C)						
		pH							pH						
		2	2.5	3	3.5	7	10	12	2	2.5	3	3.5	7	10	12
CCH-C2(2)-3.80	CCH-C2(2)-3.80(1)	No Data	No Data	No Data	No Data	No Data	No Data	No Data	No Data	No Data	No Data	No Data	No Data	No Data	No Data
	CCH-C2(2)-3.80(2)	No Data	No Data	No Data	No Data	No Data	34.88	31.37	No Data	No Data	No Data	No Data	No Data	33.11	29.65
	CCH-C2(2)-3.80(3)	33.57	32.11	33.01	33.18	32.72	No Data	No Data	31.36	29.68	30.64	30.65	30.10	No Data	No Data
	CCH-C2(2)-3.80(4)	No Data	No Data	No Data	No Data	No Data	No Data	No Data	No Data	No Data	No Data	No Data	No Data	No Data	No Data
	CCH-C2(2)-3.80(5)	No Data	No Data	No Data	No Data	No Data	No Data	No Data	No Data	No Data	No Data	No Data	No Data	No Data	No Data
	CCH-C2(2)-3.80(6)	No Data	No Data	No Data	No Data	No Data	No Data	No Data	No Data	No Data	No Data	No Data	No Data	No Data	No Data

Table 82

FTIR Measurements: CMC-g-PNIPAAm comb-type graft hydrogels

(Group of Samples: Crosslinked with citric acid)

Sample	Replica	Wave number -COOH (cm^{-1})
CCH-C3(5)-2(35%)	CCH-C3(5)-2(35%).1	1,711.9
	CCH-C3(5)-2(35%).2	1,717.1
	CCH-C3(5)-2(35%).3	1,717.7
	CCH-C3(5)-2(35%).4	1,731.6

Table 83

Equilibrium Swelling Ratio Data (Part 1):

Weight measurements from dried and swelled hydrogels in water

$t_{interval}$* (min)	Weight (g)				
	Sample CCH-C3(8)MONO-1(Al)	Sample CCH-C3(8)MONO-2(Al)		Sample CCH-C3(8)MONO-1(CA)	
	Replica CCH-C3(8)MONO-1(Al).1	Replica CCH-C3(8)MONO-2(Al).1	Replica CCH-C3(8)MONO-2(Al).2	Replica CCH-C3(8)MONO-1(CA).1	Replica CCH-C3(8)MONO-1(CA).2
Dried	0.164	0.187	0.242	1.561	1.277
10	0.681	0.540	0.653	6.120	4.668
30	0.929	0.945	0.690	7.138	5.979
30	1.119	0.681	0.861	7.701	6.772
30	1.015	0.645	0.881	7.474	5.971
30	1.044	0.671	0.879	7.667	6.033
60	1.006	0.695	0.705	7.764	5.804
140	0.952	0.634	1.053	7.527	6.260

* Time interval measured before a weight measurement was performed

Table 84

Equilibrium Swelling Ratio Data (Part 2):

Swelling degree measurements from dried and swelled hydrogels in water

t_{accu}** (min)	Swelling Degree (%)				
	Sample CCH-C3(8)MONO-1(Al)	Sample CCH-C3(8)MONO-2(Al)		Sample CCH-C3(8)MONO-1(CA)	
	Replica CCH-C3(8)MONO-1(Al).1	Replica CCH-C3(8)MONO-2(Al).1	Replica CCH-C3(8)MONO-2(Al).2	Replica CCH-C3(8)MONO-1(CA).1	Replica CCH-C3(8)MONO-1(CA).2
0	0	0	0	0	0
10	315	189	170	292	266
40	466	405	185	357	368
70	582	264	256	393	430
100	519	245	264	379	368
130	537	259	263	391	372
190	513	272	191	397	355
330	480	239	335	382	390

** Accumulated time (sum of time intervals) before a weight measurement was performed

Table 85

Equilibrium Temperature-Responsive Swelling Behavior (Part 1):

Weight measurements from dried and swelled hydrogels in water at 80 °C

$t_{interval}$* (min)	Weight (g)				
	Sample CCH-C3(8)MONO-1(Al)	Sample CCH-C3(8)MONO-2(Al)		Sample CCH-C3(8)MONO-1(CA)	
	Replica CCH-C3(8)MONO-1(Al).1	Replica CCH-C3(8)MONO-2(Al).1	Replica CCH-C3(8)MONO-2(Al).2	Replica CCH-C3(8)MONO-1(CA).1	Replica CCH-C3(8)MONO-1(CA).2
Dried	0.096	0.187	0.242	1.561	1.277
0	0.557	0.634	1.053	7.527	6.260
10	0.624	0.389	0.821	5.934	5.213
30	0.364	0.605	0.845	6.105	5.083
30	0.186	0.597	0.891	6.697	4.746
30	0.174	0.559	0.683	5.979	5.292
30	0.129	0.589	0.993	6.529	5.525

* Time interval measured before a weight measurement was performed

Table 86

Equilibrium Temperature-Responsive Swelling Behavior (Part 2):

Swelling degree measurements from swelled hydrogels in water at 80 °C

t_{accu}** (min)	Swelling Degree (%)				
	Sample CCH-C3(8)MONO-1(Al)	Sample CCH-C3(8)MONO-2(Al)		Sample CCH-C3(8)MONO-1(CA)	
	Replica CCH-C3(8)MONO-1(Al).1	Replica CCH-C3(8)MONO-2(Al).1	Replica CCH-C3(8)MONO-2(Al).2	Replica CCH-C3(8)MONO-1(CA).1	Replica CCH-C3(8)MONO-1(CA).2
0	480	239	335	382	390
10	550	108	239	280	308
40	279	224	249	291	298
70	94	219	268	329	272
100	81	199	182	283	314
130	34	215	310	318	333

** Accumulated time (sum of time intervals) before a weight measurement was performed

Table 87

Equilibrium Temperature-Responsive Swelling Behavior (Part 1):

Weight measurements from dried and swelled hydrogels in buffer pH=3 at 80 °C

$t_{interval}$* (min)	Weight (g)	
	Sample CCH-C3(8)MONO-1(CA)	
	Replica CCH-C3(8)MONO-1(CA).1	Replica CCH-C3(8)MONO-1(CA).2
Dried	1.507	2.202
0	10.785	10.547
10	4.040	5.365
30	3.360	4.223
30	3.020	5.338
30	3.196	5.312
60	2.829	4.370
30	3.226	5.553

* Time interval measured before a weight measurement was performed

Table 88

Equilibrium Temperature-Responsive Swelling Behavior (Part 2):

Swelling degree measurements from swelled hydrogels in buffer pH=3 at 80 °C

t_{accu}** (min)	Swelling Degree (%)	
	Sample CCH-C3(8)MONO-1(CA)	
	Replica CCH-C3(8)MONO-1(CA).1	Replica CCH-C3(8)MONO-1(CA).2
0	616	379
10	168	144
40	123	92
70	100	142
100	112	141
160	88	98
190	114	152

** Accumulated time (sum of time intervals) before a weight measurement was performed

Table 89

Pulsatile Temperature-Responsive Swelling Behavior (Part 1):

Weight measurements from dried and swelled hydrogels in water at 4 and 80 °C

T (°C)	Weight (g)				
	Sample CCH-C3(8)MONO-1(Al)	Sample CCH-C3(8)MONO-2(Al)		Sample CCH-C3(8)MONO-1(CA)	
	Replica CCH-C3(8)MONO-1(Al).2	Replica CCH-C3(8)MONO-2(Al).1	Replica CCH-C3(8)MONO-2(Al).2	Replica CCH-C3(8)MONO-1(CA).1	Replica CCH-C3(8)MONO-1(CA).2
Dried	0.409	0.434	0.409	1.890	3.424
80	1.263	1.807	1.651	7.279	15.439
4	1.713	1.837	1.619	11.766	23.988
80	0.780	1.857	1.670	7.430	16.937
4	1.500	1.895	1.840	12.025	25.540
80	0.767	1.909	1.910	8.363	18.634
4	1.466	2.012	1.776	12.050	24.304
80	0.432	1.913	1.770	6.651	12.322
4	1.112	1.902	1.853	11.973	23.910
80	0.387	1.976	1.804	6.272	14.231
4	1.120	2.040	1.854	12.095	25.870

Table 90

Pulsatile Temperature-Responsive Swelling Behavior (Part 2):

Swelling degree measurements from swelled hydrogels in water at 4 and 80 °C

T (°C)	Swelling Degree (%)				
	Sample CCH-C3(8)MONO-1(Al)	Sample CCH-C3(8)MONO-2(Al)		Sample CCH-C3(8)MONO-1(CA)	
	Replica CCH-C3(8)MONO-1(Al).2	Replica CCH-C3(8)MONO-2(Al).1	Replica CCH-C3(8)MONO-2(Al).2	Replica CCH-C3(8)MONO-1(CA).1	Replica CCH-C3(8)MONO-1(CA).2
80	209	316	304	285	351
4	319	323	296	523	601
80	91	328	308	293	395
4	267	337	350	536	646
80	88	340	367	342	444
4	258	364	334	538	610
80	6	341	333	252	260
4	172	338	353	533	598
80	-5	355	341	232	316
4	174	370	353	540	656

Table 91

Pulsatile Temperature-Responsive Swelling Behavior (Part 1):

Weight measurements from dried and swelled hydrogels in buffer pH=3 at 4 and 80 °C

T (°C)	Weight (g)	
	Sample CCH-C3(8)MONO-1(CA)	
	Replica CCH-C3(8)MONO-1(CA).1	Replica CCH-C3(8)MONO-1(CA).2
Dried	2.453	3.550
80	5.680	10.168
4	15.812	18.858
80	5.843	10.105
4	16.334	19.685
80	5.745	10.094
4	16.966	20.258
80	5.355	9.933
4	17.584	20.649
80	4.918	10.099
4	18.217	20.847

Table 92

Pulsatile Temperature-Responsive Swelling Behavior (Part 2):

Swelling degree measurements from swelled hydrogels in buffer pH=3 at 4 and 80 °C

T (°C)	Swelling Degree (%)	
	Sample CCH-C3(8)MONO-1(CA)	
	Replica CCH-C3(8)MONO-1(CA).1	Replica CCH-C3(8)MONO-1(CA).2
80	132	186
4	545	431
80	138	185
4	566	455
80	134	184
4	592	471
80	118	180
4	617	482
80	100	184
4	643	487

Table 93

FTIR Measurements: Functionalization of PA6 substrates

(Group of Substrates: "Concentrated Acidic Hydrolysis" NH_2 Production Method)

Substrate	Replica	Wave number -CHO (cm^{-1})
After initial activation with glutaraldehyde		
CCH-C3(8)BI-PA6(1a)	CCH-C3(8)BI-PA6(1a).1	1,738.2
	CCH-C3(8)BI-PA6(1a).2m	1,722.2
	CCH-C3(8)BI-PA6(1a).3	1,738.3
CCH-C3(8)BI-PA6(1b)	CCH-C3(8)BI-PA6(1b).1	1,722.3
	CCH-C3(8)BI-PA6(1b).2m	1,738.6
	CCH-C3(8)BI-PA6(1b).3	1,738.3
After final activation with glutaraldehyde		
CCH-C3(8)BI-PA6(1a)f	CCH-C3(8)BI-PA6(1a)f.1	1,740.6
	CCH-C3(8)BI-PA6(1a)f.2	1,738.9
	CCH-C3(8)BI-PA6(1a)f.3m	1,740.7
CCH-C3(8)BI-PA6(1b)f	CCH-C3(8)BI-PA6(1b)f.1m	1,740.9
	CCH-C3(8)BI-PA6(1b)f.2	1,740.5
	CCH-C3(8)BI-PA6(1b)f.3	1,740.7

Table 94

FTIR Measurements: Functionalization of PA6 substrates

(Group of Substrates: "Aqueous Hydrolysis" NH_2 Production Method)

Substrate	Replica	Wave number -CHO (cm^{-1})
After initial activation with glutaraldehyde		
CCH-C3(8)BI-PA6(2a)	CCH-C3(8)BI-PA6(2a).1	1,738.5
	CCH-C3(8)BI-PA6(2a).2m	1,738.4
	CCH-C3(8)BI-PA6(2a).3	1,738.1
CCH-C3(8)BI-PA6(2b)	CCH-C3(8)BI-PA6(2b).1m	1,740.7
	CCH-C3(8)BI-PA6(2b).2	1,740.3
	CCH-C3(8)BI-PA6(2b).3	1,740.9
After final activation with glutaraldehyde		
CCH-C3(8)BI-PA6(2a)f	CCH-C3(8)BI-PA6(2a)f.1	1,741.0
	CCH-C3(8)BI-PA6(2a)f.2	1,741.6
	CCH-C3(8)BI-PA6(2a)f.3m	1,741.9
CCH-C3(8)BI-PA6(2b)f	CCH-C3(8)BI-PA6(2b)f.1	1,738.4
	CCH-C3(8)BI-PA6(2b)f.2m	1,739.1
	CCH-C3(8)BI-PA6(2b)f.3	1,739.4

Table 95

FTIR Measurements: Functionalization of PA6 substrates

(Group of Substrates: "Diluted Acidic Hydrolysis" NH_2 Production Method)

Substrate	Replica	Wave number -CHO (cm^{-1})
After initial activation with glutaraldehyde		
CCH-C3(8)BI-PA6(3a)	CCH-C3(8)BI-PA6(3a).1m	1,718.8
	CCH-C3(8)BI-PA6(3a).2	1,733.4
	CCH-C3(8)BI-PA6(3a).3	1,733.8
CCH-C3(8)BI-PA6(3b)	CCH-C3(8)BI-PA6(3b).1	1,718.5
	CCH-C3(8)BI-PA6(3b).2m	1,717.4
	CCH-C3(8)BI-PA6(3b).3	1,718.7
CCH-C3(8)BI-PA6(3b.2)	CCH-C3(8)BI-PA6(3b.2).1	1,718.6
	CCH-C3(8)BI-PA6(3b.2).2	1,718.4
	CCH-C3(8)BI-PA6(3b.2).3m	1,717.8
After final activation with glutaraldehyde		
CCH-C3(8)BI-PA6(3a)f	CCH-C3(8)BI-PA6(3a)f.1	1,741.7
	CCH-C3(8)BI-PA6(3a)f.2m	1,741.8
	CCH-C3(8)BI-PA6(3a)f.3	1,741.6
CCH-C3(8)BI-PA6(3b)f	CCH-C3(8)BI-PA6(3b)f.1	1,736.2
	CCH-C3(8)BI-PA6(3b)f.2m	1,736.1
	CCH-C3(8)BI-PA6(3b)f.3	1,735.9
CCH-C3(8)BI-PA6(3b.2)f	CCH-C3(8)BI-PA6(3b.2)f.1	1,740.3
	CCH-C3(8)BI-PA6(3b.2)f.2m	1,740.9
	CCH-C3(8)BI-PA6(3b.2)f.3	1,740.7

Table 96

FTIR Measurements: Bilayer actuators based on

CMC-g-PNIPAAm comb-type graft hydrogel films on PA6 substrates

(Group of Samples: Substrate CCH-C3(8)BI-PA6(1a))

Sample	Replica	Wave number -COOH (cm^{-1})
CCH-C3(8)BI-1	CCH-C3(8)BI-1	not measured
CCH-C3(8)BI-14	CCH-C3(8)BI-14	not measured
CCH-C3(8)BI-27	CCH-C3(8)BI-27	not measured
CCH-C3(8)BI-40	CCH-C3(8)BI-40	not measured
CCH-C3(8)BI-53	CCH-C3(8)BI-53	not measured
CCH-C3(8)BI-66	CCH-C3(8)BI-66	not measured
CCH-C3(8)BI-Blanc(1)	CCH-C3(8)BI- Blanc(1)	not measured

Table 97

FTIR Measurements: Bilayer actuators based on

CMC-g-PNIPAAm comb-type graft hydrogel films on PA6 substrates

(Group of Samples: Substrate CCH-C3(8)BI-PA6(1b))

Sample	Replica	Wave number -COOH (cm^{-1})
CCH-C3(8)BI-2	CCH-C3(8)BI-2	not measured
CCH-C3(8)BI-15	CCH-C3(8)BI-15	not measured
CCH-C3(8)BI-28	CCH-C3(8)BI-28	not measured
CCH-C3(8)BI-41	CCH-C3(8)BI-41	not measured
CCH-C3(8)BI-54	CCH-C3(8)BI-54	not measured
CCH-C3(8)BI-67	CCH-C3(8)BI-67	not measured
CCH-C3(8)BI-Blanc(2)	CCH-C3(8)BI- Blanc(2)	not measured

Table 98

FTIR Measurements: Bilayer actuators based on

CMC-g-PNIPAAm comb-type graft hydrogel films on PA6 substrates

(Group of Samples: Substrate CCH-C3(8)BI-PA6(2a))

Sample	Replica	Wave number -COOH (cm^{-1})
CCH-C3(8)BI-3	CCH-C3(8)BI-PA3	1,710.0
	CCH-C3(8)BI-PA3.1	1,715.0
	CCH-C3(8)BI-PA3.2	1,720.0
	CCH-C3(8)BI-PA3.3	1,710.0
	CCH-C3(8)BI-PA3.4	1,722.0
	CCH-C3(8)BI-PA3.5	1,720.0
	CCH-C3(8)BI-PA3.6	1,715.0
	CCH-C3(8)BI-PA3.7	1,715.0
CCH-C3(8)BI-16	CCH-C3(8)BI-16	not measured
CCH-C3(8)BI-29	CCH-C3(8)BI-29	not measured
CCH-C3(8)BI-42	CCH-C3(8)BI-42	not measured
CCH-C3(8)BI-55	CCH-C3(8)BI-55	not measured
CCH-C3(8)BI-68	CCH-C3(8)BI-68	not measured
CCH-C3(8)BI-Blanc(3)	CCH-C3(8)BI- Blanc(3)	not measured

Table 99

FTIR Measurements: Bilayer actuators based on

CMC-g-PNIPAAm comb-type graft hydrogel films on PA6 substrates

(Group of Samples: Substrate CCH-C3(8)BI-PA6(2b))

Sample	Replica	Wave number -COOH (cm^{-1})
CCH-C3(8)BI-4	CCH-C3(8)BI-4	not measured
CCH-C3(8)BI-17	CCH-C3(8)BI-17	not measured
CCH-C3(8)BI-30	CCH-C3(8)BI-30	not measured
CCH-C3(8)BI-43	CCH-C3(8)BI-43	not measured
CCH-C3(8)BI-56	CCH-C3(8)BI-PA56.1	1,707.7
	CCH-C3(8)BI-PA56.2	1,701.8
	CCH-C3(8)BI-PA56.3	1,701.6
CCH-C3(8)BI-69	CCH-C3(8)BI-69	not measured
CCH-C3(8)BI-Blanc(4)	CCH-C3(8)BI- Blanc(4)	not measured

Table 100

FTIR Measurements: Bilayer actuators based on

CMC-g-PNIPAAm comb-type graft hydrogel films on PA6 substrates

(Group of Samples: Substrate CCH-C3(8)BI-PA6(3a))

Sample	Replica	Wave number -COOH (cm^{-1})
CCH-C3(8)BI-5	CCH-C3(8)BI-5	not measured
CCH-C3(8)BI-18	CCH-C3(8)BI-18	not measured
CCH-C3(8)BI-31	CCH-C3(8)BI-31	not measured
CCH-C3(8)BI-44	CCH-C3(8)BI-44	not measured
CCH-C3(8)BI-57	CCH-C3(8)BI-57	not measured
CCH-C3(8)BI-70	CCH-C3(8)BI-70	not measured
CCH-C3(8)BI-Blanc(5)	CCH-C3(8)BI- Blanc(5)	not measured

Table 101

FTIR Measurements: Bilayer actuators based on

CMC-g-PNIPAAm comb-type graft hydrogel films on PA6 substrates

(Group of Samples: Substrate CCH-C3(8)BI-PA6(3b))

Sample	Replica	Wave number -COOH (cm^{-1})
CCH-C3(8)BI-7	CCH-C3(8)BI-7	not measured
CCH-C3(8)BI-20	CCH-C3(8)BI-20	not measured
CCH-C3(8)BI-33	CCH-C3(8)BI-33	not measured
CCH-C3(8)BI-46	CCH-C3(8)BI-46	not measured
CCH-C3(8)BI-59	CCH-C3(8)BI-59	not measured
CCH-C3(8)BI-71	CCH-C3(8)BI-71	not measured
CCH-C3(8)BI-Blanc(6)	CCH-C3(8)BI- Blanc(6)	not measured

Table 102

FTIR Measurements: Bilayer actuators based on

CMC-g-PNIPAAm comb-type graft hydrogel films on PA6 substrates

(Group of Samples: Substrate CCH-C3(8)BI-PA6(3b.2))

Sample	Replica	Wave number -COOH (cm^{-1})
CCH-C3(8)BI-8	CCH-C3(8)BI-8	not measured
CCH-C3(8)BI-21	CCH-C3(8)BI-21	not measured
CCH-C3(8)BI-34	CCH-C3(8)BI-34	not measured
CCH-C3(8)BI-47	CCH-C3(8)BI-47	not measured
CCH-C3(8)BI-60	CCH-C3(8)BI-60	not measured
CCH-C3(8)BI-72	CCH-C3(8)BI-72	not measured
CCH-C3(8)BI-Blanc(7)	CCH-C3(8)BI- Blanc(7)	not measured

Table 103

FTIR Measurements: Bilayer actuators based on

CMC-g-PNIPAAm comb-type graft hydrogel films on PA6 substrates

(Group of Samples: Substrate PA6)

Sample	Replica	Wave number -COOH (cm^{-1})
CCH-C3(8)BI-84	CCH-C3(8)BI-PA84.1	no peak detected
	CCH-C3(8)BI-PA84.2	no peak detected
	CCH-C3(8)BI-PA84.3	no peak detected
CCH-C3(8)BI-85	CCH-C3(8)BI-PA85.1	no peak detected
	CCH-C3(8)BI-PA85.2	no peak detected
	CCH-C3(8)BI-PA85.3	no peak detected
CCH-C3(8)BI-86	CCH-C3(8)BI-PA86.1	no peak detected
	CCH-C3(8)BI-PA86.2	no peak detected
	CCH-C3(8)BI-PA86.3	no peak detected
CCH-C3(8)BI-87	CCH-C3(8)BI-PA87.1	no peak detected
	CCH-C3(8)BI-PA87.2	no peak detected
	CCH-C3(8)BI-PA87.3	no peak detected
CCH-C3(8)BI-88	CCH-C3(8)BI-PA88.1	no peak detected
	CCH-C3(8)BI-PA88.2	no peak detected
	CCH-C3(8)BI-PA88.3	no peak detected
CCH-C3(8)BI-89	CCH-C3(8)BI-89	not measured
CCH-C3(8)BI-Blanc(8)	CCH-C3(8)BI- Blanc(8)	not measured

Table 104

Standardsized gyration angle (|θ|) versus active layer of bilayer actuators based on CMC-g-PNIPAAm comb-type graft hydrogel films on PA6 substrates (Group of Samples: Substrate CCH-C3(8)BI-PA6(1a))

Sample	Passive Layer	Active Layer	Length[a] (mm)	Width[b] (mm)	Area[c] (mm^2)	θ	|θ|[d]
CCH-C3(8)BI-1	CCH-C3(8)BI-PA6(1a)	CCH-C3(8)BI-Sol(1)	15	2	30	1.4	0.5
CCH-C3(8)BI-14	CCH-C3(8)BI-PA6(1a)	CCH-C3(8)BI-Sol(2)	13	2	26	5.6	2.2
CCH-C3(8)BI-27	CCH-C3(8)BI-PA6(1a)	CCH-C3(8)BI-Sol(3)	11	2.5	27.5	5.5	2.0
CCH-C3(8)BI-40	CCH-C3(8)BI-PA6(1a)	CCH-C3(8)BI-Sol(4)	8	2	16	8.6	5.4
CCH-C3(8)BI-53	CCH-C3(8)BI-PA6(1a)	CCH-C3(8)BI-Sol(5)	12	2	24	4.7	2.0

[a]Length of the bilayer.

[b]Width of the bilayer.

[c]Area of the bilayer. Where: Area = Length x Width.

[d]|θ| = θ / Area.

Table 105

Standardsized gyration angle (|θ|) versus active layer of bilayer actuators based on CMC-g-PNIPAAm comb-type graft hydrogel films on PA6 substrates (Group of Samples: Substrate CCH-C3(8)BI-PA6(1b))

Sample	Passive Layer	Active Layer	Length[a] (mm)	Width[b] (mm)	Area[c] (mm^2)	θ	|θ|[d]
CCH-C3(8)BI-2	CCH-C3(8)BI-PA6(1b)	CCH-C3(8)BI-Sol(1)	16	3	48	1.6	0.3
CCH-C3(8)BI-15	CCH-C3(8)BI-PA6(1b)	CCH-C3(8)BI-Sol(2)	12	3	36	1.3	0.4
CCH-C3(8)BI-28	CCH-C3(8)BI-PA6(1b)	CCH-C3(8)BI-Sol(3)	10.5	2	21	4.5	2.1
CCH-C3(8)BI-41	CCH-C3(8)BI-PA6(1b)	CCH-C3(8)BI-Sol(4)	7	2.7	18.9	1.4	0.7
CCH-C3(8)BI-54	CCH-C3(8)BI-PA6(1b)	CCH-C3(8)BI-Sol(5)	12	2	24	6.7	2.8

[a]Length of the bilayer.

[b]Width of the bilayer.

[c]Area of the bilayer. Where: Area = Length x Width.

[d]|θ| = θ / Area.

Table 106

Standardsized gyration angle (|θ|) versus active layer of bilayer actuators based on CMC-g-PNIPAAm comb-type graft hydrogel films on PA6 substrates (Group of Samples: Substrate CCH-C3(8)BI-PA6(2a))

Sample	Passive Layer	Active Layer	Length[a] (mm)	Width[b] (mm)	Area[c] (mm^2)	θ	|θ|[d]
CCH-C3(8)BI-3	CCH-C3(8)BI-PA6(2a)	CCH-C3(8)BI-Sol(1)	13	3	39	9.2	2.4
CCH-C3(8)BI-16	CCH-C3(8)BI-PA6(2a)	CCH-C3(8)BI-Sol(2)	9	1.5	13.5	4.3	3.2
CCH-C3(8)BI-29	CCH-C3(8)BI-PA6(2a)	CCH-C3(8)BI-Sol(3)	9.5	2	19	1.7	0.9
CCH-C3(8)BI-42	CCH-C3(8)BI-PA6(2a)	CCH-C3(8)BI-Sol(4)	6.5	2.6	16.9	1.4	0.8
CCH-C3(8)BI-55	CCH-C3(8)BI-PA6(2a)	CCH-C3(8)BI-Sol(5)	11	3.1	34.1	3.4	1.0

[a]Length of the bilayer.

[b]Width of the bilayer.

[c]Area of the bilayer. Where: Area = Length x Width.

[d]|θ| = θ / Area.

Table 107

Standardsized gyration angle (|θ|) versus active layer of bilayer actuators based on CMC-g-PNIPAAm comb-type graft hydrogel films on PA6 substrates (Group of Samples: Substrate CCH-C3(8)BI-PA6(2b))

Sample	Passive Layer	Active Layer	Length[a] (mm)	Width[b] (mm)	Area[c] (mm^2)	θ	|θ|[d]
CCH-C3(8)BI-4	CCH-C3(8)BI-PA6(2b)	CCH-C3(8)BI-Sol(1)	13	2	26	0.6	0.2
CCH-C3(8)BI-17	CCH-C3(8)BI-PA6(2b)	CCH-C3(8)BI-Sol(2)	9	2.2	19.8	1.2	0.6
CCH-C3(8)BI-30	CCH-C3(8)BI-PA6(2b)	CCH-C3(8)BI-Sol(3)	9.5	2.5	23.75	2.7	1.1
CCH-C3(8)BI-43	CCH-C3(8)BI-PA6(2b)	CCH-C3(8)BI-Sol(4)	6.8	1.8	12.24	1	0.8
CCH-C3(8)BI-56	CCH-C3(8)BI-PA6(2b)	CCH-C3(8)BI-Sol(5)	9	2	18	10.3	5.7

[a]Length of the bilayer.

[b]Width of the bilayer.

[c]Area of the bilayer. Where: Area = Length x Width.

[d]|θ| = θ / Area.

Table 108

Standardsized gyration angle (|θ|) versus active layer of bilayer actuators based on CMC-g-PNIPAAm comb-type graft hydrogel films on PA6 substrates (Group of Samples: Substrate CCH-C3(8)BI-PA6(3a))

Sample	Passive Layer	Active Layer	Length[a] (mm)	Width[b] (mm)	Area[c] (mm^2)	θ	|θ|[d]
CCH-C3(8)BI-5	CCH-C3(8)BI-PA6(3a)	CCH-C3(8)BI-Sol(1)	9	2.5	22.5	10.2	4.5
CCH-C3(8)BI-18	CCH-C3(8)BI-PA6(3a)	CCH-C3(8)BI-Sol(2)	9.5	2.7	25.65	2.9	1.1
CCH-C3(8)BI-31	CCH-C3(8)BI-PA6(3a)	CCH-C3(8)BI-Sol(3)	10	2	20	1.0	0.5
CCH-C3(8)BI-44	CCH-C3(8)BI-PA6(3a)	CCH-C3(8)BI-Sol(4)	6.9	2	13.8	8.5	6.2
CCH-C3(8)BI-57	CCH-C3(8)BI-PA6(3a)	CCH-C3(8)BI-Sol(5)	10.4	2	20.8	1.0	0.5

[a]Length of the bilayer.

[b]Width of the bilayer.

[c]Area of the bilayer. Where: Area = Length x Width.

[d]|θ| = θ / Area.

Table 109

Standardsized gyration angle (|θ|) versus active layer of bilayer actuators based on CMC-g-PNIPAAm comb-type graft hydrogel films on PA6 substrates (Group of Samples: Substrate CCH-C3(8)BI-PA6(3b))

Sample	Passive Layer	Active Layer	Length[a] (mm)	Width[b] (mm)	Area[c] (mm^2)	θ	|θ|[d]
CCH-C3(8)BI-7	CCH-C3(8)BI-PA6(3b)	CCH-C3(8)BI-Sol(1)	12	3	36	0.6	0.2
CCH-C3(8)BI-20	CCH-C3(8)BI-PA6(3b)	CCH-C3(8)BI-Sol(2)	Not availabe	Not availabe	Not available	8.3	Not available
CCH-C3(8)BI-33	CCH-C3(8)BI-PA6(3b)	CCH-C3(8)BI-Sol(3)	9	2.2	19.8	6.0	3.0
CCH-C3(8)BI-46	CCH-C3(8)BI-PA6(3b)	CCH-C3(8)BI-Sol(4)	6.1	2.1	12.81	3.2	2.5
CCH-C3(8)BI-59	CCH-C3(8)BI-PA6(3b)	CCH-C3(8)BI-Sol(5)	10.2	2.8	28.56	3.1	1.1

[a]Length of the bilayer.

[b]Width of the bilayer.

[c]Area of the bilayer. Where: Area = Length x Width.

[d]|θ| = θ / Area.

Table 110

Standardsized gyration angle (|θ|) versus active layer of bilayer actuators based on CMC-g-PNIPAAm comb-type graft hydrogel films on PA6 substrates (Group of Samples: Substrate CCH-C3(8)BI- PA6(3b).2)

Sample	Passive Layer	Active Layer	Length[a] (mm)	Width[b] (mm)	Area[c] (mm^2)	θ	|θ|[d]
CCH-C3(8)BI-8	CCH-C3(8)BI-PA6(3b.2)	CCH-C3(8)BI-Sol(1)	13	2.3	29.9	21.0	7.0
CCH-C3(8)BI-21	CCH-C3(8)BI-PA6(3b.2)	CCH-C3(8)BI-Sol(2)	10.5	2.8	29.4	23.8	8.1
CCH-C3(8)BI-34	CCH-C3(8)BI-PA6(3b.2)	CCH-C3(8)BI-Sol(3)	8	2	16	4.1	2.6
CCH-C3(8)BI-47	CCH-C3(8)BI-PA6(3b.2)	CCH-C3(8)BI-Sol(4)	6	2.5	15	2.4	1.6
CCH-C3(8)BI-60	CCH-C3(8)BI-PA6(3b.2)	CCH-C3(8)BI-Sol(5)	10.5	2.3	24.15	5.9	2.4

[a]Length of the bilayer.

[b]Width of the bilayer.

[c]Area of the bilayer. Where: Area = Length x Width.

[d]|θ| = θ / Area.

Table 111

Gyration Angle (θ) vs Time

(Sample: CCH-C3(8)BI-56)

Time	Gyration Angle (θ)
0	-0.1
8	0.2
16	-0.1
24	0.0
32	0.4
40	0.3
48	0.4
56	0.4
64	0.4
72	0.7
80	0.6
88	0.4
98	2.3
106	6.4

Table 111

(Cont.)

Time	Gyration Angle (θ)
114	9.0
122	9.4
130	9.5
138	9.6
146	9.5
154	10.0
162	9.8
170	9.6
178	10.1
186	10.1
194	10.2
202	10.2
210	10.3
218	10.3

Table 112

Elemental Analysis: Aminoterminated PNIPAAm oligomers

Experimental Data - Part 1: Experimental weight percentages (%W)

(Group of Samples A ($M_{W(THEO)}$ = 5,000 g/mol))

Group of Samples A ($M_{W(THEO)}$ = 5,000 g/mol)								
Sample	**Sample Fraction**	**Replica**	**Weight (g)**	**% W - O (%)**	**% W - N (%)**	**% W - C (%)**	**% W - H (%)**	**% W - S (%)**
CCH-A15-1	CCH-A15-1	CCH-A15-1a	2.0750	16.347	11.556	59.759	9.812	0.114
		CCH-A15-1b	2.1080	16.563	11.467	58.890	9.750	0.089
CCH-A15-2	CCH-A15-2	CCH-A15-2a	1.5340	16.576	11.558	59.627	10.025	0.118
		CCH-A15-2b	1.0410	16.286	11.555	59.651	9.996	0.105
CCH-A15-3	CCH-A15-3	CCH-A15-3	1.8430	16.408	11.509	59.320	10.041	0.130
		CCH-A15-3	1.5420	16.538	11.497	59.690	10.117	0.120
CCH-C1-1	CCH-C1-1(1)	CCH-C1-1(1)a	1.9490	16.813	11.611	59.581	9.707	0.175
		CCH-C1-1(1)b	1.6220	16.710	11.579	59.306	9.656	0.165
	CCH-C1-1(2)	CCH-C1-1(2)a	1.5870	16.630	11.662	59.710	10.055	0.037
		CCH-C1-1(2)b	1.7150	16.845	11.593	59.764	10.008	0.060
CCH-C1(2)-1	CCH-C1(2)-1(1)	CCH-C1(2)-1(1)a	1.8760	16.849	11.599	59.454	9.958	0.093
		CCH-C1(2)-1(1)b	1.9370	16.847	11.566	59.292	9.913	0.095
	CCH-C1(2)-1(2)	CCH-C1(2)-1(2)a	2.0750	17.131	11.624	59.676	9.977	0.106
		CCH-C1(2)-1(2)b	2.2140	16.834	11.598	59.405	9.946	0.069

Table 112

(Cont.)

Group of Samples A (Mw(THEO) = 5,000 g/mol)								
Sample	**Sample Fraction**	**Replica**	**Weight (g)**	**% W - O (%)**	**% W - N (%)**	**% W - C (%)**	**% W - H (%)**	**% W - S (%)**
CCH-C1(2)-1	CCH-C1(2)-1(3)	CCH-C1(2)-1(3)a	1.5340	15.328	11.598	59.734	10.050	0.109
		CCH-C1(2)-1(3)b	1.7110	16.650	11.598	59.682	10.027	0.114
	CCH-C1(2)-1(4)	CCH-C1(2)-1(4)a	1.8480	16.905	11.584	59.322	9.977	0.151
		CCH-C1(2)-1(4)b	1.8420	16.471	11.562	59.399	9.978	0.119
	CCH-C1(2)-1(5)	CCH-C1(2)-1(5)a	2.1650	16.704	11.571	59.086	9.855	0.147
		CCH-C1(2)-1(5)b	1.7590	16.646	11.568	59.265	9.963	0.188
	CCH-C1(2)-1(6)	CCH-C1(2)-1(6)a	1.9720	16.866	11.568	59.367	10.007	0.137
		CCH-C1(2)-1(6)b	1.8660	16.972	11.514	59.057	9.929	0.159

Table 113

Elemental Analysis: Aminoterminated PNIPAAm oligomers

Experimental Data - Part 1: Experimental weight percentages (%W)

(Group of Samples B ($M_{W(THEO)}$ = 7,000 g/mol))

Group of Samples B ($M_{W(THEO)}$ = 7,000 g/mol)								
Sample	**Sample Fraction**	**Replica**	**Weight (g)**	**% W - O (%)**	**% W - N (%)**	**% W - C (%)**	**% W - H (%)**	**% W - S (%)**
CCH-B4-1	CCH-B4-1	CCH-B4-1	1.9650	16.513	11.540	59.326	10.014	0.049
		CCH-B4-1	1.7360	16.495	11.512	59.101	9.904	0.047
CCH-C1-2	CCH-C1-2(1)	CCH-C1-2(1)a	2.0920	16.916	11.415	58.434	9.730	0.118
		CCH-C1-2(1)b	1.5350	16.750	11.473	58.827	9.864	0.102
	CCH-C1-2(2)	CCH-C1-2(2)a	1.9670	16.861	11.604	59.400	9.999	0.098
		CCH-C1-2(2)b	1.7120	16.696	11.618	59.507	10.006	0.136
CCH-C1(2)-1	CCH-C1(2)-2(1)	CCH-C1(2)-2(1)	2.0420	16.664	11.578	59.593	10.054	0.000
		CCH-C1(2)-2(1)	0.7280	16.064	11.476	59.225	10.201	0.000
	CCH-C1(2)-2(3)	CCH-C1(2)-2(3)	2.1470	16.672	11.505	59.273	9.984	0.000
		CCH-C1(2)-2(3)	1.7420	16.630	11.589	60.012	10.360	0.000
	CCH-C1(2)-2(4)	CCH-C1(2)-2(4)a	1.8710	16.746	11.569	59.630	10.006	0.034
		CCH-C1(2)-2(4)b	1.9590	16.790	11.511	59.323	10.005	0.036
CCH-C1(2)-1	CCH-C1(2)-2(5)	CCH-C1(2)-2(5)b	1.8060	16.315	11.666	59.962	9.756	0.033
	CCH-C1(2)-2(6)	CCH-C1(2)-2(6)b	1.7100	16.718	11.136	57.299	9.316	0.050

Table 114

Elemental Analysis: Aminoterminated PNIPAAm oligomers

Experimental Data - Part 1: Experimental weight percentages (%W)

(Group of Samples C ($M_{w(THEO)}$ = 9,000 g/mol))

Group of Samples C ($M_{w(THEO)}$ = 9,000 g/mol)								
Sample	**Sample Fraction**	**Replica**	**Weight (g)**	**% W - O (%)**	**% W - N (%)**	**% W - C (%)**	**% W - H (%)**	**% W - S (%)**
CCH-B4-2	CCH-B4-2	CCH-B4-2a	1.4220	16.295	11.477	59.117	9.576	0.034
		CCH-B4-2b	1.0150	16.222	11.555	59.709	9.792	0.053
CCH-C1-3	CCH-C1-3(1)	CCH-C1-3(1)a	0.8560	16.707	11.574	59.499	10.052	0.000
		CCH-C1-3(1)b	1.4540	16.704	11.601	59.776	10.050	0.000
	CCH-C1-3(2)	CCH-C1-3(2)	1.8520	16.882	11.556	59.591	10.001	0.044
		CCH-C1-3(2)	1.4970	16.803	11.521	59.405	9.941	0.037
CCH-C1(2)-3	CCH-C1(2)-3(1)	CCH-C1(2)-3(1)a	1.6970	16.126	11.458	59.998	9.957	0.000
	CCH-C1(2)-3(2)	CCH-C1(2)-3(2)	1.4680	16.683	11.634	59.633	10.248	0.000
		CCH-C1(2)-3(2)	1.6090	16.820	11.515	59.325	10.188	0.000
	CCH-C1(2)-3(4)	CCH-C1(2)-3(4)a	1.8840	17.111	11.610	59.752	10.134	0.000
		CCH-C1(2)-3(4)b	2.1580	17.047	11.616	59.796	10.216	0.000
	CCH-C1(2)-3(5)	CCH-C1(2)-3(5)a	1.5820	16.900	11.651	60.204	10.291	0.000

Table 114
(Cont.)

Group of Samples C (Mw(THEO) = 9,000 g/mol)								
Sample	**Sample Fraction**	**Replica**	**Weight (g)**	**% W - O (%)**	**% W - N (%)**	**% W - C (%)**	**% W - H (%)**	**% W - S (%)**
CCH-C1(2)-3	CCH-C1(2)-3(6)	CCH-C1(2)-3(6)a	1.9300	16.783	11.616	59.877	10.027	0.000
		CCH-C1(2)-3(6)b	1.4800	17.316	11.586	59.687	10.007	0.000
CCH-C1(2)-3.2	CCH-C1(2)-3.2(1)	CCH-C1(2)-3.2(1)a	1.9460	17.002	11.549	59.490	10.023	0.033
		CCH-C1(2)-3.2(1)b	1.4490	16.548	11.593	59.898	10.285	0.000
	CCH-C1(2)-3.2(2)	CCH-C1(2)-3.2(2)	1.5760	16.927	11.552	59.439	10.208	0.000
		CCH-C1(2)-3.2(2)	2.0650	17.021	11.513	59.234	10.127	0.000
	CCH-C1(2)-3.2(3)	CCH-C1(2)-3.2(3)a	1.8560	17.009	11.554	59.550	10.102	0.000
		CCH-C1(2)-3.2(3)b	2.1150	17.291	11.512	59.271	10.067	0.000
	CCH-C1(2)-3.2(4)	CCH-C1(2)-3.2(4)a	1.6680	17.445	11.621	60.348	10.129	0.000
		CCH-C1(2)-3.2(4)b	2.0860	17.531	11.647	60.091	10.247	0.000
	CCH-C1(2)-3.2(5)	CCH-C1(2)-3.2(5)a	1.1490	17.352	11.569	59.662	10.177	0.000
		CCH-C1(2)-3.2(5)b	1.7280	17.412	11.537	59.531	10.191	0.000
	CCH-C1(2)-3.2(6)	CCH-C1(2)-3.2(6)	1.7260	17.553	11.422	58.975	10.079	0.000
		CCH-C1(2)-3.2(6)	2.0240	17.592	11.419	58.826	10.054	0.000

Table 114
(Cont.)

Group of Samples C ($M_{W(THEO)}$ = 9,000 g/mol)								
Sample	**Sample Fraction**	**Replica**	**Weight (g)**	**% W - O (%)**	**% W - N (%)**	**% W - C (%)**	**% W - H (%)**	**% W - S (%)**
CCH-C1(2)-3.3	CCH-C1(2)-3.3(1)	CCH-C1(2)-3.3(1)a	1.9540	17.587	11.594	59.735	9.706	0.087
		CCH-C1(2)-3.3(1)b	1.8740	17.451	11.582	59.791	9.922	0.000
	CCH-C1(2)-3.3(2)	CCH-C1(2)-3.3(2)	2.0700	17.600	11.586	59.617	10.237	0.000
		CCH-C1(2)-3.3(2)	1.9360	17.871	11.525	59.431	10.181	0.000
	CCH-C1(2)-3.3(3)	CCH-C1(2)-3.3(3)a	2.0110	15.729	11.559	59.699	9.903	0.000
		CCH-C1(2)-3.3(3)b	2.0650	17.618	11.551	59.542	9.838	0.000
	CCH-C1(2)-3.3(4)	CCH-C1(2)-3.3(4)a	1.9240	17.515	11.344	58.451	9.700	0.000
		CCH-C1(2)-3.3(4)b	1.9970	17.476	10.778	55.588	9.185	0.000
	CCH-C1(2)-3.3(5)	CCH-C1(2)-3.3(5)b	1.6570	17.404	10.523	54.312	8.922	0.000
	CCH-C1(2)-3.3(6)	CCH-C1(2)-3.3(6)	1.9660	17.915	11.576	59.612	10.180	0.000
		CCH-C1(2)-3.3(6)	1.7260	17.688	11.536	59.582	10.176	0.000

Table 115

Elemental Analysis: Aminoterminated PNIPAAm oligomers

Experimental Data - Part 2: Experimental weights

(Group of Samples A ($M_{w(THEO)}$ = 5,000 g/mol))

Group of Samples A ($M_{w(THEO)}$ = 5,000 g/mol)								
Sample	**Sample Fraction**	**Replica**	**Weight (g)**	**Weight - O (g)**	**Weight - N (g)**	**Weight - C (g)**	**Weight - H (g)**	**Weight - S (g)**
CCH-A15-1	CCH-A15-1	CCH-A15-1a	2.0750	0.3392	0.2398	1.2400	0.2036	0.0024
		CCH-A15-1b	2.1080	0.3491	0.2417	1.2414	0.2055	0.0019
CCH-A15-2	CCH-A15-2	CCH-A15-2a	1.5340	0.2543	0.1773	0.9147	0.1538	0.0018
		CCH-A15-2b	1.0410	0.1695	0.1203	0.6210	0.1041	0.0011
CCH-A15-3	CCH-A15-3	CCH-A15-3	1.8430	0.3024	0.2121	1.0933	0.1851	0.0024
		CCH-A15-3	1.5420	0.2550	0.1773	0.9204	0.1560	0.0019
CCH-C1- 1	CCH-C1-1(1)	CCH-C1-1(1)a	1.9490	0.3277	0.2263	1.1612	0.1892	0.0034
		CCH-C1-1(1)b	1.6220	0.2710	0.1878	0.9619	0.1566	0.0027
	CCH-C1-1(2)	CCH-C1-1(2)a	1.5870	0.2639	0.1851	0.9476	0.1596	0.0006
		CCH-C1-1(2)b	1.7150	0.2889	0.1988	1.0250	0.1716	0.0010
CCH-C1(2)-1	CCH-C1(2)-1(1)	CCH-C1(2)-1(1)a	1.8760	0.3161	0.2176	1.1154	0.1868	0.0017
		CCH-C1(2)-1(1)b	1.9370	0.3263	0.2240	1.1485	0.1920	0.0018
	CCH-C1(2)-1(2)	CCH-C1(2)-1(2)a	2.0750	0.3555	0.2412	1.2383	0.2070	0.0022
		CCH-C1(2)-1(2)b	2.2140	0.3727	0.2568	1.3152	0.2202	0.0015

Table 115
(Cont.)

Group of Samples A (Mw(THEO) = 5,000 g/mol)								
Sample	**Sample Fraction**	**Replica**	**Weight (g)**	**Weight - O (g)**	**Weight - N (g)**	**Weight - C (g)**	**Weight - H (g)**	**Weight - S (g)**
CCH-C1(2)-1	CCH-C1(2)-1(3)	CCH-C1(2)-1(3)a	1.5340	0.2351	0.1779	0.9163	0.1542	0.0017
		CCH-C1(2)-1(3)b	1.7110	0.2849	0.1984	1.0212	0.1716	0.0020
	CCH-C1(2)-1(4)	CCH-C1(2)-1(4)a	1.8480	0.3124	0.2141	1.0963	0.1844	0.0028
		CCH-C1(2)-1(4)b	1.8420	0.3034	0.2130	1.0941	0.1838	0.0022
	CCH-C1(2)-1(5)	CCH-C1(2)-1(5)a	2.1650	0.3616	0.2505	1.2792	0.2134	0.0032
		CCH-C1(2)-1(5)b	1.7590	0.2928	0.2035	1.0425	0.1752	0.0033
	CCH-C1(2)-1(6)	CCH-C1(2)-1(6)a	1.9720	0.3326	0.2281	1.1707	0.1973	0.0027
		CCH-C1(2)-1(6)b	1.8660	0.3167	0.2149	1.1020	0.1853	0.0030

Table 116

Elemental Analysis: Aminoterminated PNIPAAm oligomers

Experimental Data - Part 2: Experimental weights

(Group of Samples B ($M_{w(THEO)}$ = 7,000 g/mol))

Group of Samples B ($M_{w(THEO)}$ = 7,000 g/mol)								
Sample	**Sample Fraction**	**Replica**	**Weight (g)**	**Weight - O (g)**	**Weight - N (g)**	**Weight - C (g)**	**Weight - H (g)**	**Weight - S (g)**
CCH-B4-1	CCH-B4-1	CCH-B4-1	1.9650	0.3245	0.2268	1.1658	0.1968	0.0010
		CCH-B4-1	1.7360	0.2864	0.1998	1.0260	0.1719	0.0008
CCH-C1-2	CCH-C1-2(1)	CCH-C1-2(1)a	2.0920	0.3539	0.2388	1.2224	0.2036	0.0025
		CCH-C1-2(1)b	1.5350	0.2571	0.1761	0.9030	0.1514	0.0016
	CCH-C1-2(2)	CCH-C1-2(2)a	1.9670	0.3317	0.2283	1.1684	0.1967	0.0019
		CCH-C1-2(2)b	1.7120	0.2858	0.1989	1.0188	0.1713	0.0023
CCH-C1(2)-1	CCH-C1(2)-2(1)	CCH-C1(2)-2(1)	2.0420	0.3403	0.2364	1.2169	0.2053	0.0000
		CCH-C1(2)-2(1)	0.7280	0.1169	0.0835	0.4312	0.0743	0.0000
	CCH-C1(2)-2(3)	CCH-C1(2)-2(3)	2.1470	0.3579	0.2470	1.2726	0.2144	0.0000
		CCH-C1(2)-2(3)	1.7420	0.2897	0.2019	1.0454	0.1805	0.0000
	CCH-C1(2)-2(4)	CCH-C1(2)-2(4)a	1.8710	0.3133	0.2165	1.1157	0.1872	0.0006
		CCH-C1(2)-2(4)b	1.9590	0.3289	0.2255	1.1621	0.1960	0.0007
	CCH-C1(2)-2(5)	CCH-C1(2)-2(5)b	1.8060	0.2946	0.2107	1.0829	0.1762	0.0006
	CCH-C1(2)-2(6)	CCH-C1(2)-2(6)b	1.7100	0.2859	0.1904	0.9798	0.1593	0.0009

Table 117

Elemental Analysis: Aminoterminated PNIPAAm oligomers

Experimental Data - Part 2: Experimental weights

(Group of Samples C ($M_{W(THEO)}$ = 9,000 g/mol))

Group of Samples C ($M_{W(THEO)}$ = 9,000 g/mol)								
Sample	**Sample Fraction**	**Replica**	**Weight (g)**	**Weight - O (g)**	**Weight - N (g)**	**Weight - C (g)**	**Weight - H (g)**	**Weight - S (g)**
CCH-B4-2	CCH-B4-2	CCH-B4-2a	1.4220	0.2317	0.1632	0.8406	0.1362	0.0005
		CCH-B4-2b	1.0150	0.1647	0.1173	0.6060	0.0994	0.0005
CCH-C1-3	CCH-C1-3(1)	CCH-C1-3(1)a	0.8560	0.1430	0.0991	0.5093	0.0860	0.0000
		CCH-C1-3(1)b	1.4540	0.2429	0.1687	0.8691	0.1461	0.0000
	CCH-C1-3(2)	CCH-C1-3(2)	1.8520	0.3127	0.2140	1.1036	0.1852	0.0008
		CCH-C1-3(2)	1.4970	0.2515	0.1725	0.8893	0.1488	0.0006
CCH-C1(2)-3	CCH-C1(2)-3(1)	CCH-C1(2)-3(1)a	1.6970	0.2737	0.1944	1.0182	0.1690	0.0000
	CCH-C1(2)-3(2)	CCH-C1(2)-3(2)	1.4680	0.2449	0.1708	0.8754	0.1504	0.0000
		CCH-C1(2)-3(2)	1.6090	0.2706	0.1853	0.9545	0.1639	0.0000
	CCH-C1(2)-3(4)	CCH-C1(2)-3(4)a	1.8840	0.3224	0.2187	1.1257	0.1909	0.0000
		CCH-C1(2)-3(4)b	2.1580	0.3679	0.2507	1.2904	0.2205	0.0000
	CCH-C1(2)-3(5)	CCH-C1(2)-3(5)a	1.5820	0.2674	0.1843	0.9524	0.1628	0.0000

Table 117

(Cont.)

Group of Samples C ($M_{W(THEO)}$ = 9,000 g/mol)								
Sample	**Sample Fraction**	**Replica**	**Weight (g)**	**Weight - O (g)**	**Weight - N (g)**	**Weight - C (g)**	**Weight - H (g)**	**Weight - S (g)**
CCH-C1(2)-3	CCH-C1(2)-3(6)	CCH-C1(2)-3(6)a	1.9300	0.3239	0.2242	1.1556	0.1935	0.0000
		CCH-C1(2)-3(6)b	1.4800	0.2563	0.1715	0.8834	0.1481	0.0000
CCH-C1(2)-3.2	CCH-C1(2)-3.2(1)	CCH-C1(2)-3.2(1)a	1.9460	0.3309	0.2247	1.1577	0.1950	0.0006
		CCH-C1(2)-3.2(1)b	1.4490	0.2398	0.1680	0.8679	0.1490	0.0000
	CCH-C1(2)-3.2(2)	CCH-C1(2)-3.2(2)	1.5760	0.2668	0.1821	0.9368	0.1609	0.0000
		CCH-C1(2)-3.2(2)	2.0650	0.3515	0.2377	1.2232	0.2091	0.0000
	CCH-C1(2)-3.2(3)	CCH-C1(2)-3.2(3)a	1.8560	0.3157	0.2144	1.1052	0.1875	0.0000
		CCH-C1(2)-3.2(3)b	2.1150	0.3657	0.2435	1.2536	0.2129	0.0000
	CCH-C1(2)-3.2(4)	CCH-C1(2)-3.2(4)a	1.6680	0.2910	0.1938	1.0066	0.1690	0.0000
		CCH-C1(2)-3.2(4)b	2.0860	0.3657	0.2430	1.2535	0.2138	0.0000
	CCH-C1(2)-3.2(5)	CCH-C1(2)-3.2(5)a	1.1490	0.1994	0.1329	0.6855	0.1169	0.0000
		CCH-C1(2)-3.2(5)b	1.7280	0.3009	0.1994	1.0287	0.1761	0.0000
	CCH-C1(2)-3.2(6)	CCH-C1(2)-3.2(6)	1.7260	0.3030	0.1971	1.0179	0.1740	0.0000
		CCH-C1(2)-3.2(6)	2.0240	0.3561	0.2311	1.1906	0.2035	0.0000

Table 117

(Cont.)

Group of Samples C ($Mw_{(THEO)}$ = 9,000 g/mol)								
Sample	**Sample Fraction**	**Replica**	**Weight (g)**	**Weight - O (g)**	**Weight - N (g)**	**Weight - C (g)**	**Weight - H (g)**	**Weight - S (g)**
CCH-C1(2)-3.3	CCH-C1(2)-3.3(1)	CCH-C1(2)-3.3(1)a	1.9540	0.3436	0.2265	1.1672	0.1897	0.0017
		CCH-C1(2)-3.3(1)b	1.8740	0.3270	0.2170	1.1205	0.1859	0.0000
	CCH-C1(2)-3.3(2)	CCH-C1(2)-3.3(2)	2.0700	0.3643	0.2398	1.2341	0.2119	0.0000
		CCH-C1(2)-3.3(2)	1.9360	0.3460	0.2231	1.1506	0.1971	0.0000
	CCH-C1(2)-3.3(3)	CCH-C1(2)-3.3(3)a	2.0110	0.3163	0.2325	1.2005	0.1991	0.0000
		CCH-C1(2)-3.3(3)b	2.0650	0.3638	0.2385	1.2295	0.2032	0.0000
	CCH-C1(2)-3.3(4)	CCH-C1(2)-3.3(4)a	1.9240	0.3370	0.2183	1.1246	0.1866	0.0000
		CCH-C1(2)-3.3(4)b	1.9970	0.3490	0.2152	1.1101	0.1834	0.0000
	CCH-C1(2)-3.3(5)	CCH-C1(2)-3.3(5)b	1.6570	0.2884	0.1744	0.8999	0.1478	0.0000
	CCH-C1(2)-3.3(6)	CCH-C1(2)-3.3(6)	1.9660	0.3522	0.2276	1.1720	0.2001	0.0000
		CCH-C1(2)-3.3(6)	1.7260	0.3053	0.1991	1.0284	0.1756	0.0000

Table 118

Elemental Analysis: Aminoterminated PNIPAAm oligomers

Experimental Data - Part 3: Experimental moles (mol_{exp})

(Group of Samples A ($M_{W(THEO)}$ = 5,000 g/mol))

Group of Samples A ($M_{W(THEO)}$ = 5,000 g/mol)							
Sample	**Sample Fraction**	**Replica**	**mol_{exp} - O (mol)**	**mol_{exp} - N (mol)**	**mol_{exp} - C (mol)**	**mol_{exp} - H (mol)**	**mol_{exp} - S (mol)**
CCH-A15-1	CCH-A15-1	CCH-A15-1a	0.0212	0.0171	0.1032	0.2020	$7.38x10^{-5}$
		CCH-A15-1b	0.0218	0.0173	0.1034	0.2039	$5.85x10^{-5}$
CCH-A15-2	CCH-A15-2	CCH-A15-2a	0.0159	0.0127	0.0762	0.1526	$5.65x10^{-5}$
		CCH-A15-2b	0.0106	0.0086	0.0517	0.1032	$3.41x10^{-5}$
CCH-A15-3	CCH-A15-3	CCH-A15-3	0.0189	0.0151	0.0910	0.1836	$7.47x10^{-5}$
		CCH-A15-3	0.0159	0.0127	0.0766	0.1548	$5.77x10^{-5}$
CCH-C1-1	CCH-C1-1(1)	CCH-C1-1(1)a	0.0205	0.0162	0.0967	0.1877	$1.06x10^{-4}$
		CCH-C1-1(1)b	0.0169	0.0134	0.0801	0.1554	$8.35x10^{-5}$
	CCH-C1-1(2)	CCH-C1-1(2)a	0.0165	0.0132	0.0789	0.1583	$1.83x10^{-5}$
		CCH-C1-1(2)b	0.0181	0.0142	0.0853	0.1703	$3.21x10^{-5}$
CCH-C1(2)-1	CCH-C1(2)-1(1)	CCH-C1(2)-1(1)a	0.0198	0.0155	0.0929	0.1853	$5.44x10^{-5}$
		CCH-C1(2)-1(1)b	0.0204	0.0160	0.0956	0.1905	$5.74x10^{-5}$
	CCH-C1(2)-1(2)	CCH-C1(2)-1(2)a	0.0222	0.0172	0.1031	0.2054	$6.86x10^{-5}$
		CCH-C1(2)-1(2)b	0.0233	0.0183	0.1095	0.2185	$4.77x10^{-5}$

Table 118
(Cont.)

Group of Samples A ($M_{W(THEO)}$ = 5,000 g/mol)							
Sample	**Sample Fraction**	**Replica**	**mol_{exp} - O (mol)**	**mol_{exp} - N (mol)**	**mol_{exp} - C (mol)**	**mol_{exp} - H (mol)**	**mol_{exp} - S (mol)**
CCH-C1(2)-1	CCH-C1(2)-1(3)	CCH-C1(2)-1(3)a	0.0147	0.0127	0.0763	0.1529	$5.22x10^{-5}$
		CCH-C1(2)-1(3)b	0.0178	0.0142	0.0850	0.1702	$6.08x10^{-5}$
	CCH-C1(2)-1(4)	CCH-C1(2)-1(4)a	0.0195	0.0153	0.0913	0.1829	$8.70x10^{-5}$
		CCH-C1(2)-1(4)b	0.0190	0.0152	0.0911	0.1823	$6.84x10^{-5}$
	CCH-C1(2)-1(5)	CCH-C1(2)-1(5)a	0.0226	0.0179	0.1065	0.2117	$9.93x10^{-5}$
		CCH-C1(2)-1(5)b	0.0183	0.0145	0.0868	0.1739	$1.03x10^{-4}$
	CCH-C1(2)-1(6)	CCH-C1(2)-1(6)a	0.0208	0.0163	0.0975	0.1958	$8.43x10^{-5}$
		CCH-C1(2)-1(6)b	0.0198	0.0153	0.0917	0.1838	$9.25x10^{-5}$

Table 119

Elemental Analysis: Aminoterminated PNIPAAm oligomers

Experimental Data - Part 3: Experimental moles (mol_{exp})

(Group of Samples B ($Mw_{(THEO)}$ = 7,000 g/mol))

Group of Samples B ($Mw_{(THEO)}$ = 7,000 g/mol)							
Sample	**Sample Fraction**	**Replica**	**mol_{exp} - O (mol)**	**mol_{exp} - N (mol)**	**mol_{exp} - C (mol)**	**mol_{exp} - H (mol)**	**mol_{exp} - S (mol)**
CCH-B4-1	CCH-B4-1	CCH-B4-1	0.0203	0.0162	0.0971	0.1952	$3.00x10^{-5}$
		CCH-B4-1	0.0179	0.0143	0.0854	0.1706	$2.54x10^{-5}$
CCH-C1-2	CCH-C1-2(1)	CCH-C1-2(1)a	0.0221	0.0170	0.1018	0.2019	$7.70x10^{-5}$
		CCH-C1-2(1)b	0.0161	0.0126	0.0752	0.1502	$4.88x10^{-5}$
	CCH-C1-2(2)	CCH-C1-2(2)a	0.0207	0.0163	0.0973	0.1951	$6.01x10^{-5}$
		CCH-C1-2(2)b	0.0179	0.0142	0.0848	0.1699	$7.26x10^{-5}$
CCH-C1(2)-2	CCH-C1(2)-2(1)	CCH-C1(2)-2(1)	0.0213	0.0169	0.1013	0.2037	0.00
		CCH-C1(2)-2(1)	0.0073	0.0060	0.0359	0.0737	0.00
	CCH-C1(2)-2(3)	CCH-C1(2)-2(3)	0.0224	0.0176	0.1060	0.2127	0.00
		CCH-C1(2)-2(3)	0.0181	0.0144	0.0870	0.1790	0.00
	CCH-C1(2)-2(4)	CCH-C1(2)-2(4)a	0.0196	0.0155	0.0929	0.1857	$1.98x10^{-5}$
		CCH-C1(2)-2(4)b	0.0206	0.0161	0.0968	0.1944	$2.20x10^{-5}$
	CCH-C1(2)-2(5)	CCH-C1(2)-2(5)b	0.0184	0.0150	0.0902	0.1748	$1.86x10^{-5}$
	CCH-C1(2)-2(6)	CCH-C1(2)-2(6)b	0.0179	0.0136	0.0816	0.1580	$2.67x10^{-5}$

Table 120

Elemental Analysis: Aminoterminated PNIPAAm oligomers

Experimental Data - Part 3: Experimental moles (mol_{exp})

(Group of Samples C ($M_{W(THEO)}$ = 9,000 g/mol))

Group of Samples C ($M_{W(THEO)}$ = 9,000 g/mol)							
Sample	**Sample Fraction**	**Replica**	**mol_{exp} - O (mol)**	**mol_{exp} - N (mol)**	**mol_{exp} - C (mol)**	**mol_{exp} - H (mol)**	**mol_{exp} - S (mol)**
CCH-B4-2	CCH-B4-2	CCH-B4-2a	0.0145	0.0117	0.0700	0.1351	$1.51x10^{-5}$
		CCH-B4-2b	0.0103	0.0084	0.0505	0.0986	$1.68x10^{-5}$
CCH-C1-3	CCH-C1-3(1)	CCH-C1-3(1)a	0.0089	0.0071	0.0424	0.0854	0.00
		CCH-C1-3(1)b	0.0152	0.0120	0.0724	0.1450	0.00
	CCH-C1-3(2)	CCH-C1-3(2)	0.0195	0.0153	0.0919	0.1837	$2.54x10^{-5}$
		CCH-C1-3(2)	0.0157	0.0123	0.0740	0.1476	$1.73x10^{-5}$
CCH-C1(2)-3	CCH-C1(2)-3(1)	CCH-C1(2)-3(1)a	0.0171	0.0139	0.0848	0.1676	0.00
	CCH-C1(2)-3(2)	CCH-C1(2)-3(2)	0.0153	0.0122	0.0729	0.1492	0.00
		CCH-C1(2)-3(2)	0.0169	0.0132	0.0795	0.1626	0.00
	CCH-C1(2)-3(4)	CCH-C1(2)-3(4)a	0.0201	0.0156	0.0937	0.1894	0.00
		CCH-C1(2)-3(4)b	0.0230	0.0179	0.1074	0.2187	0.00
	CCH-C1(2)-3(5)	CCH-C1(2)-3(5)a	0.0167	0.0132	0.0793	0.1615	0.00

Table 120

(Cont.)

Group of Samples C ($Mw_{(THEO)}$ = 9,000 g/mol)							
Sample	**Sample Fraction**	**Replica**	**mol_{exp} - O (mol)**	**mol_{exp} - N (mol)**	**mol_{exp} - C (mol)**	**mol_{exp} - H (mol)**	**mol_{exp} - S (mol)**
CCH-C1(2)-3	CCH-C1(2)-3(6)	CCH-C1(2)-3(6)a	0.0202	0.0160	0.0962	0.1920	0.00
		CCH-C1(2)-3(6)b	0.0160	0.0122	0.0735	0.1469	0.00
CCH-C1(2)-3.2	CCH-C1(2)-3.2(1)	CCH-C1(2)-3.2(1)a	0.0207	0.0160	0.0964	0.1935	2.00×10^{-5}
		CCH-C1(2)-3.2(1)b	0.0150	0.0120	0.0723	0.1478	0.00
	CCH-C1(2)-3.2(2)	CCH-C1(2)-3.2(2)	0.0167	0.0130	0.0780	0.1596	0.00
		CCH-C1(2)-3.2(2)	0.0220	0.0170	0.1018	0.2075	0.00
	CCH-C1(2)-3.2(3)	CCH-C1(2)-3.2(3)a	0.0197	0.0153	0.0920	0.1860	0.00
		CCH-C1(2)-3.2(3)b	0.0229	0.0174	0.1044	0.2112	0.00
	CCH-C1(2)-3.2(4)	CCH-C1(2)-3.2(4)a	0.0182	0.0138	0.0838	0.1676	0.00
		CCH-C1(2)-3.2(4)b	0.0229	0.0173	0.1044	0.2121	0.00
	CCH-C1(2)-3.2(5)	CCH-C1(2)-3.2(5)a	0.0125	0.0095	0.0571	0.1160	0.00
		CCH-C1(2)-3.2(5)b	0.0188	0.0142	0.0856	0.1747	0.00
	CCH-C1(2)-3.2(6)	CCH-C1(2)-3.2(6)	0.0189	0.0141	0.0847	0.1726	0.00
		CCH-C1(2)-3.2(6)	0.0223	0.0165	0.0991	0.2019	0.00

Table 120

(Cont.)

Group of Samples C ($Mw_{(THEO)}$) = 9,000 g/mol)							
Sample	**Sample Fraction**	**Replica**	**mol_{exp} - O (mol)**	**mol_{exp} - N (mol)**	**mol_{exp} - C (mol)**	**mol_{exp} - H (mol)**	**mol_{exp} - S (mol)**
CCH-C1(2)-3.3	CCH-C1(2)-3.3(1)	CCH-C1(2)-3.3(1)a	0.0215	0.0162	0.0972	0.1882	$5.30x10^{-5}$
		CCH-C1(2)-3.3(1)b	0.0204	0.0155	0.0933	0.1845	0.00
	CCH-C1(2)-3.3(2)	CCH-C1(2)-3.3(2)	0.0228	0.0171	0.1027	0.2102	0.00
		CCH-C1(2)-3.3(2)	0.0216	0.0159	0.0958	0.1955	0.00
	CCH-C1(2)-3.3(3)	CCH-C1(2)-3.3(3)a	0.0198	0.0166	0.1000	0.1976	0.00
		CCH-C1(2)-3.3(3)b	0.0227	0.0170	0.1024	0.2015	0.00
	CCH-C1(2)-3.3(4)	CCH-C1(2)-3.3(4)a	0.0211	0.0156	0.0936	0.1851	0.00
		CCH-C1(2)-3.3(4)b	0.0218	0.0154	0.0924	0.1820	0.00
	CCH-C1(2)-3.3(5)	CCH-C1(2)-3.3(5)b	0.0180	0.0124	0.0749	0.1467	0.00
	CCH-C1(2)-3.3(6)	CCH-C1(2)-3.3(6)	0.0220	0.0162	0.0976	0.1986	0.00
		CCH-C1(2)-3.3(6)	0.0191	0.0142	0.0856	0.1742	0.00

Table 121

Elemental Analysis: Aminoterminated PNIPAAm oligomers

Experimental Data - Part 4: Average experimental moles (mol_{avg})

(Group of Samples A ($M_{W(THEO)}$ = 5,000 g/mol))

Group of Samples A ($M_{W(THEO)}$ = 5,000 g/mol)					
Sample	**mol_{avg} - O (mol)**	**mol_{avg} - N (mol)**	**mol_{avg} - C (mol)**	**mol_{avg} - H (mol)**	**mol_{avg} - S (mol)**
CCH-A15-1	0.0215	0.0172	0.1033	0.2029	$6.62x10^{-5}$
CCH-A15-2	0.0132	0.0106	0.0639	0.1279	$4.53x10^{-5}$
CCH-A15-3	0.0174	0.0139	0.0838	0.1692	$6.62x10^{-5}$
CCH-C1-1	0.0180	0.0142	0.0852	0.1679	$6.01x10^{-5}$
CCH-C1(2)-1	0.0198	0.0157	0.0939	0.1878	$7.30x10^{-5}$

Table 122

Elemental Analysis: Aminoterminated PNIPAAm oligomers

Experimental Data - Part 4: Average experimental moles (mol_{avg})

(Group of Samples B ($M_{W(THEO)}$ = 7,000 g/mol))

Group of Samples B ($M_{W(THEO)}$ = 7,000 g/mol)					
Sample	**mol_{avg} - O (mol)**	**mol_{avg} - N (mol)**	**mol_{avg} - C (mol)**	**mol_{avg} - H (mol)**	**mol_{avg} - S (mol)**
CCH-B4-1	0.0191	0.0152	0.0912	0.1829	$2.77x10^{-5}$
CCH-C1-2	0.0192	0.0150	0.0898	0.1793	$6.46x10^{-5}$
CCH-C1(2)-2	0.0182	0.0144	0.0863	0.1715	$1.32x10^{-5}$

Table 123

Elemental Analysis: Aminoterminated PNIPAAm oligomers

Experimental Data - Part 4: Average experimental moles (mol_{avg})

(Group of Samples C ($Mw_{(THEO)}$ = 9,000 g/mol))

Group of Samples C ($Mw_{(THEO)}$ = 9,000 g/mol)					
Sample	**mol_{avg} - O (mol)**	**mol_{avg} - N (mol)**	**mol_{avg} - C (mol)**	**mol_{avg} - H (mol)**	**mol_{avg} - S (mol)**
CCH-B4-2	0.0124	0.0100	0.0602	0.1168	$1.59x10^{-5}$
CCH-C1-3	0.0148	0.0117	0.0702	0.1404	$1.07x10^{-5}$
CCH-C1(2)-3	0.0179	0.0141	0.0851	0.1717	0.00
CCH-C1(2)-3.2	0.0192	0.0147	0.0883	0.1792	$1.67x10^{-6}$
CCH-C1(2)-3.3	0.0207	0.0154	0.0925	0.1842	$4.42x10^{-6}$

Table 124

Elemental Analysis: Aminoterminated PNIPAAm oligomers

Experimental Data - Part 5: Experimental mol percentages ($\%mol_{exp}$)

Group of Samples A ($Mw_{(THEO)}$ = 5,000 g/mol)					
Sample	**$\%mol_{exp}$ - O (%)**	**$\%mol_{exp}$ - N (%)**	**$\%mol_{exp}$ - C (%)**	**$\%mol_{exp}$ - H (%)**	**$\%mol_{exp}$ - S (%)**
CCH-A15-1	6.2353	4.9820	29.9408	58.8227	0.0192
CCH-A15-2	6.1394	4.9240	29.6317	59.2840	0.0210
CCH-A15-3	6.1255	4.8877	29.4760	59.4875	0.0233
CCH-C1-1	6.3035	4.9895	29.8641	58.8218	0.0210
CCH-C1(2)-1	6.2540	4.9496	29.6033	59.1701	0.0230

Table 125

Elemental Analysis: Aminoterminated PNIPAAm oligomers

Experimental Data - Part 5: Experimental mol percentages ($\%mol_{exp}$)

(Group of Samples B ($Mw_{(THEO)}$ = 7,000 g/mol))

Group of Samples B ($Mw_{(THEO)}$ = 7,000 g/mol)					
Sample	**$\%mol_{exp}$ - O (%)**	**$\%mol_{exp}$ - N (%)**	**$\%mol_{exp}$ - C (%)**	**$\%mol_{exp}$ - H (%)**	**$\%mol_{exp}$ - S (%)**
CCH-B4-1	6.1884	4.9367	29.5774	59.2886	0.0090
CCH-C1-2	6.3280	4.9544	29.5901	59.1062	0.0213
CCH-C1(2)-2	6.2597	4.9492	29.7305	59.0560	0.0046

Table 126

Elemental Analysis: Aminoterminated PNIPAAm oligomers

Experimental Data - Part 5: Experimental mol percentages ($\%mol_{exp}$)

(Group of Samples C ($Mw_{(THEO)}$ = 9,000 g/mol))

Group of Samples C ($Mw_{(THEO)}$ = 9,000 g/mol)					
Sample	**$\%mol_{exp}$ - O (%)**	**$\%mol_{exp}$ - N (%)**	**$\%mol_{exp}$ - C (%)**	**$\%mol_{exp}$ - H (%)**	**$\%mol_{exp}$ - S (%)**
CCH-B4-2	6.2097	5.0191	30.1896	58.5736	0.0080
CCH-C1-3	6.2606	4.9242	29.5919	59.2188	0.0045
CCH-C1(2)-3	6.2047	4.8894	29.4695	59.4364	0.0000
CCH-C1(2)-3.2	6.3705	4.8714	29.2981	59.4594	0.0006
CCH-C1(2)-3.3	6.6277	4.9179	29.5743	58.8787	0.0014

Table 127

Elemental Analysis: Aminoterminated PNIPAAm oligomers

Theoretical Data - Part 1: Theoretical moles (mol_{theo})

(Group of Samples A ($M_{W(THEO)}$ = 5,000 g/mol))

Group of Samples A ($M_{W(THEO)}$ = 5,000 g/mol)						
Sample	**mol_{theo} – olig. (mol)**	**mol_{theo} - O (mol)**	**mol_{theo} - N (mol)**	**mol_{theo} - C (mol)**	**mol_{theo} - H (mol)**	**mol_{theo} - S (mol)**
CCH-A15-1	866	45	46	272	502	1
CCH-A15-2	866	45	46	272	502	1
CCH-A15-3	866	45	46	272	502	1
CCH-C1-1	866	45	46	272	502	1
CCH-C1(2)-1	866	45	46	272	502	1

Table 128

Elemental Analysis: Aminoterminated PNIPAAm oligomers

Theoretical Data - Part 1: Theoretical moles (mol_{theo})

(Group of Samples B ($Mw_{(THEO)}$ = 7,000 g/mol))

	Group of Samples B ($Mw_{(THEO)}$ = 7,000 g/mol)						
Sample	**mol_{theo} – olig. (mol)**	**mol_{theo} - O (mol)**	**mol_{theo} - N (mol)**	**mol_{theo} - C (mol)**	**mol_{theo} - H (mol)**	**mol_{theo} - S (mol)**
CCH-B4-1	1208	63	64	380	700	1
CCH-C1-2	1208	63	64	380	700	1
CCH-C1(2)-2	1208	63	64	380	700	1

Table 129

Elemental Analysis: Aminoterminated PNIPAAm oligomers

Theoretical Data - Part 1: Theoretical moles (mol_{theo})

(Group of Samples C ($Mw_{(THEO)}$ = 9,000 g/mol))

Group of Samples C ($Mw_{(THEO)}$ = 9,000 g/mol)						
Sample	**mol_{theo} – olig. (mol)**	**mol_{theo} - O (mol)**	**mol_{theo} - N (mol)**	**mol_{theo} - C (mol)**	**mol_{theo} - H (mol)**	**mol_{theo} - S (mol)**
CCH-B4-2	1550	81	82	488	898	1
CCH-C1-3	1550	81	82	488	898	1
CCH-C1(2)-3	1550	81	82	488	898	1
CCH-C1(2)-3.2	1550	81	82	488	898	1
CCH-C1(2)-3.3	1550	81	82	488	898	1

Table 130

Elemental Analysis: Aminoterminated PNIPAAm oligomers

Theoretical Data - Part 2: Theoretical mol percentages ($\%mol_{theo}$)

(Group of Samples A ($M_{W(THEO)}$ = 5,000 g/mol))

Group of Samples A ($M_{W(THEO)}$ = 5,000 g/mol)					
Sample	**$\%mol_{theo}$ - O (%)**	**$\%mol_{theo}$ - N (%)**	**$\%mol_{theo}$ - C (%)**	**$\%mol_{theo}$ - H (%)**	**$\%mol_{theo}$ - S (%)**
CCH-A15-1	5.1963	5.3118	31.4088	57.9677	0.1155
CCH-A15-2	5.1963	5.3118	31.4088	57.9677	0.1155
CCH-A15-3	5.1963	5.3118	31.4088	57.9677	0.1155
CCH-C1-1	5.1963	5.3118	31.4088	57.9677	0.1155
CCH-C1(2)-1	5.1963	5.3118	31.4088	57.9677	0.1155

Table 131

Elemental Analysis: Aminoterminated PNIPAAm oligomers

Theoretical Data - Part 2: Theoretical mol percentages ($\%mol_{theo}$)

(Group of Samples B ($M_{W(THEO)}$ = 7,000 g/mol))

Group of Samples B ($M_{W(THEO)}$ = 7,000 g/mol)					
Sample	**$\%mol_{theo}$ - O (%)**	**$\%mol_{theo}$ - N (%)**	**$\%mol_{theo}$ - C (%)**	**$\%mol_{theo}$ - H (%)**	**$\%mol_{theo}$ - S (%)**
CCH-B4-1	5.2152	5.2980	31.4570	57.9470	0.0828
CCH-C1-2	5.2152	5.2980	31.4570	57.9470	0.0828
CCH-C1(2)-2	5.2152	5.2980	31.4570	57.9470	0.0828

Table 132

Elemental Analysis: Aminoterminated PNIPAAm oligomers

Theoretical Data - Part 2: Theoretical mol percentages ($\%mol_{theo}$)

(Group of Samples C ($Mw_{(THEO)}$ = 9,000 g/mol))

Group of Samples C ($Mw_{(THEO)}$ = 9,000 g/mol)					
Sample	**$\%mol_{theo}$ - O (%)**	**$\%mol_{theo}$ - N (%)**	**$\%mol_{theo}$ - C (%)**	**$\%mol_{theo}$ - H (%)**	**$\%mol_{theo}$ - S (%)**
CCH-B4-2	5.2258	5.2903	31.4839	57.9355	0.0645
CCH-C1-3	5.2258	5.2903	31.4839	57.9355	0.0645
CCH-C1(2)-3	5.2258	5.2903	31.4839	57.9355	0.0645
CCH-C1(2)-3.2	5.2258	5.2903	31.4839	57.9355	0.0645
CCH-C1(2)-3.3	5.2258	5.2903	31.4839	57.9355	0.0645

Table 133

Elemental Analysis: CMC-g-PNIPAAm graft copolymers

Experimental Data - Part 1: Experimental weight percentages of N (%W - N)

Group of Samples A (Mw(Graft)$_{(THEO)}$ = 5,000 g/mol)

Group of Samples A (Mw(Graft)$_{(THEO)}$ = 5,000 g/mol)				
Sub-Group A.1 (%Graft(THEO)=40%)				
Sample	**Sample Fraction**	**Replica**	**Weight (g)**	**% W - N (%)**
CCH-A27-1	CCH-A27-1(1)	CCH-A27-1(1)	1.2440	3.659
	CCH-A27-1(2)	CCH-A27-1(2)	1.1230	3.706
		CCH-A27-1(2).1ASE	1.7740	3.672
		CCH-A27-1(2).2ASE	1.1870	3.757
		CCH-A27-1(2).3ASE	0.5820	3.790
	CCH-A27-1(3)	CCH-A27-1(3)	1.0380	3.583
	CCH-A27-1(4)	CCH-A27-1(4)	1.4750	3.527
	CCH-A27-1(5)	CCH-A27-1(5)	1.7930	3.533
CCH-C2-1.40	CCH-C2-1.40	CCH-C2_1.40.1ASE	1.2780	1.307
		CCH-C2_1.40.2ASE	1.0520	1.356
CCH-C2(2)-1.40	CCH-C2(2)-1.40(1)	No replica	Not measured	Not measured
	CCH-C2(2)-1.40(2)	CCH-C2(2)-1.40(2)ASE.1	1.3550	5.318
		CCH-C2(2)-1.40(2)ASE.3	1.3040	5.420
	CCH-C2(2)-1.40(3)	No replica	Not measured	Not measured
	CCH-C2(2)-1.40(4)	No replica	Not measured	Not measured

Table 133

(Cont.)

Group of Samples A (Mw(Graft)(THEO) = 5,000 g/mol)				
Sub-Group A.2 (%Graft(THEO)=50%)				
Sample	**Sample Fraction**	**Replica**	**Weight (g)**	**% W - N (%)**
CCH-B5-1.50	CCH-B5-1.50	CCH-B5-1.50.1ASE	1.8630	5.044
		CCH-B5-1.50.2ASE	1.6520	5.129
		CCH-B5-1.50.3ASE	1.2090	5.508
		CCH-B5-1.50	1.6670	4.569
		CCH-B5-1.50	1.3850	4.548
CCH-C2(2)-1.50	CCH-C2(2)-1.50(1)	No replica	Not measured	Not measured
	CCH-C2(2)-1.50(2)	CCH-C2(2)-1.50(2).1ASE	1.1950	6.619
		CCH-C2(2)-1.50(2).2ASE	1.6970	6.468
		CCH-C2(2)-1.50(2).3ASE	1.0090	6.685
	CCH-C2(2)-1.50(3)	No replica	Not measured	Not measured
	CCH-C2(2)-1.50(4)	No replica	Not measured	Not measured
	CCH-C2(2)-1.50(5)	No replica	Not measured	Not measured

Table 133

(Cont.)

Group of Samples A (Mw(Graft)(THEO) = 5,000 g/mol)				
Sub-Group A.3 (%Graft(THEO)=80%)				
Sample	**Sample Fraction**	**Replica**	**Weight (g)**	**% W - N (%)**
CCH-C2(2)-1.80	CCH-C2(2)-1.80(1)	No replica	Not measured	Not measured
	CCH-C2(2)-1.80(2)	No replica	Not measured	Not measured
	CCH-C2(2)-1.80(3)	No replica	Not measured	Not measured
	CCH-C2(2)-1.80(4)	No replica	Not measured	Not measured
	CCH-C2(2)-1.80(5)	CCH-C2(2)-1.80(5).1ASE	1.0490	9.197
		CCH-C2(2)-1.80(5).2ASE	1.1540	9.101
		CCH-C2(2)-1.80(5).3ASE	1.1690	9.078
	CCH-C2(2)-1.80(6)	No replica	Not measured	Not measured
	CCH-C2(2)-1.80(7)	No replica	Not measured	Not measured
	CCH-C2(2)-1.80(8)	No replica	Not measured	Not measured
	CCH-C2(2)-1.80(9)	No replica	Not measured	Not measured
	CCH-C2(2)-1.80(10)	No replica	Not measured	Not measured

Table 134

Elemental Analysis: CMC-g-PNIPAAm graft copolymers

Experimental Data - Part 1: Experimental weight percentages of N (%W-N)

(Group of Samples B ($Mw(Graft)_{(THEO)}$ = 7,000 g/mol))

Group of Samples B ($Mw(Graft)_{(THEO)}$ = 7,000 g/mol)				
Sub-Group B.1 (%Graft(THEO)=40%)				
Sample	**Sample Fraction**	**Replica**	**Weight (g)**	**% W - N (%)**
CCH-B5-2.40	CCH-B5-2.40	CCH-B5-2.40.2ASE	1.7540	2.177
		CCH-B5-2.40.3ASE	1.2020	1.443
CCH-C2(2)-2.40	CCH-C2(2)-2.40(1)	No replica	Not measured	Not measured
	CCH-C2(2)-2.40(2)	No replica	Not measured	Not measured
	CCH-C2(2)-2.40(3)	CCH-C2(2)-2.40(3).1ASE	1.5270	1.841
		CCH-C2(2)-2.40(3).2ASE	1.1540	1.576
		CCH-C2(2)-2.40(3).3ASE	1.1420	1.166
	CCH-C2(2)-2.40(4)	No replica	Not measured	Not measured
	CCH-C2(2)-2.40(5)	No replica	Not measured	Not measured

Table 134

(Cont.)

Group of Samples B (Mw(Graft)(THEO) = 7,000 g/mol)				
Sub-Group B.2 (%Graft(THEO)=50%)				
Sample	**Sample Fraction**	**Replica**	**Weight (g)**	**% W - N (%)**
CCH-B5-2.50	CCH-B5-2.50	CCH-B5-2.50.2ASE	1.2220	4.459
CCH-C2(2)-2.50	CCH-C2(2)-2.50(1)	No replica	Not measured	Not measured
	CCH-C2(2)-2.50(2)	CCH-C2(2)-2.50(2).1ASE	1.0800	6.173
		CCH-C2(2)-2.50(2).2ASE	1.3790	6.088
	CCH-C2(2)-2.50(3)	No replica	Not measured	Not measured
	CCH-C2(2)-2.50(4)	No replica	Not measured	Not measured

Table 134

(Cont.)

Group of Samples B (Mw(Graft)(THEO) = 7,000 g/mol)				
Sub-Group B.3 (%Graft(THEO)=80%)				
Sample	**Sample Fraction**	**Replica**	**Weight (g)**	**% W - N (%)**
CCH-C2(2)-2.80	CCH-C2(2)-2.80(1)	No replica	Not measured	Not measured
	CCH-C2(2)-2.80(2)	No replica	Not measured	Not measured
	CCH-C2(2)-2.80(3)	No replica	Not measured	Not measured
	CCH-C2(2)-2.80(4)	CCH-C2(2)-2.80(4).1ASE	1.3090	8.817
		CCH-C2(2)-2.80(4).2ASE	1.2610	8.883
	CCH-C2(2)-2.80(5)	No replica	Not measured	Not measured
	CCH-C2(2)-2.80(6)	No replica	Not measured	Not measured
	CCH-C2(2)-2.80(7)	No replica	Not measured	Not measured

Table 135

Elemental Analysis: CMC-g-PNIPAAm graft copolymers

Experimental Data - Part 1: Experimental weight percentages of N (%W-N)

(Group of Samples C (Mw(Graft)$_{(THEO)}$ = 9,000 g/mol))

Group of Samples C (Mw(Graft)$_{(THEO)}$ = 9,000 g/mol)				
Sub-Group C.1 (%Graft(THEO)=40%)				
Sample	**Sample Fraction**	**Replica**	**Weight (g)**	**% W - N (%)**
CCH-B5-3.40	CCH-B5-3.40	CCH-B5-3.40.2ASE	1.7570	2.989
		CCH-B5-3.40.3ASE	1.6840	2.631
CCH-C2(2)-3.40	CCH-C2(2)-3.40(1)	No replica	Not measured	Not measured
	CCH-C2(2)-3.40(2)	CCH-C2(2)-3.40(2).2ASE	1.2930	2.761
		CCH-C2(2)-3.40(2).3ASE	1.2540	2.305
	CCH-C2(2)-3.40(3)	No replica	Not measured	Not measured

Table 135

(Cont.)

Group of Samples C (Mw(Graft)(THEO) = 9,000 g/mol)				
Sub-Group C.2 (%Graft(THEO)=50%)				
Sample	**Sample Fraction**	**Replica**	**Weight (g)**	**% W - N (%)**
CCH-B5-3.50	CCH-B5-3.50	CCH-B5-3.50.1ASE	1.1440	4.568
		CCH-B5-3.50.2ASE	1.1110	4.605
		CCH-B5-3.50.3ASE	1.8840	4.427
CCH-C2(2)-3.50	CCH-C2(2)-3.50(1)	No replica	Not measured	Not measured
	CCH-C2(2)-3.50(2)	No replica	Not measured	Not measured
	CCH-C2(2)-3.50(3)	CCH-C2(2)-3.50(3).1ASE	1.0490	6.221
		CCH-C2(2)-3.50(3).2ASE	1.3330	6.116
		CCH-C2(2)-3.50(3).3ASE	1.6180	6.070

Table 135

(Cont.)

Group of Samples C (Mw(Graft)(THEO) = 9,000 g/mol)				
Sub-Group C.3 (%Graft(THEO)=80%)				
Sample	**Sample Fraction**	**Replica**	**Weight (g)**	**% W - N (%)**
CCH-C2(2)-3.80	CCH-C2(2)-3.80(1)	No replica	Not measured	Not measured
	CCH-C2(2)-3.80(2)	No replica	Not measured	Not measured
	CCH-C2(2)-3.80(3)	CCH-C2(2)-3.80(3).1ASE	1.2100	8.800
		CCH-C2(2)-3.80(3).2ASE	1.1660	8.790
	CCH-C2(2)-3.80(4)	No replica	Not measured	Not measured
	CCH-C2(2)-3.80(5)	No replica	Not measured	Not measured
	CCH-C2(2)-3.80(6)	No replica	Not measured	Not measured

Table 136

Elemental Analysis: CMC-g-PNIPAAm graft copolymers

Experimental Data - Part 2: Average experimental weight percentage of N (%W_{avg} - N)

(Group of Samples A ($Mw(Graft)_{(THEO)}$ = 5,000 g/mol))

Group of Samples A ($Mw(Graft)_{(THEO)}$ = 5,000 g/mol)	
Sub-Group A.1 (%Graft(THEO)=40%)	
Sample	**% W_{avg} - N (%)**
CCH-A27-1	3.653
CCH-C2-1.40	1.332
CCH-C2(2)-1.40	5.369
Sub-Group A.2 (%Graft(THEO)=50%)	
Sample	**% W_{avg} - N (%)**
CCH-B5-1.50	4.960
CCH-C2(2)-1.50	6.591
Sub-Group A.3 (%Graft(THEO)=80%)	
Sample	**% W_{avg} - N (%)**
CCH-C2(2)-1.80	9.125

Table 137

Elemental Analysis: CMC-g-PNIPAAm graft copolymers

Experimental Data - Part 2: Average experimental weight percentage of N (%W_{avg} - N)

(Group of Samples B (Mw(Graft)$_{(THEO)}$ = 7,000 g/mol))

Group of Samples B (Mw(Graft)$_{(THEO)}$ = 7,000 g/mol)	
Sub-Group B.1 (%Graft(THEO)=40%)	
Sample	**% W_{avg} - N (%)**
CCH-B5-2.40	1.810
CCH-C2(2)-2.40	1.528
Sub-Group B.2 (%Graft(THEO)=50%)	
Sample	**% W - N (%)**
CCH-B5-2.50	4.459
CCH-C2(2)-2.50	6.131
Sub-Group B.3 (%Graft(THEO)=80%)	
Sample	**% W_{avg} - N (%)**
CCH-C2(2)-2.80	8.850

Table 138

Elemental Analysis: CMC-g-PNIPAAm graft copolymers

Experimental Data - Part 2: Average experimental weight percentage of N (%W_{avg} - N)

(Group of Samples C (Mw(Graft)$_{(THEO)}$ = 9,000 g/mol))

Group of Samples C (Mw(Graft)$_{(THEO)}$ = 9,000 g/mol)	
Sub-Group C.1 (%Graft(THEO)=40%)	
Sample	**% W_{avg} - N (%)**
CCH-B5-3.40	2.810
CCH-C2(2)-3.40	2.533
Sub-Group C.2 (%Graft(THEO)=50%)	
Sample	**% W_{avg} - N (%)**
CCH-B5-3.50	4.533
CCH-C2(2)-3.50	6.136
Sub-Group C.3 (%Graft(THEO)=80%)	
Sample	**% W_{avg} - N (%)**
CCH-C2(2)-3.80	8.795

Table 139

Elemental Analysis: CMC-g-PNIPAAm graft copolymers

Experimental Data - Part 3: Degree of substitution of PNIPAAm grafts per anhydroglucose unit (AGU) in CMC (DS)

(Group of Samples A ($Mw(Graft)_{(THEO)}$ = 5,000 g/mol))

Group of Samples A ($Mw(Graft)_{(THEO)}$ = 5,000 g/mol)							
Sub-Group A.1 (%Graft(THEO)=40%)							
Sample	**PC_1 (%)**	**MW_1 (g/mol)**	**N_1 (mol)**	**MWU (g/mol)**	**MWG_1 (= $Mw(Graft)_{(EXP)}$) (g/mol)**	**$d.s_1$**	**DS**
CCH-A27-1 Backbone: CMC Grafts: Sample CCH-A15-1	3.653	14.007	44	223	5,101.340	0.0189	0.0171
CCH-C2-1.40 Backbone: CMC Grafts: Sample CCH-C1-1	1.332	14.007	44	223	5,103.026	0.0054	0.0038
CCH-C2(2)-1.40 Backbone: CMC Grafts: Samples CCH-A15-1, CCH-A15-2, CCH-A15-3, CCH-C1-1 and CCH-C1(2)-1	5.369	14.007	44	223	5,071.776	0.0345	0.0242

Table 139

(Cont.)

Group of Samples A ($Mw(Graft)_{(THEO)}$ = 5,000 g/mol)							
Sub-Group A.2 (%Graft(THEO)=50%)							
Sample	**PC_1 (%)**	**MW_1 (g/mol)**	**N_1 (mol)**	**MWU (g/mol)**	**MWG_1 (= $Mw(Graft)_{(EXP)}$) (g/mol)**	**$d.s_1$**	**DS**
CCH-B5-1.50 Backbone: CMC Grafts: Sample CCH-A15-1	4.960	14.007	44	223	5,101.340	0.0304	0.0274
CCH-C2(2)-1.50 Backbone: CMC Grafts: Samples CCH-A15-1, CCH-A15-2, CCH-A15-3, CCH-C1-1 and CCH-C1(2)-1	6.591	14.007	44	223	5,071.776	0.0516	0.0361
Sub-Group A.3 (%Graft(THEO)=80%)							
Sample	**PC_1 (%)**	**MW_1 (g/mol)**	**N_1 (mol)**	**MWU (g/mol)**	**MWG_1 (= $Mw(Graft)_{(EXP)}$) (g/mol)**	**$d.s_1$**	**DS**
CCH-C2(2)-1.80 Backbone: CMC Grafts: Samples CCH-A15-1, CCH-A15-2, CCH-A15-3, CCH-C1-1 and CCH-C1(2)-1	9.125	14.007	44	223	5,071.776	0.1302	0.0911

Table 140

Elemental Analysis: CMC-g-PNIPAAm graft copolymers

Experimental Data - Part 3: Degree of substitution of PNIPAAm grafts per anhydroglucose unit (AGU) in CMC (DS)

(Group of Samples B ($Mw(Graft)_{(THEO)}$ = 7,000 g/mol))

Group of Samples B ($Mw(Graft)_{(THEO)}$ = /,000 g/mol)							
Sub-Group B.1 (%Graft(THEO)=40%)							
Sample	**PC_1 (%)**	**MW_1 (g/mol)**	**N_1 (mol)**	**MWU (g/mol)**	**MWG_1 (= $Mw(Graft)_{(EXP)}$) (g/mol)**	**$d.s_1$**	**DS**
CCH-B5-2.40 Backbone: CMC Grafts: Sample CCH-B4-1	1.810	14.007	60	223	7,048.210	0.0057	0.0051
CCH-C2(2)-2.40 Backbone: CMC Grafts: Samples CCH-B4-1, CCH-C1-2 and CCH-C1(2)-2	1.528	14.007	60	223	7,071.348	0.0047	0.0033

Table 140

(Cont.)

Group of Samples B (Mw(Graft)(THEO) = /,000 g/mol)							
Sub-Group B.2 (%Graft(THEO)=50%)							
Sample	**PC_1 (%)**	**MW_1 (g/mol)**	**N_1 (mol)**	**MWU (g/mol)**	**MWG_1 (= Mw(Graft)(EXP)) (g/mol)**	**$d.s_1$**	**DS**
CCH-B5-2.50 Backbone: CMC Grafts: Sample CCH-B4-1	4.459	14.007	60	223	7,048.210	0.0189	0.0170
CCH-C2(2)-2.50 Backbone: CMC Grafts: Samples CCH-B4-1, CCH-C1-2 and CCH-C1(2)-2	6.131	14.007	60	223	7,071.348	0.0336	0.0235
Sub-Group B.3 (%Graft(THEO)=80%)							
Sample	**PC_1 (%)**	**MW_1 (g/mol)**	**N_1 (mol)**	**MWU (g/mol)**	**MWG_1 (= Mw(Graft)(EXP)) (g/mol)**	**$d.s_1$**	**DS**
CCH-C2(2)-2.80 Backbone: CMC Grafts: Samples CCH-B4-1, CCH-C1-2 and CCH-C1(2)-2	8.850	14.007	60	223	7,071.348	0.0920	0.0644

Table 141

Elemental Analysis: CMC-g-PNIPAAm graft copolymers

Experimental Data - Part 3: Degree of substitution of PNIPAAm grafts per anhydroglucose unit (AGU) in CMC (DS)

(Group of Samples C ($Mw(Graft)_{(THEO)}$ = 9,000 g/mol))

Group of Samples C ($Mw(Graft)_{(THEO)}$ = 9,000 g/mol)							
Sub-Group C.1 (%Graft(THEO)=40%)							
Sample	**PC_1 (%)**	**MW_1 (g/mol)**	**N_1 (mol)**	**MWU (g/mol)**	**MWG_1 (= $Mw(Graft)_{(EXP)}$) (g/mol)**	**$d.s_1$**	**DS**
CCH-B5-3.40 Backbone: CMC Grafts: Sample CCH-B4-2	2.810	14.007	78	223	9,169.140	0.0075	0.0068
CCH-C2(2)-3.40 Backbone: CMC Grafts: Samples CCH-B4-2, CCH-C1-3, CCH-C1(2)-3, CCH-C1(2)-3.2 and CCH-C1(2)-3.3	2.533	14.007	78	223	9,080.610	0.0066	0.0046

Table 141

(Cont.)

Group of Samples C ($Mw(Graft)_{(THEO)}$ = 9,000 g/mol)							
Sub-Group C.2 (%Graft(THEO)=50%)							
Sample	**PC_1 (%)**	**MW_1 (g/mol)**	**N_1 (mol)**	**MWU (g/mol)**	**MWG_1 (= $Mw(Graft)_{(EXP)}$) (g/mol)**	**$d.s_1$**	**DS**
CCH-B5-3.50 Backbone: CMC Grafts: Sample CCH-B4-2	4.533	14.007	78	223	9,169.140	0.0149	0.0134
CCH-C2(2)-3.50 Backbone: CMC Grafts: Samples CCH-B4-2, CCH-C1-3, CCH-C1(2)-3, CCH-C1(2)-3.2 and CCH-C1(2)-3.3	6.136	14.007	78	223	9,080.610	0.0258	0.0181

Table 141
(Cont.)

Group of Samples C (Mw(Graft)$_{(THEO)}$ = 9,000 g/mol)								
Sub-Group C.3 (%Graft(THEO)=80%)								
Sample	**PC_1 (%)**	**MW_1 (g/mol)**	**N_1 (mol)**	**MWU (g/mol)**	**MWG_1 (= Mw(Graft)$_{(EXP)}$) (g/mol)**	**$d.s_1$**	**DS**
CCH-C2(2)-3.80 Backbone: CMC Grafts: Samples CCH-B4-2, CCH-C1-3, CCH-C1(2)-3, CCH-C1(2)-3.2 and CCH-C1(2)-3.3	8.795	14.007	78	223	9,080.610	0.0680	0.0476